DEPARTMENT OF CIVIL ENGINEERING

Water Resources Research Group

UNIVERSITY ℃SALFORD

ARIP REPORT No. 4

~~~~~~

ANGLIAN RADAR INFORMATION PROJECT

~~~~~~

ANGLIAN RADAR INFORMATION PROJECT

REPORT NO. ◆ 5

OI/309/5/A

*Quantitative Precipitation Estimation with Weather Radar:
Problems and Solutions for the National Rivers Authority,
Anglian Region*

Water Resources Research Group
Department of Civil Engineering
University of Salford
Salford, M5 4WT

Report prepared by

K.A. Tilford and Prof. I.D. Cluckie
September 1991

Contents

List of figures

List of tables

Chapter 1. Introduction

This is the fifth report to be submitted as part of the Anglian Radar Information Project (ARIP).

Chapter 2 discusses in detail aspects of radar systems that have a direct influence on Regional precipitation estimation accuracy using weather radar data. In particular the chapter covers such topics as radar site horizons, beam infilling and the effect of range on rainfall observation and quantitative estimation. The range problem becomes particularly important at long range (i.e. beyond about 125 km) where the beam height and volume introduce significant error into observation and estimation. A simple range correction procedure is introduced to remove some the systematic effects of range underestimation (at long range) and also overestimation (at close range) for use with historical data, especially when cumulated over extended periods (e.g. several weeks or more). The chapter also examines in some detail the influence of altitude on radar rainfall estimation in the Region, a study which is supported by comprehensive raingauge data from the northern area. Finally, the chapter investigates the extent of problems due to the presence of bright-band.

Chapter 3 provides an introduction to a three-phase raingauge-based procedure for Regionwide adjustment of real-time radar rainfall data. The procedure incorporates a sophisticated numerical algorithm for fitting a two-dimensional surface to irregularly distributed assessment factors to produce a regular assessment factor field. In addition, two-dimensional interpolation is used to produce a spatial rainfall field from raingauge data which can be compared the radar images. The choice of assessment factor (i.e. the ratio of rainfalls estimated by raingauge and radar), and the surface smoothness are both influential in the subsequent adjustment and available choices and recommendations are discussed and justified. A worked example illustrates the adjustment procedure in operation. Theoretical aspects of the surface-fitting and interpolation algorithms are covered in an Appendices 9 and 10.

The adjustment procedure is verified and evaluated in Chapter 4. Emphasis is placed on the estimation of areal rainfall amounts and the procedure is assessed for a number of individual case study rainfall events in addition to an overall assessment from all the available data (23-days). The case study events were selected to include different types of rainfall system (the main discrimination being between widespread, low spatial variability stratiform rainfall, and highly localised convective rainfall) for which a large number of raingauges were available, and during which significant rainfall occurred. An additional appraisal considered the influence of the adjustment procedure on storm frequency estimation for selected test catchments, using the Flood Studies Report procedure for design storm derivation. Finally, the impact of adjustment was assessed in terms of an end-point application. The EPA assessment used the different rainfall types as an input into a flow-forecasting model, and compared the accuracy of the flow-forecasts from each. The latter assessment was invaluable in that it provided the only truly independent assessment of the adjustment procedure.

The influence of raingauge network density on radar adjustment is an important issue addressed in chapter 5. The extent to which the spatial variability of the rainfall process influences areal estimation from raingauge data alone is examined for a highly spatially variable convective event and a lower spatially variable stratiform rainfall event. This study is then extended to the radar adjustment procedure and areal and point rainfall estimates made from raingauge data, and unadjusted and adjusted radar data. The analysis is based on a limited number of case studies for which the rainfall process differs and for which rainfall is significant, and a large number of raingauges were available. On the basis of the study, a tentative recommendation is made for the density of raingauges required for real-time adjustment to provide acceptable results.

The findings detailed in the Report are summarised and the implications discussed in the final chapter. A substantial amount of additional information pertinent to radar adjustment is contained in the twelve appendices collected at the end of the report. The Report is fully cross-referenced and attention is drawn to relevant information in other ARIP Reports and Software Profiles.

Footnote:

Reference is made throughout the report to radar adjustment and calibration. The differentiation is an important one and not self-explanatory. The term calibration in the context of this report is reserved for hardware tuning procedures typically carried out by radar manufacturers, but also to the Meteorological Office real-time raingauge calibration process. The use of the term calibration in the second case is misleading, and all subsequent processing of the radar data (for example the procedures developed as part of this study) with the exception of the Meteorological Office calibration scheme, are referred to as adjustment procedures.

Chapter 2. Analysis of Weather Radar Performance in Anglian Region

The general characteristics of the weather radars serving the Anglian Region (i.e. Chenies [London] and Ingham [Lincoln]) are shown in Appendices 2 and 4. This chapter discusses in greater detail aspects of the radar systems which directly affect precipitation estimation accuracy in the Region and describes the results of an initial appraisal into the performance of the radars. The analysis highlights problems in estimation accuracy due to range related affects and proposes a radar range correction algorithm for use in real-time. The problems arising from bright-band are also highlighted and discussed.

2.1. Radar Horizons

The importance of a relatively clear sight horizon was discussed in ARIP 4 (sections 3.2.1 and 3.2.2). The sight horizons for Ingham and Chenies radar are shown in figure 2.1 and 2.2. Two horizons are shown for each radar, a distant horizon (obtained from a digitised terrain map), and a horizon which includes local obstructions (made by theodolite survey). The Ingham site is shown to have an excellent obstruction free horizon, mainly because of the subdued nature of the topography in the coverage area but also due to the rural location providing a location free from large buildings close to the radar. The Chenies site is less ideal and suffers from a significant local obstruction problem, and also a permanent echo problem due to ground clutter.

2.2. Beam Infilling

The problems that arise from ground clutter and the approaches taken to help minimise them were discussed in ARIP 4 section 3.2. In particular the technique of beam infilling was mentioned, whereby data derived from a higher beam elevation are used in place lower beam elevation data where permanent echo, ground clutter, or local obstructions are known to be a problem.

The beam infilling (5 km) cartesian grids used for the Chenies and Ingham radars are shown in figure 2.3. The grids indicate the areas precipitation data are derived from a beam elevation other than the lowest (0.5°) beam. Beam infilling for the Ingham radar utilises two higher elevation beams whereas only one is used for the Chenies radar. Though not directly affecting precipitation estimates over the Region (the infilling takes place beyond the Regional boundaries), the infilling grids for Chenies are reproduced for comparison with the Ingham infill grid.

Beam infilling of the Ingham radar is particularly important for the Anglian Region because it takes place within the Region thereby directly affecting local precipitation estimates (i.e. rainfall
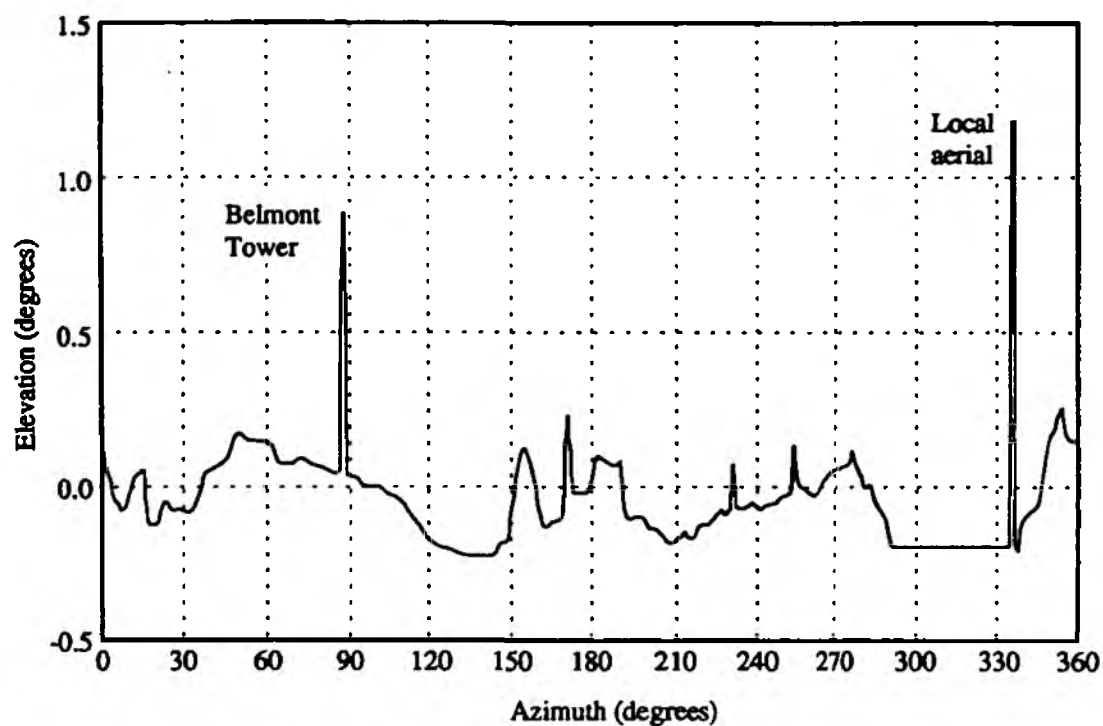
i). including local obstructions
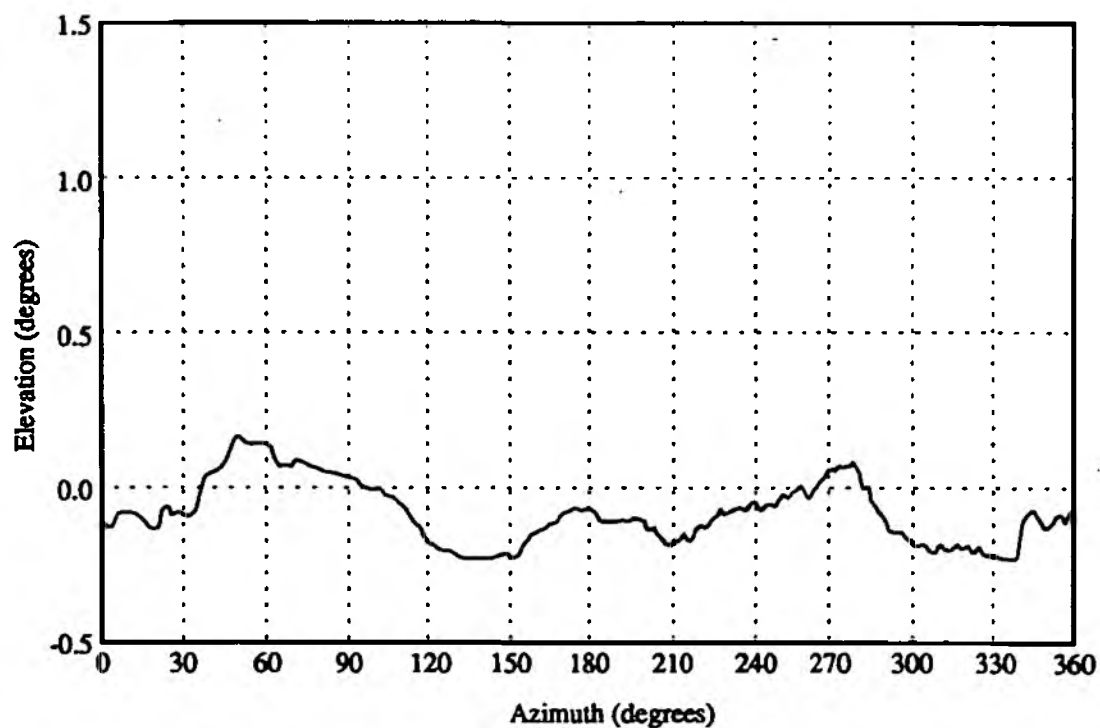
ii). distant horizon

Figure 2.1: Horizon diagrams for Ingham radar
(source: Meteorological Office)
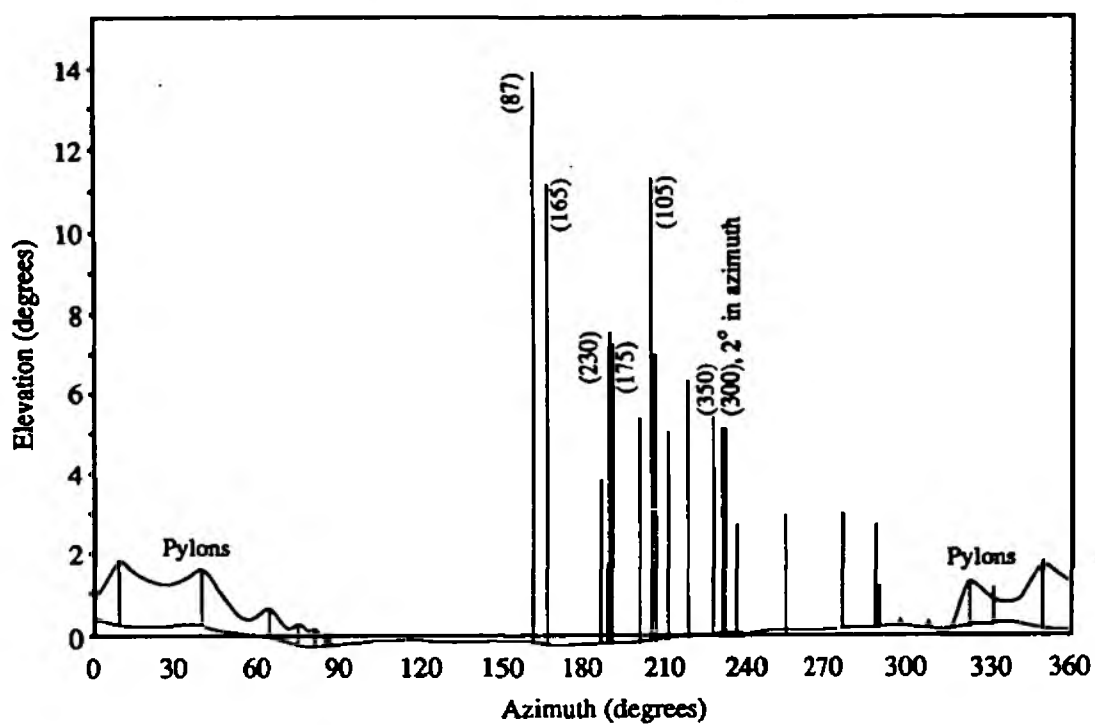
i). local obstructions
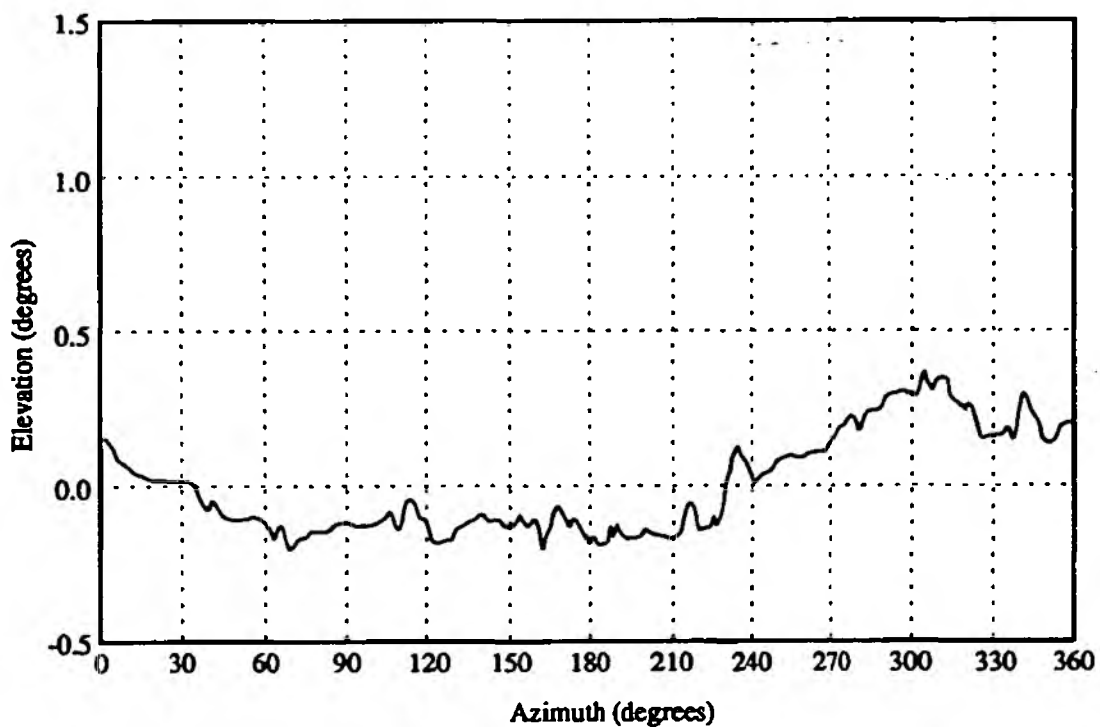
ii). distant horizon

Figure 2.2: Horizon diagrams for Chenies radar
(source: Meteorological Office)

estimates for the Lincoln area). Of the range effects discussed in section 2.3, near range overestimation is shown to be a major source of precipitation estimation error. This is largely due to the presence of bright-band (which for the reasons discussed in ARIP 4 section 3.4.2, results in larger errors close to the radar rather than at longer ranges), but remains a problem even when bright-band is absent. Beam infilling seems to be the reason for this and is probably explained by inhomogenities in the vertical reflectivity profile (i.e. a beam at one elevation produces an echo which differs to the echo received from a beam at a different elevation). For the same reasons, beam infilling can introduce spatial discontinuities in the beam height used to estimate surface precipitation. The effect is most severe for the Chenies radar which is restricted to two beam elevations, the altitude steps being less severe for Ingham which has an additional intermediate beam elevation (1.1°). The spatial discontinuity effect is illustrated by figure 2.4 which shows longitudinal profiles of the radar beam centres used to derive surface rainfall at selected azimuths (as indicated by the arrows on figure 2.3).
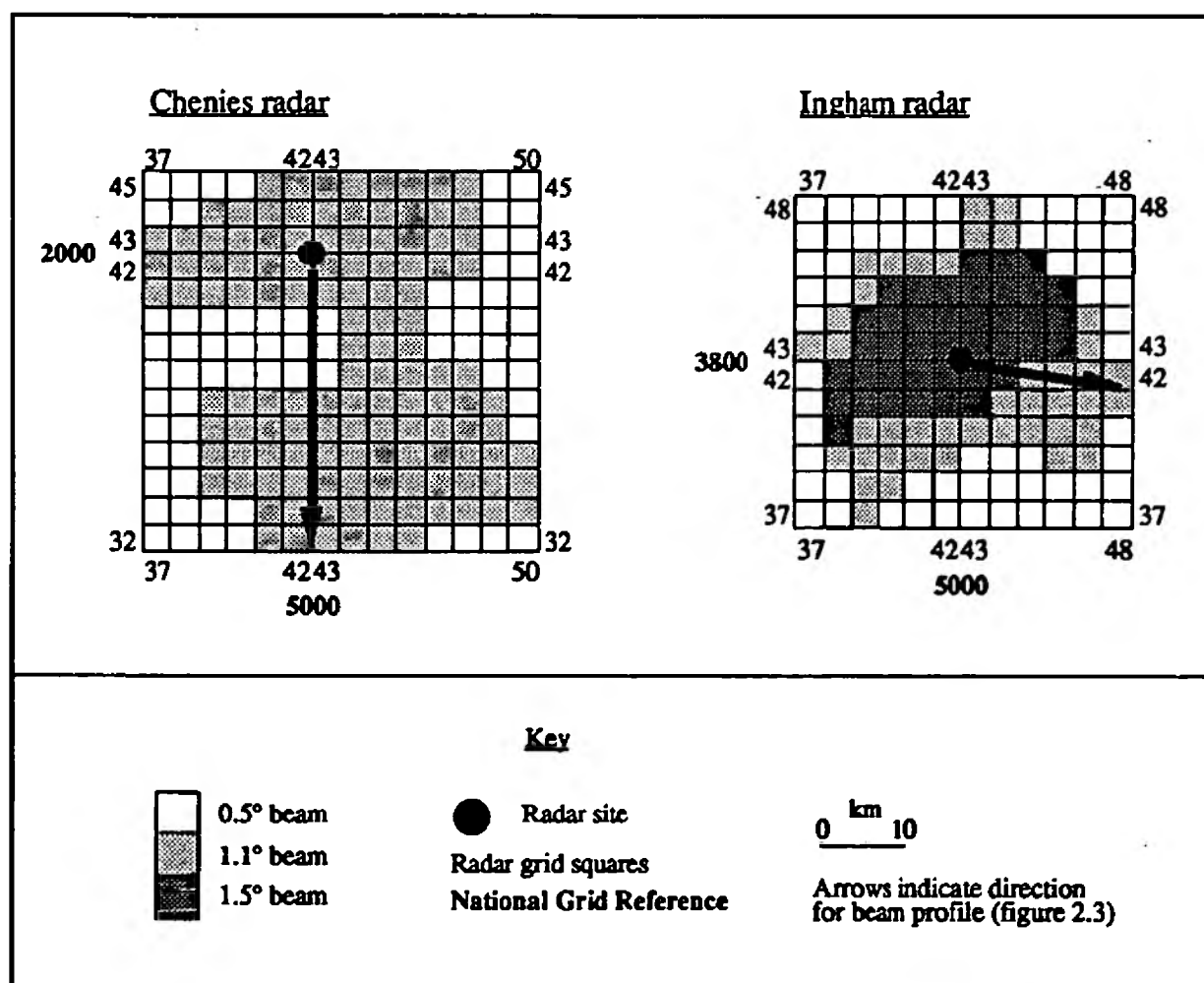
Figure 2.3: Beam infilling grids for Ingham and Chenies radars
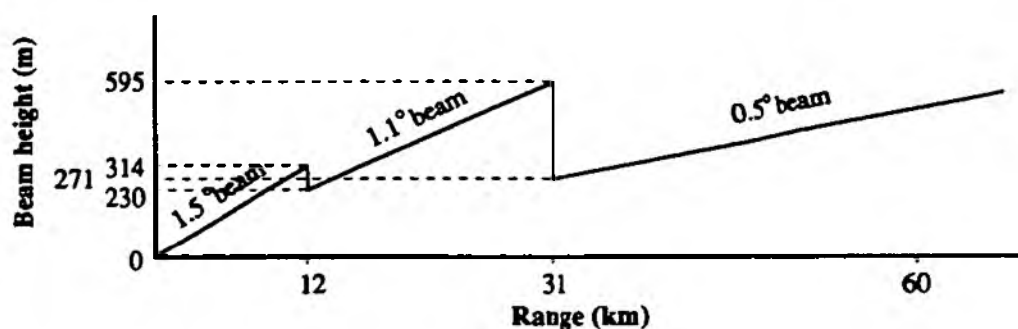
i). Ingham radar. 120 azimuth
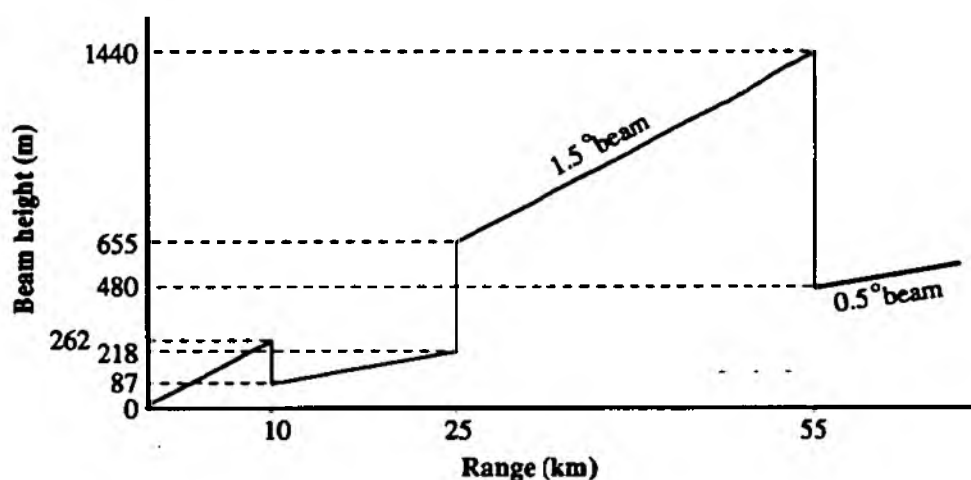
ii). Chenies radar. 180 azimuth

Figure 2.4: Effect of beam infilling at near range (beam heights neglect earth curvature and beam refraction)

2.3. The Effect of Range on Quantitative Precipitation Estimation

The ways in which range from radar affect precipitation estimation are discussed in ARIP 4 chapter 3 in a theoretical manner: this section presents the results of an in-depth analysis based upon data primarily from the Ingham radar. The analysis has revealed that estimation problems occur not only at far range, but also close to the radar (albeit for different reasons), and proposes a simple range correction procedure.

2.3.1. Analysis of Range Related Precipitation Estimation Accuracy Problems

A useful initial assessment of radar performance can be made by cumulating rainfall over a long period of time and examining the resultant rainfall field. Such a procedure can be invaluable in identifying problems which affect precipitation estimation systematically, such as ground clutter or beam occultation due to local obstacles which may have been overlooked by the at-site range calibration. In addition, the procedure highlights the effect of range.

A total of 27 days data were available for this analysis (see Appendix 5 for a listing and Appendix 11 for event radar image cumulations), spanning the period from late 1988 (when the Ingham radar first became operational) to mid-December 1989. Unadjusted rainfall data on a 5 km grid (to a range of 210 km) for all 27 days were cumulated and the depths averaged over time to produce a time independent average rainfall intensity field (in mm/hr units). The procedure was repeated for two additional data (sub)sets, the first being all data having a bright-band present, and the second excluding all bright-band data[1]. The average rainfall intensity fields for each of the data sets are shown in figure 2.5 in two forms, a regular gridded format, and a linearly interpolated contour representation.

The average rainfall intensity fields are also represented in the form of a rainfall intensity / range scattergraph, i.e. the average rainfall intensity of each of the grid squares for the period plotted against the range of the cell from the radar site.

Finally, the information contained in the scattergraphs is 'distilled' in a range averaged rainfall intensity / range line graph. To produce these, range slicing was introduced across 5 km bounds (i.e. 0-5 km, 5-10 km, . . . , 205-210 km), and the rainfall intensities of all cells falling within each of the range slices averaged to produce a mean rainfall intensity for each. Variability between the rainfall intensities of the cells within each range slice is computed by the standard deviation.

- the average rainfall intensity fields are shown in figure 2.5.
- the rainfall intensity / range scattergraphs are shown in figure 2.6.
- the range averaged rainfall intensity / range line graphs are shown in figure 2.7.

The figures clearly indicate that the mean estimated precipitation intensity for the 27 day period is inversely related to range. In addition to underestimation at longer ranges (i.e. beyond 100 km), rainfall intensities close to the radar, (i.e. in the range 0-60 km) appear to be overestimated, most significantly within 30 km range. The effect of bright-band on quantitative precipitation estimation is clearly illustrated, the average rainfall intensities when bright-band is present being considerably higher than when absent, typically by a factor of five or more and sometimes by as much as a factor of ten.

---

[1] The radar data header block was used to determine whether bright-band was present (the header block flag being driven by the objective real-time Meteorological Office bright-band detection algorithm).

i). All data
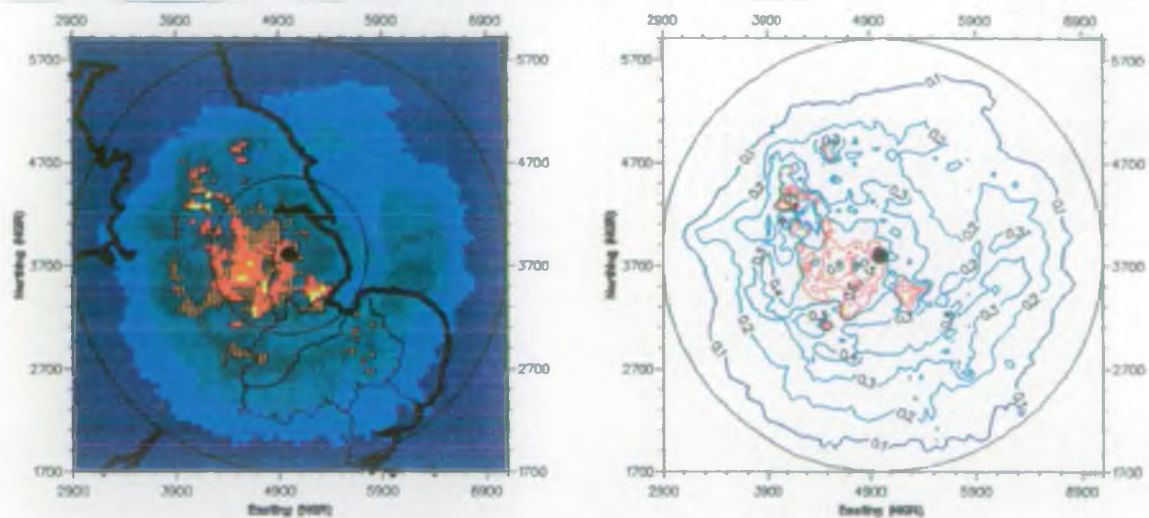
ii). Bright-band affected data only
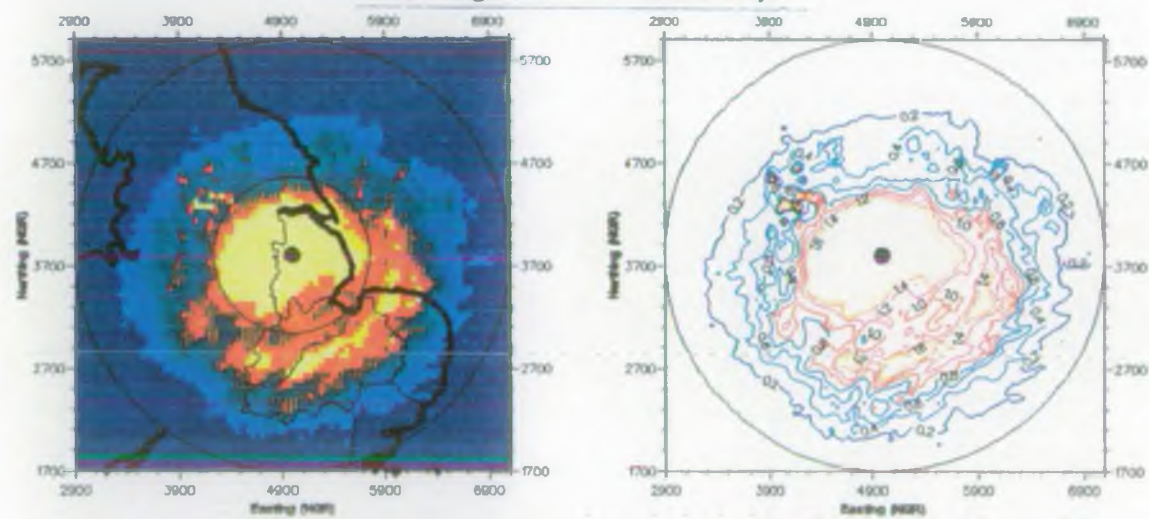
iii). Bright-band affected data removed
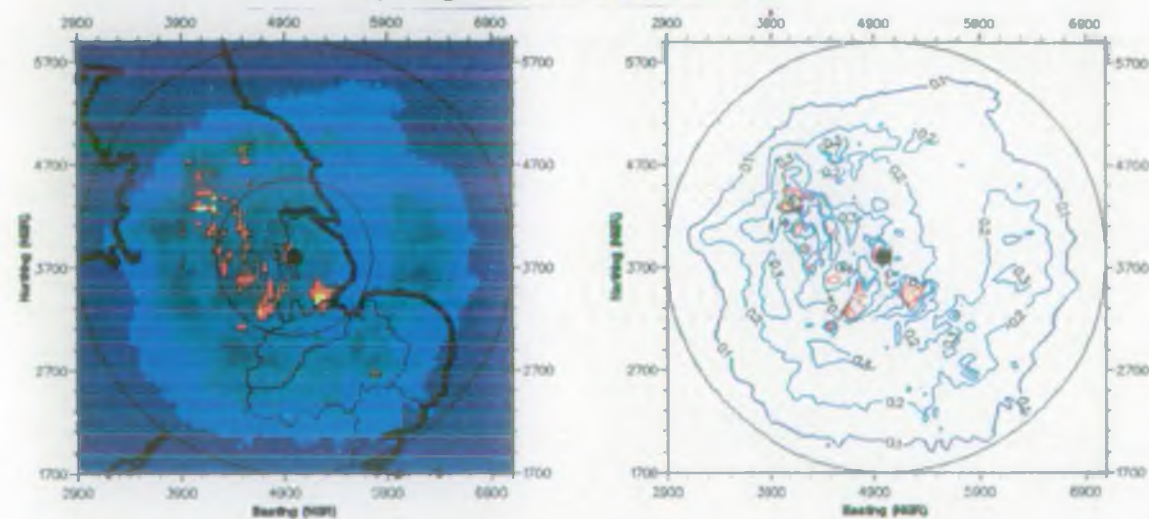
Figure 2.5: Average rainfall intensity fields (Ingham radar, 27 days, unadjusted 5 km data)

i). All available data

ii). Bright-band frames only

iii). Bright-band frames removed
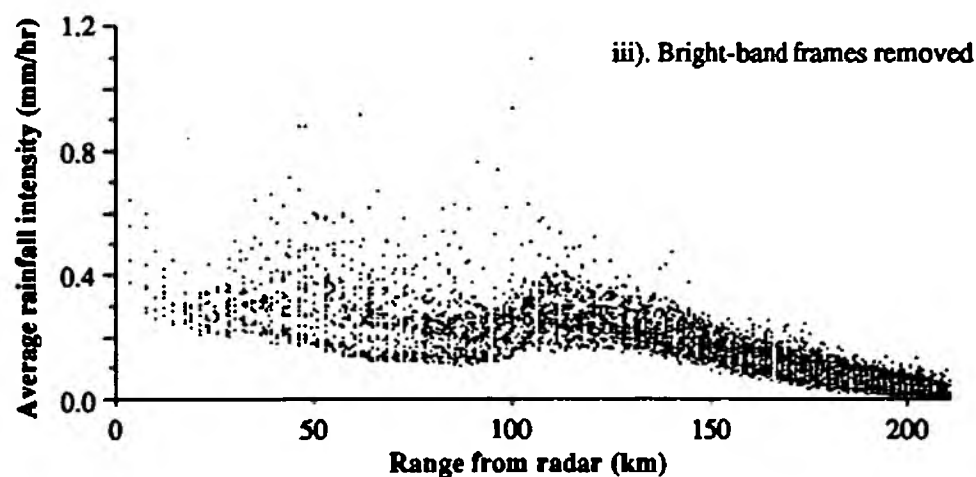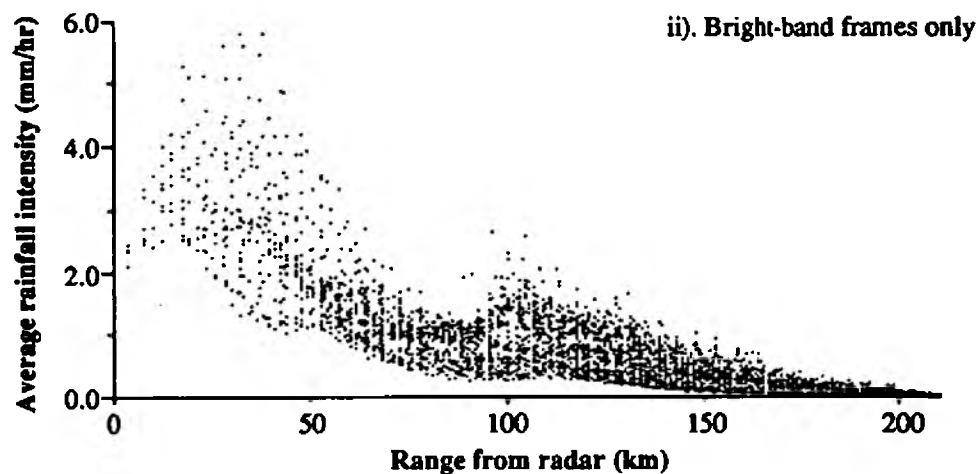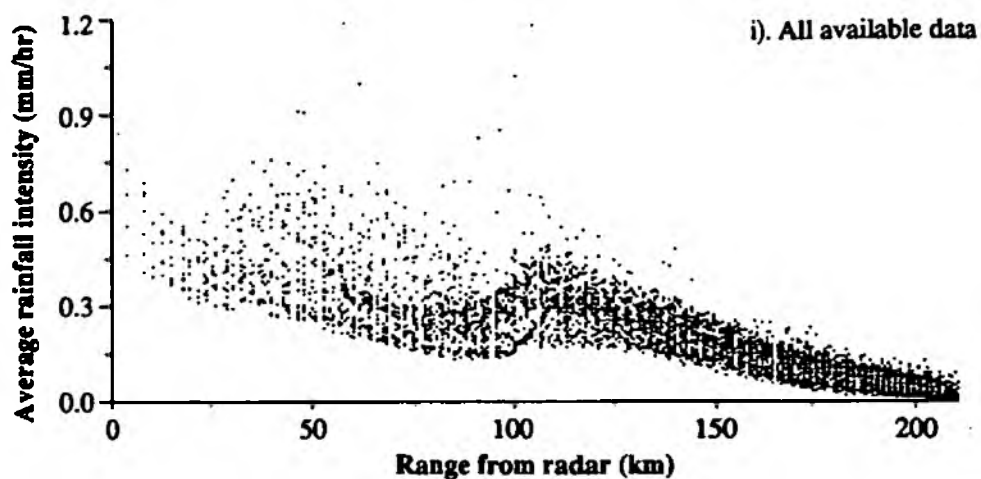
Figure 2.6: Average rainfall intensity as a function of range from the radar
(Ingham radar, 5 km, unadjusted data, from a total of 27 days data)
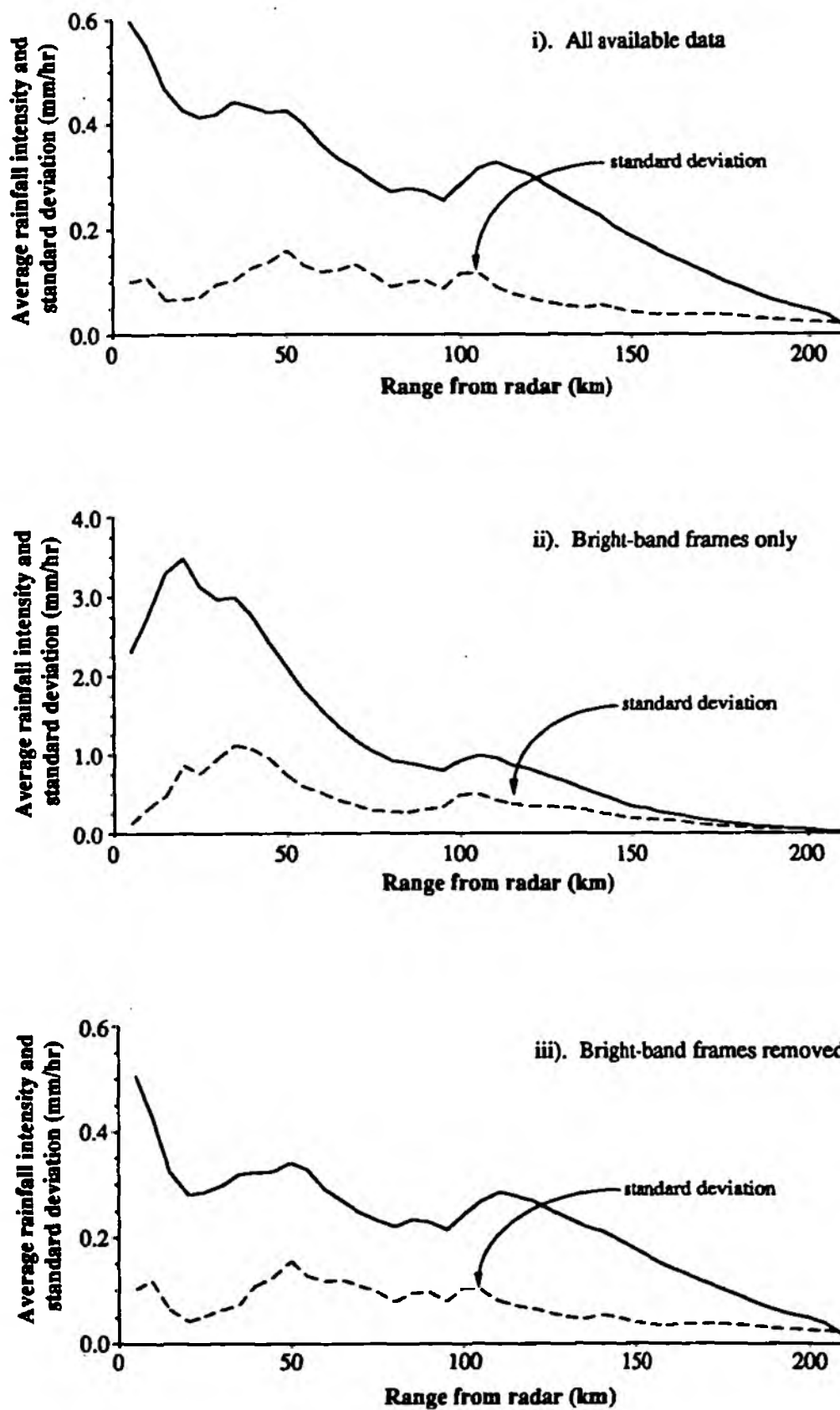
Figure 2.7: Average rainfall intensity as a function of range for the entire radar image (Ingham radar, 5 km unadjusted data from a total of 27 days data)

Range averaged rainfall intensity / range line graphs have also been derived for radar cells overlying the northern area of the Anglian Region for which raingauge data are also available (refer to Appendix 6 for the 5 km radar cell mapping scheme used to represent the area). This enabled a direct comparison of the radar derived rainfall intensities with raingauge values. The study was made for two data sets; individual daily data, and a 23 day subset of the main data set. The latter was the longest duration for which raingauge and radar data were both available and rainfall over the Region was significant, i.e. 4 days were excluded from the analysis. In order to avoid the introduction of storm bias into the analysis, only raingauges present for all 23 days or 22 days were included, and gauges absent for longer than 1 day excluded.

The range averaged mean radar rainfall intensity / range line graph for the 23 day period is shown in figure 2.8. Raingauge data are also shown on the graph. The raingauges used, their range from the radar, mean rainfall intensity and number of days data used for each are tabulated in table 2.1. Whilst the average radar rainfall intensities show a strong range dependency, the raingauge data exhibit little dependency. This visual interpretation is borne out by the (Pearson) product moment correlation coefficients[2] for each distribution:

Raingauge data,   PMC = 0.2, i.e. a very weak positive correlation.
Unadjusted radar data,   PMC = -0.8, i.e. a very strong negative correlation.
Adjusted radar data,   PMC = -0.8, i.e. a very strong negative correlation.

The raingauge data tend to confirm that in the northern area of Anglian Region the spatial distribution of the rainfall over the 23 day period is not one of decreasing rainfall intensity with range from the radar site and therefore confirms the presence of range related estimation accuracy problems with the Ingham radar.

Range averaged rainfall intensity / range line graphs for each of the 23 days on an individual basis are shown in figure 2.9. Radar - raingauge ratios for the daily rainfall totals are plotted on the same figures. Over the shorter daily duration, the range effect is less obvious. However, it should be noted that the maximum range of any of the raingauges located in the northern area from the radar is 140 km, and consequently underestimation at long ranges, i.e. 150 km and beyond, (together with a tendency of radar / raingauge ratios to decrease with range) cannot be studied in detail. Despite this, there are a number of occasions when range effects can be seen. Overestimation at near range is also readily observable, particularly when bright-band is present (e.g. 14th, 16th and 18th December 1989).

Finally, a study was conducted to determine whether the range effect was azimuth dependent. Azimuth dependent range averaged rainfall intensity / range line graphs for the 27 day period are

[2] The (Pearson) product-moment correlation coefficient measures a linear relationship, and has a value which varies from -1.0 to 1.0. A coefficient of 0.0 indicates that no linear relationship exists; a +1.0 coefficient implies a 'perfect' positive relationship (i.e. an increase in one variable is always associated with a corresponding increase in the other variable); and a coefficient of -1.0 indicates a 'perfect' negative relationship (i.e. an increase in one variable is always associated with a corresponding decrease in the other variable).
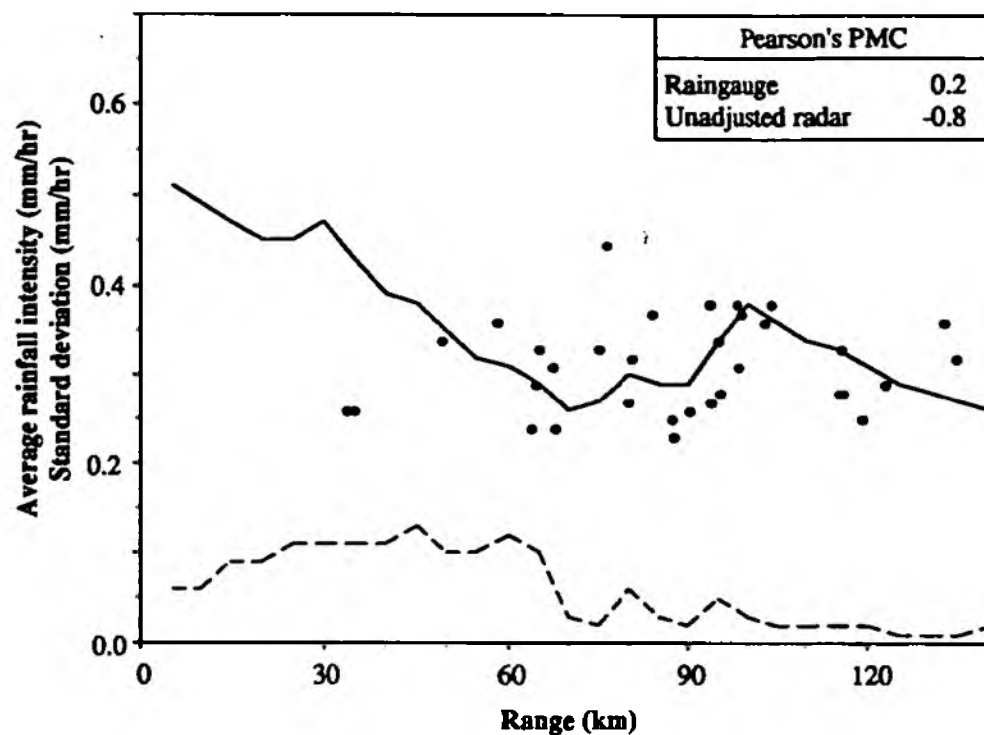
Figure 2.8: Comparison of unadjusted radar and raingauge mean rainfall intensity estimates for a 23 day period as a function of range for the northern area of Anglian Region. (Only raingauges not absent for more than one day included)

Column 1: Raingauge reference
Column 2: Number of days data
Column 3: Range from radar (km)
Column 4: Average rainfall intensity (mm/hr)

U01	22	65	0.29	V03	23	98	0.31	V21	23	95	0.28
U04	23	58	0.36	V04	22	81	0.32	V22	22	94	0.27
U05	22	79	0.24	V05	22	95	0.34	V23	23	116	0.28
U06	23	35	0.26	V06	23	90	0.26	V24	23	134	0.32
U07	23	80	0.27	V08	22	98	0.38	V26	23	116	0.28
U11	23	67	0.31	V12	23	119	0.25	V27	23	104	0.38
U12	23	83	0.24	V13	22	87	0.25	V28	23	88	0.23
U17	22	50	0.34	V16	22	103	0.36	V29	23	123	0.29
U18	23	75	0.33	V18	22	93	0.38	V31	22	84	0.37
U19	22	65	0.33	V19	22	132	0.36	V32	23	116	0.33
U25	22	34	0.26	V20	22	99	0.37				

Table 2.1: Station breakdown of raingauge rainfall intensity/range data

Average rainfall
intensity (mm/hr)   Log GR Ratio
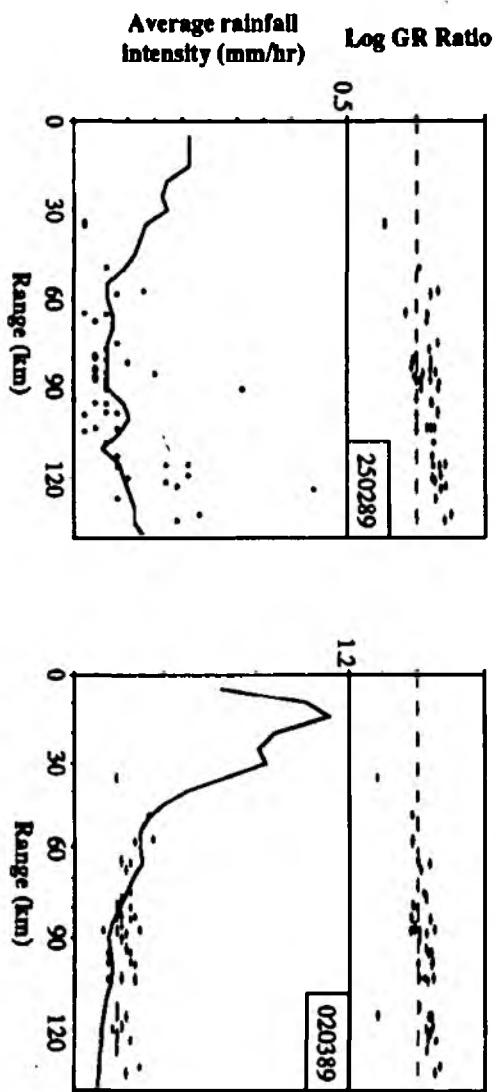
Figure 2.9(i): Unadjusted radar and raingauge derived rainfall intensities, and RG ratios as a function of range for daily data

Average rainfall intensity (mm/hr)　Log GR Ratio

Average rainfall intensity (mm/hr)　Log GR Ratio

1.5

0.5

0.8

0.4

291188

191088

240289

091188

14
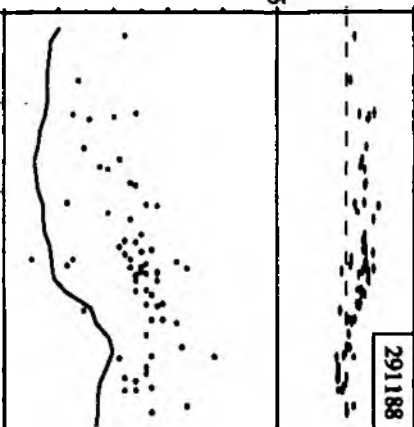
Average rainfall intensity (mm/hr)   **Log GR Ratio**
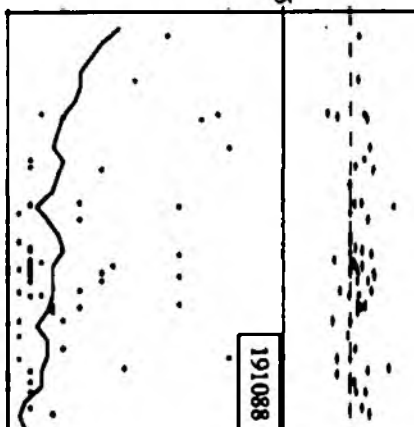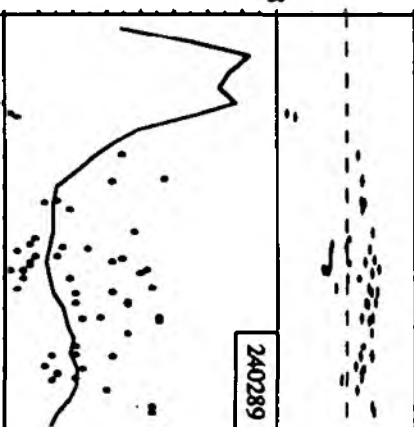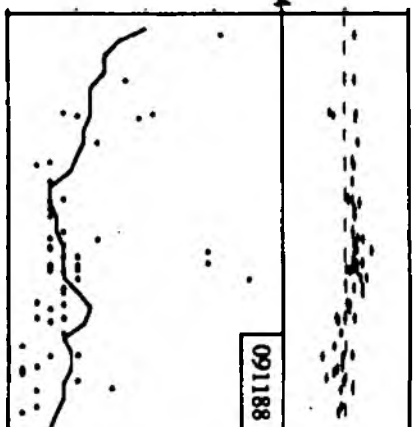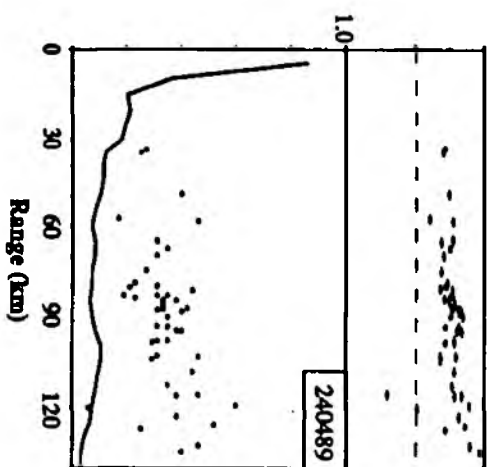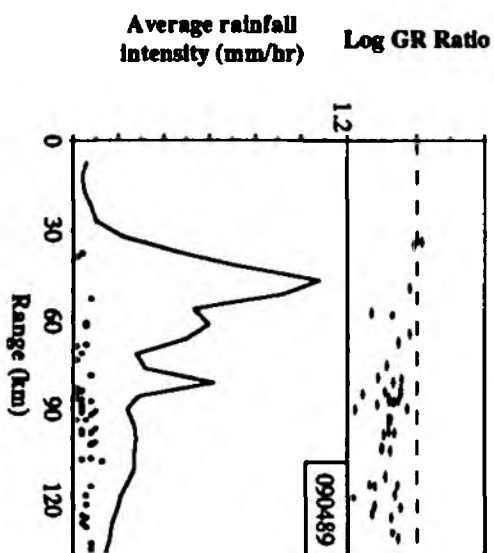
Figure 2.9(ii): Unadjusted radar and raingauge derived rainfall intensities, and RG ratios as a function of range for daily data

Average rainfall intensity (mm/hr) Log GR Ratio

Average rainfall intensity (mm/hr) Log GR Ratio

0.15

1.0

230389

140389

1.0

1.0

040489

200389

15
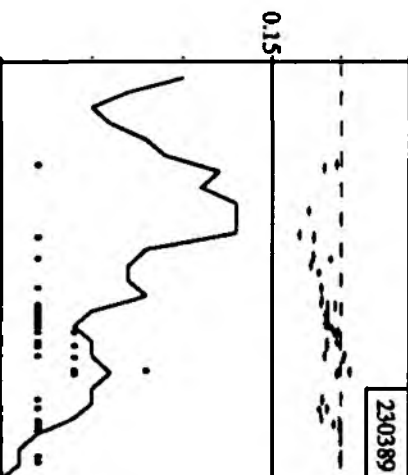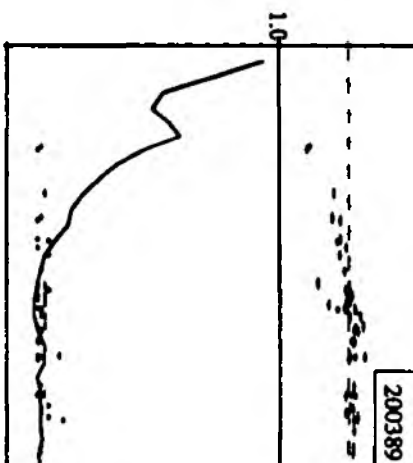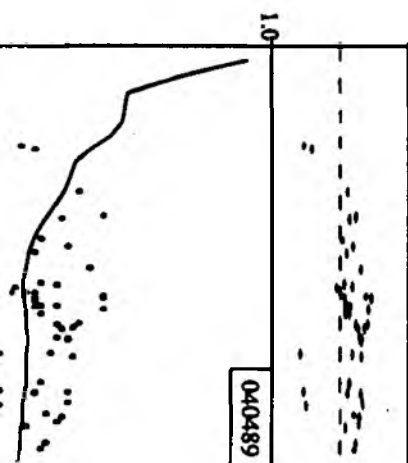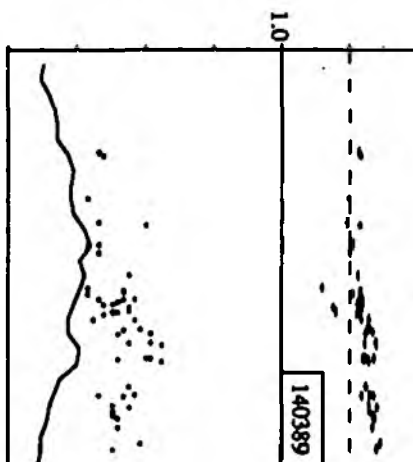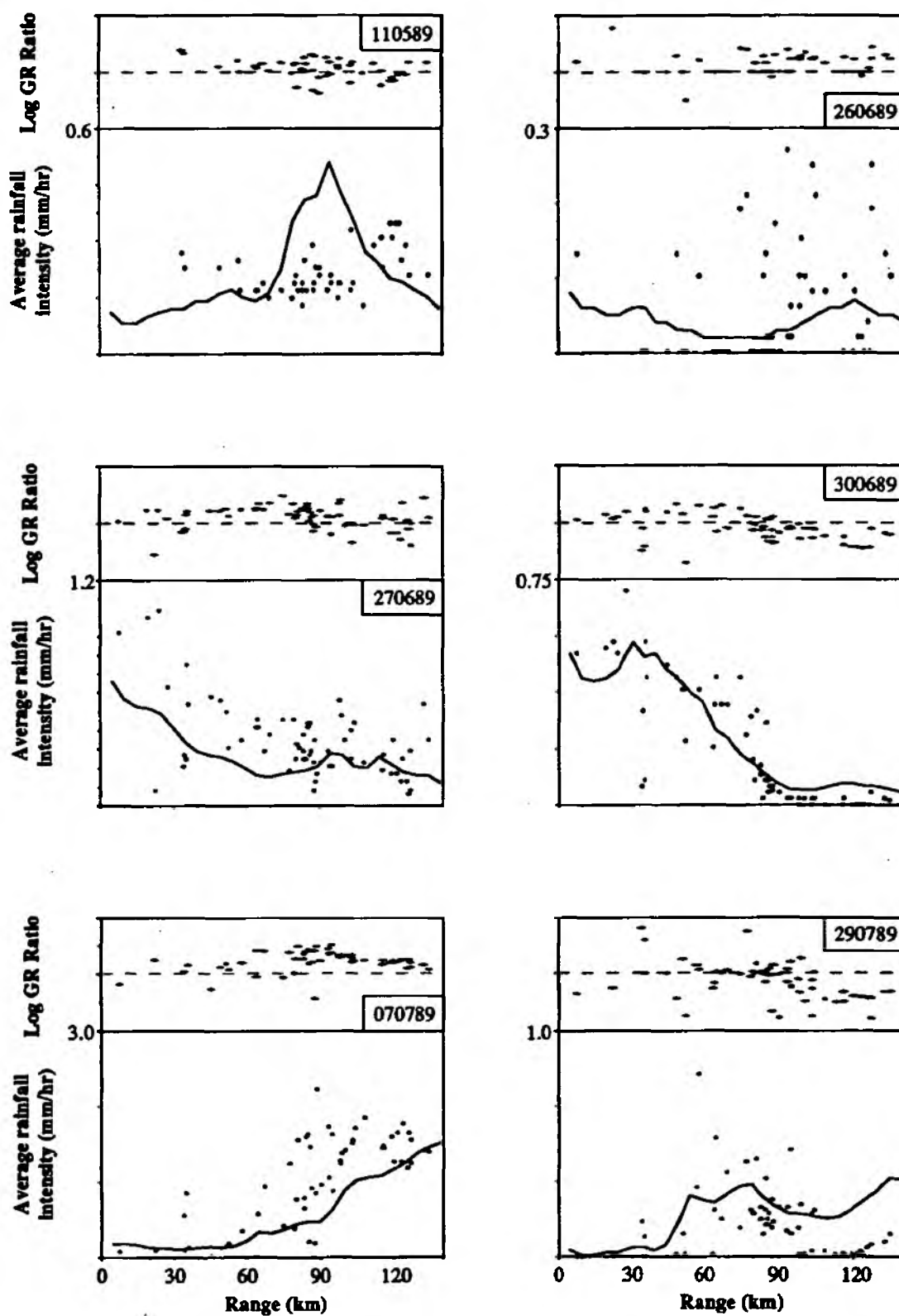
Figure 2.9(iii): Unadjusted radar and raingauge derived rainfall intensities, and RG ratios as a function of range for daily data
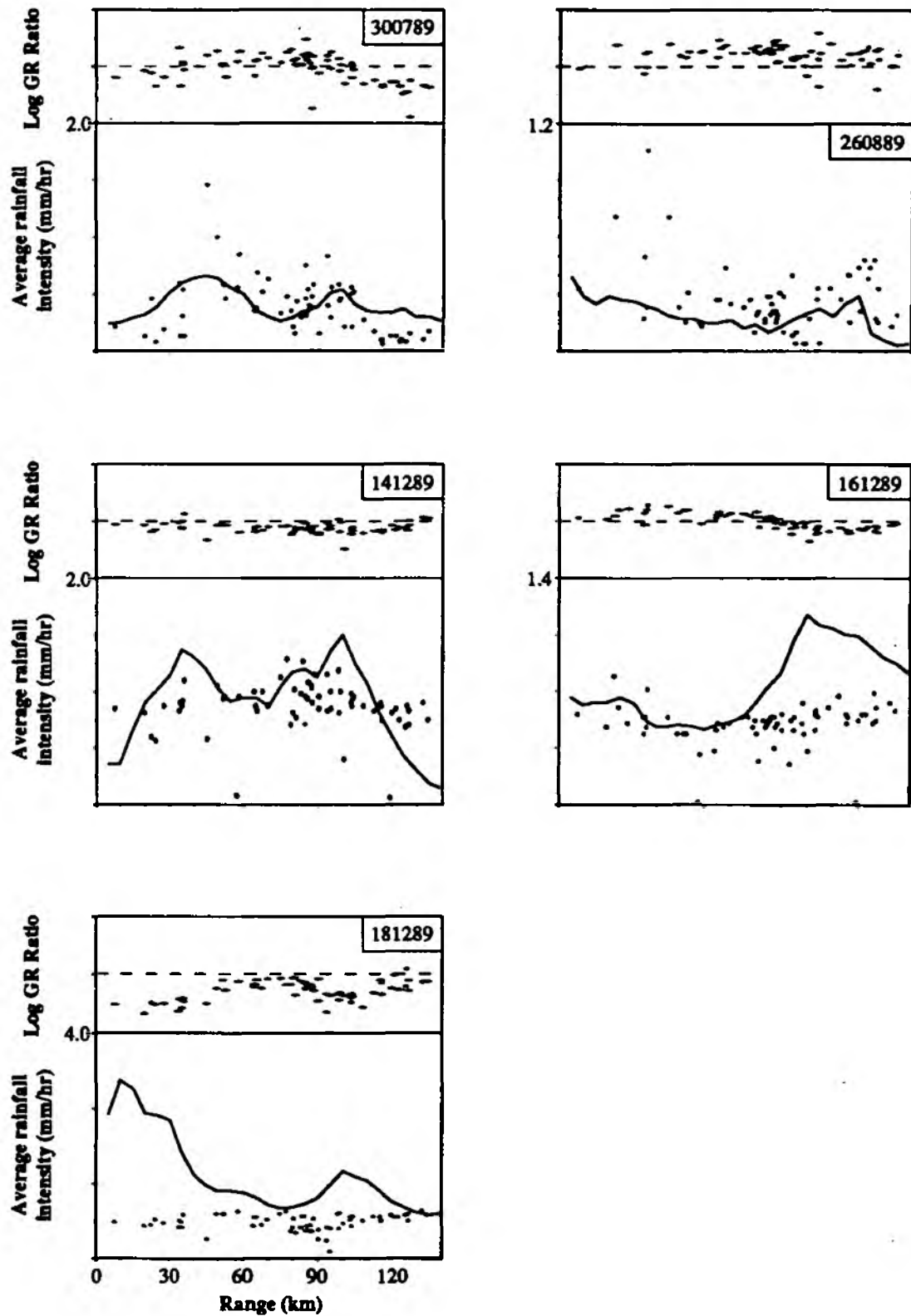
Figure 2.9(iv): Unadjusted radar and raingauge derived rainfall intensities, and RG ratios as a function of range for daily data

shown in figure 2.10. These are the same as those shown in figure 2.7(i) but break down the radar image into four 30° sectors centred on azimuths 0°, 90°, 180°, and 270° (north, south, east and west) from the radar site. Thus, only those radar grid cells falling within the sectors centred on the study directions are included in computation of the range averaged mean rainfall intensity for that particular azimuth. The figures indicate that the range effect is largely azimuth independent though near range overestimation seems less at azimuths in the range 315 - 360° (NW - N), and suggest some anomalous overestimation at azimuth 315° between 100 and 200 km range. It is concluded that azimuth dependency is not significant.

2.3.2. Development of a Range Correction Procedure

Two variants on a simple range correction procedure were investigated and derived from unadjusted 5 km, Ingham radar data. For reasons described later in this section, a 'bright-band free' data set were used in derivation of the correction procedure, from a total of 27 days of data. The procedure assumes that the range effect is due to problems in radar precipitation estimation and not real, (an assumption which is reasonable based upon the analysis conducted in section 2.3.1) and consequently discounts any naturally occurring spatial variations in rainfall over the area of radar coverage. For reasons discussed in section 2.3.1, the correction procedure does not incorporate an azimuth correction component.

An average rainfall intensity for the entire radar coverage area is computed for the 27 day period (0.27 mm/hr). From this and the average rainfall intensity observed within each range bound, a range correction factor for each range is computed where the range correction factor for the cell being range corrected is defined as the ratio of mean rainfall intensity for the entire area to the rainfall intensity for the uncorrected cell. A value greater than unity indicates underestimation of rainfall intensity by the radar and a value of less than unity indicates overestimation. Range correction is then made simply by multiplying each radar grid cell with the appropriate range correction factor. For convenience, 5 km range slicing is used and 42 range correction factors are derived.

The range correction factors obtained by this method are shown in figure 2.11. The factor exhibits near linearity until about 110 km range. Beyond this, and with increasing severity with range, the correction factor shows a non-linear behaviour, reflecting the increasing severity of rainfall underestimation at ranges exceeding this point. Rather than utilise these range correction factors, a modified form was derived, the derivation based upon fitting a straight line to the factors optimised over the range 0-150 km. Factors beyond 150 km were derived from extrapolation of the linear relationship. Reference to figure 2.11 illustrates that the range correction tends to reduce rainfall intensities within a range of 60 km and increases them beyond this range (the maximum decrease is 53 % [at ranges 0-5 km] and the maximum decrease is 150 % [at 205-210 km]). Furthermore, the correction factors derived via optimisation are conservative at ranges exceeding 150 km and under-correct beyond this point. However, they
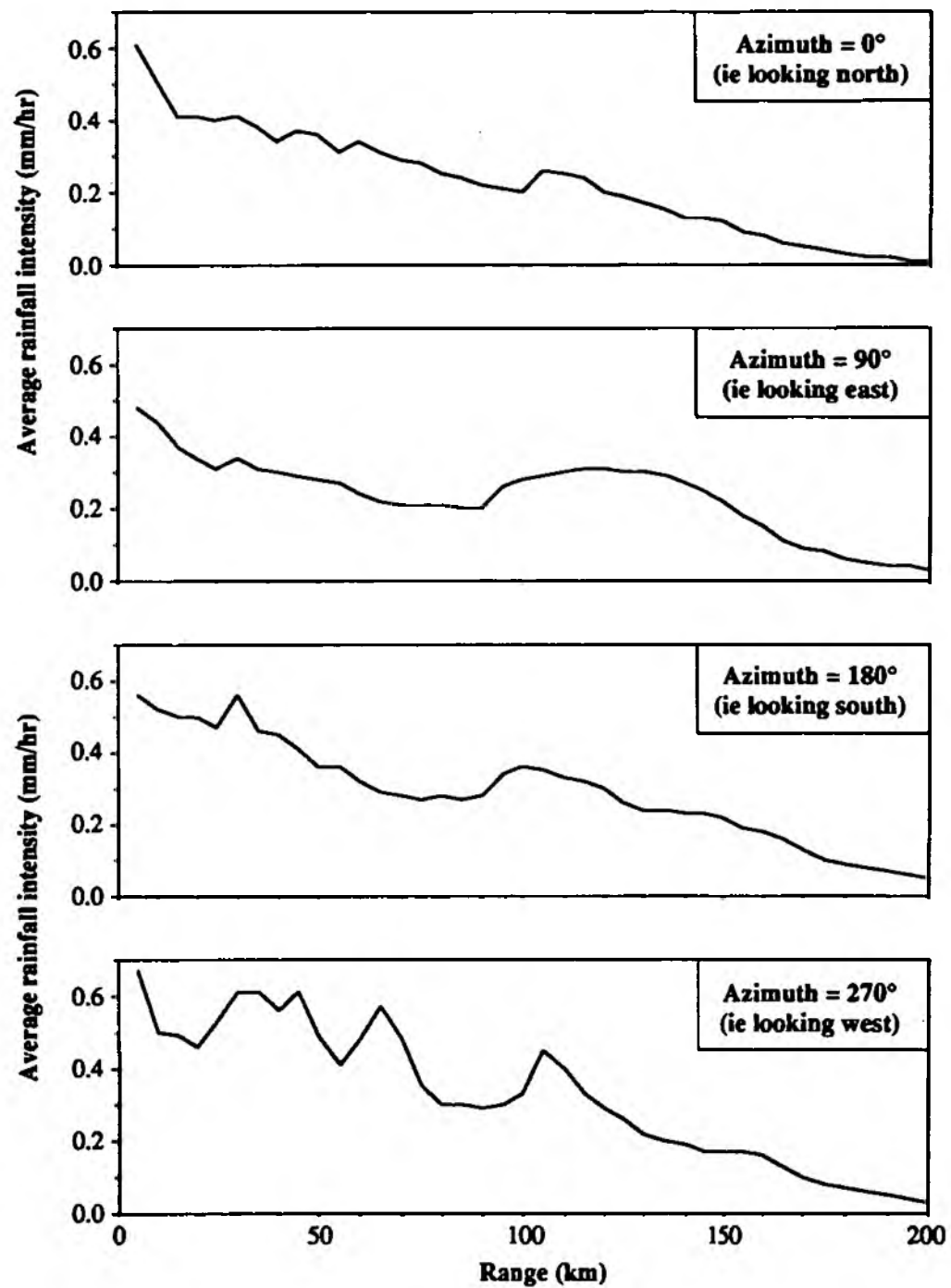
Figure 2.10: Anisotropy of range effect on radar rainfall estimation
(Ingham data, 27 days, 5 km grid, unadjusted)
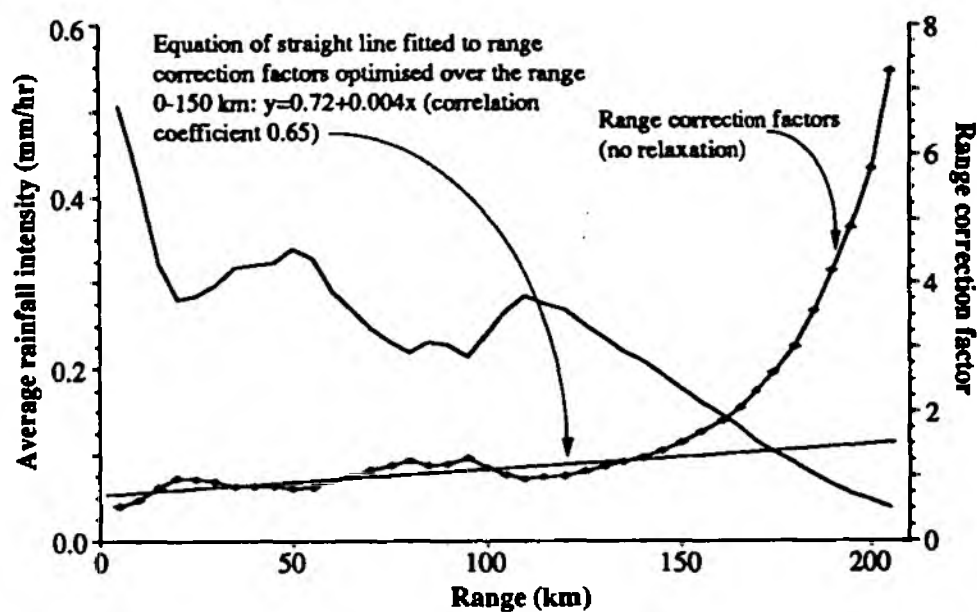
Figure 2.11: Average rainfall intensity and range correction
factors as a function of range (derived from 5 km Ingham
data, with bright-band affected frames omitted)

have the advantage of adjusting data beyond these ranges by an amount that is consistent with the estimation uncertainty of the data.

The range averaged range corrected rainfall intensity / range line graphs are shown in figure 2.12 for all three data sets, on the same scale as figure 2.7 for ease of comparison. The standard deviation of cells within each of the range groups is also plotted. The average rainfall intensity fields in figure 2.13 demonstrate the effect of range correction using range correction factors derived from straight-line optimisation, and can be compared directly with the corresponding (but uncorrected) fields in figure 2.5.

The range correction procedure corrects for a systematic error (inadequacy) in the at-site range correction procedure and consequently produces on average more realistic estimates of precipitation amounts particularly at very near and very long ranges. The procedure has been optimised over the range 0 - 150 km for rainfall where bright-band is not a major factor. It is recognised that the correction is conservative beyond 150 km, and the radar rainfall intensities may therefore continue to be underestimates beyond this range. The range correction is unable to correct for gross overestimation arising from bright-band occurring within 60 km from the radar, though it will partly correct for it. In addition, should a bright-band be present beyond 60 km the range correction will increase overestimation. Optimisation of an alternative set of range correction factors for bright-band periods is recommended but has not been developed at this stage since application would ultimately be dependent on reliable bright-band detection and height estimation in real-time.

2.4.   Anomalies in the Time Averaged Rainfall Field

The time averaged rainfall fields shown in figure 2.5 illustrate that the Ingham radar is remarkably free from anomalous echoes. This must largely be attributable to the quality of the radar site with regards an obstruction free horizon.

An anomalous 'spoke echo' is discernible in the time averaged rainfall fields for some of the daily data (see Appendix 3). The spoke which emanates from a point close to the radar site (within 50 km range) at a bearing of 170°, causes an anomalously high return echo from points along it, such that daily cumulations for affected cells can be in error by as much as a factor of five. Since the anomaly does not appear on data after March 1989, it is assumed that the at-site calibration procedure identified the problem and corrected for it early in the year. Consequently, it is not considered further.
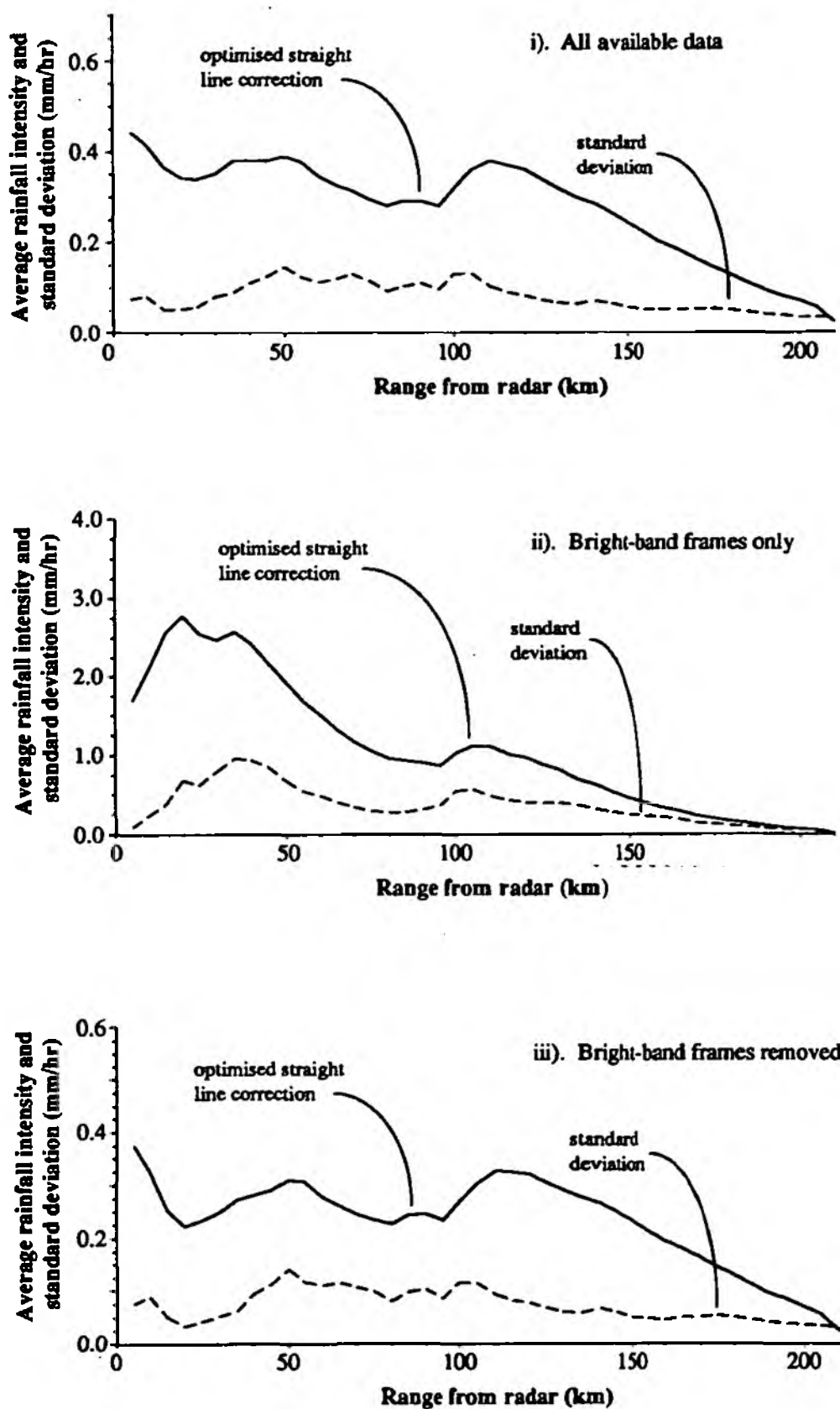
Figure 2.12: Average rainfall intensity as a function of range for the entire radar image after range correction. (Ingham radar, 5 km unadjusted data from a total of 27 days data)

i). All data
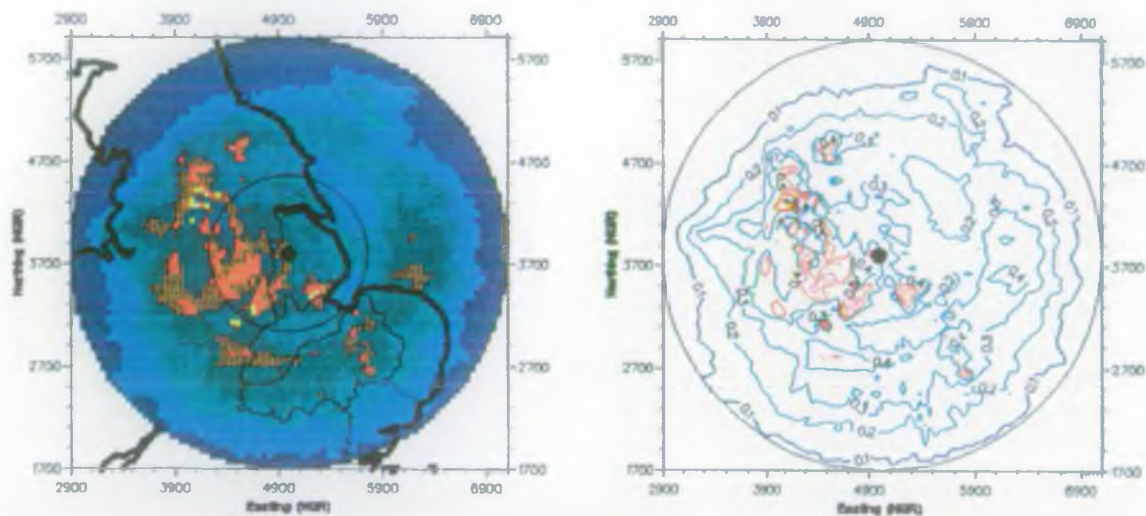
ii). Bright-band affected data only
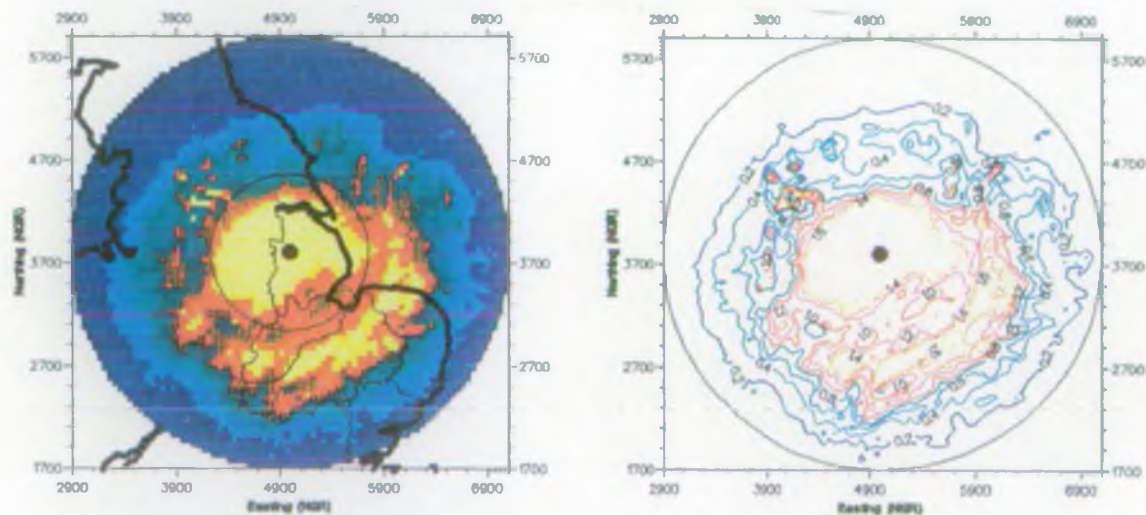
iii). Bright-band affected data removed
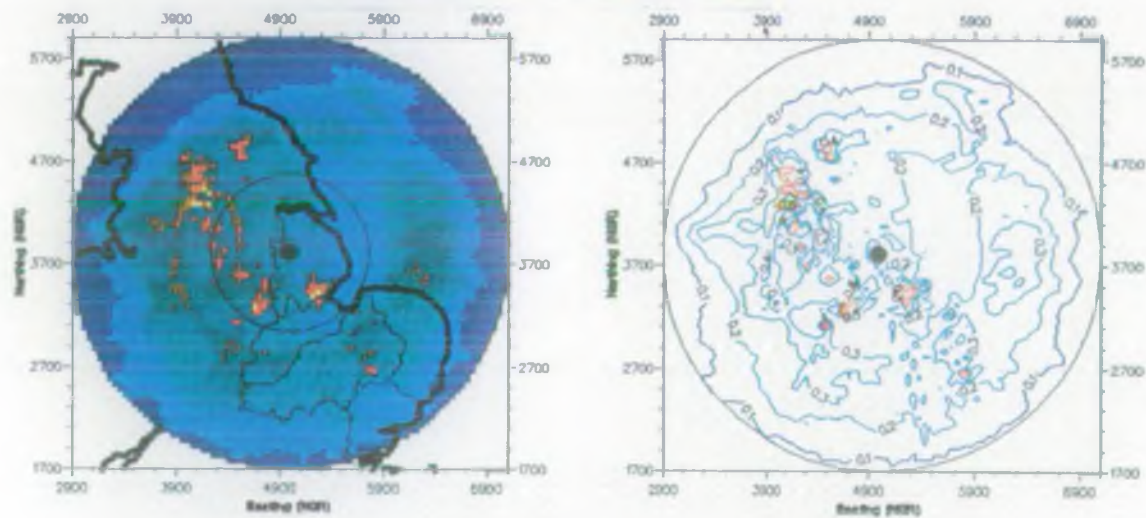
Figure 2.13: Average rainfall intensity fields after range correction
(Ingham radar 27 days, unadjusted 5 km data)

2.5 The Significance of Altitude on the Precipitation Process

Though the topography of the region is subdued, the role of orography in enhancing precipitation formation is recognised and in certain locations can be very significant (e.g. moisture laden air traversing the Pennines). A clear relationship between long-term average annual rainfall and topography in the northern area of Anglian Region exists and can be assessed by referring to figure 2.14 and figure 2.15. In order to determine the strength of the correlation between topography and rainfall over shorter durations (days to weeks) in the northern area, a raingauge-based study was conducted. Two analyses were conducted, the first examining the effect of topography over a long (23 day) period, and the second investigating the effect on a daily basis.

The study was based on the longest period for which raingauge (and for comparison) radar data were available. After excluding two days during which the rainfall over the region was insignificant and three days when raingauge data were not available, a period of 23 days was left. In order to avoid the introduction of storm bias into the analysis, only raingauges present for all 23 days or 22 days were included, and gauges absent for longer than 1 day excluded. Thus, although for any particular day as many as 68 raingauges may have been available, only 32 of these were available for all 23 days or 22 days.

The spatial rainfall pattern for the northern area for the 23 day period is shown in figure 2.16. The figure shows the average rainfall intensity for:

- the entire Ingham radar image (i.e. on an 84*84, 5 km grid, to a range of 210 km).
- a surface interpolated from northern area raingauge data.
- the radar image for the northern area (linearly interpolated for spatial smoothing).

The average rainfall intensities for each of the raingauges for the 23 day period is plotted against its altitude above mean sea level in figure 2.17, and details of stations used, their altitude and average recorded intensity are shown in table 2.2. The bivariate (Pearson's) product moment correlation coefficient computed for the data is 0.7, indicating a reasonably strong positive correlation (between raingauge altitude and rainfall intensity). A straight line fitted to the scattered data points using a least squares objective function provides a quick means of estimating rainfall for any elevation and any duration in the Anglian Region (assuming the assumptions underlying the regionalisation are valid). According to the relationship average rainfall intensity increases by 0.0325 mm/hr per 50 m altitude: for example a station at 100 m will record about 23 mm more rainfall than one located at 50 m over a 30 day period (and 280 mm more over a year). The relationship should not be extrapolated beyond about 150 m altitude and the data are actually fitted better by a second order polynomial.

The analysis was repeated for the daily data making up the 23 day period. The rainfall intensity and altitude data are plotted as scattergraphs for each day (figure 2.18), and the product moment

Key

- ■ Over 122m
- ▨ 61-122m
- ☐ Below 61m

⊙ Lincoln radar

N

0 km 25
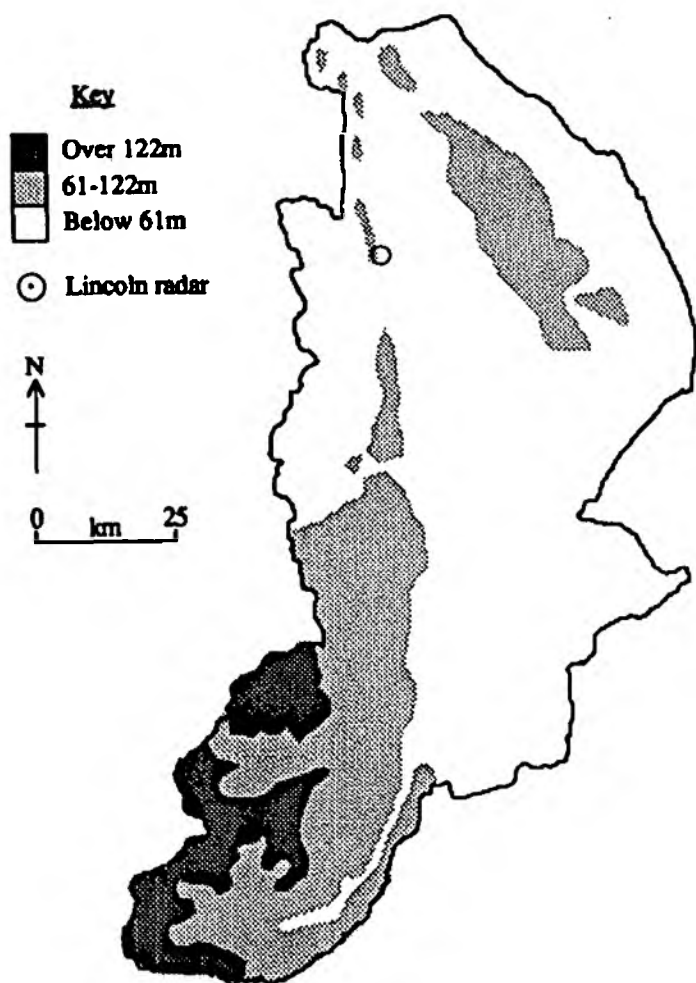
Figure 2.14: Northern Area topography (simplified)

Key

- Over 800mm/yr
- 700-800mm/yr
- 650-700mm/yr
- 600-650mm/yr
- 550-600mm/yr
- ⊙ Lincoln radar

N

0 km 25
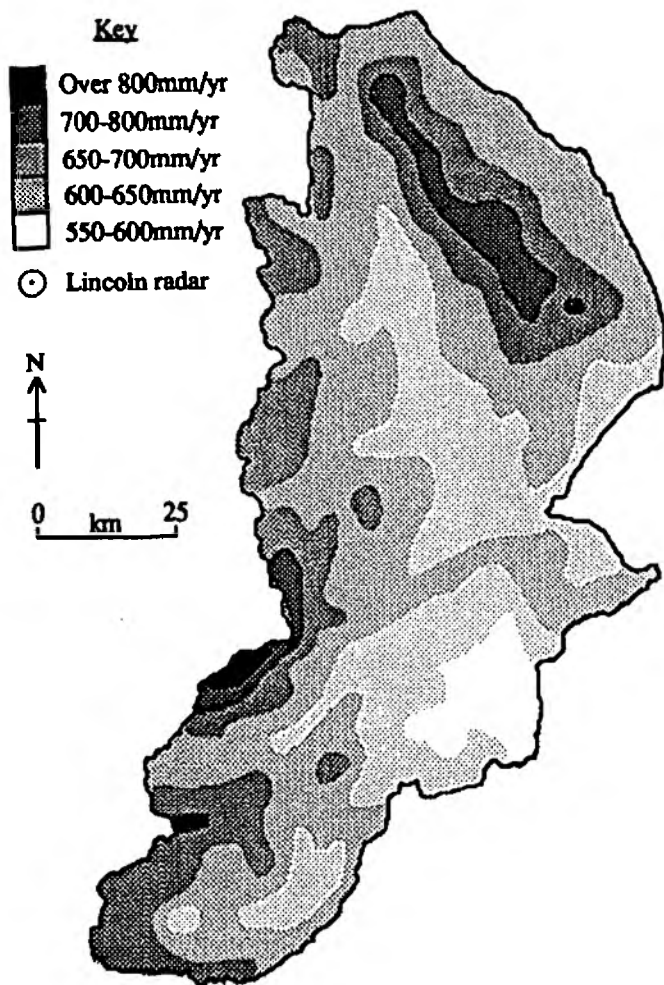
Figure 2.15: Northern Area average annual rainfall. 1941-1971 (adapted from NERC, 1975)

i). Complete radar

ii). Interpolated raingauge

iii). Regional radar

Above	0.800
0.700 -	0.800
0.600 -	0.700
0.500 -	0.600
0.400 -	0.500
0.300 -	0.400
0.200 -	0.300
0.100 -	0.200
Below	0.100
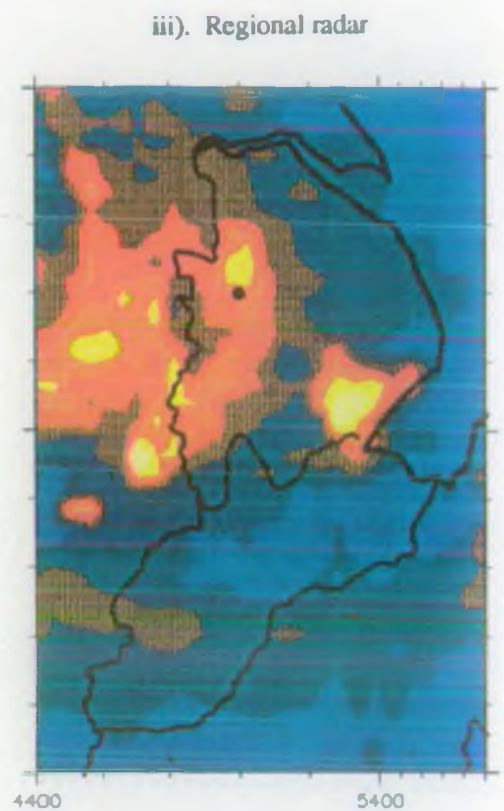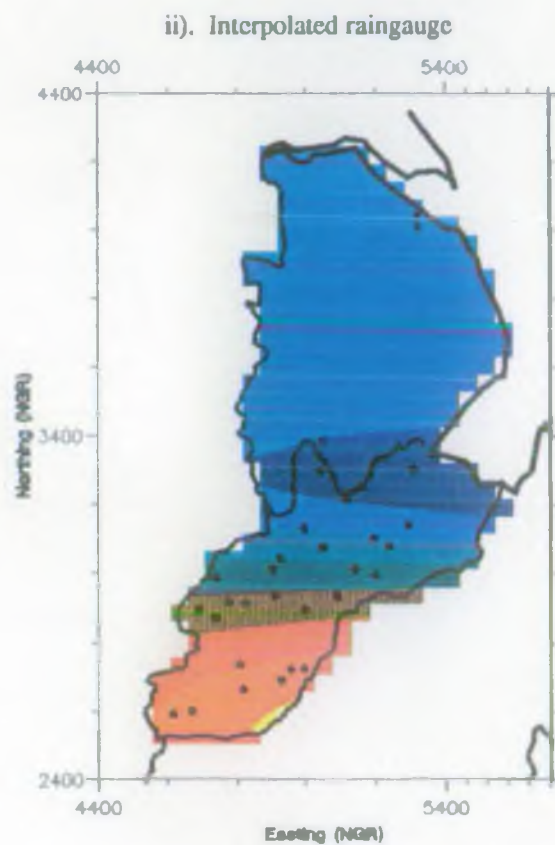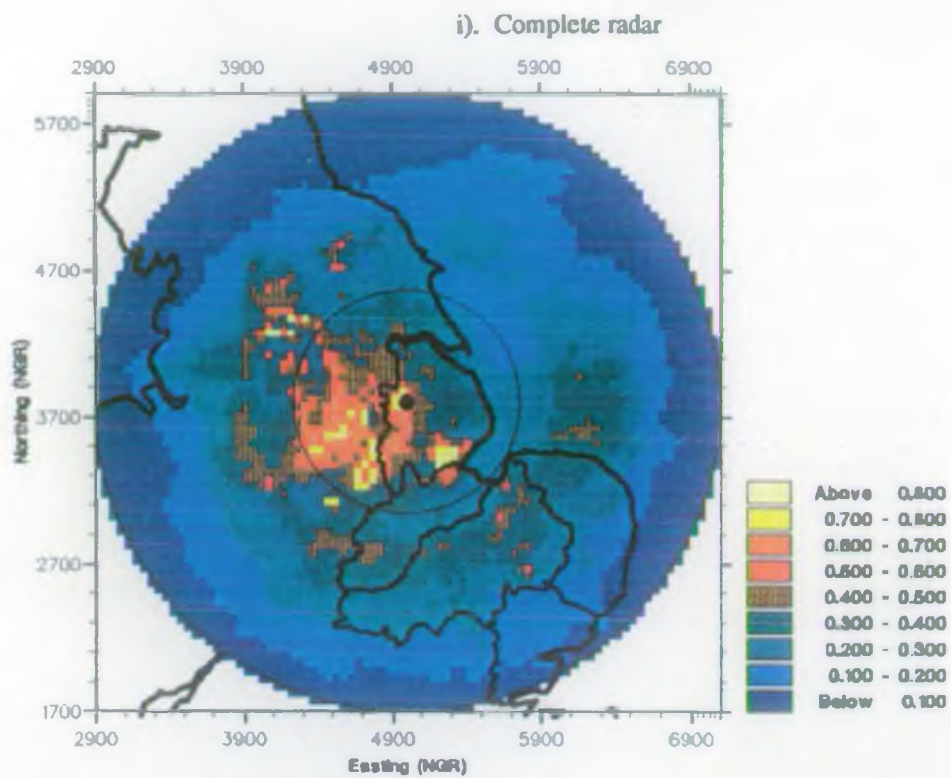
Figure 2.16: Radar and raingauge rainfall fields for altitude study data
(Ingham radar, unadjusted 5 km data)

Average rainfall intensity (mm/hr)

0.4

0.3

0.2

0.1

0.0

0   50   100   150   200

Station altitude (metres AMSL)

Least-squares straight-line:
$y = 0.27 + 0.00065x$ $R^2 = 0.49$

Pearson's PMC = 0.7
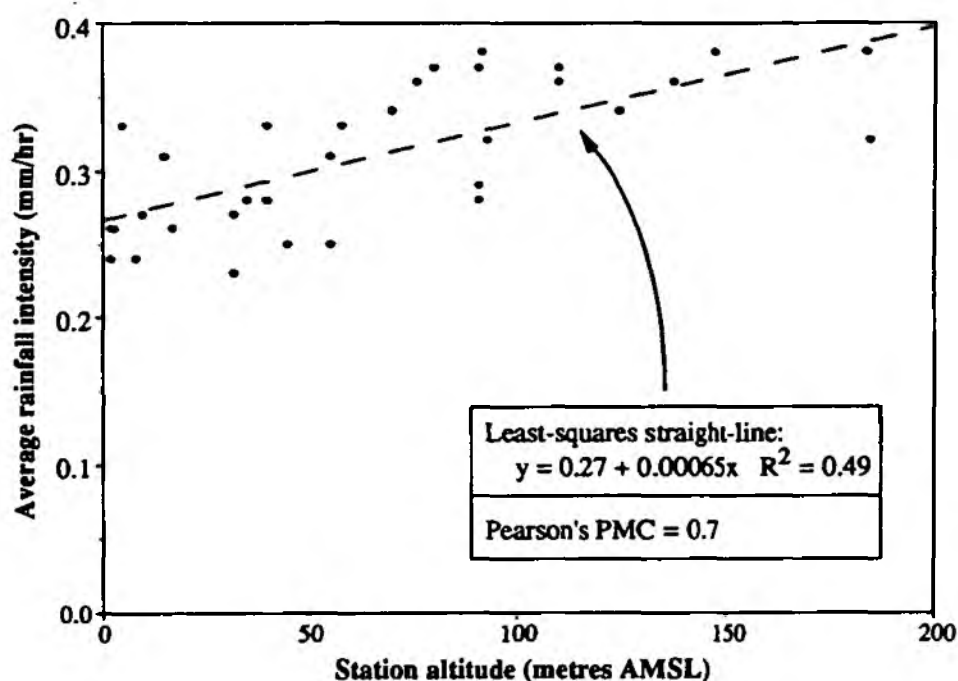
Figure 2.17: Average raingauge rainfall intensity over a 23 day period as a function of station altitude (only raingauges not absent for more than 1 day included)

Column 1: Raingauge reference
Column 2: Number of days data
Column 3: Station altitude (m)
Column 4: Average rainfall intensity (mm/hr)

U01	22	4	0.29	V03	23	55	0.31	V21	23	35	0.28
U04	23	76	0.36	V04	22	93	0.32	V22	22	32	0.27
U05	22	2	0.24	V05	22	125	0.34	V23	23	91	0.28
U06	23	2	0.26	V06	23	17	0.26	V24	23	185	0.32
U07	23	10	0.27	V08	22	148	0.38	V26	23	40	0.28
U11	23	15	0.31	V12	23	45	0.25	V27	23	184	0.38
U12	23	8	0.24	V13	22	55	0.25	V28	23	32	0.23
U17	22	70	0.34	V16	22	137	0.36	V29	23	91	0.29
U18	23	58	0.33	V18	22	92	0.38	V31	22	110	0.37
U19	22	5	0.33	V19	22	110	0.36	V32	23	40	0.33
U25	22	3	0.26	V20	22	80	0.37				

Table 2.2: Station breakdown of raingauge rainfall intensity/altitude data

Table 2.3: Raingauge rainfall intensity - raingauge altitude correlation

Date	Number of gauges	Mean gauge altitude (m)	Mean rainfall intensity (mm/hr)	Rainfall SD (mm/hr)	Pearson PMC [1]
191088	67	56	0.10	0.11	-0.1
091188	58	49	0.09	0.07	-0.3
291188	66	58	0.48	0.12	0.3
240289	52	62	0.25	0.15	0.8
250289	52	62	0.09	0.08	0.1
020389	44	64	0.22	0.06	0.3
140389	50	59	0.40	0.07	0.5
200389	51	58	0.19	0.03	-0.1
230389	50	59	0.02	0.02	0.3
040489	48	63	0.19	0.10	0.4
090489	50	61	0.05	0.03	0.6
240489	50	62	0.33	0.10	0.0
110589	49	62	0.22	0.06	0.1
260689	64	57	0.07	0.10	0.4
270689	68	57	0.35	0.20	0.0
300689	62	52	0.17	0.19	-0.2
070789	58	63	1.02	0.06	0.5
290789	64	58	0.21	0.23	-0.1
300789	68	58	0.36	0.26	0.0
260889	65	61	0.26	0.18	-0.1
141289	68	61	0.89	0.22	0.0
161289	68	61	0.50	0.13	0.0
181289	68	61	0.63	0.18	0.2
All days [2]	32	64	0.32	0.05	0.7

Notes:

[1] PMC is product moment correlation

[2] Only gauges not absent for more than 1 day out of 23 are included in the analysis
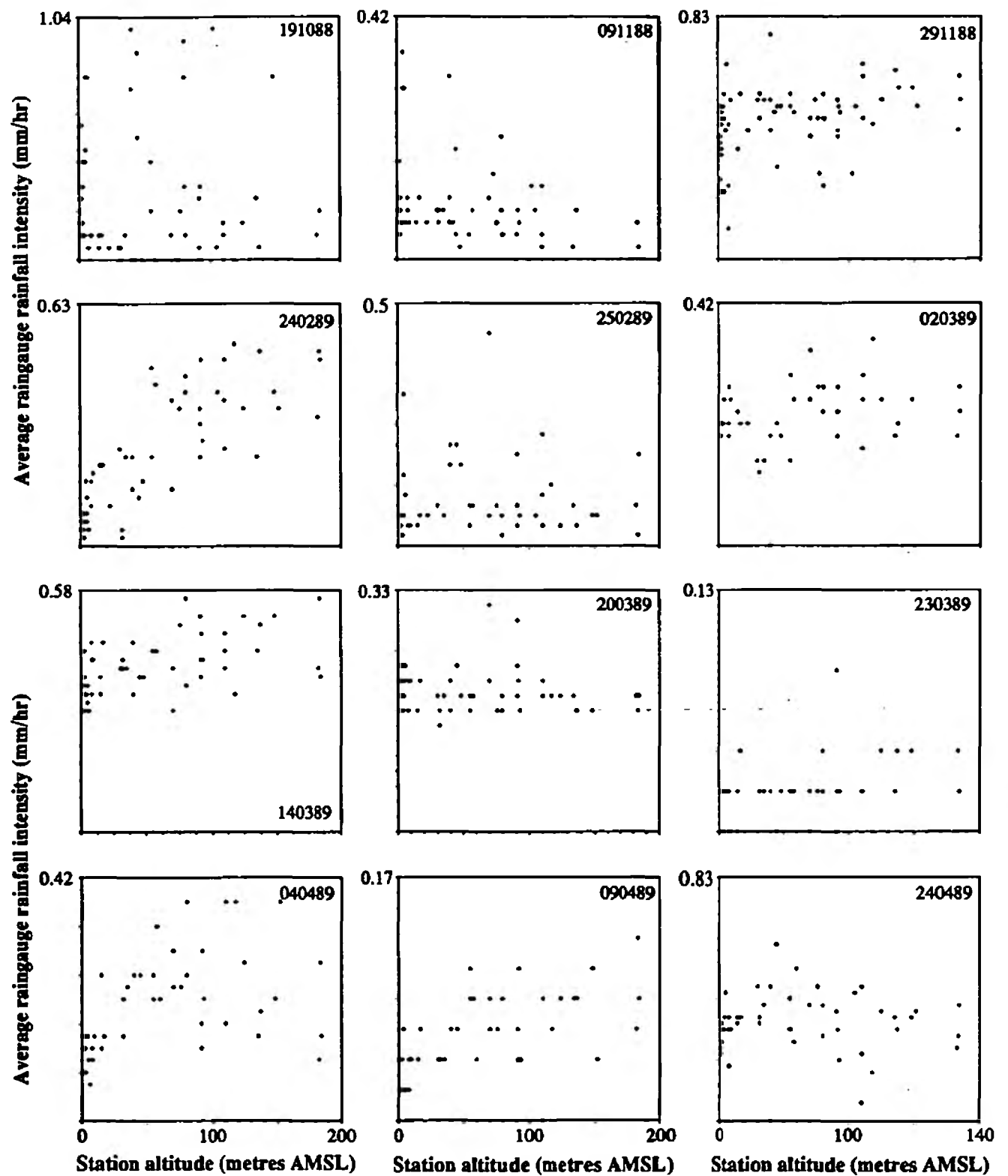
Figure 2.18(i): Daily raingauge rainfall intensity as a function of station altitude
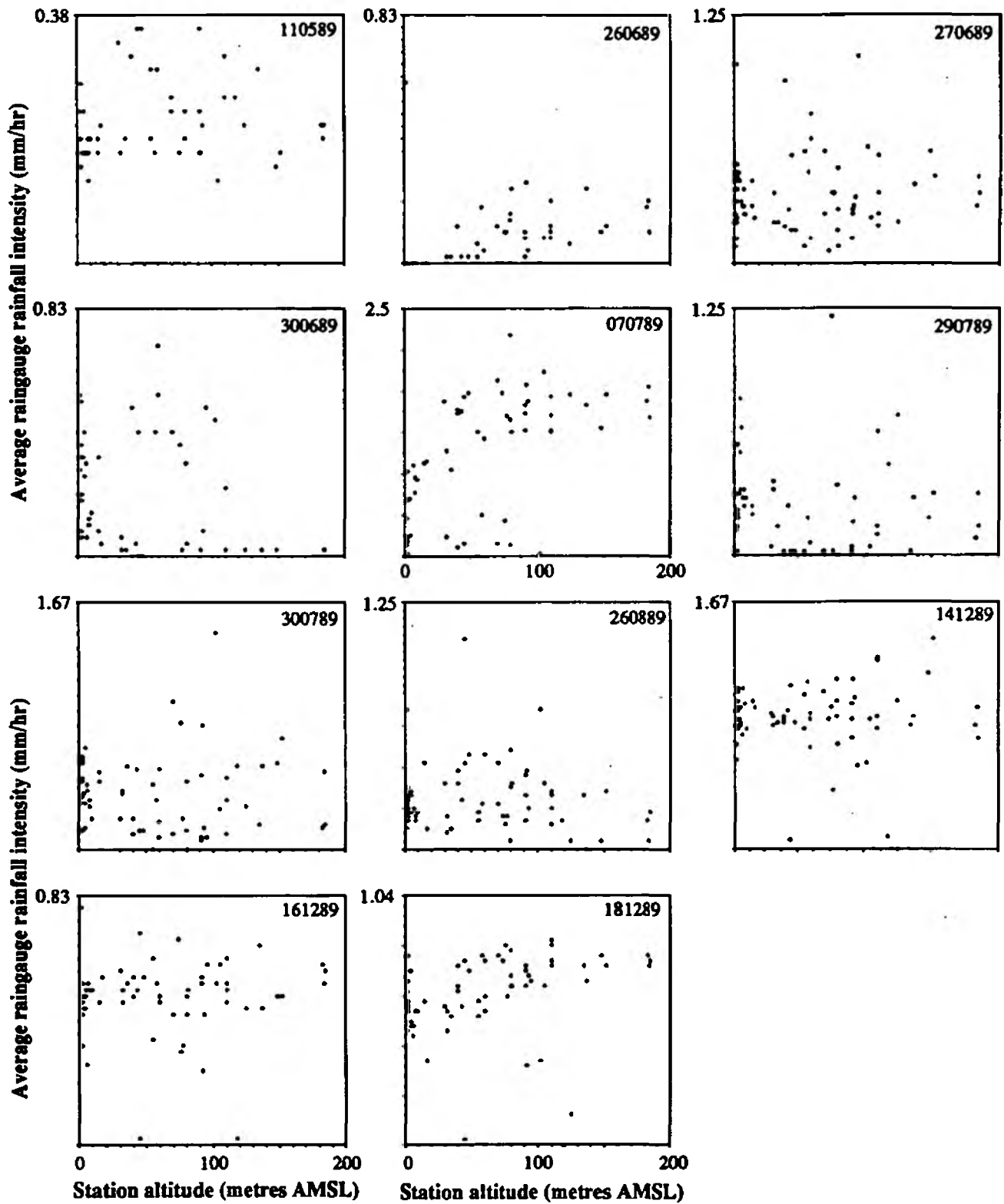
Figure 2.18(ii): Daily raingauge rainfall intensity as a function of station altitude

correlation computed for each (table 2.3). Also tabulated is the number of raingauges used for each day, their mean altitude, mean rainfall intensity and the standard deviation between all the gauges for each days data (which provides an indication of inter-gauge variability for each days data). The results show that the relationship between altitude and rainfall weakens as the duration decreases, so that some days show no significant positive correlation at all whilst some do continue to demonstrate such a correlation. It is noticeable that the strongest positive correlations occur during widespread frontal rainfall rather than the localised showers associated with convective cells.

The significant difference between the radar and raingauge rainfall fields in figure 2.16 is explained by the following factors:

- the radar data are unadjusted (no ground truth data has been used to improve the radar rainfall estimates).
- bright-band was present on a number of occasions during the period used for the analysis.
- part of the area used for the comparison is close to (surrounds) the radar, and is subject to significant overestimations in the rainfall intensity.
- the study area extends to 134 km range from the radar, the radar rainfall estimates suffering from those inaccuracies attributable to long range.
- sampling considerations, i.e. raingauges provide a point rainfall measurement, radar a volume sampled some distance above the ground.

It is therefore concluded that altitude correction of the radar data is not appropriate for short-time periods (i.e. less than a week), and consequently for real-time hydrological applications, although for longer time periods (egseveral months or more) an altitude correction may be more appropriate. The corollary of this is that the potential of unadjusted radar rainfall estimates in the study of orographic effects in the Region is severely limited, since the often subtle effects of orography are masked by errors arising from the radar rainfall estimation process.

2.6.   Bright-band

The theoretical aspects of bright-band were discussed in section ARIP 4 section 2.4.2. This section discusses the bright-band phenomena as it affects precipitation estimation by the Ingham radar in the Anglian Region. Throughout the analysis, information regarding the presence (or absence) of bright-band is taken from the header block of the single-site radar data, and therefore assumes that the real-time bright-band detection algorithm (described in ARIP 4 section 2.4.2) used at the radar site is reliable.

Of the 27 days data for the Ingham radar analysed, just over half were adjusted in real-time by the Meteorological Office. Of these, bright-band was present approximately 15% of the time (in the region of 2 days), with the occurrences being concentrated within four days in December

1989, a notable period of persistent rainfall within a large-scale frontal system. It should be noted that the Meteorological Office bright-band detection algorithm estimates the average height of the bright-band layer.

The effect of bright-band on radar precipitation estimates has been demonstrated in the preceding sections. In particular, the scattergraphs in figure 2.6 illustrate the often dramatic increases in estimated rainfall intensity (and hence depth) if the data are unadjusted, the overestimation being accentuated at close range (for reasons discussed in ARIP 4 section 2.4.2) especially within 60 km of the radar. Figures 2.6(ii) and 2.7(ii) in particular show increased scatter centred (approximately) at ranges 40 km and 110 km, confirmed by the standard deviation trace as localised maxima in variance. Two interpretations are possible: range repetition of bright-band, first being observed by the 1.1° elevation beam, and then (at the farther range) the 0.5° beam; or two bright-band heights being observed by the same beam. Reference to cumulated hyetographs for raingauges and overlying 5 km (and if within 70 km range, 2 km grid cell) for bright-band events (e.g. Appendix 12, figures A12.23 - A12.25) illustrate the dramatic effect at the onset of bright-band, the gradient of the hyetographs being considerably greater for the radar cells than for the raingauges.

The estimated height of the bright-band layer for days which bright-band was present for longer than three hours per day is shown in figure 2.19. The figures illustrate the dynamic temporal and spatial nature of the bright-band phenomena, the layer changing altitude quite rapidly. The enhancement coefficient trace (i.e. the ratio of echoes observed from a bright-band affected beam with an unaffected beam), illustrates the extent to which signal echo enhancement may occur due to bright-band.

A good example of bright-band is provided by Ingham radar data from the 14th December 1989, a day in which bright-band was present for many hours. Figure 2.20 shows unadjusted radar data over a 5 km grid cumulated over a one hour period from 10:00 to 11:00 GMT for four beam elevations (0.5°, 1.1°, 1.5° and 2.5°). The size of each image reflects the range to which each of the beam elevations operates (i.e 210 km, 210 km, 140 km and 105 km respectively). The example demonstrates two important characteristics of bright-band:

• increase in estimated rainfall intensity especially close to the radar.
• classic annular nature of the bright-band (for the higher beam elevations).

The form of the bright-band only becomes clearly apparent for the higher beam elevations and (except in the strongest cases) when the data are cumulated over time. Consequently, the presence of bright-band can be difficult to ascertain, even subjectively, in real-time.

Overestimation due to bright-band will be implicitly ameliorated by the range correction procedure when it occurs within 60 km (i.e. where the range correction procedure lowers the estimated rainfall intensity). However, since range correction is optimised for conditions when
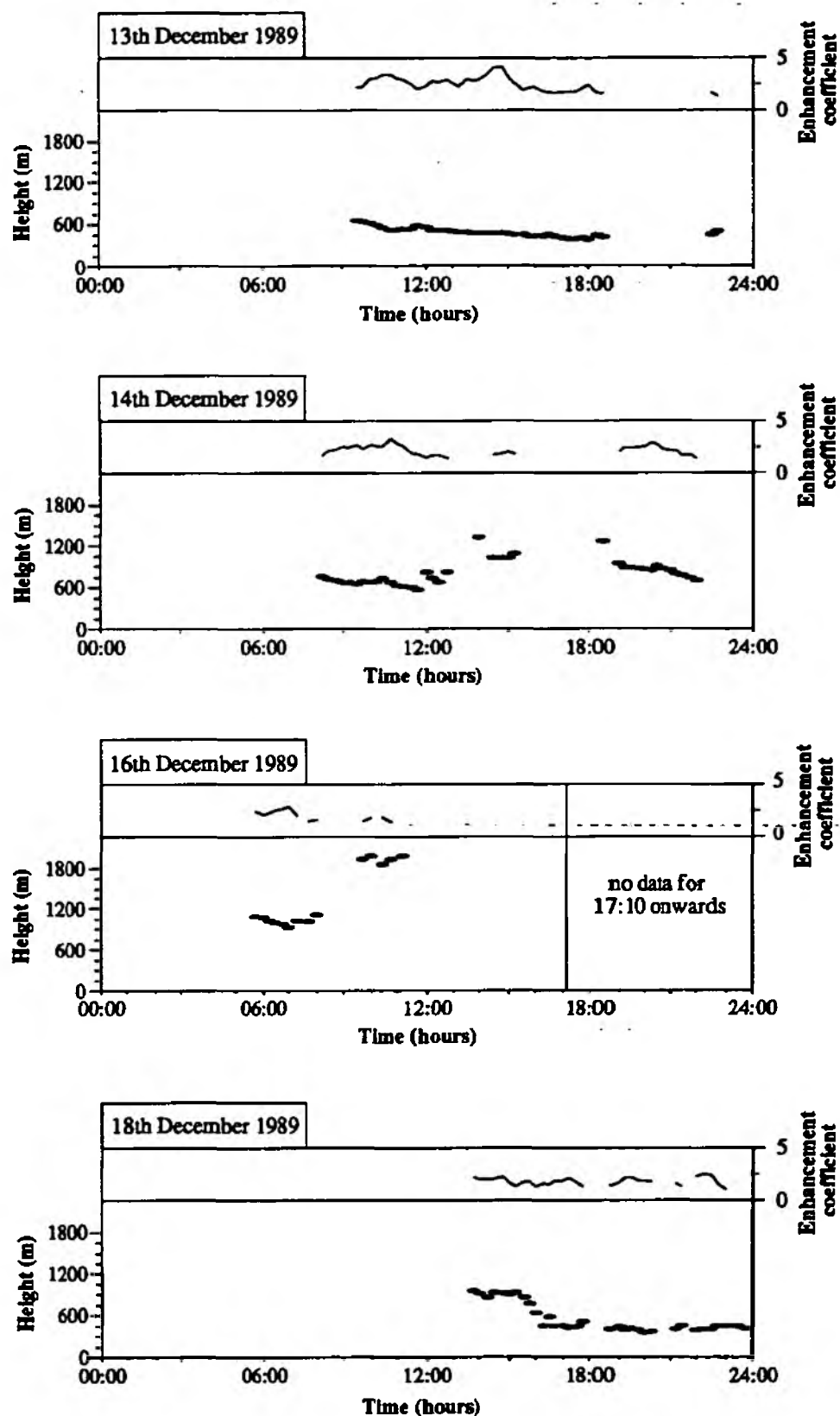
Figure 2.19: Bright band layer height and reflectivity enhancement for days on which a bright band was identified as for at least three hours (Ingham data)

i). surface beam

ii). 1.1° beam

iii). 1.5° beam

iv). 2.5° beam
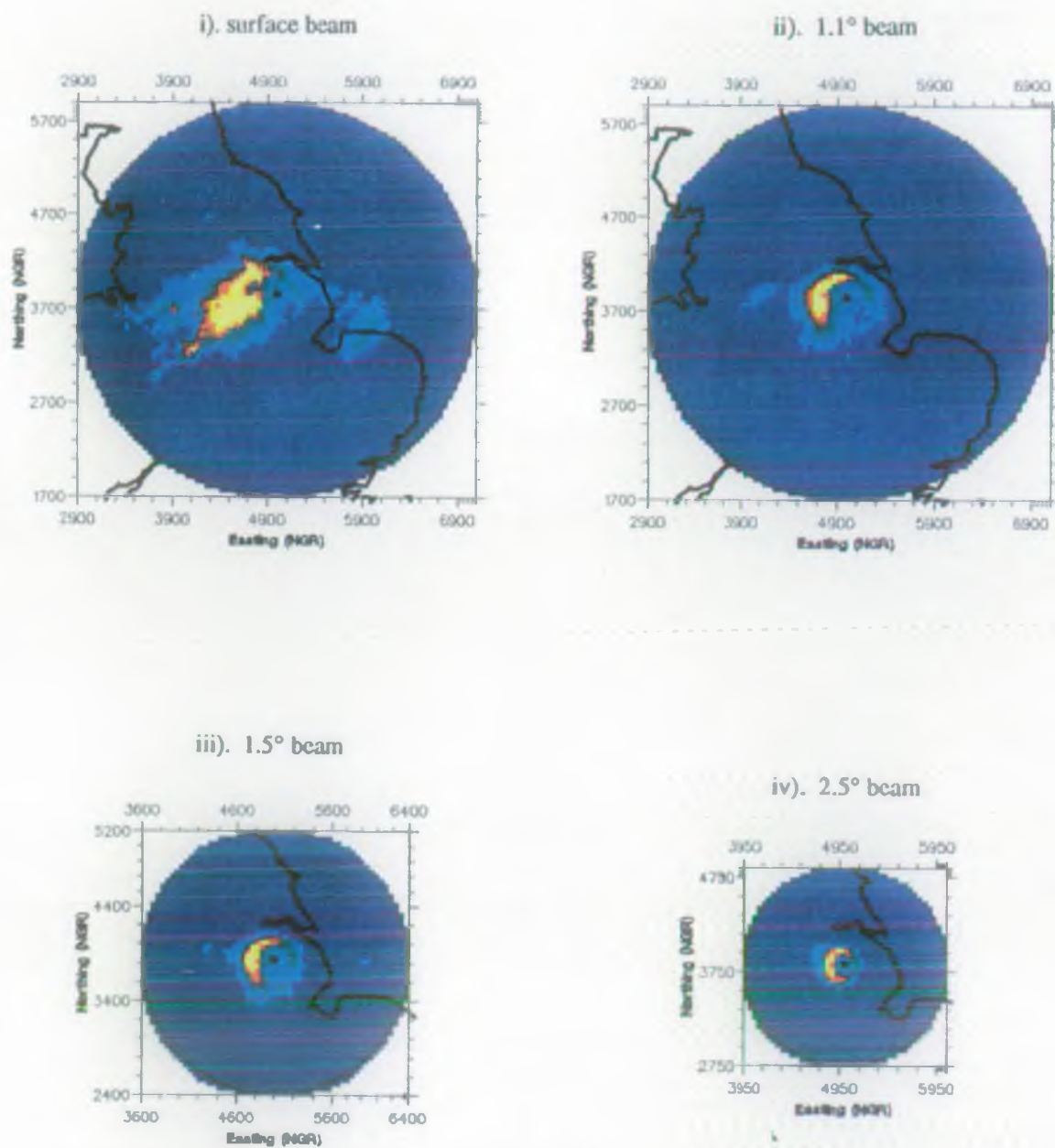
Figure 2.20: Example of bright-band; 10:00-11:00 GMT, 14th December 1989
(Ingham radar, unadjusted 5 km data)

bright-band is not present, corrections applied during the presence of bright-band will inevitably be conservative, and the overall effect limited. It should be noted that the range correction procedure is not recommended for real-time operation and any correction in real-time will be restricted to that arising from the real-time raingauge-based adjustment procedure described in Chapter 4 although satisfactory correction will only occur if the raingauges are collocated with a grid-square experiencing bright-band (something which is impossible to guarantee due to the dynamic nature of bright-band). Further comments together with a correction case studies for bright-band affected data are made in Chapter 5.

The dynamic nature of bright-band has largely defeated attempts by workers around the world to develop reliable correction algorithms which can operate in real-time. The hit-and-miss nature of point raingauge measurements precludes the use of all but the densest (and hence uneconomic) raingauge networks for adjustment, and whilst the dual-beam algorithm discussed in ARIP 4 section 2.4.2 enables reliable identification, the potential for reliable correction remains largely unfulfilled.

The key to unlocking the problems posed by bright-band rest with detailed physical knowledge of the vertical reflectivity profile of the atmosphere. Until recently attempts to acquire this knowledge have been rather limited, largely because they have utilised data from existing scanning radars operating in a RHI mode or from information built up from a small number of different beam elevations operated as part of a PPI scanning strategy, such devices having inadequate vertical resolution. Far fewer studies have utilised radar devices dedicated to vertical observations (i.e. non scanning). A joint research and development project between the Water Resources Research Group at Salford and the Radar Research Laboratory in McGill University, Montreal (Canada) is using a small vertically pointing, X-band radar to directly observe the vertical reflectivity profile in high spatial (7.5 m) and temporal resolution (2 s). Preliminary results have already demonstrated the immense potential of such a device, and will enable significant progress on real-time bright-band correction algorithms.

2.7. Conclusion

This chapter has presented the results of a detailed analysis of the performance of the Ingham radar over the northern area of the Anglian Region. The analysis has illustrated the consequences of beam infilling close to the radar site, the effect of range from the radar site, and the problems due to bright-band. Each of these are intrinsically interlinked by the over-riding factor - beam height. Thus, whilst beam infilling helps overcome problems due to ground clutter problems at close range, significant overestimation of rainfall within the beam infill zone is introduced. This is almost certainly due to the exacerbation of the bright-band problem, the higher beam elevation intersecting the bright-band (if present) closer to the radar site, the lower beam elevation only intersecting the layer at longer ranges where the effect is less severe. The analyses have illustrated the problem of underestimation of rainfall intensities at long range,

underestimation which is particularly severe at ranges beyond 150 km. A simple range correction algorithm for single site radar data has been developed for off-line use with historical data. The correction procedure has been optimised for ranges 0 - 150 km and beyond this only provides partial (conservative) correction consistent with the reduced rainfall information content of the radar signal at these ranges. The best correction of underestimation of rainfall intensity occurs in the range 70 km - 150 km. The correction factors also help compensate for the close range overestimation, though since the routine is optimised for non-bright-band events will only provide partial (conservative) correction of over-estimation due to the presence of bright-band.

The range correction procedure described is regarded as a correction for a systematic error in the radar data applicable to long-term data accumulations (i.e. greater than several weeks). For shorter durations, some implicit range correction will be made by the real-time raingauge-based adjustment procedure described in the chapter 4.

An analysis of the effect of altitude on the rainfall process within the northern area of the Anglian Region revealed a positive correlation between raingauge altitude and average recorded rainfall intensity (i.e. correlation strengthening with increasing duration) for the (relatively short period of) available data. The correlation between raingauge altitude and rainfall quantity being duration dependent, the relationship being weak for periods of the order days to weeks and even for a period of almost one month altitude still has only a small influence. Furthermore, uncertainty and errors in the radar rainfall estimates swamp any altitude effect which may be implicit within the radar data and it is not feasible to quantitatively examine short-term topographical influences on the rainfall process using radar data. In terms of real-time utilisation of radar data, for operational water resource management, the altitude affect in the northern area, and almost certainly the rest of the Region can be regarded as insignificant.

Time averaged radar rainfall images for the Ingham radar for periods up to one month indicate a marked absence of anomalous echoes. This is attributed primarily to the site of the radar and the relatively clutter free sight horizon.

Chapter 3. An Introduction to Raingauge-based Radar Adjustment

Water resource management usually requires estimates of areal rainfall rather than point rainfall estimates. In particular, an accurate assessment of areal rainfall is a necessary basic input to rainfall-runoff models (perhaps the most substantial user of real-time rainfall data), especially conceptual models which utilise a water balance approach. Catchment rainfall derived from a (usually relatively sparse) real-time raingauge network can only be regarded as an index of true areal rainfall, and this tends to restrict the ability to model the rainfall-runoff process accurately. Even at a point, where the gauge is ideally sited, raingauges do not measure true point rainfall, primarily because of wind influences.

Numerous methods of determining areal rainfall from point raingauge measurements have been proposed (e.g. see the review conducted by Hall and Barclay, 1975, and the objective comparisons of Creutin and Obled, 1982). Techniques vary greatly in terms of complexity, from the simplest deterministic methods, e.g. nearest neighbour method, arithmetic mean, Thiessen, subjective isohyetal, to the more sophisticated stochastic methods such as bicubic-spline surfaces, optimal interpolation, and kriging.

Increasing attention has focussed on the use of sophisticated and powerful interpolation and surface fitting algorithms as a means of improving the accuracy of radar-rainfall estimates. The rationale underlying this is that the point accuracy of raingauges can be used in conjunction with the high spatial resolution of the radar data to derive an adjusted rainfall field which portrays the actual rainfall field with higher accuracy than either of the rainfall fields in isolation. This chapter introduces the use of two dimensional interpolation and surface fitting for radar-raingauge adjustment, and an adjustment procedure suitable for implementation in an operational environment in Anglian Region is described in detail. A number of case studies are presented.

3.1. Introduction to Radar Rainfall Adjustment Using Raingauge Data

The raingauge-based radar rainfall adjustment procedure is conceptually quite simple and can be considered as a three phase process, the phases being summarised as:

- computation of assessment factors (see section 3.2) at each of the raingauge locations.
- two dimensional surface fitting of the scattered assessment factors. This results in a regularly distributed assessment factor field on a grid coincident with the cartesian grid used by the radar (5 km grid).
- node by node multiplication of the unadjusted radar data by the 'mapped' assessment factors to produce an adjusted rainfall field.

Each phase in the process is shown below in figure 3.1.
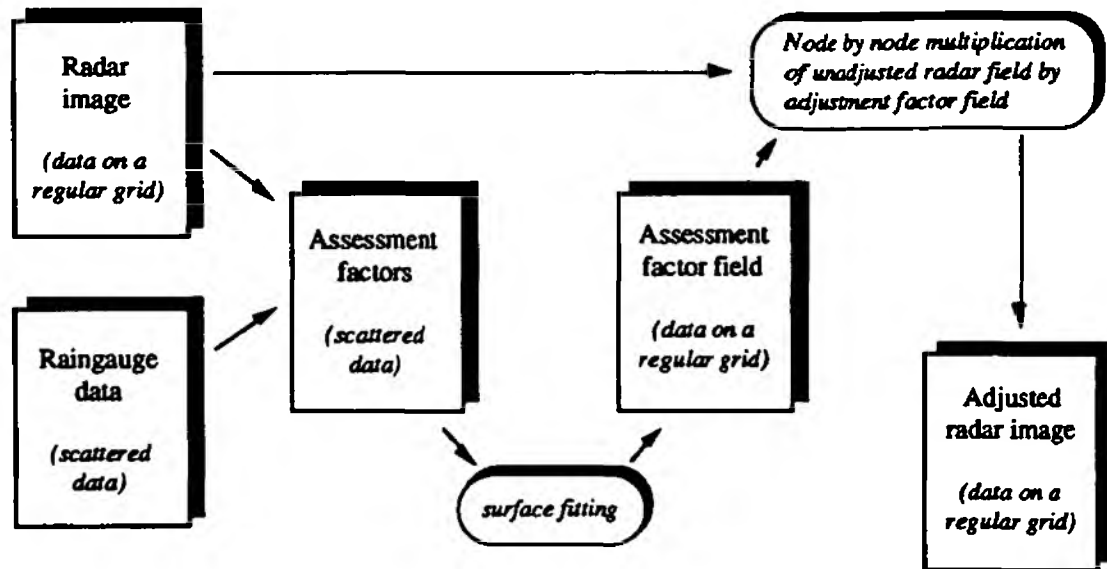
Figure 3.1: <u>Schematic representation of radar rainfall data adjustment incorporating two-dimensional surface fitting of assessment factors</u>

No attempt is made to relate or modify the assessment factors by physically related factors e.g. synoptic type, altitude, distance from sea, or prevailing wind direction / strength, although it would be possible to incorporate explanatory variables into the surface fitting algorithm. Consequently the technique differs from the raingauge-based adjustment approach used by the Meteorological Office which uses a system of physiographically defined adjustment domains and storm type identification algorithms.

3.2. Assessment Factors

Assessment factors are derived at each of the raingauge locations. The most basic form of the assessment factor is the simple ratio of radar rainfall value to raingauge rainfall value shown below:

$$AF = \frac{G}{R}$$

(eq. 3.1)

where AF = assessment factor, G is the raingauge rainfall value and R the radar rainfall value.

In order to overcome discontinuities in this form when $R=0$, an amended form shown in eq 3.2. is used. Selection of the constants ρ and λ is not straightforward and is important since the

constants have a direct influence on the value of the assessment factors. In the interests of generality this report assigns values of unity to both parameters (no parameter optimisation has been used to objectively select may lead to different values). It is worth noting that many other definitions of assessment factors can be derived (e.g. see Moore, *et al.*, 1989) though the benefits of alternative forms are difficult to assess. The representativeness of different forms of assessment factors remains unresolved and is still the subject of ongoing investigation. Incorporation of a different form of assessment factor in the radar data adjustment scheme would be straightforward.

It is recognised that the selection of the constants will influence the resultant value of the assessment factor and further work to assess the extent of these errors together with a detailed study into the representativeness of assessment factors (both the simple definition as well as the many modified forms proposed, [e.g. Moore *et al.*, 1990]) is required.

$$AF_i = \frac{G_i + \lambda}{R_i + \rho}$$

(eq. 3.2)

where there are n raingauges and λ and ρ both equal 1.0.

It should be noted that tipping bucket raingauges inherently have a quantisation error, the magnitude of which is a function of the bucket size. The two most common bucket capacities are 0.2 mm and 0.5 mm (equivalent rainfall depth), the maximum quantisation error associated with these being 0.8 mm/hr and 2.0 mm/hr respectively. No form of quantisation correction component has been included in the assessment factor definition.

Although the assessment factors can be formed over any time (limited only by the temporal resolution of the rainfall data), preliminary studies indicate that a cumulation period of one hour produces reasonable results and cumulation over this duration reduces the number of occasions where there is no or minimal rainfall (thereby reducing error in the assessment factor).

3.3. Two-Dimensional Interpolation and Surface Fitting

A number of two dimensional interpolation and surface fitting algorithms have been investigated. Of these, two interpolation and one surface fitting algorithm are favoured. All the algorithms work with irregularly distributed data (although many solutions to related problems in two-dimensional interpolation have been in long use, interpolation functions making an exact fit for irregularly spaced data are rare [when the data points are on a regular grid, many solutions are possible]). The interpolation algorithm is not explicitly used for radar adjustment but to derive a representation of the spatial rainfall field from the point raingauge data facilitating a visual comparison of the radar and raingauge rainfall fields. The surface fitting routine is used to map the irregularly distributed assessment factors to a regular grid coincident with the

cartesian grid of the radar data. All algorithms are more fully described in Appendices 9 and 10.

The fundamental problem that any interpolation or surface fitting procedure for data scattered in the plane (such as raingauge rainfall data) addresses is the following (after Renka and Cline, 1984):

'...given a set of nodes (abscissae) (x_i, y_i) arbitrarily distributed in the x-y plane, with corresponding ordinates z_i, $i=1,2,....,M$, construct a bivariate function $F(x,y)$ which interpolates/fits a surface to, the data values, ie, $F(x_i, y_i)=z_i$, $i=1,2,....,M...$'.

The problem arises in a wide variety of scientific fields in which the data represents observed or computed values of some physical phenomenon such as temperature, elevation, stress obtained by finite element methods, or as in this case, rainfall amounts. Information usually derives from points whose locations are determined logistically rather than as a result of network optimisation considerations, so that in practice most existing operational raingauge networks can be considered as randomly distributed as regards the observed rainfall process.

Regardless of the algorithm used, a satisfactory fit cannot be expected if the number and arrangement of the data points do not adequately represent the character of the underlying relationship. Ideally data points should extend over the whole domain of interest of the independent variable and extrapolation outside the data ranges is most unwise. It is advantageous to have additional points near the boundaries of the estimation domain, and also in special high priority areas (e.g. major towns liable to flooding such as Lincoln, Norwich etc).

It should not be forgotten that the rainfall process is highly dynamic and spatially variable, ("a mosaic-like phenomenon not always occurring and not everywhere existing" [Stol, 1986]), and the extent to which fitting a smooth surface i.e. a surface that is continuous and once differentiable, can ever provide an accurate estimation of rainfall at unsampled points needs to be questioned. Also, it is worth remembering that aesthetics are not necessarily synonymous with accuracy.

3.3.1. Two-dimensional Interpolation

A smooth interpolatory surface is often desired when a visual impression of the surface is required. The main requirements for an interpolation scheme are (Shepherd, 1968):

- the two dimensional interpolation function is to be 'smooth'.
- the interpolated surface must pass exactly through the specified data points.
- the interpolated surface should meet the user's intuitive expectations about the phenomenon under investigation.

Interpolation methods may be either local or global. In a global method the interpolant is dependent on all the data points regardless of their distance from the interpolation point, whereas in a local method, the interpolant does not depend on data points more than a certain distance from the interpolation point. Often a local method is used to avoid prohibitive computation time, although for rainfall, especially localised convective storms, a global method would not be appropriate.

By fitting data points exactly it is assumed that the data points are accurate measures of the process at that point: consequently the chance to reduce observation / measurement error is lost.

3.3.2. Two-dimensional Surface Fitting

The main constraint applied to interpolation schemes is that the interpolating function passes exactly through each of the data points. This ensures an exact rendition of the rainfall field at the sampled points, though can in the case of rainfall result in a contorted surface. This is because the rainfall process is spatially dynamic (i.e. may be highly localised) and discontinuous. If this constraint is relaxed such that the interpolation function need not fit the given values exactly, trend surface fitting (Krumbein, 1959) may be appropriate. An advantage of this approach is that distortion of the estimated rainfall arising from possible random error in the data (measurement / observation error) may be reduced. Many surface fitting procedures, including the one described, provide user control of the smoothness of fit / closeness of fit balance by way of a smoothness parameter. It should be noted that if the fit is too smooth the signal will be lost (underfit), and if too close the surface may pick up too much noise (overfit).

3.3.3. Interpolation and Surface Fitting in Practice

Two dimensional interpolation and surface fitting can be applied to three data types:

Radar data: Since the radar data are already on a regular grid, a surface fitting algorithm for regularly distributed data may be applied, the smoothness / fit of the surface being controlled by a smoothness parameter. Surface fitting can be used in this context to remove random error in the radar data and identify the overall trend of the spatial rainfall field. However in practice it is recommended that the radar data are unaltered. Figure 3.2 shows a bicubic spline surface fitted to radar data integrated over the period 1000-1100 GMT, 14th December 1989 for different smoothing factors. As the smoothing factor decreases in value, the surface fits the data more and more closely. Figure 3.2(i) represents a bicubic polynomial, the smoothest surface the algorithm can fit, whilst in figure 3.2(viii), the surface passes through the data points exactly (i.e. the surface has become an interpolating function).

i). $S = 1\,000\,000$ ii). $S = 17\,000$ iii). $S = 14\,000$

iv). $S = 11\,000$ v). $S = 8\,000$ vi). $S = 6\,000$

vii). $S = 4\,000$ viii). $S = 0$

	Above 35.00
	30.00 - 35.00
	25.00 - 30.00
	20.00 - 25.00
	15.00 - 20.00
	10.00 - 15.00
	5.00 - 10.00
	0.00 - 5.00
	Below 0.00
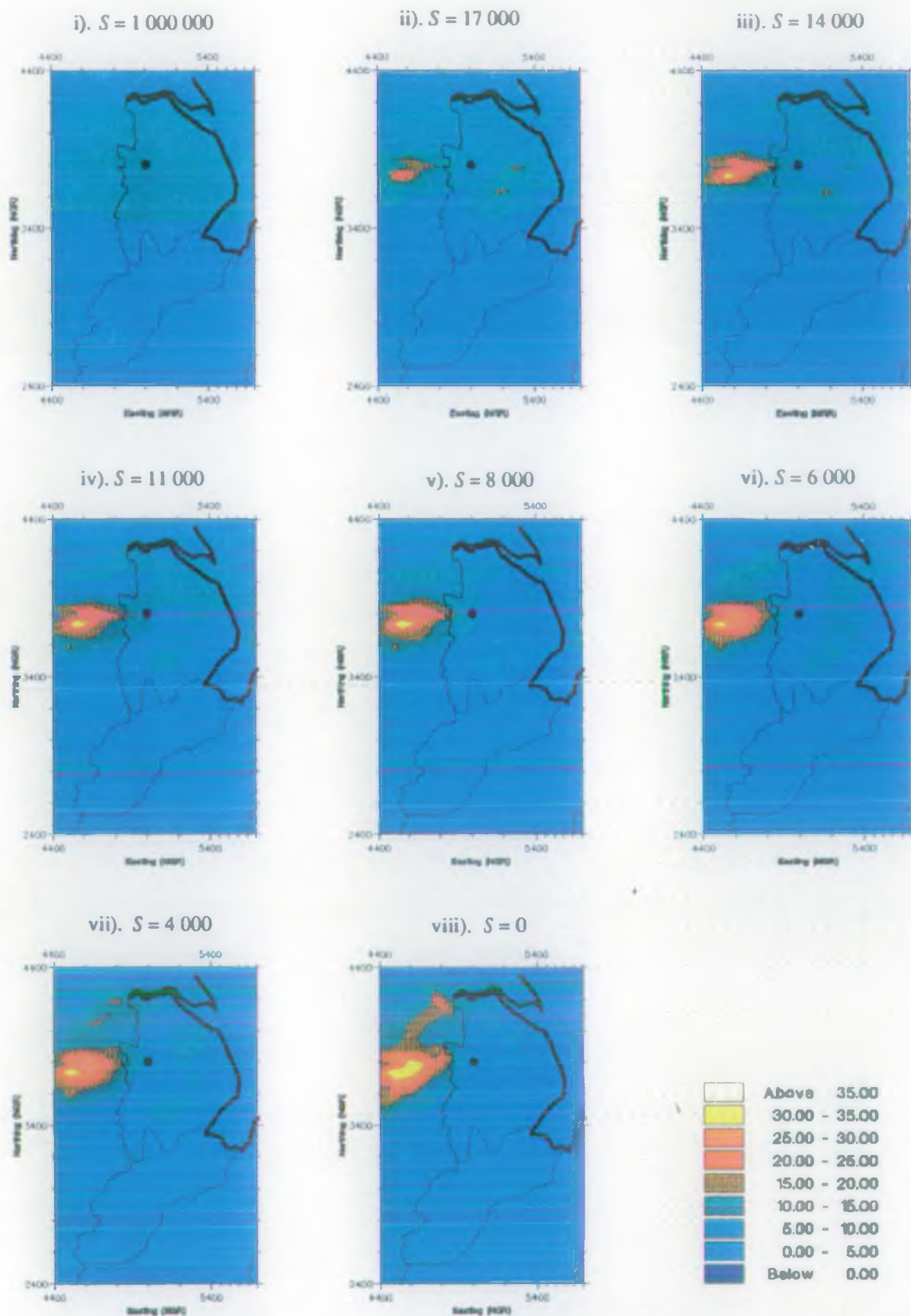
Figure 3.2: Bicubic spline surface fitted to radar data cumulated over the period 10:00-11:00 GMT, 14th December 1989 (Ingham radar, unadjusted 5 km data)

Raingauge data: Objective mapping of point rainfall raingauge measurements scattered in the plane onto a regular grid can provide a useful indication of the spatial distribution of the rainfall field in the event of radar failure. Two interpolation procedures have been tested (see Appendix 9) and preliminary studies indicate that there is no significant difference between the two algorithms in terms of areal rainfall computation. As with all interpolation procedures, caution should be exercised in the interpretation of such a field, particularly close to the interpolation domain boundaries, and in areas of poor raingauge coverage. Spatial rainfall fields derived from raingauge data have a larger high frequency component than assessment factor fields (see below), and display sharper peaks. Examples of interpolated raingauge fields can be found in chapter 4 (e.g. figures 4.3, 4.5, 4.8, and 4.11), as well as the Software Profile for QUANTARE.

Assessment factors: The assessment factor field tends to be a low frequency field and is consequently better suited to surface fitting or interpolation than the previous fields. An evaluatory analysis indicates that the bicubic spline surface fitting procedure (see Appendix 10) produces acceptable results and is preferred over an interpolation function. A logarithmic transformation of the assessment factors prior to surface fitting was investigated as a means of easing the problem of fitting a smooth field to the assessment factors but was found not to be necessary. In order to prevent unwanted fluctuations in the surface towards the boundaries of the fitting domain, a mask is applied around the fitting domain and all values within this region set to an adjustment factor corresponding to no adjustment (i.e AF=1.0) - fuller details may be found in the RADGAP Software Profile. Example surfaces fitted to the assessment factor field for a range of smoothing parameters are shown in figure 3.3 (10:00-11:00 GMT 14th Dec 1989) and figure 3.4 (mean assessment factor field for the period 00:00-23:45 GMT, 14th Dec 1989).

3.4. Adjustment of the Radar Rainfall Estimates

The instantaneous radar rainfall intensities for five minute periods are averaged at hourly intervals to produce mean rainfall depths for that hour at each grid cell. Likewise the raingauge rainfall depths are cumulated over the hour for each raingauge. At each raingauge location *(i)*, assessment factors *(AF)* are derived by applying equation 3.2 introduced in section 3.2 with values substituted in for ρ and λ (see below):

$$AF_i = \frac{G_i + 1}{R_i + 1}$$

where G_i is the raingauge rainfall depth for gauges $i=1,...,n$ and R_i is the 5 km radar estimated rainfall depth for the overlying radar grid cell. The constants ρ and γ (both set to unity) prevent discontinuities in the definition of the ratio when R_i is zero. It is recognised that the selection of the constants will influence the resultant value of the assessment factor and further work to assess the extent of these errors together with a detailed study into the representativeness of assessment factors is required.
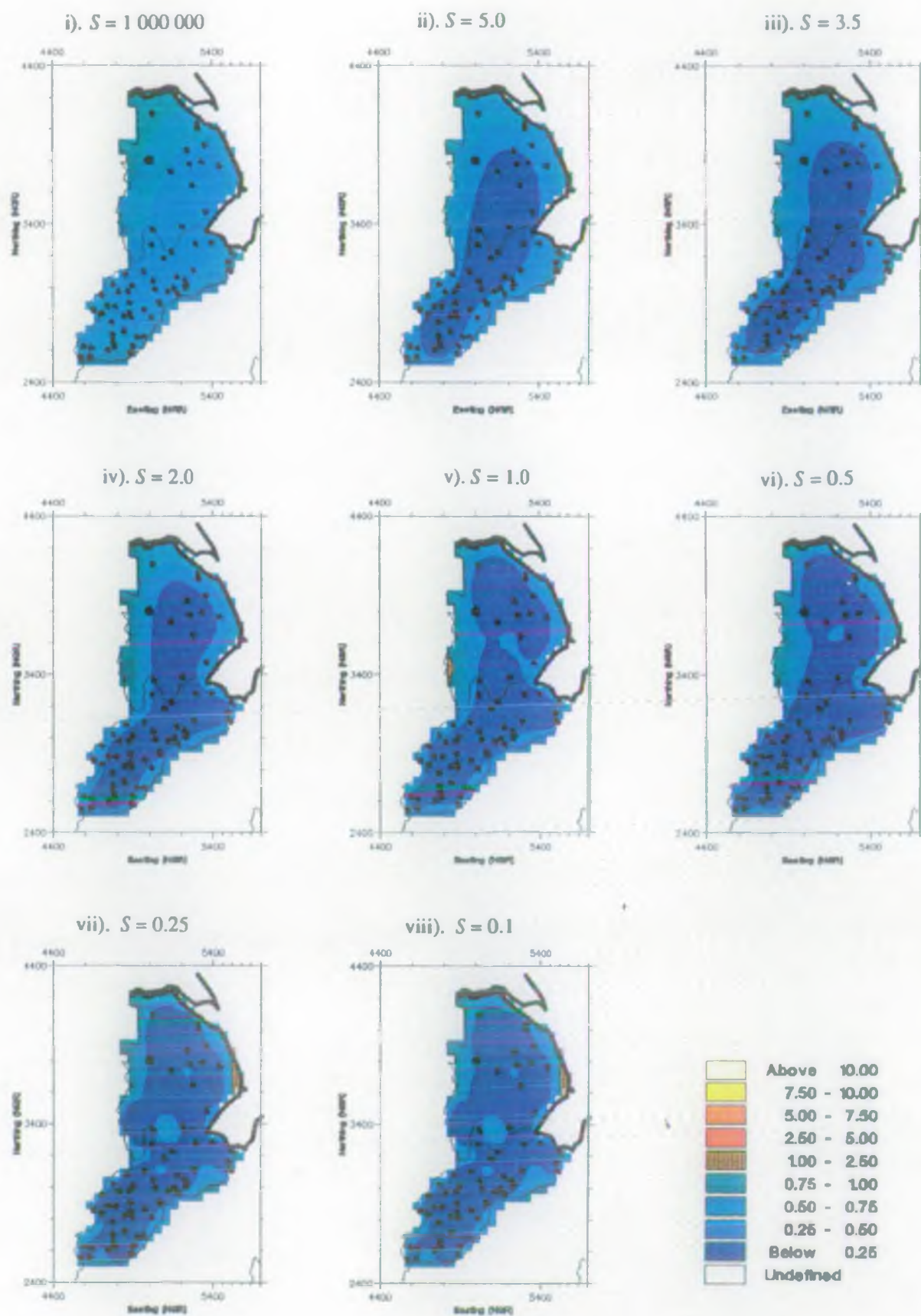
Figure 3.3: Bicubic spline surface fit to assessment factors: 14th December 1989 (Ingham radar, unadjusted 5 km data)
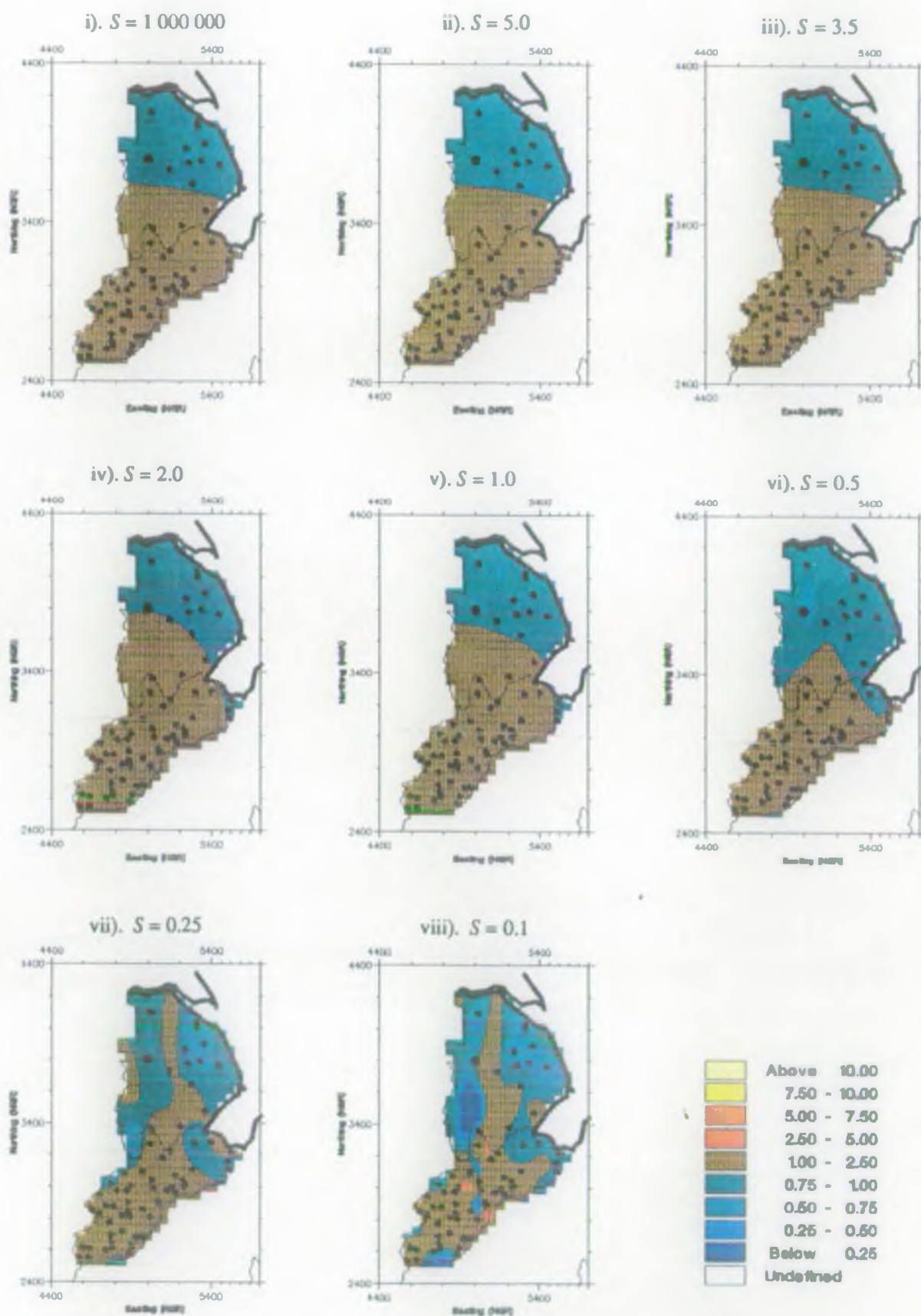
Figure 3.4: Bicubic spline surface fit to assessment factors: 10:00-11:00 GMT, 14th December 1989 (Ingham radar, unadjusted 5 km data)

Upper and lower bound constraints are applied to the assessment factors to prevent adjustment from being too radical or unstable in time. The constraining condition is shown in equation 3.3.

$$0.1 \leq AF_i \leq 10.0$$

<div align="right">(eq. 3.3)</div>

AF values greater than 1.0 indicate that the unadjusted radar values will be increased by adjustment (inferring overestimation by the radar), whilst values less than 1.0 indicate that the unadjusted radar values will be reduced by adjustment (inferring underestimation by the radar). A value of exactly 1.0 indicates no change.

Once the assessment factors have been defined for all raingauge locations a bicubic spline surface is fitted. The result is a regular assessment factor field with AF defined for points coincident with the 5 km cartesian radar grid. Adjustment of the hourly radar image is then achieved by multiplying each of the unadjusted radar rainfall values by the collocated assessment factor at each point (i,j) in the rectangular adjustment domain $(i_{min}, i_{min})*(i_{max}, j_{max})$, ie,

$$R_{adj}(ij) = R_{unadj}(ij) * AF(ij), \ i=1, np: j=1, nq$$

<div align="right">(eq. 3.4)</div>

where there are np points along the x-axis and nq points along the y-axis.

The form of assessment factor utilised (eq. 3.2. and eq. 3.3) implicitly assumes that at each raingauge location, the raingauge rainfall amount is correct and differences between the raingauge value and value of the overlying radar grid square are attributed to radar estimation error.

The process is then repeated for following hours, adjustment being made at the end of each hourly integration period. The use of hourly integration periods reduces the impact of temporal sampling errors in the raingauge data, and also reduces quantisation error due to the raingauge bucket size.

For the analysis described in chapter 4 and 5, radar data are adjusted only within the northern area of the Anglian Region, although a surface is fitted to the assessment factors over a larger domain. This default surface fitting domain which extends over the rectangle defined by points given by the north-eastern*most* and south-western*most* raingauges is extended by the addition of two pseudo-raingauges located just beyond the extreme south-west and north-east corners of the northern area. These points have zero weighting and do not influence the computed surface ensures that the estimated assessment factor field covers the northern area completely. In order to prevent fluctuations in the assessment factor field at the boundaries of the raingauge coverage, the assessment factors at all grid points beyond the boundary of the northern area yet within the surface fitting domain are set to unity (i.e. no change in the unadjusted radar field). This

constrains the field to be conservative in adjustment at and towards the area boundaries (the possibility of setting these to another value, e.g. the average of the computed assessment factors, is subject to further investigation).

3.5. Choice of the Surface Fitting Smoothing Parameter

Figures 3.3 and 3.4 demonstrate that the form of the assessment factor field surface and hence, the adjusted radar data is controlled by the surface smoothness parameter S of the surface fitting algorithm. In addition, S also controls (in addition to the grid mesh size, field complexity and number of data points) the execution speed of the surface fitting algorithm.

Figure 3.5 provides an indication of the relationship between the average computational speed of the RADGAP adjustment program (which incorporates surface fitting and interpolation) per adjustment[1] to the value of the S parameter, for a 68 raingauge network. The figure shows that routine timing is exponentially related to S, very small values of S (e.g. less than about 5) note the smaller the value of S the more complex the surface fitted to the data points) drastically effecting execution speed though this rapidly falls to a near constant minimum beyond a 'threshold value' of about 10.
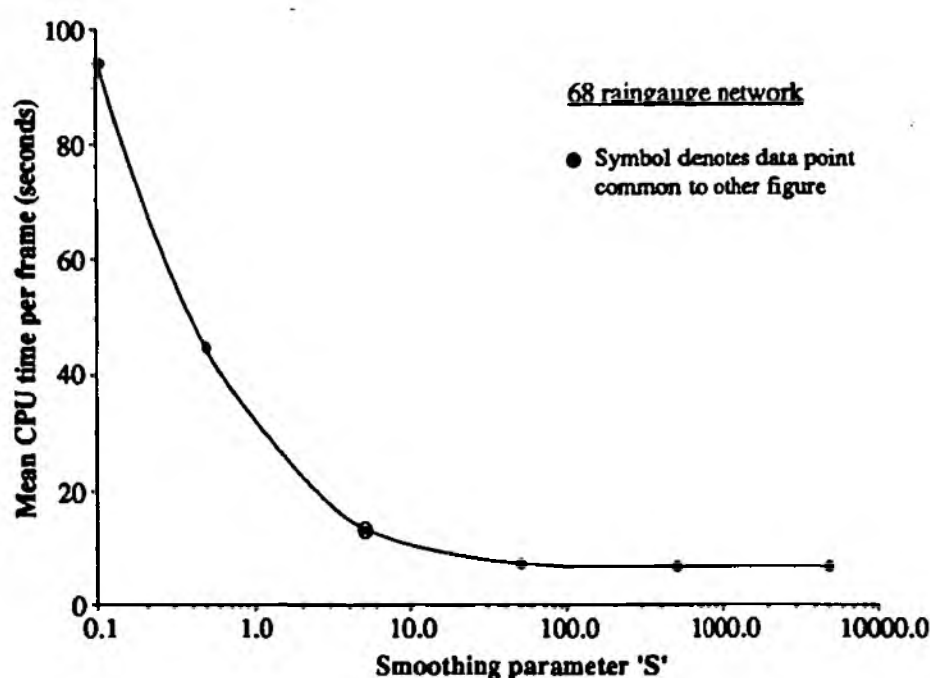
Figure 3.5: Relationship between routine execution speed and surface smoothness

The results of a preliminary investigation into the influence of the assessment factor surface

---

[1] computation was performed over a 24 hour data period and mean computation speed per adjustment frame computed. The computer used for this testing was a DEC 3100 VAXstation.

smoothness on areal rainfall estimates derived from the adjusted radar data, areal rainfall amounts were computed for five test catchments for three different values of S (0.5, 5, and 50). Figure 3.6 shows cumulative hyetographs for each case in addition to the cumulative hyetographs obtained from unadjusted radar and interpolated raingauge data. The figure indicates that generally, the adjusted radar amounts converge toward the raingauge derived amounts as the field complexity increases (i.e. as S gets smaller). However, this effect appears to be scale influenced, and for the larger test catchments of St. Andrews and Upton (233 km^2, 222 km^2) this relationship breaks down beyond a threshold value which for these areas appears to be $S=5$.

Figure 3.7 presents the relationship between computional speed and the number of gauges in the raingauge network for $S=5$. The relationship is tentatively extrapolated beyond the data set upper bound and interpretation beyond should be cautionary. The relationship shows that the mean computation time is less than 60 seconds for 100 raingauges (however, computational time for different adjustment frames may vary considerably due to changes in the complexity of the assessment factor and rainfall fields). The number of raingauges in the network does not include additional data points include in the adjustment domain mask (see section 3.4 and also the RADGAP Software Profile) which are used to prevent fluctuations in the assessment factor surface. Considerable scope for execution speed of RADGAP therefore exists via a reduction in the number of mask data points: the effect of this reduction on the field stability has not been fully investigated.
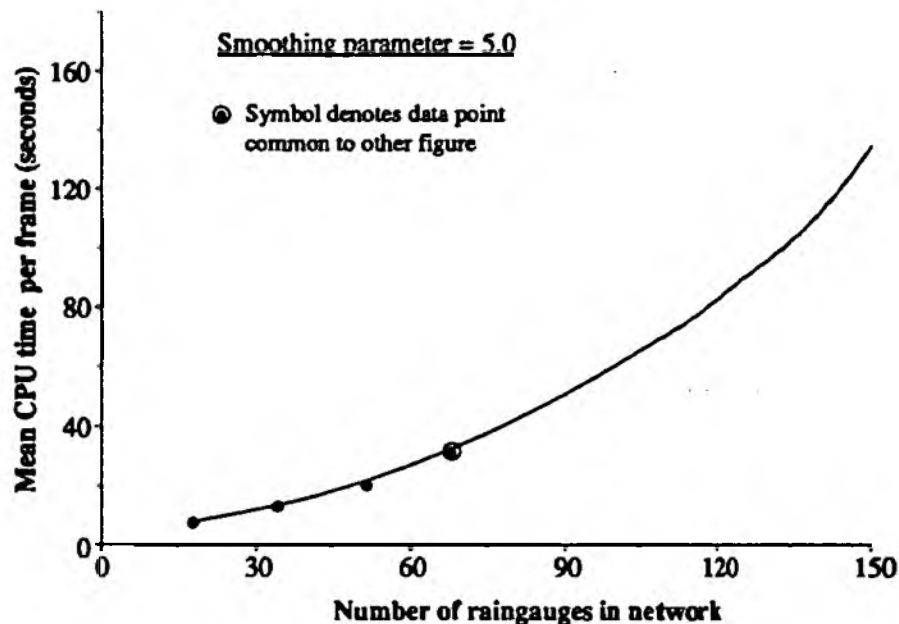
Figure 3.7: Relationship between routine execution speed and number of raingauges in network
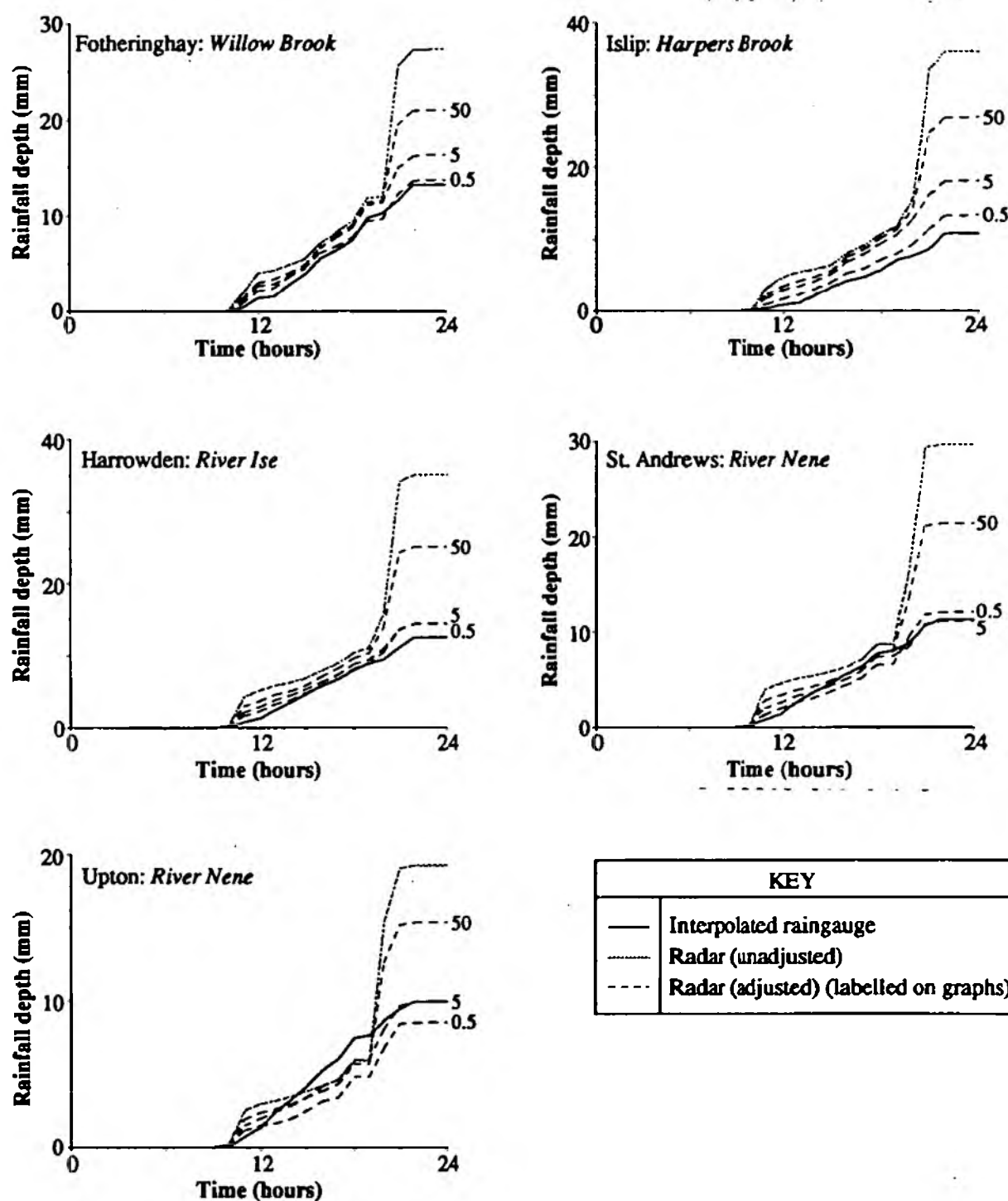
Figure 3.6: Comparison of areally averaged catchment rainfall amounts for the period 00:00-23:59. 18th December 1989 derived for different surface smoothing parameter settings

Overall the timing of the routine is acceptable for real-time applications for raingauge networks of up to about 150 gauges (with no more than 500 mask data points) for an S value of 5 the mean timing for the test case being about 14 seconds/frame for a 68 gauge network. Beyond this, the routine timing becomes limiting. A smoothing parameter value, $S=5$ constitutes in terms of routine timing and surface fitting.

3.6. Radar Adjustment Example

Simplified examples for four different adjustment cases are shown in figure 3.8. Each of the examples show a rainfall cell passing through an area where there are three raingauges.

Case 1: The cell is located between all three raingauges which consequently register no rainfall. The radar cells overlying each raingauge also do not detect any rain. The assessment factor at each of these locations is therefore unity, the assessment factor field also has the spatially constant value of unity, and the adjusted radar field is identical to the unadjusted radar field in this region.

Case 2: The cell falls on one of the raingauges (G_3) which measures 10 units of rainfall. The radar cell overlying this raingauge also detects 10 units of rain. At the other two raingauge locations, no rain is detected either by raingauge or radar. The assessment factor at each of these locations is unity, the assessment factor field once again has the spatially constant value of unity, and the adjusted radar field is identical to the unadjusted radar field in this region.

Case 3: The cell falls on one of the raingauges (G_3) which measures 5 units of rainfall whilst the radar cell overlying this raingauge detects 10 units of rain. At the other two raingauge locations, no rain is detected either by raingauge or radar. The assessment factor at the first location is 0.55, and at the other two locations, unity. The assessment factor field therefore slopes from a value of unity to a value of 0.55 in the vicinity of the first raingauge. The adjusted radar field differs from the unadjusted radar field, the radar cell overlying G_3 having a value of 5.5 (reduced from 10 units).

Case 4: The cell falls on one of the raingauges (G_3) which measures 10 units of rainfall whilst the radar cell overlying this raingauge detects 5 units of rain. At the other two raingauge locations, no rain is detected either by raingauge or radar. The assessment factor at the first location is 1.83 and at the other two locations, unity. The assessment factor field therefore slopes from a value of unity to a value of 1.83 in the vicinity of the first raingauge. The adjusted radar field differs from the unadjusted radar field, the radar cell overlying G_3 having a value of 9.15 (increased from 5 units).
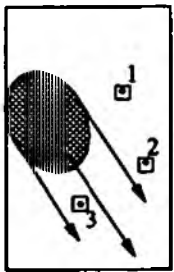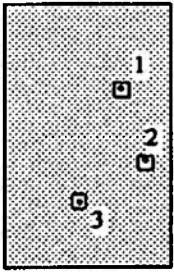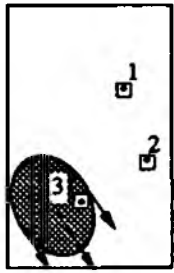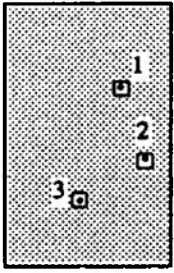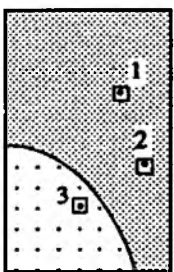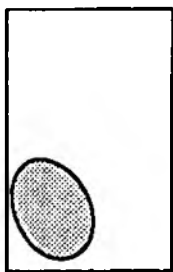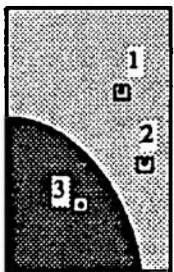
Unadjusted radar image	Assessment factor field	Adjusted radar image

Case 1

$\left.\begin{array}{l}G_1\\G_2\\G_3\end{array}\right\}=0$

$\left.\begin{array}{l}R_1\\R_2\\R_3\end{array}\right\}=0$

$\left.\begin{array}{l}AF_1\\AF_2\\AF_3\end{array}\right\}=1$

Radar field unchanged

Case 2

$\left.\begin{array}{l}G_1\\G_2\end{array}\right\}=0$
$G_3=10$

$\left.\begin{array}{l}R_1\\R_2\end{array}\right\}=0$
$R_3=10$

$\left.\begin{array}{l}AF_1\\AF_2\\AF_3\end{array}\right\}=1$

Radar field unchanged

Case 3

$\left.\begin{array}{l}G_1\\G_2\end{array}\right\}=0$
$G_3=5$

$\left.\begin{array}{l}R_1\\R_2\end{array}\right\}=0$
$R_3=10$

$\left.\begin{array}{l}AF_1\\AF_2\end{array}\right\}=1$
$AF_3=0.55$

Radar field adjusted. Cell intensity reduced in accordance with recorded raingauge value (R_3 adjusted = 5.5).

Case 4

$\left.\begin{array}{l}G_1\\G_2\end{array}\right\}=0$
$G_3=10$

$\left.\begin{array}{l}R_1\\R_2\end{array}\right\}=0$
$R_3=5$

$\left.\begin{array}{l}AF_1\\AF_2\end{array}\right\}=1$
$AF_3=1.83$

Radar field adjusted. Cell intensity increased in accordance with recorded raingauge value R_3 adjusted = 9.15).

Figure 3.8: Adjustment Examples (Simplified)

3.7. Concluding Comments

This chapter has introduced a procedure for adjusting radar data using a network of ground-based raingauges. The procedure incorporates a sophisticated two-dimensional surface fitting algorithm which fits a surface to assessment factors computed for each of the raingauge sites. The procedure assumes that the raingauges provide an accurate measure of rainfall at a point though because the surface is not constrained to pass exactly through the assessment factors, random measurement errors (in both raingauge and radar data) are intrinsically accommodated and problems due to the mismatch in sampling between radar and raingauge partially overcome. The field is constrained to be conservative in its adjustment towards the adjustment domain boundary by the application of a data mask which constrains the field at these points and prevents instabilities in the surface. In addition upper and lower bounds in the value any assessment factor can assume prevent temporal and spatial instabilities in the surface. The assessment factor surface is used to adjust the radar data on a cell by cell basis multiplicatively.

The smoothness of the surface fitted to the irregularly distributed assessment factors can be controlled by a single smoothness parameter, which can be set by the user. The number of data points the surface is required to fit, the surface smoothing parameter, and the grid-mesh size all influence the computational speed of the surface fitting routine. A brief study determined an optimal value for the smoothing parameter which provides the best compromise between field complexity, computational time, and the areal estimates derived from the adjusted radar data (compared to a raingauge-truth index). The number of data points the field is fitted to is shown not to influence the computational speed as significantly as the field smoothness parameter. Potential exists for increasing CPU speed simply by reducing the number of null data points in the data mask applied around the adjustment domain.

Chapter 4. Adjustment Case Studies and Procedure Evaluation

This chapter introduces a number of case studies which demonstrate the performance of the radar adjustment scheme under different synoptic conditions. Performance assessment is carried by comparing unadjusted and adjusted radar data and raingauge data, both subjectively via visual comparison of the spatial rainfall fields, and objectively by comparing cumulative rainfall hyetographs for a number of test river catchments. In the latter the raingauge derived rainfall estimates are used as an index of true surface rainfall. Two hydrological applications of rainfall data provide an additional assessment: design storm return period derivation and river flow forecasting. The 'end-point application' (EPA) assessment provided by the flow forecasting comparison enables a direct indication of the effectiveness (and therefore indirectly, the accuracy) of radar and raingauge rainfall measurement for a real-time hydrological procedure: the rainfall data are used as an input to a river flow forecasting model and the quality of the flow forecasts obtained from each compared. This technique overcomes the problems associated with the sampling mismatch resulting from comparing raingauge point and radar volume measures, using instead the river catchment as a gauge of rainfall amounts. Finally, the chapter assesses the impact of radar data intensity resolution.

4.1. The Adjustment Domain

For reasons of raingauge data availability the adjustment procedure has been limited to the northern area of the Anglian Region for all the case studies. As well as having a rainfall archive for a relatively large number of raingauges (up to a maximum of 68 gauges, made up from a combination of telemetering gauges and recording loggers - see Appendices 5, 7, and 8), the area also extends to a range of approximately 140 km from the Ingham radar thereby enabling the influence of range to be directly studied. Essentially, adjustment takes place over a rectilinear area large enough to cover the entire area plus a minimum 10 km border all the way around the area. The mapping scheme used for this adjustment area is shown in Appendix 6.

4.2. Overall Assessment of Radar Adjustment

Before looking at individual case studies, the overall results of adjustment appraisal over a 23 day period are presented. For the appraisal, unadjusted radar data were adjusted on an hourly basis as described in section 3.4 for all the available data. Using the raingauge derived rainfall estimates as an index of true surface rainfall, a comparison was made between areal rainfall amounts derived from interpolated raingauge data and from unadjusted and adjusted radar data. Mean percentage deviations of the radar data from the raingauge derived index of areal rainfall for one to 24 hour cumulations were computed for each of the days data, a mean percentage error being computed from all the daily deviations. The mean percentage deviations for the five

test catchments are shown in figure 4.1, and the deviations expressed by the root mean square error statistic (see eq. 4.1) are listed in table 4.1 for each catchment, together with an overall catchment percentage improvement.

$$RMSE = \sqrt{\frac{1}{n} \sum_{i=1}^{24} \left[RAD_i - GAU_i \right]^2}$$

(eq. 4.1)

where RAD and GAU are the areal rainfall amounts cumulated to time i, derived from radar data (unadjusted or adjusted) and from raingauge data respectively.

Table 4.1: Error statistics and overall percentage improvement in areal rainfall amounts

Catchment	RMSE unadjusted	adjusted	% Improvement
Fotheringhay	9.194	7.480	18.6
Islip	4.216	2.240	46.9
Harrowden	5.189	2.543	51.0
St. Andrews	5.904	3.586	39.3
Upton	4.645	4.908	-5.7
Overall	29.148	20.757	28.8

The results show that the adjustment procedure achieves a significant reduction in the deviation of the radar derived catchment averaged rainfall compared to that derived from the unadjusted radar data. The overall percentage improvement attained averaged over all the data and for all the test catchments is just under 29 %, with improvement on an individual catchment basis ranging from 18.6 % to 51 % (with the Upton catchment deviation increasing after adjustment by nearly 6 %).

4.3. Case Studies

The following sections present the results of a number of case studies. From the data available (almost four weeks), examples were taken to include convective summer rainfall - short periods of intense and localised rainfall, and stratiform rainfall - more widespread, longer duration and lower intensity. Case study choice was also restricted to those days where rainfall was significant and where a large number of raingauges were available.

Stratiform rainfall, most common during periods of atmospheric stability typical of cyclonic
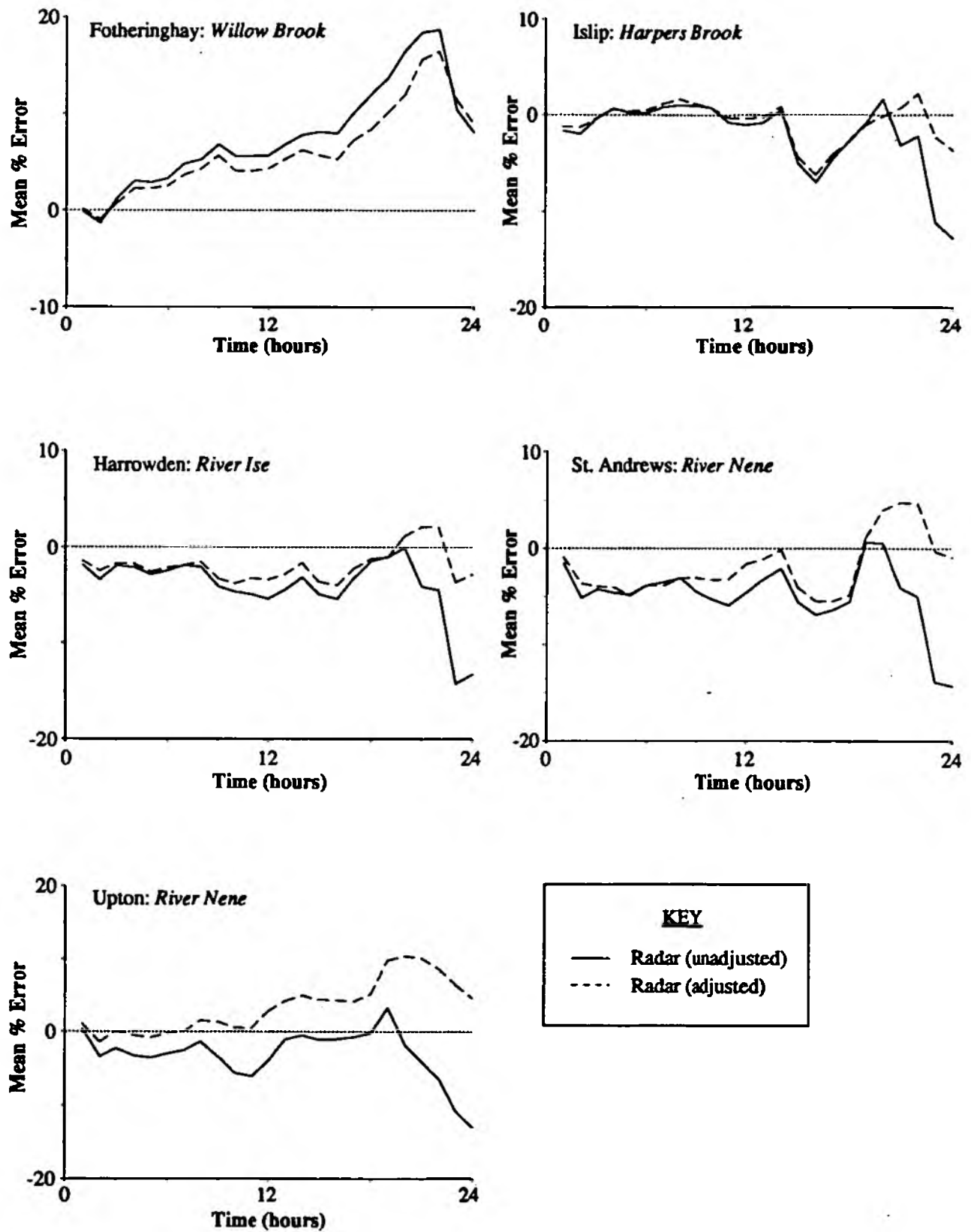
Figure 4.1: Comparison of error in cumulative rainfall amounts for catchment averaged rainfall for adjusted and unadjusted radar rainfall data for test catchments (derived from a total of 23 days data)

cumulated (up to a factor of five in this example: 60-70 mm of radar rainfall compared to 14-16 mm of raingauge rainfall). This is even more significant when it is realised that in some cases, the dominant jump is confined to a period of less than two hours.
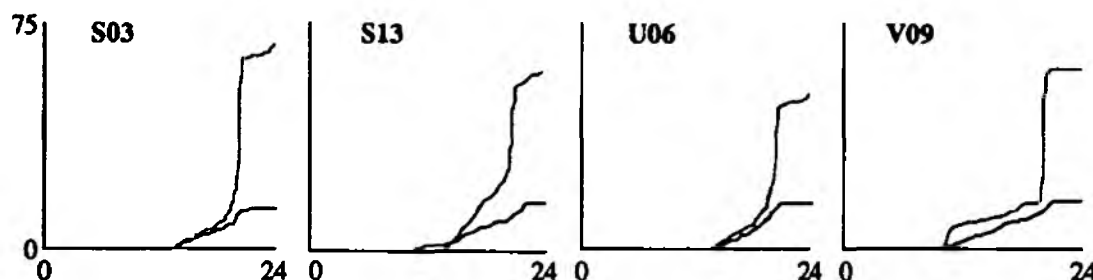
Figure 4.2: Example raingauge/radar hyetographs for bright-band affected rainfall

Figure 4.3 shows four different images: unadjusted radar rainfall field (i), the corresponding radar image after adjustment (ii), the interpolated raingauge rainfall field (iv) and the mean assessment factor field (iii) applied to the 24 hourly radar rainfall images. All the rainfall fields (i.e. [i], [ii] and [iv]) are cumulated over the entire available period and are in mm depth units.

There is a striking difference between the unadjusted radar and raingauge derived rainfall fields with significant overestimation by the unadjusted radar data throughout the area, but strongest within 50 km range of the radar. The mean assessment factor field reflects this, having a mean value of less than unity for the day, signifying that the adjustment procedure is on average lowering the unadjusted radar rainfall estimates). The adjusted radar rainfall field more closely resembles the raingauge field, with the worst of the bright-band overestimation removed.

Figure 4.4 compares cumulative areal rainfall hyetographs for five test catchments derived from interpolated raingauge data, unadjusted and adjusted radar data, and also Meteorological Office calibrated radar data. If the raingauge derived amounts are used as an index of actual areal rainfall, it can be concluded that:

• Met. Office radar calibration has a very limited impact, and can makes the data worse,
• unadjusted radar data deviate significantly from the raingauge derived index in this case overestimating rainfall amounts,
• radar adjustment using the procedure described in chapter 3 reduces deviation from the raingauge amounts.

The extent to which the local adjustment procedure is reducing error rather than just making the radar data 'look' more like the raingauge data is difficult to assess from the catchment hyetographs, since the comparison is heavily biased (i.e. comparisons are made with raingauge data used for adjustment) although as commented in the introduction to this section, it is
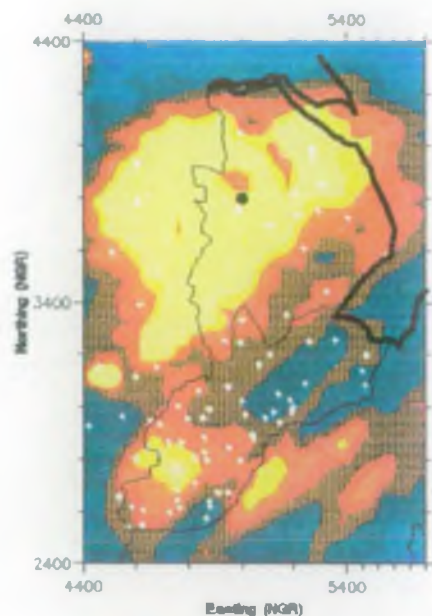
i). unadjusted radar
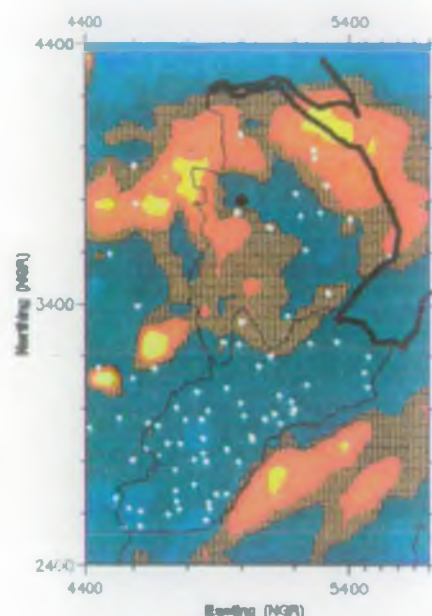
ii). adjusted radar
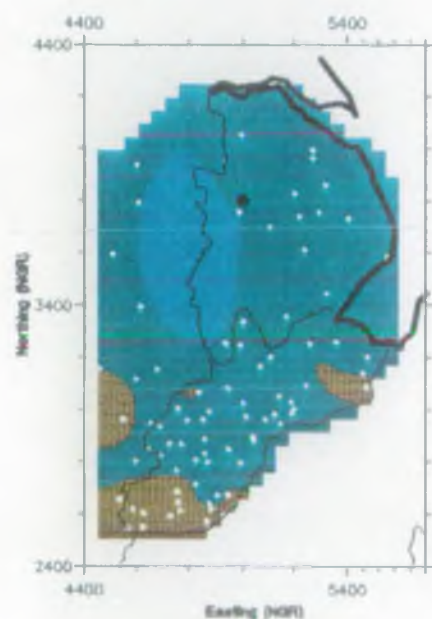
iii). assessment factors

iv). interpolated raingauge

Figure 4.3: Radar adjustment fields, 18th December 1989 (Ingham radar)
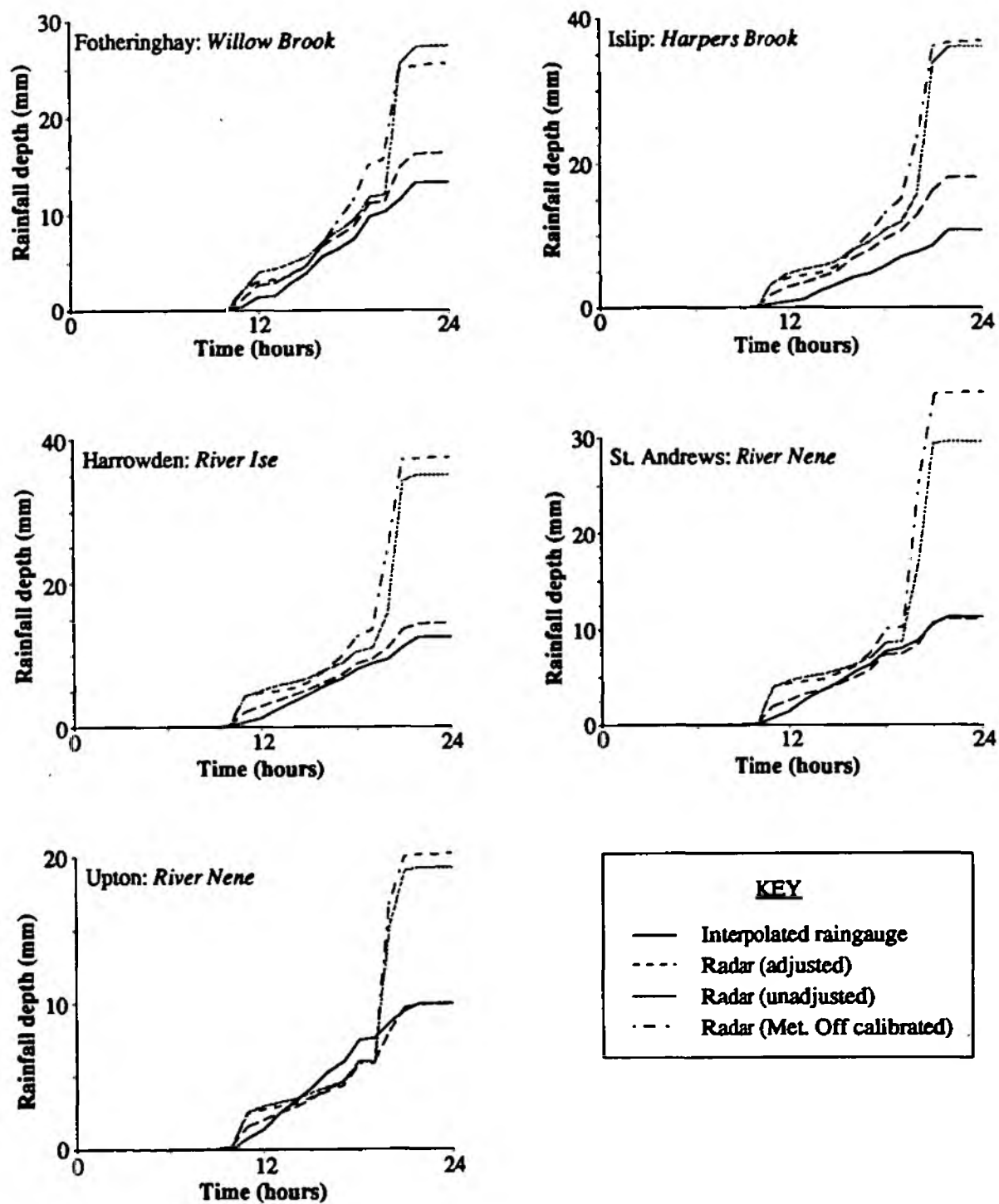
Figure 4.4: Catchment averaged rainfall amounts: 18th December 1989

reasonable to assume that the point raingauge measurements are highly representative of rainfall over the area and that the adjustment applied to the radar data is indeed an error correction. Other forms of assessment using storm frequency computation and flow forecasting are described in section 4.4 and 4.5.

• Case Study 2: 16th December 1989

This event spans the period 00:00-17:00 GMT 16th December 1989. Significant amounts of widespread rainfall occurred during the day the bulk after 06:00 GMT. The average raingauge rainfall total for the 66 available gauges is 14 mm (mostly occurring in 11 hours, i.e. approx. 1.3 mm/hr) with a standard deviation of the gauge measurements of 3 mm. A bright-band presence is flagged, but is not severe because the bright-band is at higher altitude (1 km to 2 km), and is only intersected by the radar beam at longer ranges (100 km and beyond) where the partial beam filling limits the error it introduces.

A glance at figure A12.26 (Appendix 12) reveals that radar overestimation is limited to raingauges at long range from the radar i.e. to the south of the area. Figure 4.5 illustrates this long range bright-band overestimation graphically, whilst figure A11.26 (Appendix 11) shows a well defined annulus of high reflectivity at range of about 100 km. Examination of the adjusted radar rainfall field reveals that adjustment has effectively 'capped' the rainfall in the areas most affected by overestimation. Figure 4.6 shows that for four of the five test catchments (all of which li.e. within a bright-band affected area) the radar data overestimate actual areal rainfall, and that after adjustment the overestimation is significantly reduced.

4.3.2. Convective rainfall systems

Two case studies have been drawn from the available data for convective rainfall systems, both occurring in July 1989.

• Case Study 3: 7th July 1989

This event spans the period 00:00-14:00 GMT 7th July 1989. The event is a typical convective event with localised cells of intense rainfall moving though the south of the case study area. The average raingauge rainfall total for the 58 available gauges is 25 mm and the high spatial variability of rainfall over the area is reflected by an inter-gauge standard deviation of 15 mm. Some raingauges measure only a trace of rainfall whilst others record over 40 mm (e.g. gauge S17 measured 0.5 mm of rain, whilst gauge V14, 40 km south-west measured 53.5 mm). Most of the rainfall occurs in the period 04:00-10:00 GMT so the average rainfall intensity is approx. 4.2 mm/hr, considerably higher than either of the stratiform rainfall cases. This case is a good example of the dynamic and spatially discontinuous nature of (convective) rainfall fields.
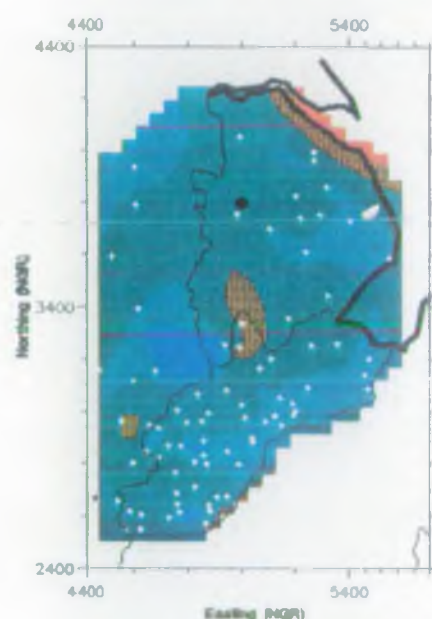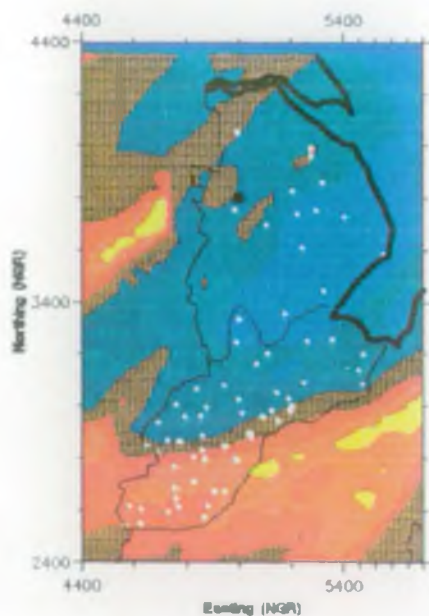
i). unadjusted radar
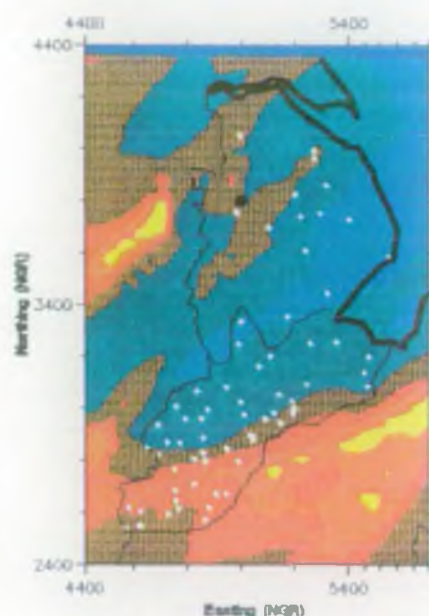
ii). adjusted radar
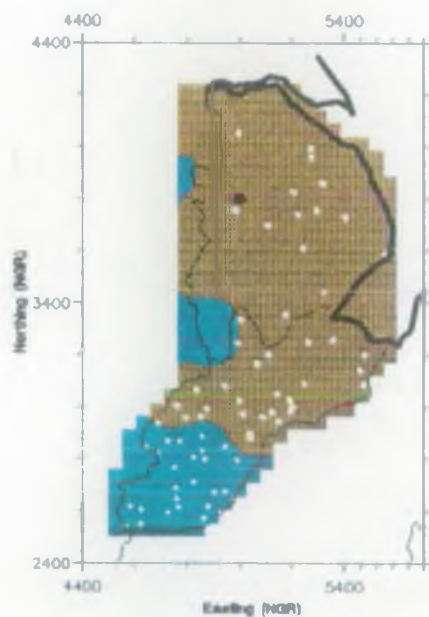
iii). assessment factors
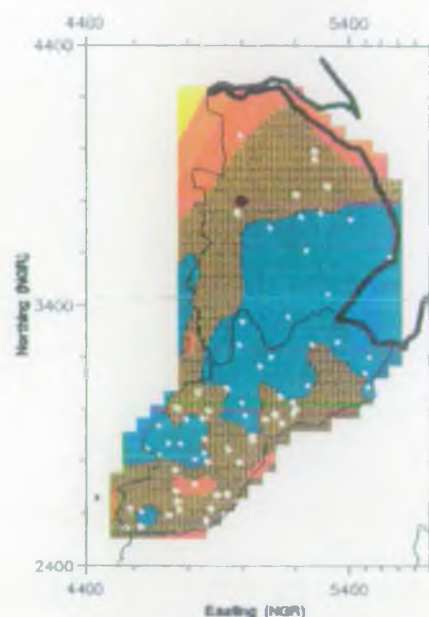
iv). interpolated raingauge
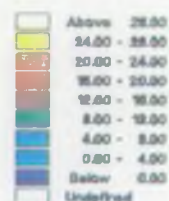
Figure 4.5: Radar adjustment fields, 16th December 1989 (Ingham radar)
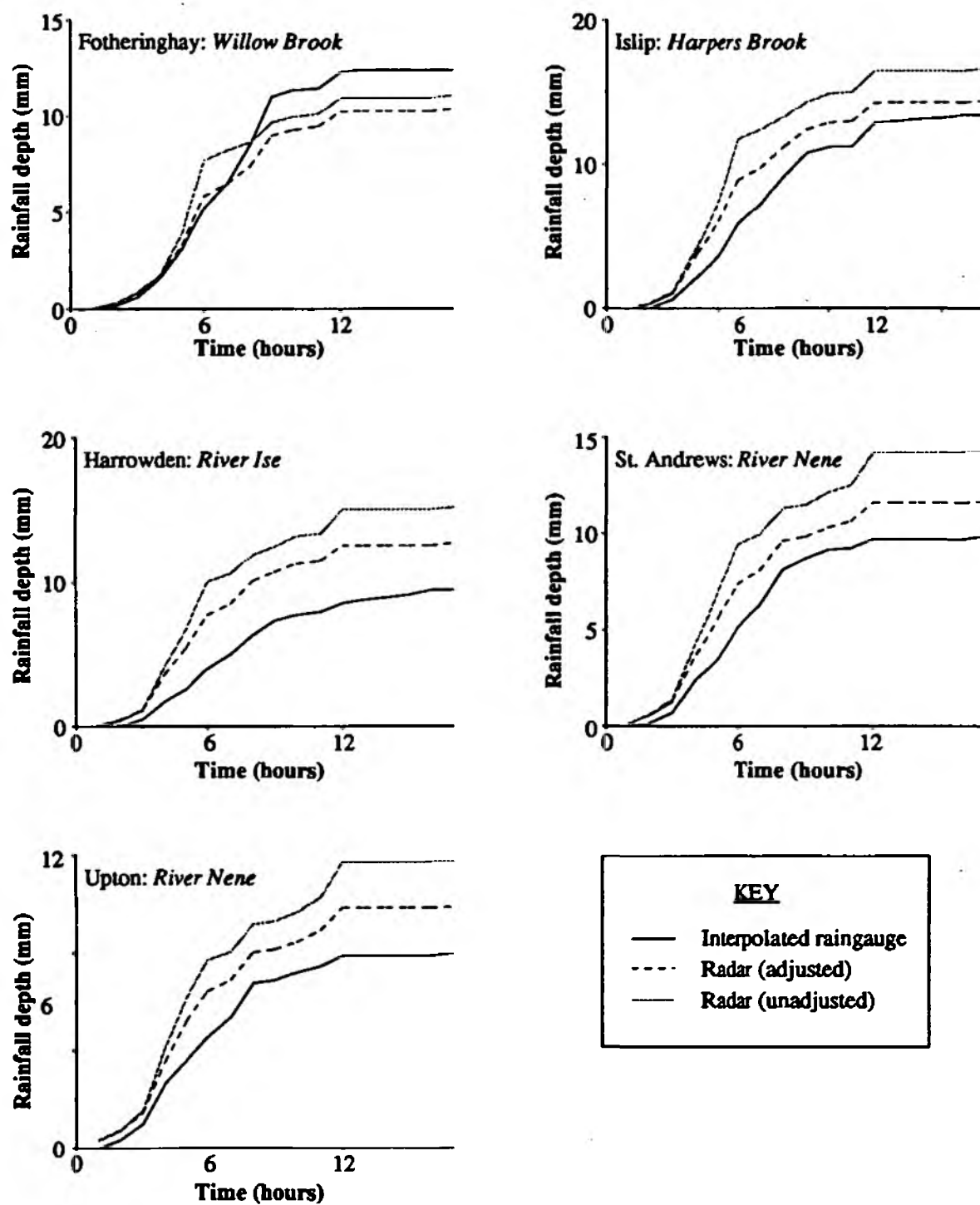
Figure 4.6: Catchment averaged rainfall amounts: 16th December 1989

Figure 4.7 shows cumulative hyetographs of four selected raingauges and the 5 km radar cells which overly them (refer also to Appendix 12). The hyetographs clearly illustrate the passage of a number of rain-bearing convective cells over the raingauge sites. For almost all the gauge sites, the raingauges measure more rainfall than is observed by the radar. This is directly attributable to the dynamism of rainfall process, and the sampling problems it poses for a point measurement device. In such circumstances, the representativeness of the raingauges must be questioned critically, especially since it is in precisely these conditions that a weather radar is of most benefit and subject to the least error. The EPA assessment in section 4.5 provides further evidence for these statements. The hyetograph for gauge V24 provides a good example of agreement between raingauge and radar rainfall estimates.

Figure 4.7: Example raingauge/ radar hyetographs for convective rainfall

Figure 4.8 shows four different images: unadjusted radar rainfall field (i), the corresponding radar image after adjustment (ii), the interpolated raingauge rainfall field (iv), and the mean assessment factor field (iii) applied to the 24 hourly radar rainfall images. All the rainfall fields (i.e. [i], [ii] and [iv]) are cumulated over the entire available period and are in mm depth units.

The unadjusted radar field illustrates how the heaviest rainfall is confined to the south of the area with rainfall amounts decreasing to the north. This overall pattern is also reflected in the interpolated raingauge rainfall field although the field is more complex, due to the inter-gauge variability. The form of the unadjusted radar field is changed quite dramatically by adjustment: the adjusted rainfall field generally having higher rainfall intensities in the south of the area. However, the case illustrates a shortcoming of a surface fitting approach whereby the assumption of gauge truth forces an unsatisfactory 'circus tent pole' effect on the radar field. Although a smoother assessment factor field would partially overcome this, this case reveals that the assumption of gauge truth is fundamentally flawed and illustrates the limitations of a point measurement.

Figure 4.9 compares cumulative areal rainfall hyetographs for the five test catchments derived from interpolated raingauge data, unadjusted and adjusted radar data, and Meteorological Office calibrated radar data. The hyetographs show that deviation between the unadjusted radar derived areal rainfall amounts and those derived from raingauge amounts can be large, often by

i). unadjusted radar
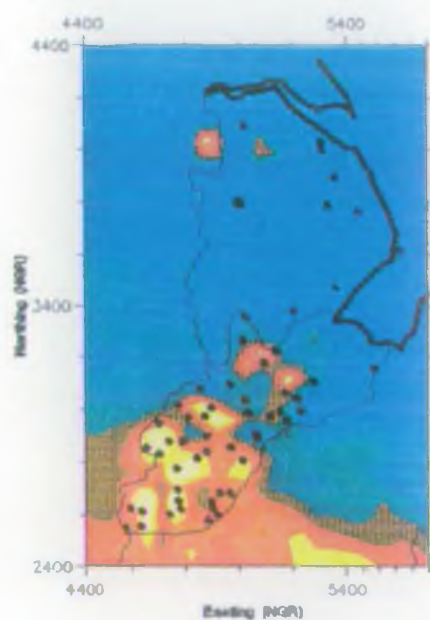
ii). adjusted radar
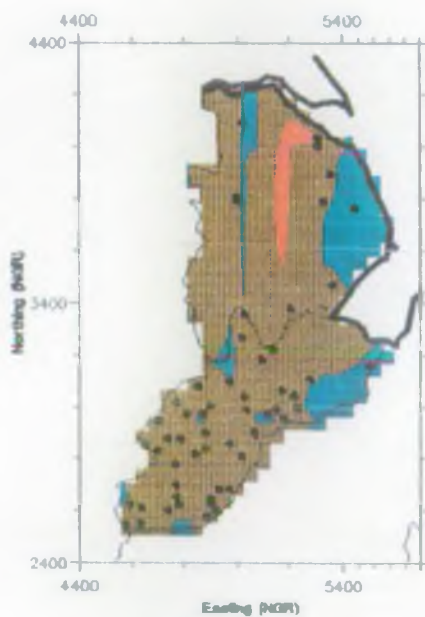
iii). assessment factors

iv). interpolated raingauge

Figure 4.8: Radar adjustment fields, 7th July 1989 (Ingham radar)
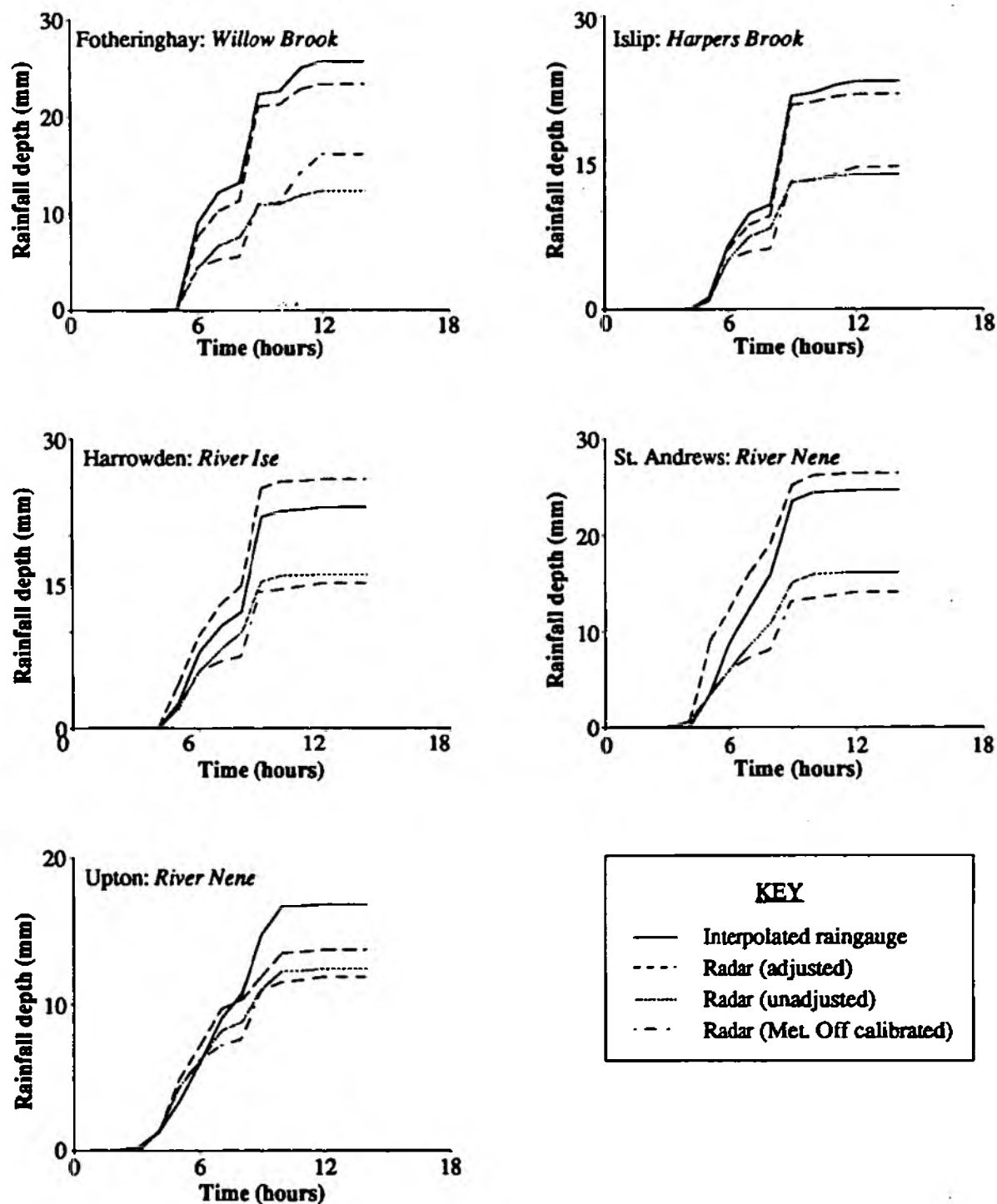
Figure 4.9: Catchment averaged rainfall amounts: 7th July 1989

as much as 93 % at the event end (Fotheringhay catchment: 12.4 mm for raingauge; 25.8 mm for unadjusted radar). As in the other cases, the radar adjustment procedure is successful in reducing these deviations, but given the comments regarding gauge-truth it appears likely that the adjustment procedure is actually 'correcting' a good quality rainfall field with a less accurate one (discussed more fully in section 4.5). As in previous case studies the Meteorological Office real-time gauge calibration has a limited impact.

• Case Study 4: 30th July 1989

This event spans the period 00:00-23:45 GMT 30th July 1989. The event selected is another typical convective event with localised cells of intense rainfall moving though the area particularly in a north-easterly direction from the south-west at a range of between 25-55 km from the radar. The average raingauge rainfall total for the 67 available gauges is 9 mm and as with case study 3, there is high spatial variability of rainfall over the area (inter-gauge standard deviation of 6 mm) and the range of raingauge measured rainfalls is large - 35 mm. An example of high inter-gauge variability is provided by gauge S14 which measured 30.5 mm of rain whilst a nearby cluster of gauges about 15 km to the west (gauges S05, S06, S07, S11) all measured about 4 mm. Most of the rainfall occurs in the period 04:00 - 12:00 GMT so the average rainfall intensity is approximately 1 mm/hr. This case is a good example of the dynamic and spatially discontinuous nature of (convective) rainfall fields.

Figure 4.10 shows cumulative hyetographs of four selected raingauges and the 5 km radar cells which overly them (refer also to Appendix 12). The hyetographs clearly illustrate the passage of a number of rain-bearing convective cells over the raingauge sites. As with the previous convective case study, the raingauges measure more rainfall than is observed by the radar for many of the gauge sites, and as before this is attributed to the dynamism of rainfall process, and the sampling problems it poses for a point measurement device.
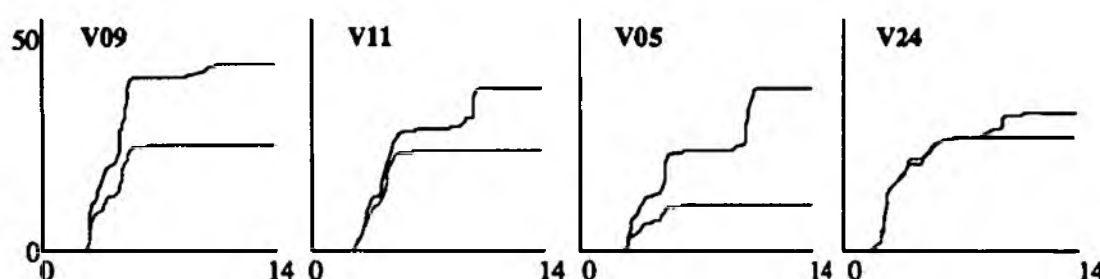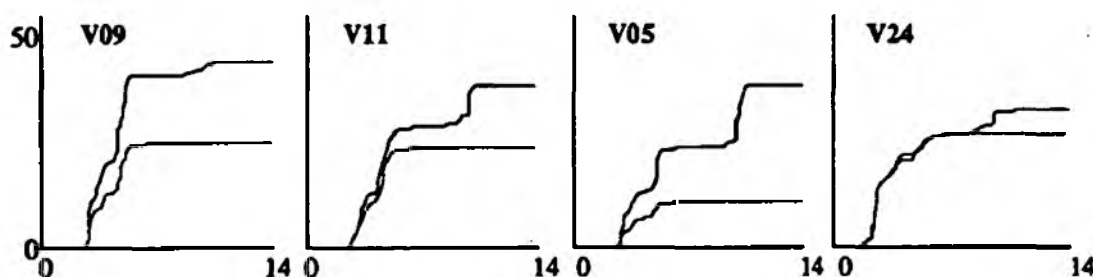

Figure 4.10: Example raingauge / radar hyetographs for convective rainfall

Figure 4.11 shows four different images: unadjusted radar rainfall field (i), the corresponding radar image after adjustment (ii), the interpolated raingauge rainfall field (iv), and the mean

assessment factor field (iii) applied to the 24 hourly radar rainfall images. All the rainfall fields (i.e. [i], [ii] and [iv]) are cumulated over the entire available period and are in mm depth units.

The unadjusted radar and raingauge rainfall fields generally exhibit excellent correlation both clearly defining the band of high rainfall running through the centre of the area, lower rainfall about 15 km east to southeast to the radar site, and in the south of the area. The influence of a few high gauge readings causes the interpolation procedure to produce some 'islands' of high rainfalls, and the influence of these high gauge readings can also seen in the adjusted radar image although the effect is less dramatic than in case study 3.

Figure 4.12 compares cumulative areal rainfall hyetographs for the five test catchments derived from interpolated raingauge data, unadjusted and adjusted radar data. The hyetographs show that deviation between the unadjusted radar derived areal rainfall amounts and those derived from raingau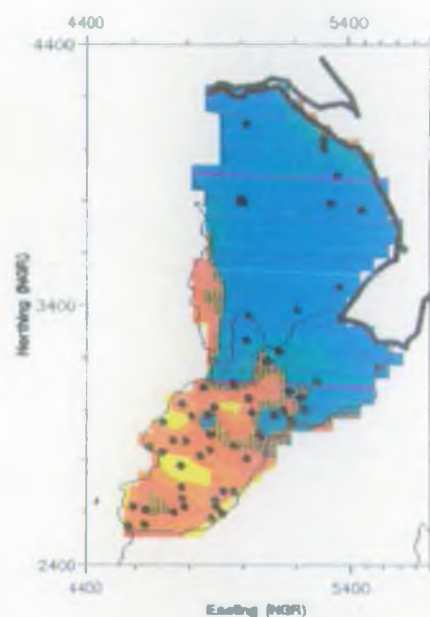ge amounts can be large, often by as much as 93 % at the event end (Fotheringhay catchment: 12.4 mm for raingauge; 25.8 mm for unadjusted radar). As in the other cases, the radar adjustment procedure is successful in reducing these deviations, but it appears likely that the adjustment procedure is actually 'correcting' a good quality rainfall field with a less accurate one (discussed more fully in section 4.5).

4.4. Storm Return Period Estimation

One common hydrological application of rainfall data is its use in determining the return period of a rainfall event. In order to assess the impact of radar data adjustment on storm frequency computation, the flood studies report procedure (NERC, 1975) for estimating storm return periods over ungauged catchments[1] was applied. The procedure was used to yield a family of storm hyetographs having return periods of 1, 2, 5, 10, 50 and 100 years for five test catchments with which event data from the radar and raingauges could be compared. By comparing the observed hyetographs for the unadjusted and adjusted radar data and raingauge data with the computed design hyetographs, it has been possible to assess the utility of the different data types in terms of a 'front-end rainfall product', i.e. storm frequency estimation and in particular:

* the influence of the bright-band on the unadjusted radar data and the extent to which the real-time adjustment procedure could remove it (case 1),
* the possible implications of raingauge representativeness (particularly in convective rainfall, case 2).

The analysis has been performed for two of the case study events of section 4.3, a severely bright-band affected winter stratiform event and an intense summer convective event.

[1] This is a procedure which enables design storm profiles to be derived (i.e. storm having a particular return period) from physical catchment characteristics and regional storm coefficients. The design storm profiles can have either winter or summer profiles, with varying degrees of 'peakedness'. The storm profiles are symmetrical. The duration of the design storms is controlled by the estimation algorithm.
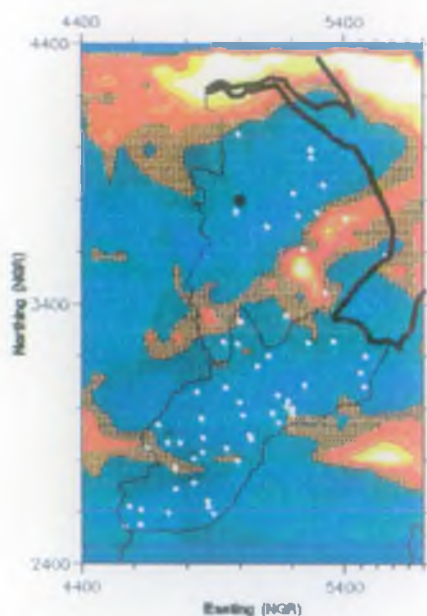
i). unadjusted radar
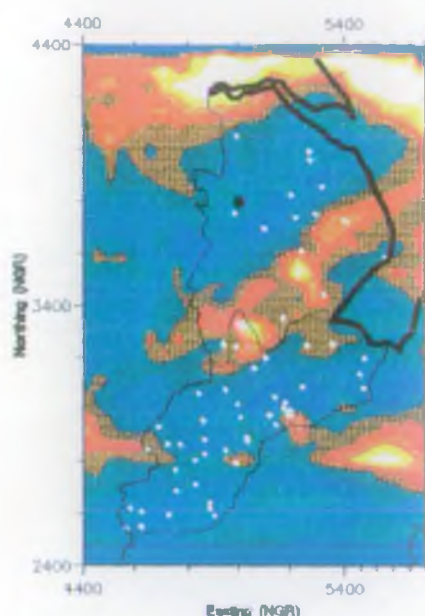
ii). adjusted radar
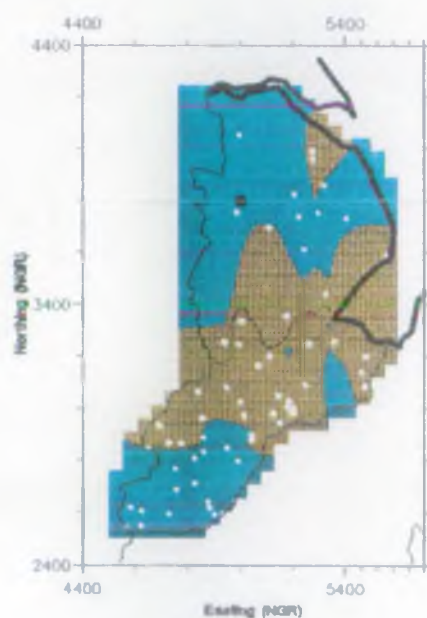
iii). assessment factors
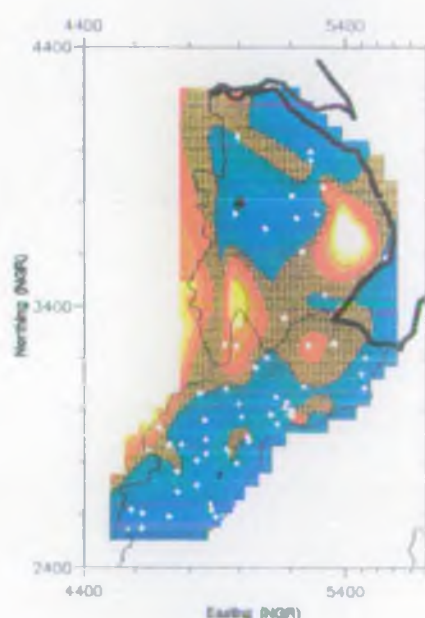
iv). interpolated raingauge
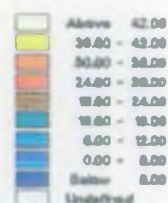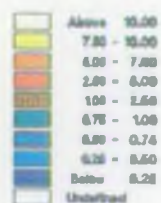
Figure 4.11: Radar adjustment fields, 30th July 1989 (Ingham radar)
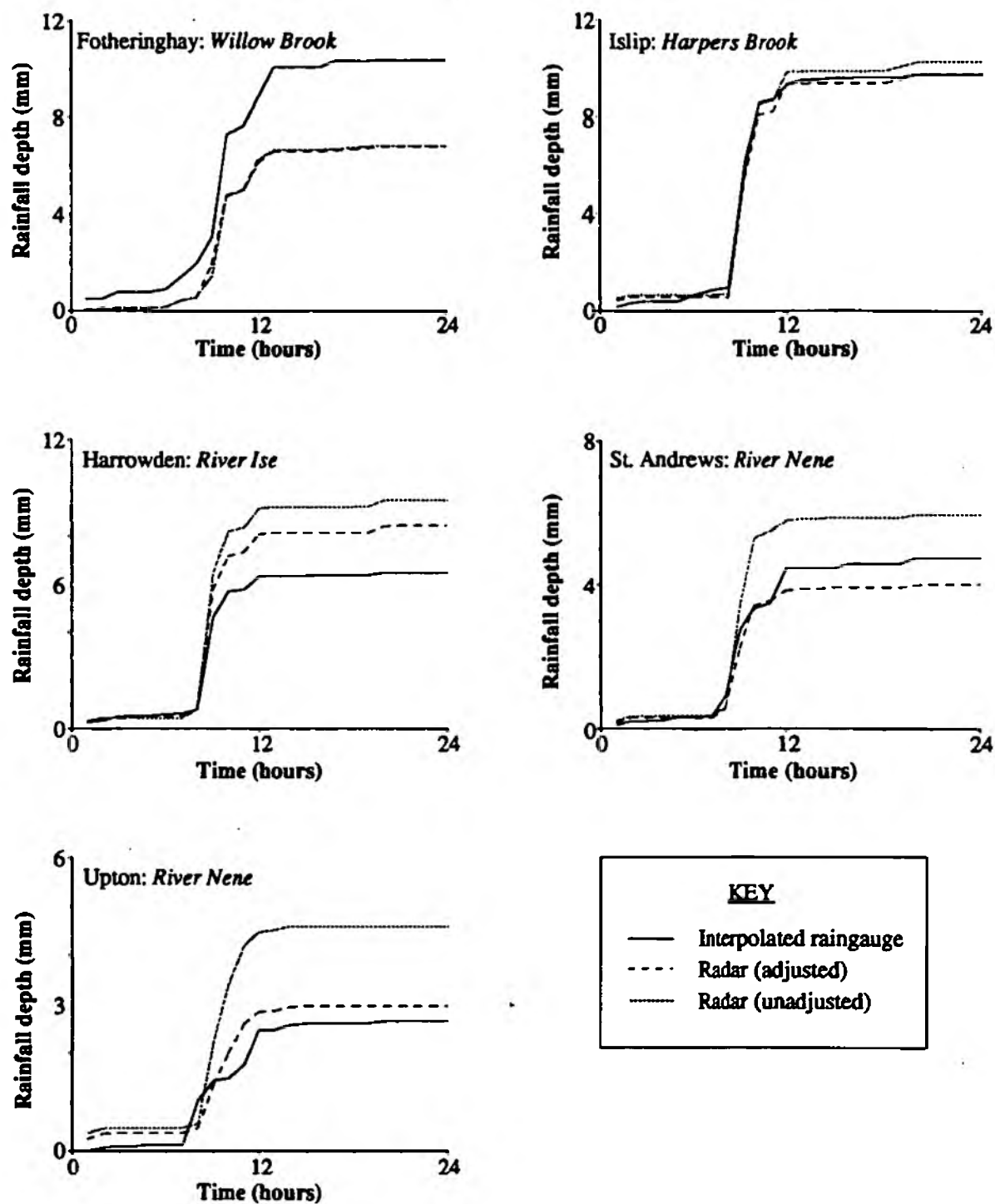
Figure 4.12: Catchment averaged rainfall amounts: 30th July 1989

Case 1: 18th December 1989

For this event a family of design storms with winter profiles having 75% peakedness was generated. The cumulative hyetographs derived from the storm profiles are shown in figure 4.13 ([a] and [b]) for each of the test catchments. Superimposed on each are cumulative hyetographs for the respective catchments derived from unadjusted and adjusted radar data and from raingauge data. The superimposition enables the return period of the observed storm hyetographs to be estimated and these are shown in table 4.2. For all catchments, the bright-band presence has a major influence on the estimated return periods which in storm frequency estimation terms is unacceptable. In all cases except the Upton catchment, the unadjusted radar data storm hyetograph exceed in magnitude even the 100-year return period curve whilst the raingauge and adjusted radar data hyetographs suggest a storm return periods ranging from 3-17 years. The extent to which adjustment of the radar data produces storm hyetographs having the same or similar estimated return periods to those derived from the raingauge data appears to be related to the catchment area, the greatest similarity being achieved for the larger catchments (Upton and St. Andrews) (see Appendix 13 for study catchment locations and areas).

Table 4.2: Storm return periods for different data types: 18th December 1989

	Raingauge	Unadjusted radar	Adjusted radar
Fotheringhay	17	>100	80
Islip	5	>100	35
Harrowden	5	>100	3
St. Andrews	3	>100	3
Upton	< 1	5	< 1

Clearly in this case storm frequencies estimated from unadjusted radar data are gravely in error, the error being directly attributable to a short-period of intense bright-band, and there is no doubt that the magnitude of the error renders the data unusable for storm return period estimation in this instance. Adjustment of the data however produces estimates which far more closely represent the raingauge derived values, although in certain cases, e.g. Islip catchment there is still a significant difference.

Figure 4.13(a): Cumulative hyetographs for 18th December 1989 data superimposed on 1, 2, 5, 10, 50, and 100 year design storm cumulative hyetographs (75 % peakedness, winter profile)

Figure 4.13(b): Cumulative hyetographs for 18th December 1989 data superimposed on 1, 2, 5, 10, 50, and 100 year design storm cumulative hyetographs (75 % peakedness, winter profile)

Case 2: 7th July 1989

For this event a family of design storms with summer profiles having 75% peakedness was generated. The cumulative hyetographs derived from the storm profiles are shown in figure 4.14 ([a] and [b]) for each of the test catchments. Superimposed on each are cumulative hyetographs for the respective catchments derived from unadjusted and adjusted radar data and from raingauge data. The superimposition enables the return period of the observed storm hyetographs to be estimated and these are shown in table 4.3.

For all the catchments, a major difference exists between the return period of the storm hyetographs generated from the unadjusted radar and raingauge data, but in this case the reverse of that observed in the previous case is seen, with the raingauge derived hyetographs significantly exceeding those derived from unadjusted radar data (by as much as 93 % in term of rainfall depth - see section 4.3.2) and storm return periods estimated from the raingauge data exceed those derived from unadjusted radar data by a factor of four up to a factor of ten, the largest differences tending to occur for the smaller catchments (i.e. Fotheringhay, Islip).

Table 4.3:   Storm return periods for different data types: 7th July 1989

	Raingauge	Unadjusted - radar -	Adjusted - radar -
Fotheringhay	> 100	12	> 100
Islip	100	9	90
Harrowden	40	9	75
St. Andrews	30	8	50
Upton	4	1	2

Even though adjustment reduces the deviation between the raingauge and radar data, whether this corresponds to a reduction in error is doubtful especially given the comments in section 4.3.2 regarding raingauge representativeness. In this case there is no good reason for the radar data to be grossly in error (no bright-band), indeed weather radar estimates are usually high quality in convective conditions. Consequently, in this situation it is more reasonable to look to the raingauges for the source of error which probably arises through sampling error resulting from inadequate representativeness of the point raingauge measurements in a highly dynamic rainfall field. Consequently it is concluded that estimation of storm return period on the basis of point raingauge data in this type of rainfall system is liable to involve large errors due to sampling problems and that better estimates could be obtained from unadjusted radar data. This is discussed further in section 4.5.
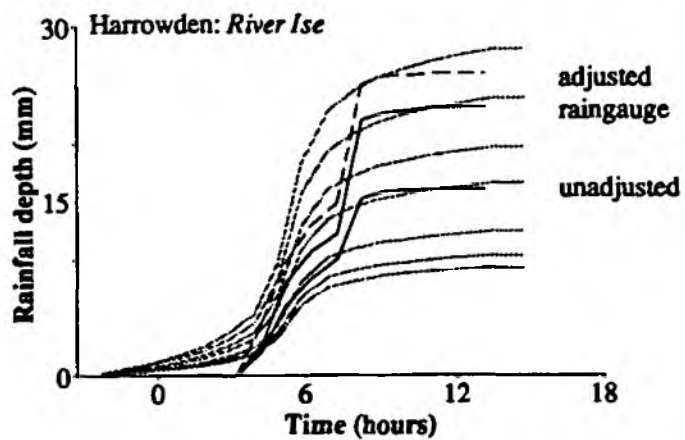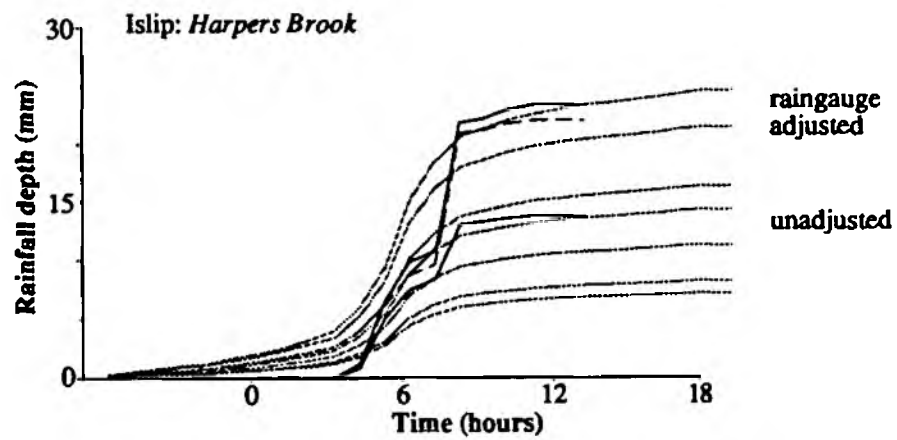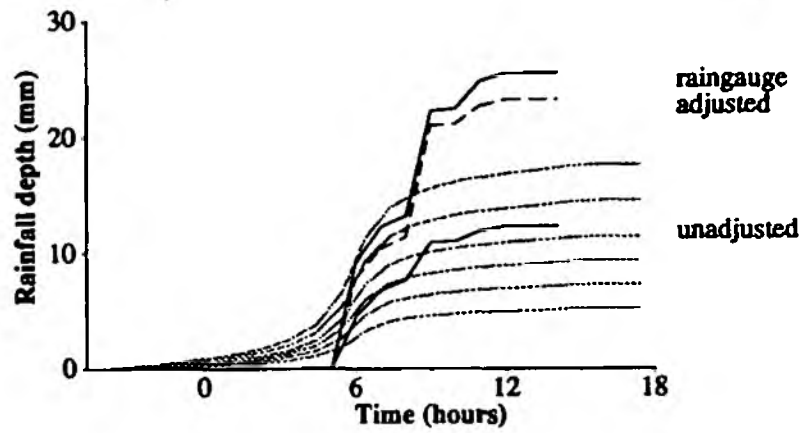
Figure 4.14(a): Cumulative hyetographs for 7th July 1989 data superimposed on 1, 2, 5, 10, 50, and 100 year design storm cumulative hyetographs (75 % peakedness. summer profile)

St. Andrews: *River Nene*

adjusted
raingauge

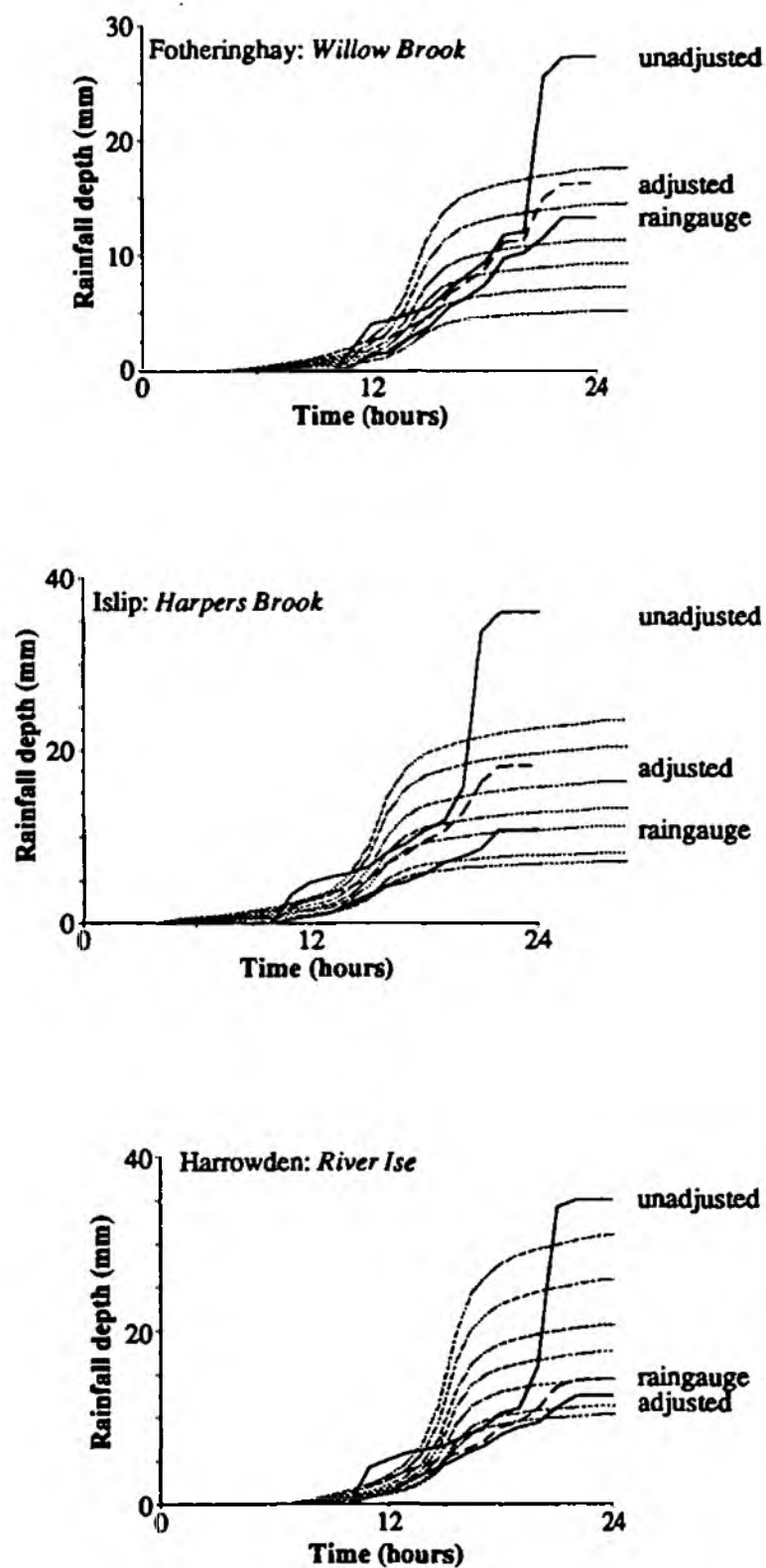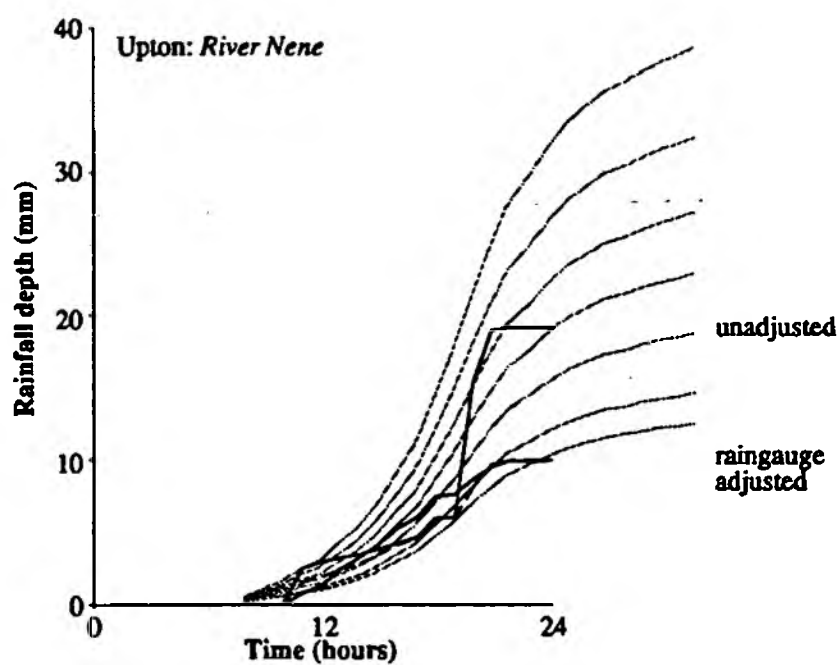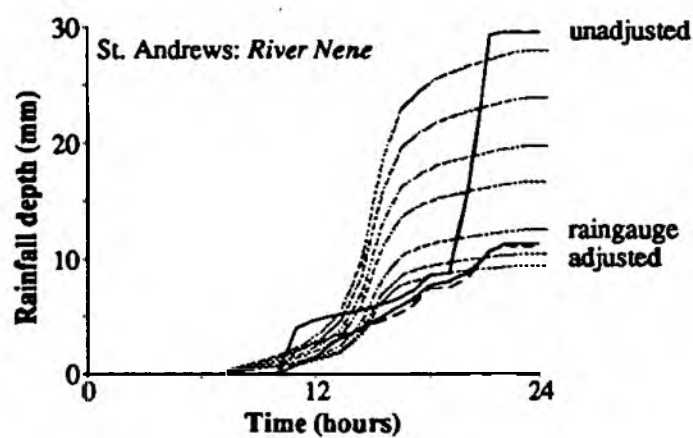unadjusted

Upton: *River Nene*

raingauge
adjusted
unadjusted
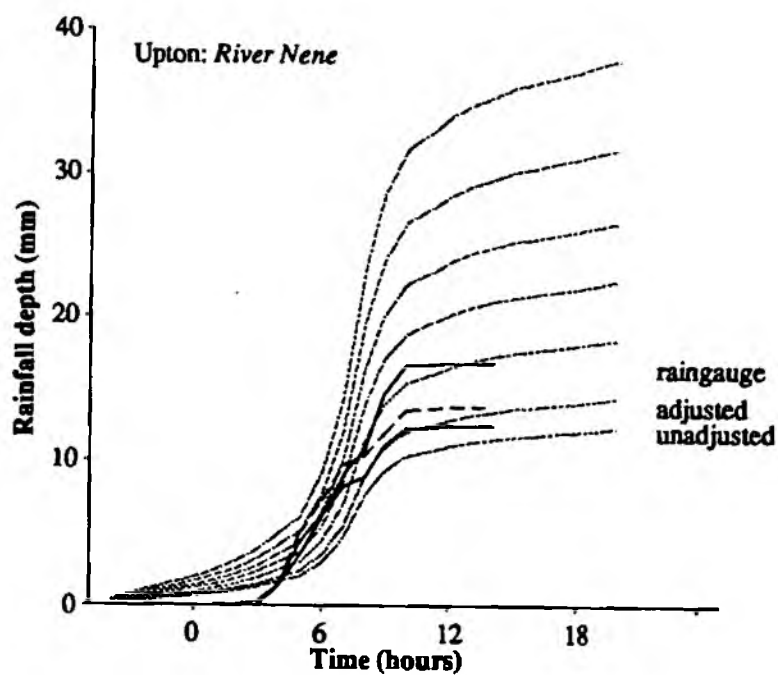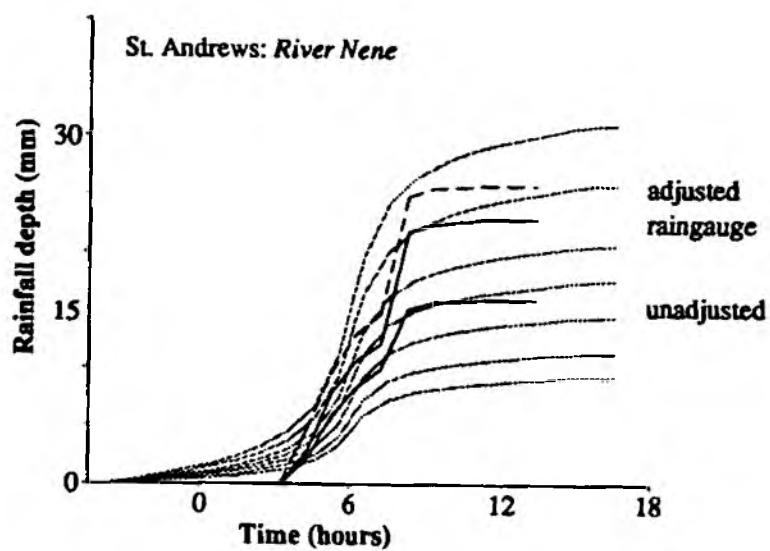
Figure 4.14(b): Cumulative hyetographs for 7th July 1989 data superimposed on 1, 2, 5, 10, 50, and 100 year design storm cumulative hyetographs (75 % peakedness, summer profile)

4.5. End-point Application (EPA) Assessment: River Flow -forecasting

The basis of the EPA assessment is to use the rainfall estimates as input to a common hydrological application. Flood forecasting is perhaps the major use for real-time rainfall data, and it is common for National Rivers Authority Regions to routinely operate many rainfall-runoff models continuously in real-time, so that potential flooding can be forecasted in advance and the necessary warnings processed and disseminated in advance of actual flooding

Flow forecasting also provides a convenient, independent and unbiased means of comparing areal rainfall amounts derived from radar and raingauge data. Simple lumped transfer-function rainfall-runoff models (see ARIP Report 2) were calibrated for two test catchments from existing unit hydrograph ordinates[2] (see Software Profile for TFUH), and catchment averaged rainfall estimates derived from unadjusted and adjusted radar data and raingauge data used as a model input in simulated real-time. The quality of the river flow-forecasts were then objectively compared and each of the data inputs independently assessed. This procedure thereby uses the river catchment as a gauge of areal rainfall. The two test catchments used for the EPA assessment are the Willow Brook catchment to the Fotheringhay gauging station, and the upper section of the River Witham gauged at Colsterworth. The flow modelling was conducted for a number of a total of five days where significant rainfall occurred, three days in December 1989 and two in July 1989.

4.5.1. Case Study 1: 29th-30th July 1989

In this case, flow forecasting was conducted over a two day period during which significant rainfall occurred. The rain was associated with a convective system having high variability in space and time (described more fully in section 4.3.2).

The mean root mean square errors (RMSE) of the flow-forecasts (lead-times ranging from 1-8 hours) for the Fotheringhay and Colsterworth catchments are shown in figure 4.15. The figure shows that for the convective event, the best forecasts are produced using a rainfall input derived from unadjusted radar rainfall data. In both cases raingauge and adjusted radar data inputs produce lower quality flow forecasts. The results are summarised in table 4.4 which shows the overall RMSE of the flow-forecasts (i.e. the mean of the RMSE's for 1, 2, 3,..., 8 step-ahead forecasts). The results demonstrate that overall, flow forecasts derived from an unadjusted radar derived rainfall input are more accurate than those derived from a raingauge data derived input (26% more accurate for the Fotheringhay catchment and 26.5% for the Colsterworth catchment).

---

[2] These unit hydrograph ordinates were derived from a number of past events (using raingauge derived areal rainfall estimates).
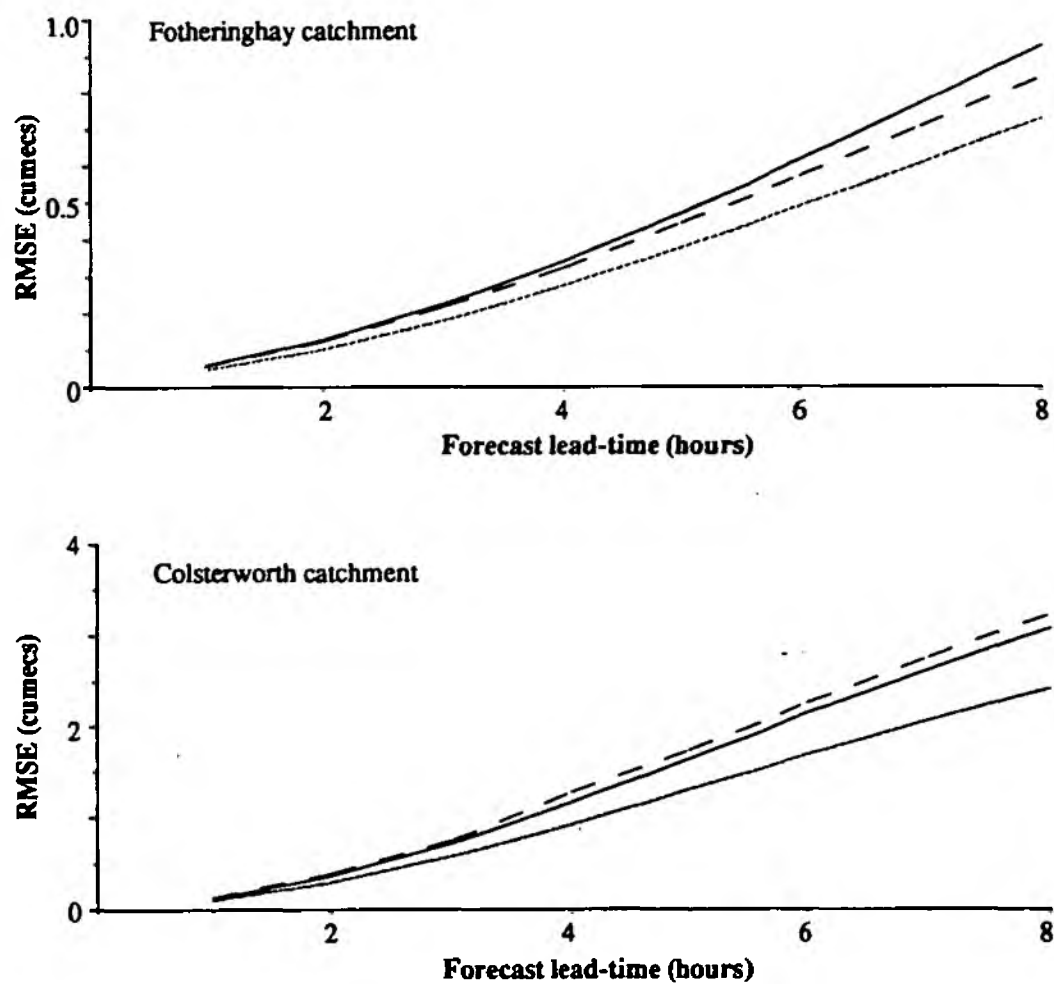
Figure 4.15: Error plots for flow-forecasts: 29-30th July 1989

Table 4.4: <u>Overall root mean square errors of flow-forecasts: convective rainfall</u>

	Fotheringhay	Colsterworth
Unadjusted	0.351	1.172
Adjusted	0.410	1.561
Raingauge	0.442	1.482

From these observations it is possible to conclude that the raingauge network does not accurately represent the spatial structure of the rainfall field. The validity of the gauge-truth assumption, questioned in previous sections is again questioned and it is surmised that in cases such as this, where the rainfall field is highly dynamic in space and time, and where there is no bright-band problem, unadjusted radar derived observations provide the best estimates of areal rainfall. Furthermore, adjustment of the unadjusted radar data with gauge data produces an adjusted radar field that, though more closely resembling the raingauge data, is actually accuracy degraded.

4.5.2. Case Study 2: 14th, 16th and 18th December 1989

In this case, flow forecasting was conducted over three days in December 1989. This was a period of prolonged rainfall during which widespread rainfall associated with a frontal weather system sweeping across the British Isles occurred (refer to section 3.4.1 for further information). The rainfall was stratiform and although there are some localised showers associated with the system, spatial and temporal variation is low. A bright-band was present much of the time and was most intense on the 18th.

The mean root mean square errors (RMSE) of the flow-forecasts (lead-times ranging from 1-8 hours) for the Fotheringhay and Colsterworth catchments are shown in figure 4.16(a) Fotheringhay catchment and 4.16(b) Colsterworth catchment.

In every case, forecasting errors were reduced when adjusted radar rainfall data were used as a model input compared to unadjusted radar rainfall inputs. The results are summarised in table 4.5 which shows the overall RMSE of the flow-forecasts (i.e. the mean of the RMSE's for 1, 2, 3,..., 8 step-ahead forecasts).
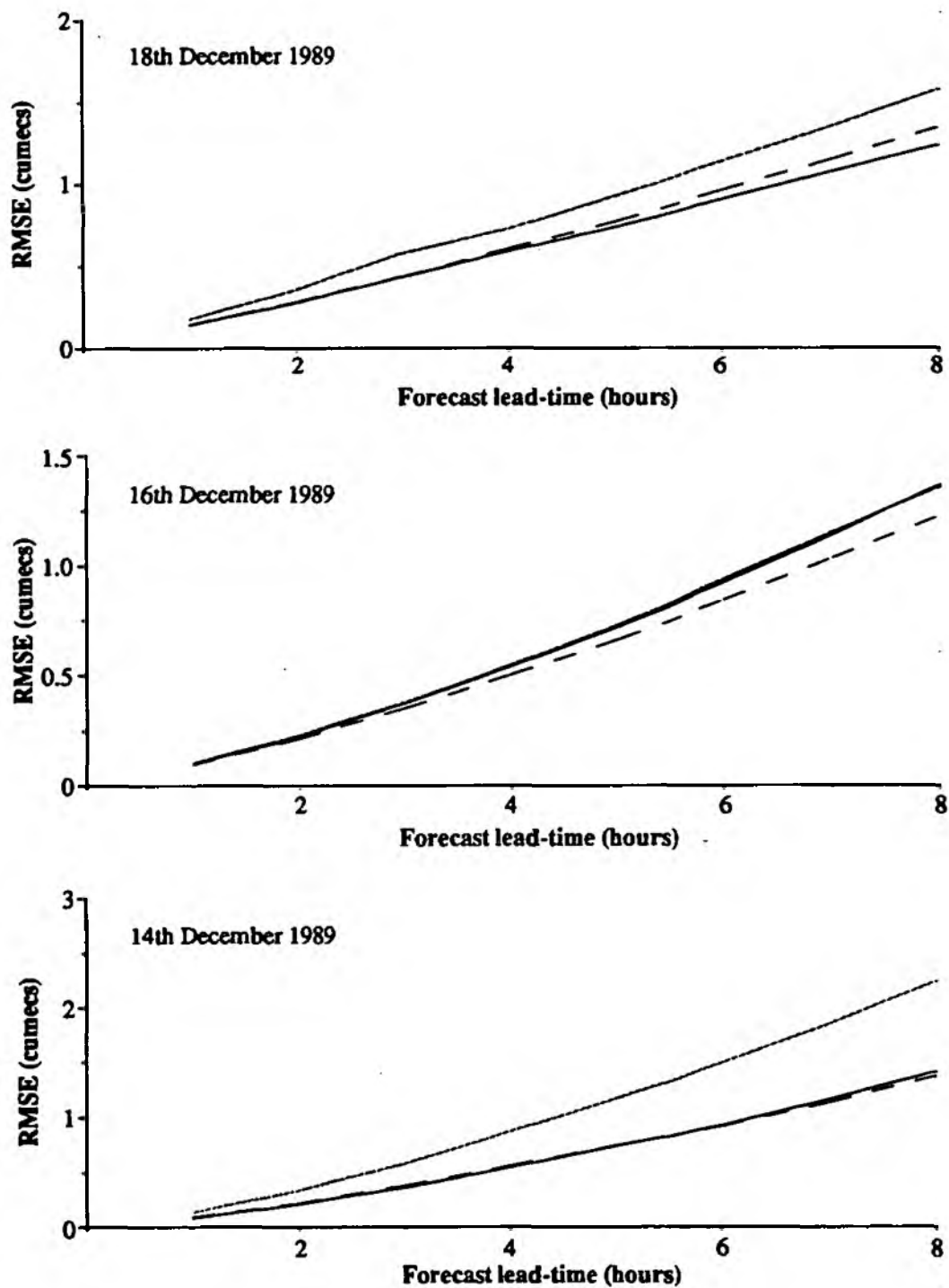
Figure 4.16(a): Error plots for flow-forecasts: Fotheringhay catchment
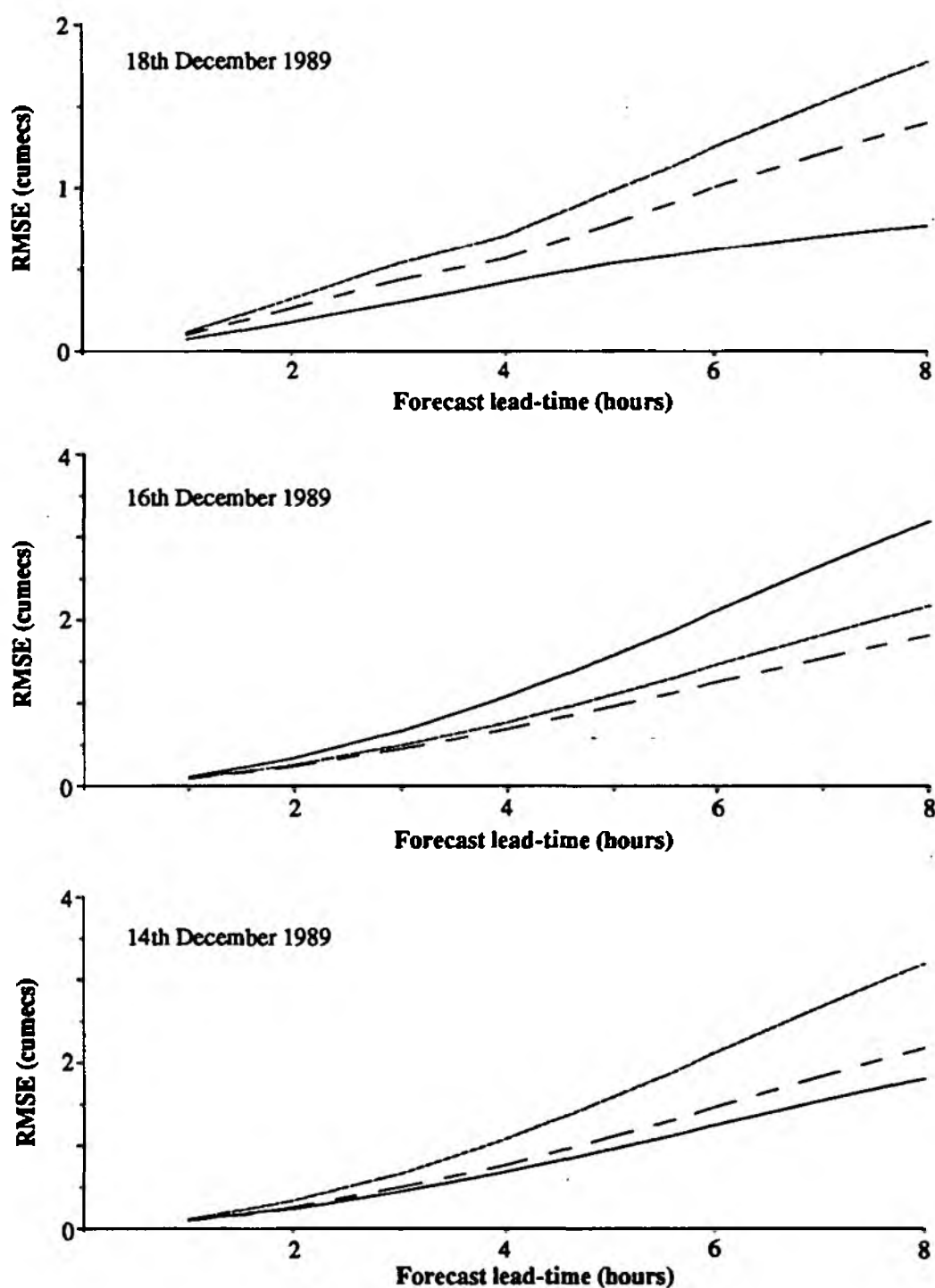
Figure 4.16(b): Error plots for flow-forecasts: Colsterworth catchment

Table 4.5: Overall root mean square errors of flow-forecasts: stratiform rainfall

	14th Dec	16th Dec	18th Dec
i. Fotheringhay			
Unadjusted	1.084	0.679	0.857
Adjusted	0.674	0.614	0.712
Raingauge	0.680	0.673	0.678
ii. Colsterworth			
Unadjusted	1.473	0.502	0.903
Adjusted	1.025	0.483	0.719
Raingauge	0.881	0.569	0.453

Most striking of all are the results for the 18th December where the best quality forecasts were obtained from the use of a raingauge derived input whilst forecasts from an unadjusted radar derived rainfall input were significantly worse. In this case it appears that although adjustment improves the quality of the forecasts significantly, the severe effect of the bright-band is not completely removed. For the 14th and 16th the best performance for the Fotheringhay catchment resulted from use of the adjusted radar rainfall input and the forecasts produced from an unadjusted radar derived rainfall input were the worst. For Colsterworth on the 14th the raingauge derived rainfall input produced the best forecasts whilst the worst were those from an unadjusted radar rainfall input.

There is no clear overall pattern for these events, except that when the bright-band affect is particularly severe, as it was on the 18th December, the adjustment procedure struggles to remove all the bright-band artifacts and unadjusted radar data forecasts are invariably of poorer quality than adjusted radar or raingauge derived inputs. In such circumstances areal rainfall estimates derived from the raingauge data provide the best flow-forecasts. It should be remembered however, that for the comparison the transfer function was used with parameter updating disabled and the capability of the model to compensate for exactly this type of input data error was removed. In the other cases adjustment does produce a better quality product suggesting that the adjustment procedure has been successful in combining the point accuracy of the raingauges with the spatial information content of the radar data.

As a cautionary note to the interpretation of statistics: the difference between forecasts is often far less dramatic than the statistics often imply. An example is provided by the Fotheringhay model on the 14th December, a case where adjustment produces an overall improvement of 61% in overall RMSE over the unadjusted data. Figure 4.17 shows five 8-hour ahead forecasts made through the course of the event for unadjusted (i) and adjusted radar data inputs (ii), and mean

RMSE's of the 2, 4, 6, and 8 step-ahead forecasts for both are shown on figure 4.18. The figures show that although impressive in statistical error terms, there is only a minor difference in terms of a visual assessment of future flows and the consequences in terms of real-time flood-forecasting and warning need to be carefully considered.

4.6. Radar Intensity Resolution: Three-bit and Eight-bit Radar Data

The utility of three-bit rainfall data for forecasting flows in small-medium sized rural catchments has already been investigated in detail and is not covered further in this report. The general conclusion was that the use of three-bit radar rainfall data for flood forecasting did not compromise forecast accuracy significantly, and models calibrated using three-bit data do not vary significantly to those derived from eight-bit data. For further information the reader is referred to ARIP Report 2.

A brief study investigated the influence of data intensity resolution on areal rainfall estimation and consequently storm frequency estimation using data for two rainfall events, the 7th July 1989 and 18th December 1989 (see section 4.3.1 and 4.3.2 for further information on these events). Cumulative storm hyetographs derived from unadjusted and adjusted eight and three-bit data, for five test catchments are shown in figure 4.19 for the 7th July 1989 and figure 4.20 for 18th December 1989.

The RMSE's of the cumulative hyetographs derived from eight and three-bit radar rainfall data are shown in table 4.6. The statistics show that for the 7th July rainfall the overall deviation between hyetographs is small (never exceeding 0.31 mm for unadjusted data) and in all cases, adjustment of the radar data increases the deviation, in the case of the two larger catchments (St. Andrews and Upton) significantly. However given the comments of previous sections this is not serious since the unadjusted radar data better represent the actual rainfall field. The hyetographs show that the impact of reduced intensity resolution is scale related and becomes more significant for the larger catchments. The errors of the bright-band affected stratiform rainfall on the 18th December are considerably higher, and unlike the previous case, adjustment reduces the difference between the eight and three-bit derived hyetographs. The scale relationship is not clearly defined for this case.

The impact of reduced intensity resolution on storm frequency estimation is not severe. Table 4.7 and 4.8 shows return periods of storms estimated from three and eight-bit radar data for the 7th July data and the 18th December events respectively.

In all cases the return periods estimated from the three-bit data are broadly in-line with those estimated from eight-bit data particularly for the 18th December data. Although the storm frequency estimation procedure does not benefit from the data processing that a flow-forecasting model provides, and is therefore more sensitive to any differences in the rainfall data, intensity

i). unadjusted radar rainfall input
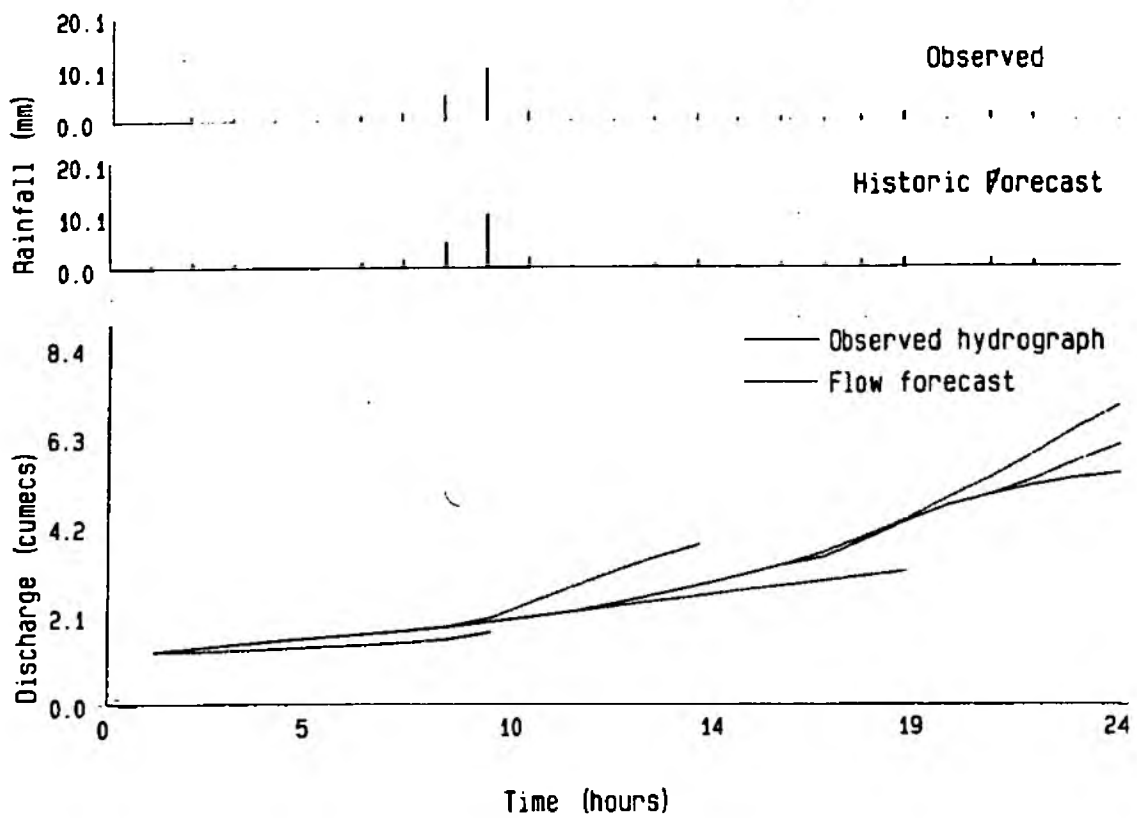
ii). adjusted radar rainfall input
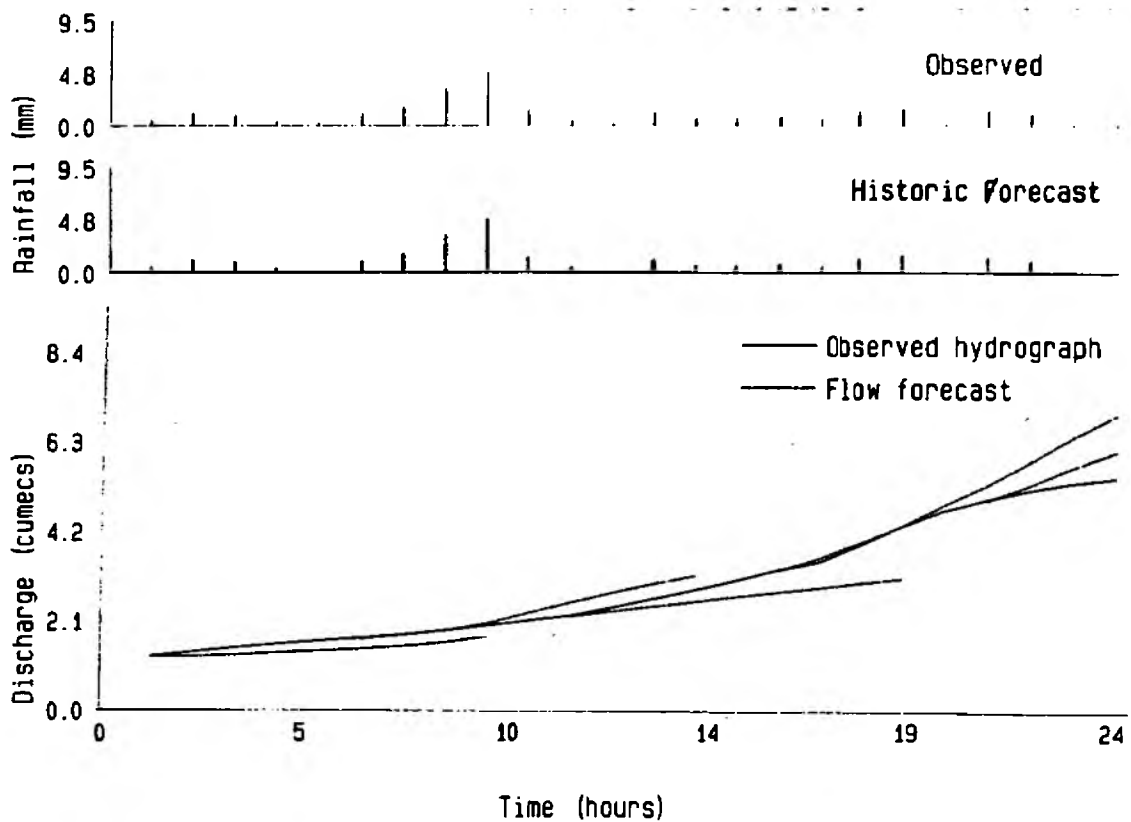
Figure 4.17: Flow forecasting comparison: 14th December 1989, Fotheringhay catchment
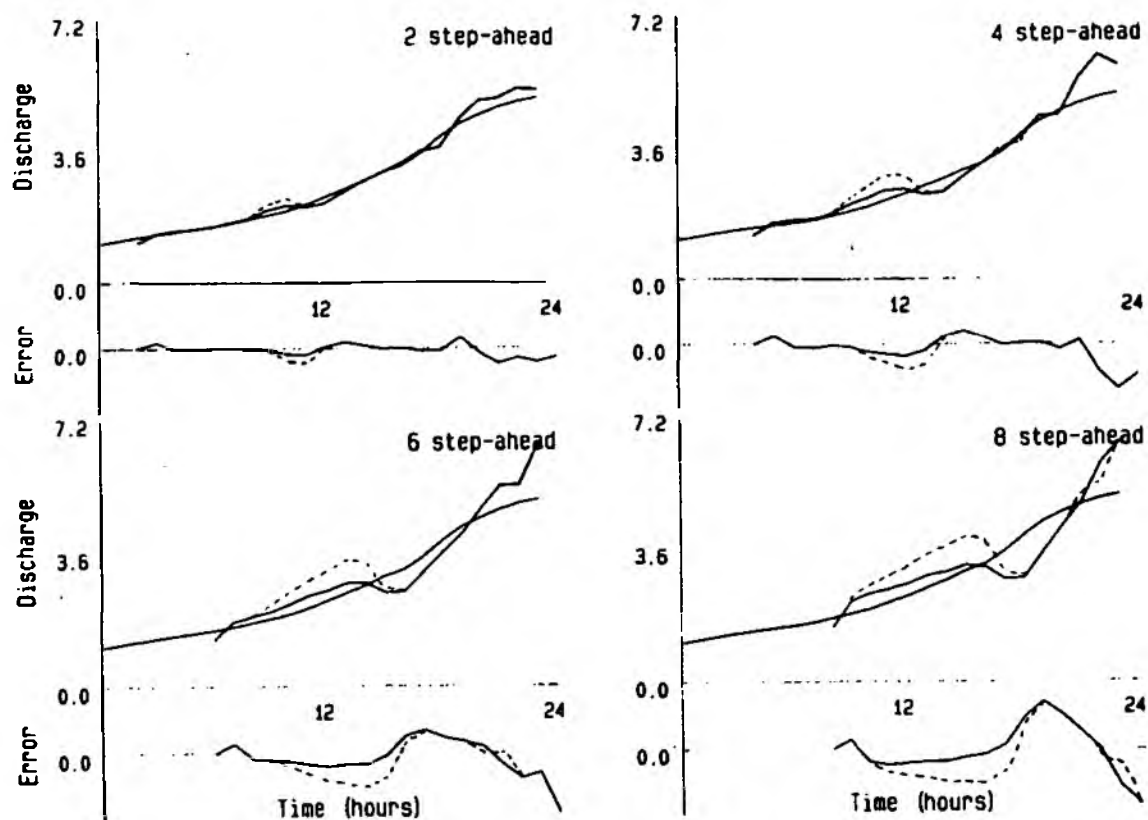
Figure 4.18: Flow forecasting error comparison: 14th December 1989, Fotheringhay catchment
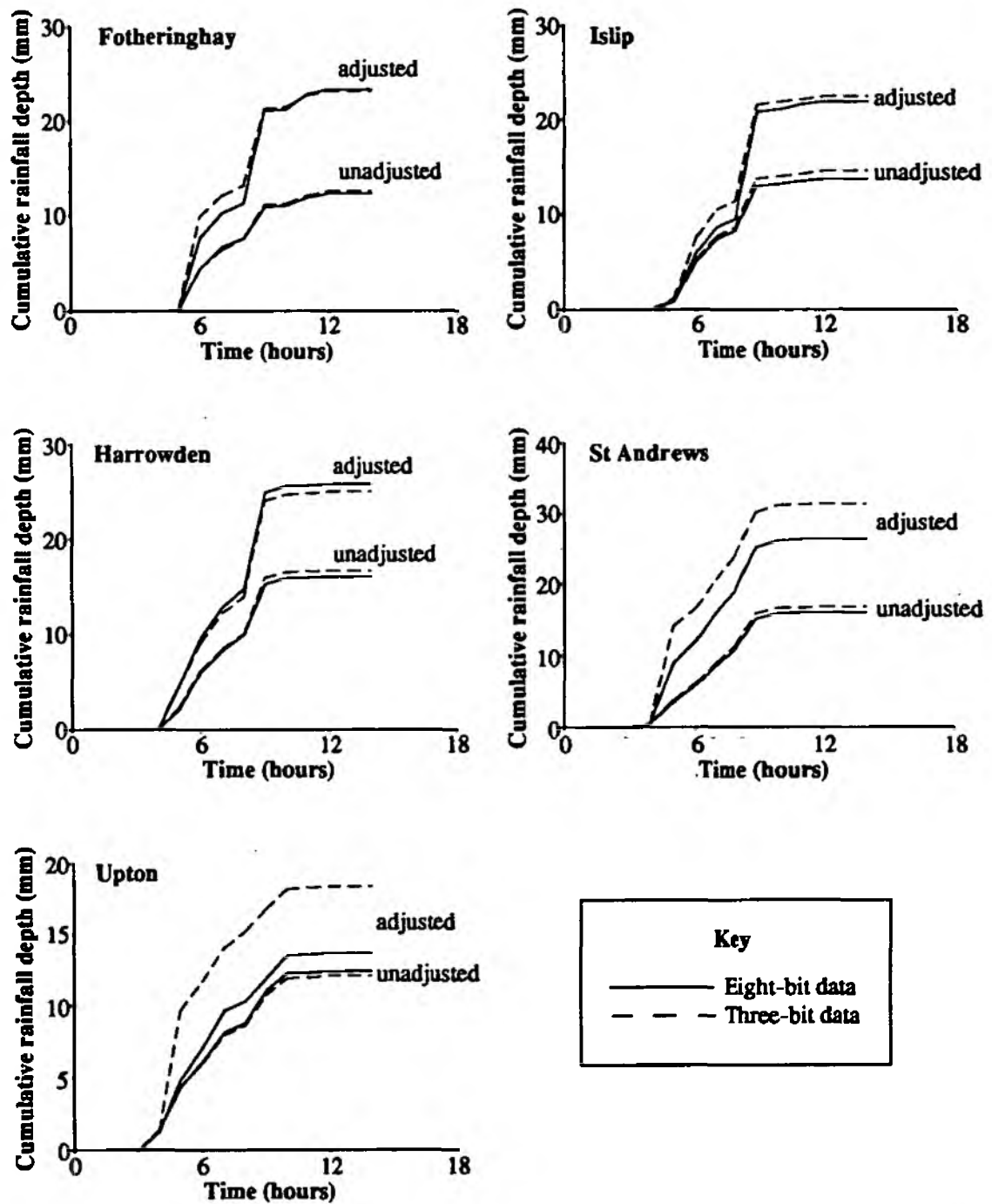
Figure 4.19: Cumulative hyetographs derived from unadjusted and adjusted eight-bit and three-bit radar rainfall data: 7th July 1989
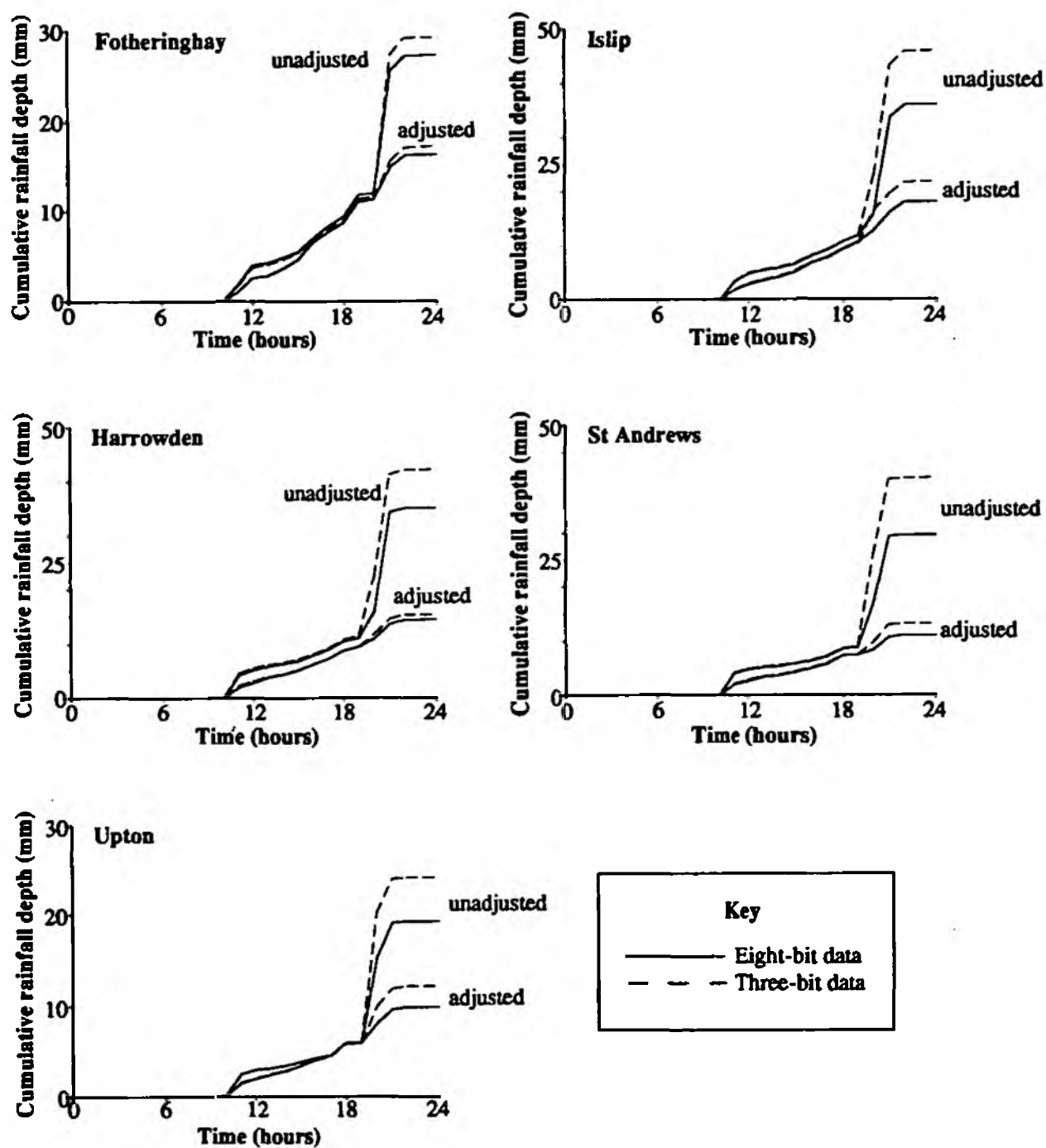
Figure 4.20: Cumulative hyetographs derived from unadjusted and adjusted eight-bit and three-bit radar rainfall data: 18th December 1989

resolution does not have a major impact on the estimation of areal rainfall amounts, and therefore on storm frequency estimation.

Table 4.6: <u>Root mean square errors of cumulative hyetographs derived from eight and three radar rainfall data</u>

	7th July 1989		18th December 1989	
	unadjusted	adjusted	unadjusted	adjusted
Fotheringhay	0.090	0.400	0.448	0.114
Islip	0.232	0.623	1.964	0.787
Harrowden	0.246	0.434	1.545	0.214
St. Andrews	0.308	2.881	2.159	0.431
Upton	0.169	2.745	1.040	0.474

Table 4.7: <u>Storm return periods for three and eight-bit data: 7th July 1989</u>

	Eight-bit		Three-bit	
	unadjusted	adjusted	unadjusted	adjusted
Fotheringhay	12	> 100	12	> 100
Islip	9	90	10	90
Harrowden	9	75	10	60
St. Andrews	8	50	9	100
Upton	1	2	<1	5

Table 4.8: <u>Storm return periods for three and eight-bit data: 18th December 1989</u>

	Eight-bit		Three-bit	
	unadjusted	adjusted	unadjusted	adjusted
Fotheringhay	>100	80	>100	85
Islip	>100	35	>100	45
Harrowden	>100	3	>100	5
St. Andrews	>100	3	>100	5
Upton	5	< 1	10	1

4.7. Concluding Comments

The chapter has presented the results of investigations into the use of adjusted radar data for areal rainfall estimation, storm period return period estimation, and river flow-forecasting. In addition, the influence of data intensity resolution on radar adjustment for areal rainfall estimation and storm frequency analysis has been examined. In all cases, assessment has been carried out with a minimum of two different rainfall events of different rainfall types: convective summer showers and winter stratiform rainfall.

Over a 23 day evaluation period which embraced rainfall data for a wide range of synoptic conditions, the adjustment procedure achieves a reduction in the deviation of the radar derived catchment averaged rainfall compared to that derived from the unadjusted radar data of 29%. In comparison, the impact of the real-time Meteorological Office 'calibration' procedure is shown to be slight and even the cause of additional errors in the data.

The low spatial variability of stratiform rainfall means that point raingauge measurements are generally representative of rainfall over an area. Consequently, raingauge-based adjustment of radar data can be quite successful in such rainfall systems. This is particularly true in cases where a bright-band effect is present. A severe bright-band can introduce large errors into radar rainfall estimates, to the extent that even if the bright-band is only present for a few hours, areal rainfall estimates for a 24 hour period can be error by as much as a factor of five. The adjustment procedure has been shown to be effective in dealing with these errors and significantly reduces the deviation between the raingauge and radar data.

In convective rainfall systems where the rainfall process is highly dynamic and spatial and temporal variability can be extremely high (a case is cited where two raingauges separated by 15 km measured 4 mm and 31 mm of rainfall respectively), raingauges typically overestimate areal rainfall. Weather radar data tend to be high quality in such rainfall systems because of the high spatial resolution and the absence of a bright-band to degrade quantitative accuracy. Thus, whilst the adjustment procedure effectively reduces the deviation between the unadjusted radar and raingauge rainfalls (the procedure implicitly assumes that raingauge amounts are correct), an accurate rainfall field is in fact being accuracy degraded by being 'corrected' with a less accurate raingauge field (the gauge-truth assumption is violated). This hypothesis was backed-up by the end-point application (EPA) analysis where in convective rainfall the best quality flow-forecasts for two catchments were those derived from an unadjusted radar rainfall input. The unsatisfactory nature of raingauge adjustment in these circumstances is graphically illustrated by a 'circus tent-pole' effect where gauge unrepresentativeness produces an unreasonable adjusted radar rainfall field.

An investigation into storm return period estimation using raingauge and radar data found that a severe bright-band can introduce unacceptable errors into the radar data. Whilst adjustment of the radar data significantly reduces these errors, in the severest bright-band cases the error was

still significant.

The influence of the intensity resolution of radar data on 'front-end' rainfall products has been investigated for a stratiform rainfall event and a convective system. The results indicate that for stratiform rainfall, adjustment reduces the difference between cumulative hyetographs derived from eight and three-bit radar data to the extent that storm frequency estimates for five test catchments derived from the three and eight-bit data do not differ significantly. A scale relationship appears to operate for stratiform rainfall whereby the difference between eight and three-bit derived cumulative hyetographs increases with area. For the convective event, the difference between the three and eight-bit cumulative hyetographs increases after adjustment. This is not regarded as serious in the light of comments made earlier regarding raingauge representativeness in such circumstances and the difference between unadjusted three and eight-bit hyetographs is insignificant for hydrological applications (either front-end products or end-point applications). It is concluded that three-bit radar data are sufficient for hydrological applications.

The adjustment procedure is useful in all but summer convective rainfalls where the raingauge-truth assumption of the adjustment procedure is violated. The procedure provides a significant bright-band correction capability which means that radar data can be used operationally with higher confidence in circumstances where confidence would otherwise be low. In rainfall conditions where the adjustment raingauges are representative of rainfall, the procedure successfully combines the point accuracy of the raingauges whilst retaining the spatial information content of the radar data. This is illustrated in the EPA assessment where areal rainfall estimates derived from adjusted radar data provide better forecast accuracy than either raingauge or unadjusted derived amounts.

Chapter 5.   Raingauge Network Density

Intrinsically linked with raingauge adjustment of radar data is the question of raingauge density. In the analyses described in chapter 4, all available raingauge data have been used. However, the question of 'how many raingauges, and where ?' invariably occurs and consequently a brief study was conducted to address these questions and investigate the influence of network density on areal and point rainfall estimates derived from the adjusted radar data. Raingauge network density and network rationalisation are complex topics and a detailed study was not possible in the time available, so a limited number of case studies have been used in conjunction with five test catchments. Despite these limitations, the study does provide a good indication of the sensitivity of areal rainfall estimation, and of the adjustment procedure in particular for different synoptic conditions.

5.1.   Influence of Raingauge Network Density on Areal Rainfall Estimates

This section presents the results of an analysis into the influence that the density of the raingauge network used for adjusting the radar data has on quantitative areal rainfall estimation.

The approach taken was to select case study events for different types of rainfall, i.e. one winter stratiform the other summer convective, for which significant rainfall occurred, and for which a large number of raingauges were available. Areal rainfall amounts were then estimated from raingauge data, and unadjusted and adjusted radar for each of the test catchments, for different raingauge network densities. Four different densities for each case study were used corresponding to a full network, i.e. all available raingauges, and 75%, 50% and 25% networks. To form the reduced density networks, raingauges were removed subjectively. An attempt was made to maintain even coverage across the entire adjustment area.

For each of the test catchments, cumulative hyetographs of catchment rainfall derived from raingauge data and from unadjusted and adjusted radar data have been plotted, for each of the network densities. Visual comparison between the figures provides a subjective indication of the impact of network density, and a more objective assessment is provided the error figures and statistics. In these, the cumulative rainfall amounts derived from the full raingauge network are assumed to be the actual areal rainfall, and error of the radar data is computed as the deviation from these raingauge 'truth-indices'.

In addition to assessing the impact of the raingauge network density on the adjustment procedure, areal rainfall totals were also computed directly from the raingauge data (via interpolation to a regular grid, and nodal averaging - see QUANTARE Software Profile) for the different densities and the resulting areal amounts compared. It has therefore been possible to assess the influence of network density on areal rainfall amounts derived solely from the raingauge data and thereby

assess the sensitivity of the estimation procedure (interpolation algorithm) to network density for different rainfall types.

5.1.1.   Case Study 1: 18th December 1989

As discussed in chapter 4 (section 4.3.1) widespread, significant, and spatially uniform rainfall occurred on this day. The event is also of interest because of the influence of a severe bright-band effect (see ARIP Report 4, and section 2.6) causing major overestimation of rainfall in the area by the radar. A total of 68 gauges were available and the three 'reduced density' networks therefore have 51, 34, and 17 raingauges (75%, 50%, 25%). The four networks are shown in figure 5.1. Also on the figure are the locations of the five test catchments.

Figure 5.2 shows cumulative hyetographs for each of the test catchments derived from raingauge data alone with the four different raingauge networks. A visual comparison suggests only a small variation between hyetographs despite the difference in the number of raingauges used to determine the rainfall amounts. The results are summarised in table 5.1 which shows the total areal rainfall for each catchment derived from each the networks, and the maximum difference between them in percentage difference terms. The table shows that the maximum difference between any of the areal totals for any catchment is 23%, the average maximum difference being just over 12%. The low variation in the rainfall estimates is attributable to the low spatial variation of the event.

Table 5.1: Areal rainfall estimation using different raingauge network densities: 18th December 1989

Catchment	Raingauge network density				Mean	Maximum % difference
	25%	50%	75%	100%		
Fotheringhay	14.211	15.206	13.464	13.269	14.038	12.8
Islip	14.022	13.266	11.088	10.790	12.292	23.0
Harrowden	12.037	12.210	12.438	12.505	12.298	3.7
St. Andrews	11.043	12.372	11.547	11.298	11.565	10.7
Upton	11.301	10.868	10.946	9.952	10.767	11.9

Figure 5.3 shows the unadjusted (i) and adjusted (ii) radar rainfall fields and the raingauge rainfall field (iv) together with the mean assessment factor field (iii) for the day for each of the raingauge network densities ([a] 75%, [b] 50%, [c] 25%, for full network see figure 4.3). The figures provide a visual illustration of the impact of network density on the adjustment procedure. It is immediately apparent that as the density decreases, the impact of the adjustment lessens.

25 % network (17 gauges)   50 % network (34 gauges)
75 % network (51 gauges)   100 % network (68 gauges)
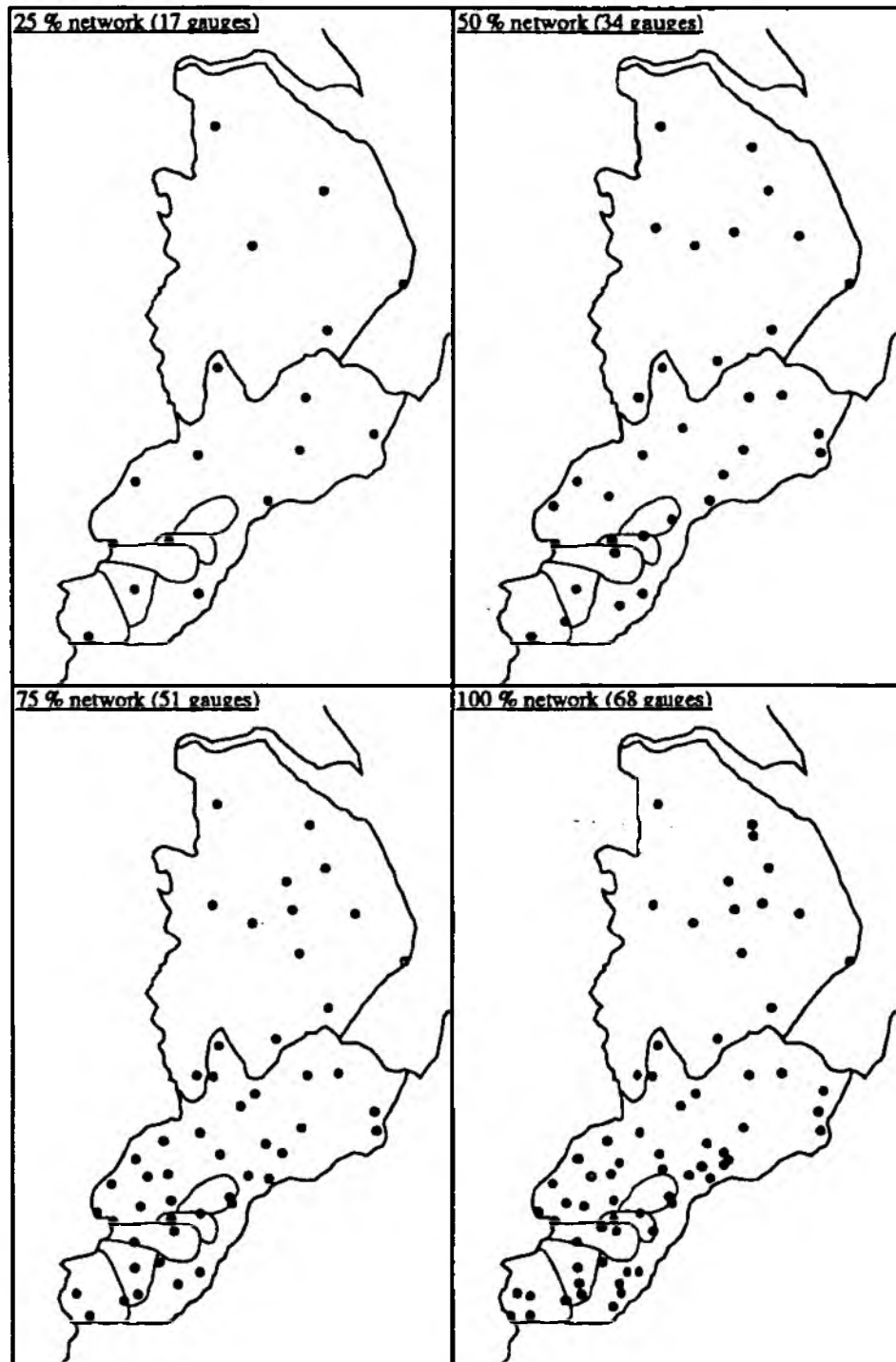
Figure 5.1: Raingauge networks: 18th December 1989
(test catchments superimposed)
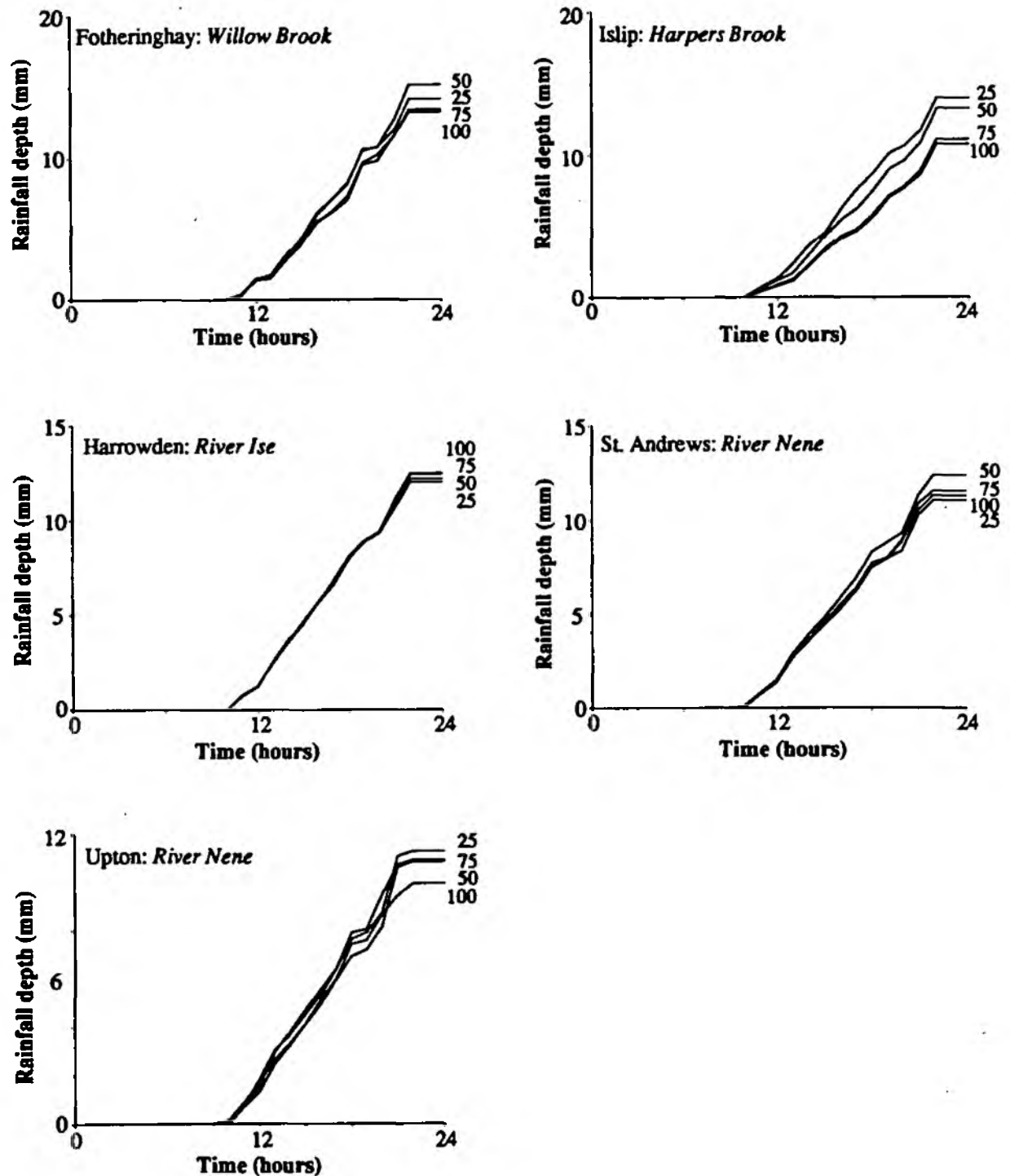
Figure 5.2: Catchment averaged rainfall amounts derived from interpolated raingauge data from networks of varying densities: 18th December 1989
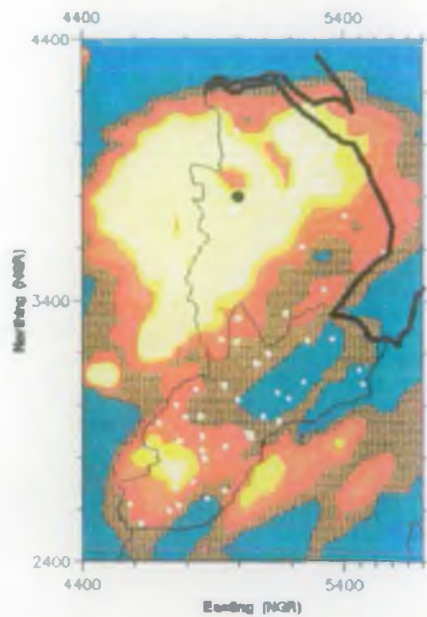
i). unadjusted radar
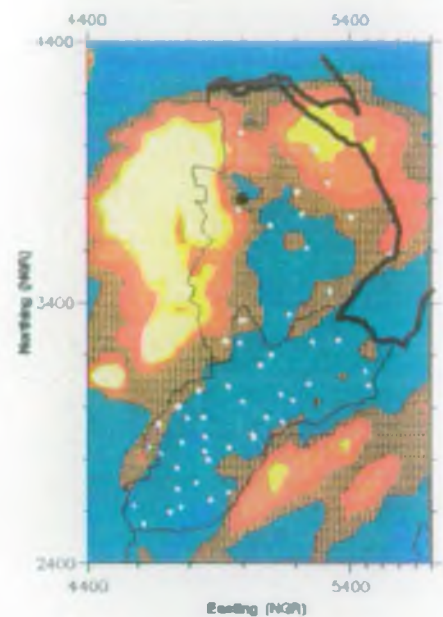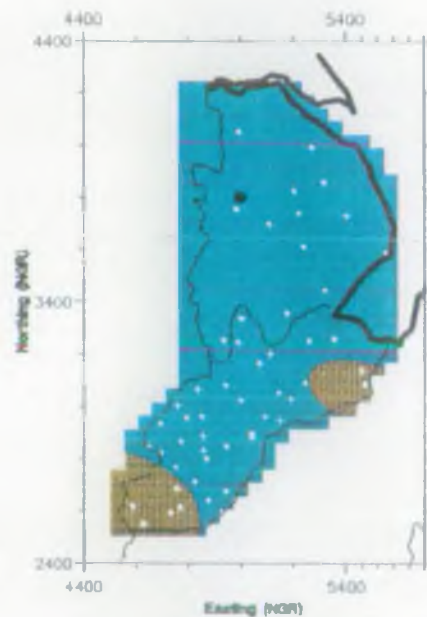
ii). adjusted radar

iii). assessment factors
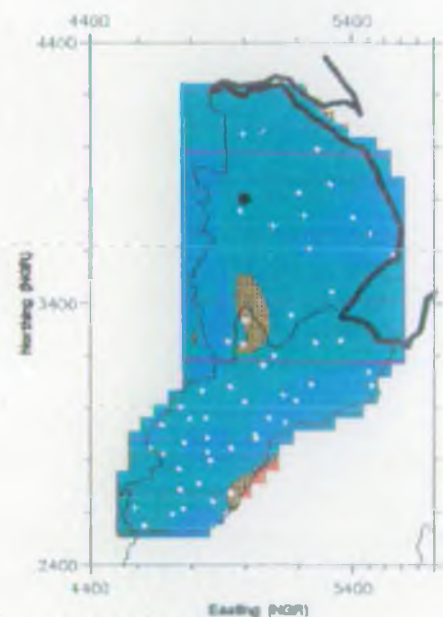
iv). interpolated raingauge
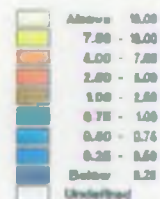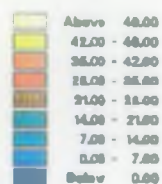
Figure 5.3a: Radar adjustment fields, 75%, 18th December 1989 (Ingham radar)
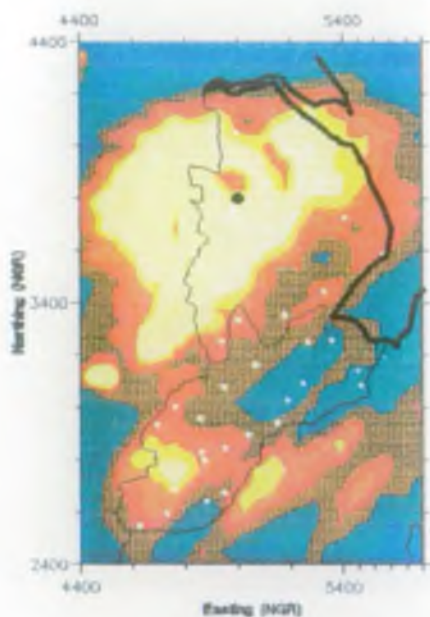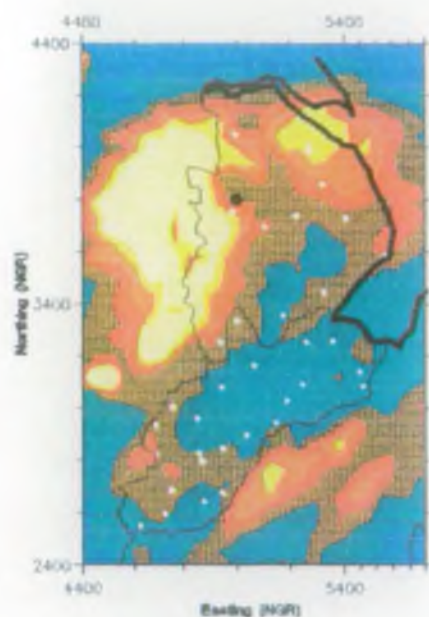
i). unadjusted radar
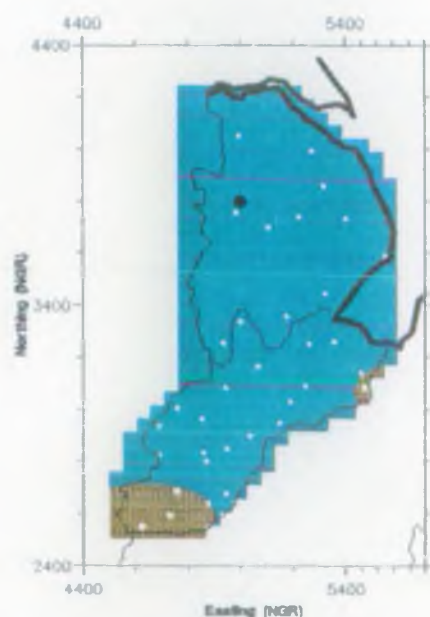
ii). adjusted radar

iii). assessment factors
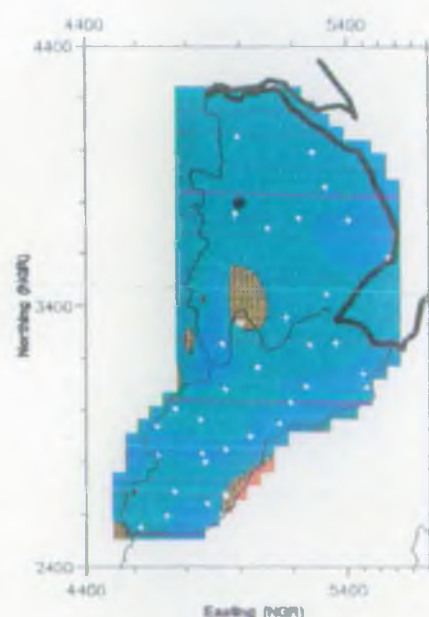
iv). interpolated raingauge
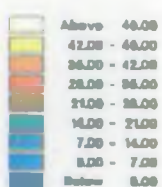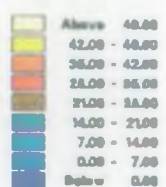
Figure 5.3b: Radar adjustment fields, 50%, 18th December 1989 (Ingham radar)
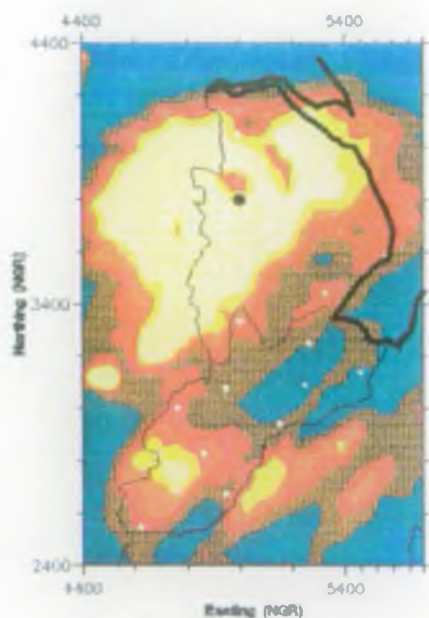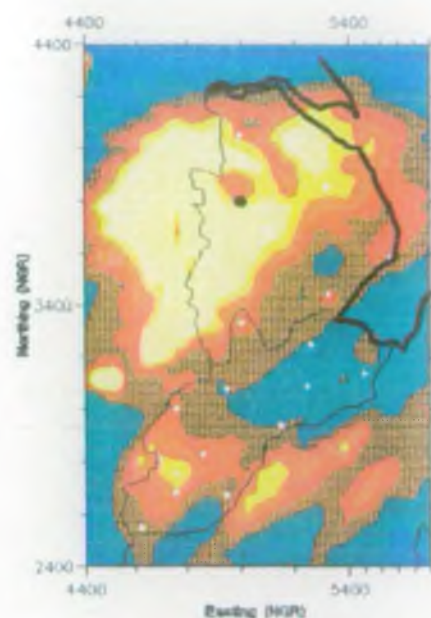
i). unadjusted radar

ii). adjusted radar
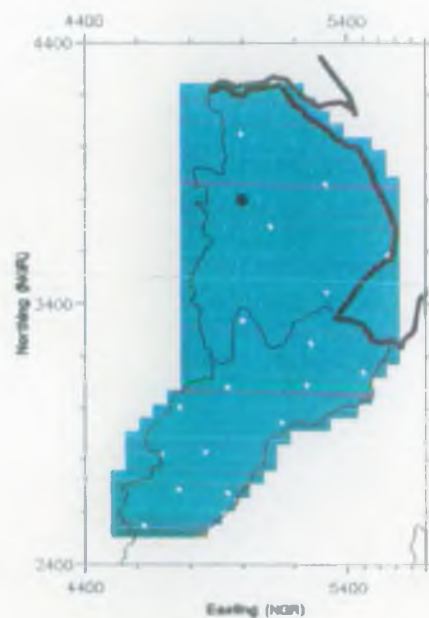
iii). assessment factors
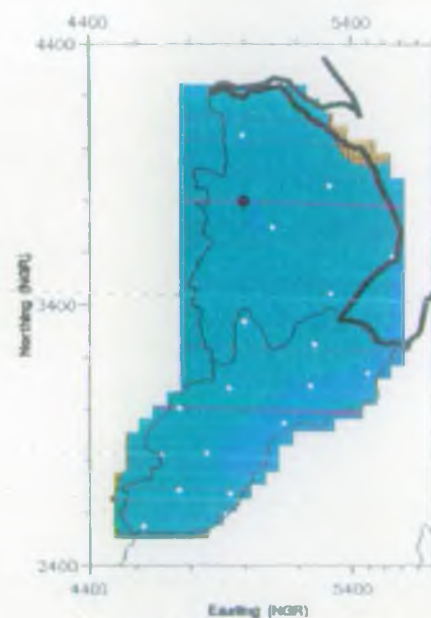
iv). interpolated raingauge
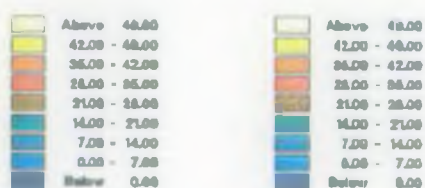
Figure 5.3c: Radar adjustment fields, 25%, 18th December 1989 (Ingham radar)

Cumulative hyetographs for each of the test catchments derived from all available raingauges (assumed truth), unadjusted radar data and radar data adjusted with the four different raingauge networks are shown in figures 5.4(a) full network, (b) 75% network, (c) 50% network, and (d) 25% network. Visual assessment shows that despite the low spatial variability of the rainfall event, the density of the raingauge network exerts a major influence on the areal totals derived from the adjusted radar data, and the extent to which the deviation between raingauge and radar derived amounts is reduced falls with decreasing network density. This pattern is highlighted in figure 5.5 which shows the mean percentage 'error' (i.e. deviation from the 100% raingauge network derived amounts) in the adjusted radar rainfall amounts. The figure shows that for all catchments, the error increases with falling network density although it should be noted that the difference between the errors for the full (100%) network and the 75% network are not large. The results illustrated in the figure are statistically summarised in table 5.2. Here, a single statistic (RMSE) is computed for each error trace in the figure, so since there are five traces per catchment (unadjusted radar, 25%, 50%, 75%, and 100% error), each catchment has five RMSE statistics which provide an indication of mean percentage error over the entire 24 hour period. The results shown in table 5.2 are represented graphically in figure 5.6.

Table 5.2: <u>Root mean square (%) error of areal rainfall estimates: 18th December 1989</u>

Catchment	Unadjusted	Network density			
		100%	75%	50%	25%
Fotheringhay	23.9	7.3	8.9	11.2	19.5
Islip	55.9	21.9	22.2	30.1	48.3
Harrowden	40.6	5.8	5.6	16.9	33.3
St Andrews	35.7	2.4	2.4	12.3	27.5
Upton	22.8	3.9	5.2	9.5	17.0

Figure 5.6 shows that the relationship between the density of the raingauge network used for radar adjustment is related to areal estimation error by an S-curve. Hence, adjustment using very low density networks has only marginal benefits in terms of error reduction, and beyond an upper threshold density errors are no longer reduced as the raingauge network density increases. In between these upper and lower bounds (the top and bottom portions of the S), there is a middle segment where errors are reduced quite considerably with an increase in network density. Overall, the figure suggests that the best compromise between error reduction and network density for this case study is for the 75% network which corresponds to 51 gauges. This is equivalent to a network density of 185 km^2/gauge, or a mean inter-gauge spacing of just under 14 km.

Figure 5.4(a): Catchment averaged rainfall amounts. 100% network:
18th December 1989

Figure 5.4(b): Catchment averaged rainfall amounts. 75% network:
18th December 1989

Figure 5.4(c): Catchment averaged rainfall amounts, 50% network:
18th December 1989

Figure 5.4(d): Catchment averaged rainfall amounts, 25% network: 18th December 1989

Figure 5.5: Error in cumulative catchment averaged rainfall:
18th December 1989
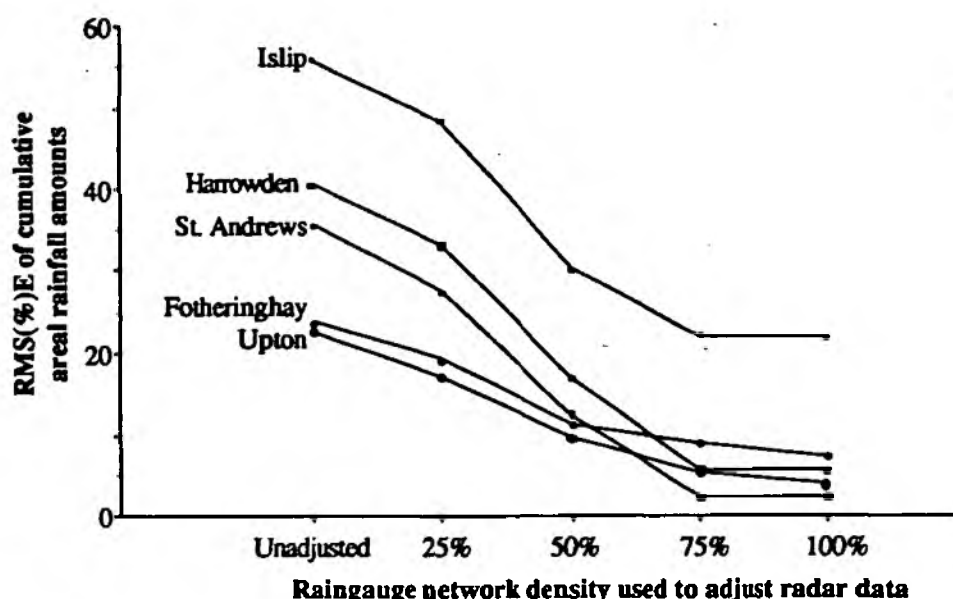
Figure 5.6: Mean RMS(%)E of areal rainfall estimates: 18th December 1989

5.1.2. Case Study 2: 30th July 1989

As discussed in Chapter 3 (section 3.2.2) localised, significant, and spatially variable rainfall occurred on this day. A total of 67 gauges were available and the three 'reduced density' networks therefore have 50, 33, and 17 raingauges (75%, 50%, 25%) respectively. The four networks are shown in figure 5.7. Also on the figure are the locations of the five test catchments.

Figure 5.8 shows cumulative hyetographs for each of the test catchments derived from raingauge data alone with the four different raingauge networks. A visual comparison reveals a large variation between hyetographs. The results are summarised in table 5.3 which shows the total areal rainfall derived from each the networks for each catchment, and the maximum difference between them in percentage difference terms. The table shows that the maximum difference between any of the areal totals for any catchment is 49.3%, the average maximum difference being just over 32%. This variation is considerably higher than for the stratiform event in case study 1, and is indicative of the higher spatial variation of convective rainfalls.

Figure 5.9 shows the unadjusted (i) and adjusted (ii) radar rainfall fields and the raingauge rainfall fields (iv) together with the mean assessment factor field (iv) for the day for each of the raingauge network densities ([a] 75%, [b] 50%, [c] 25%, for full network see figure 4.11). The figures provide a visual illustration of the impact of network density on the adjustment procedure.
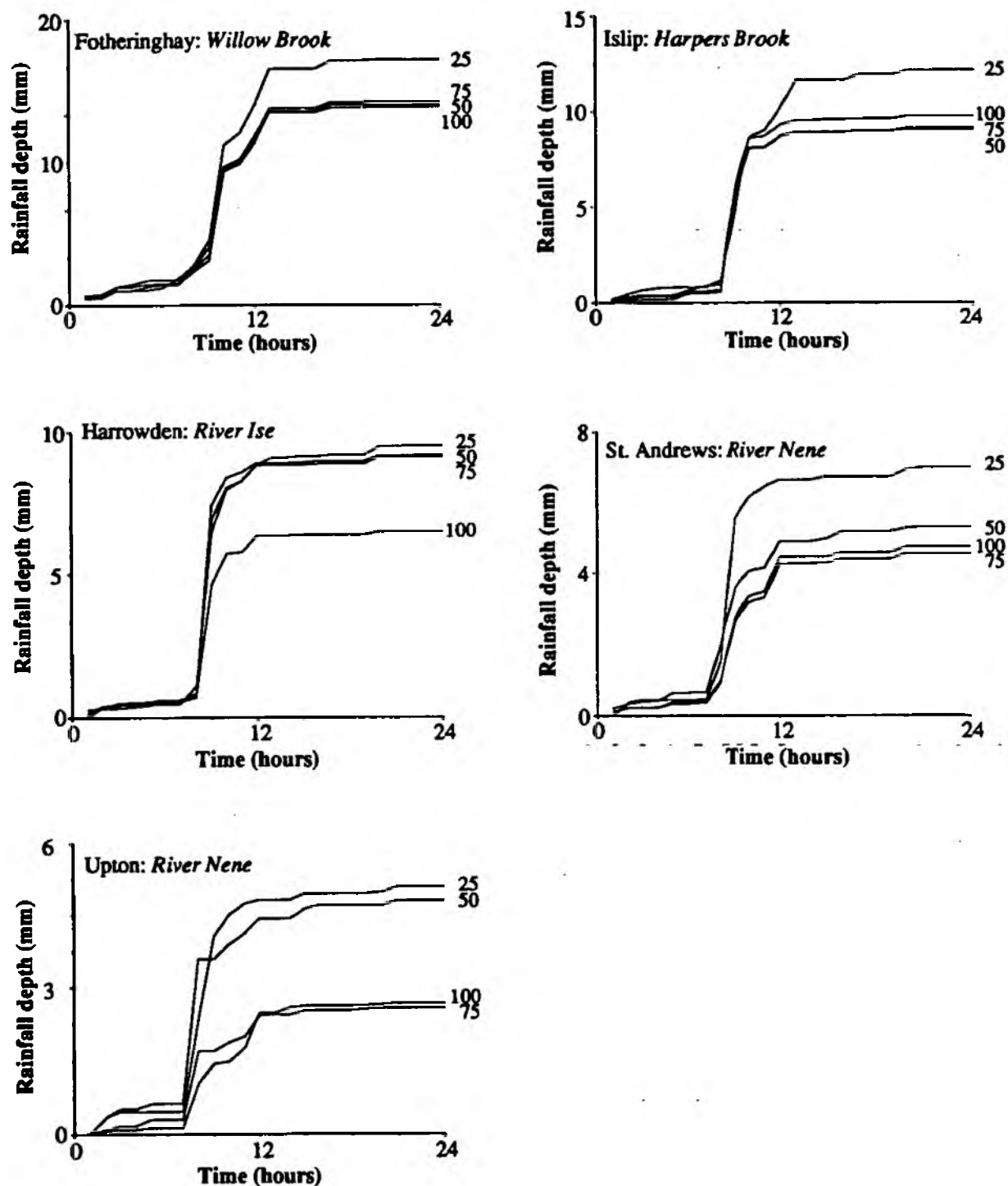
Figure 5.8: Catchment averaged rainfall amounts derived from interpolated raingauge data from networks of varying densities: 30th July 1989
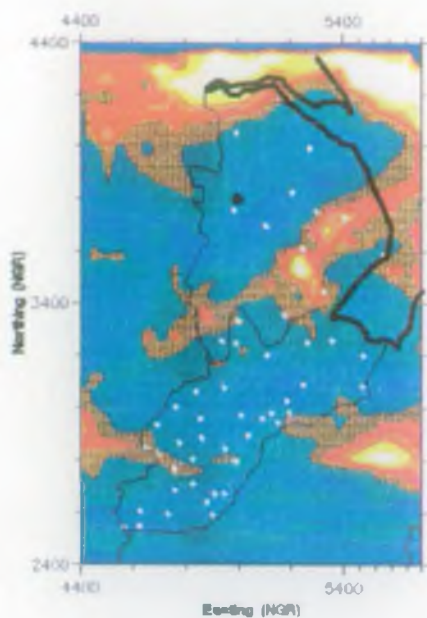
i). unadjusted radar
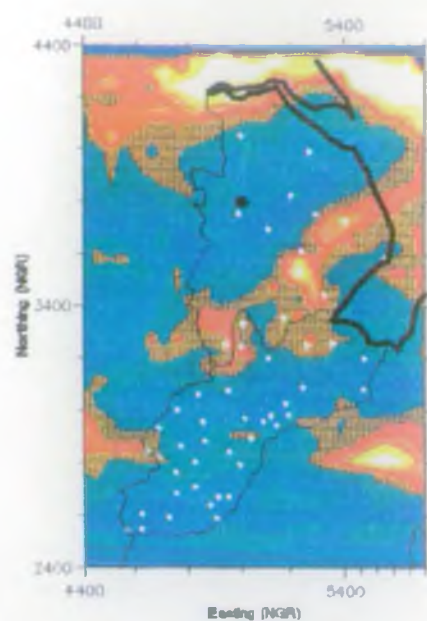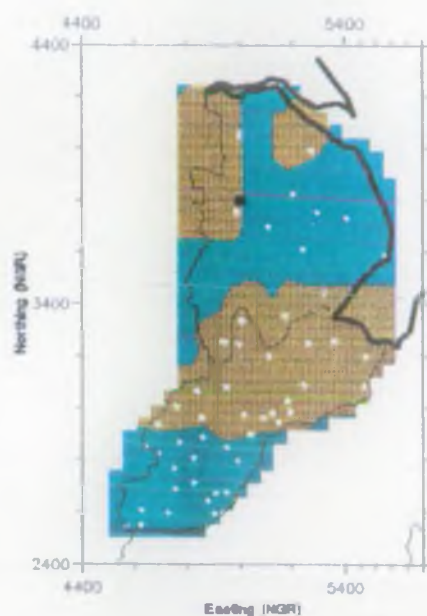
ii). adjusted radar

iii). assessment factors
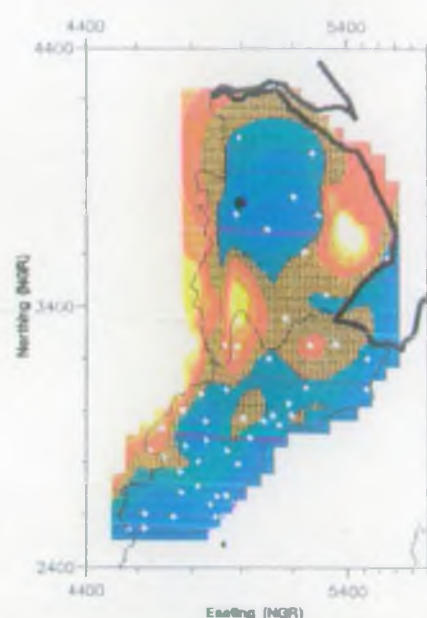
iv). interpolated raingauge

Figure 5.9a: Radar adjustment fields, 75%, 30th July 1989 (Ingham radar)
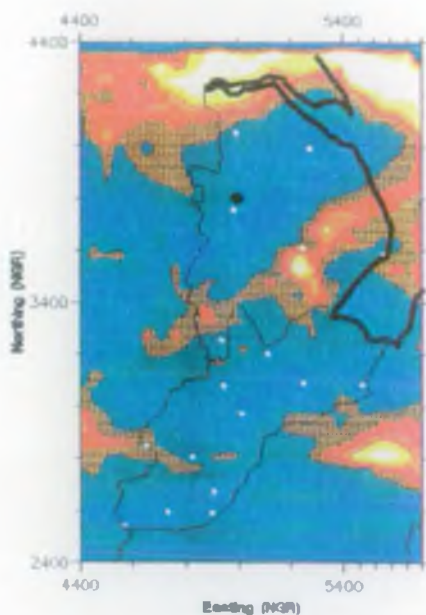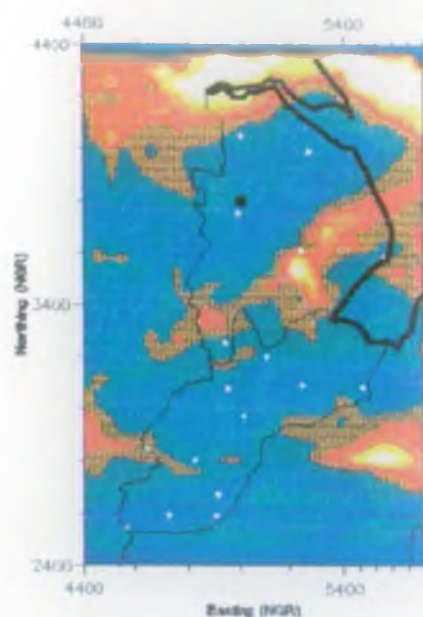
i). unadjusted radar
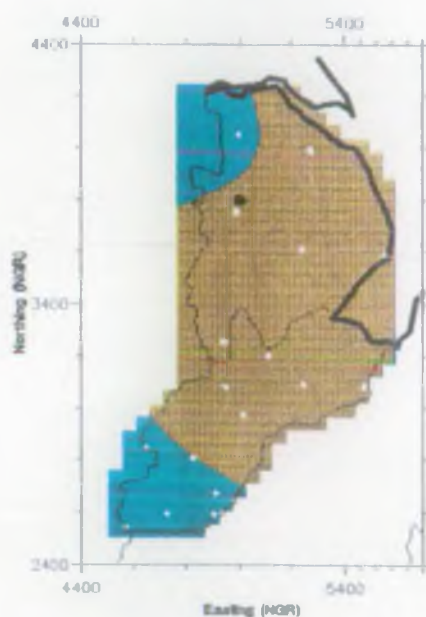
ii). adjusted radar

iii). assessment factors
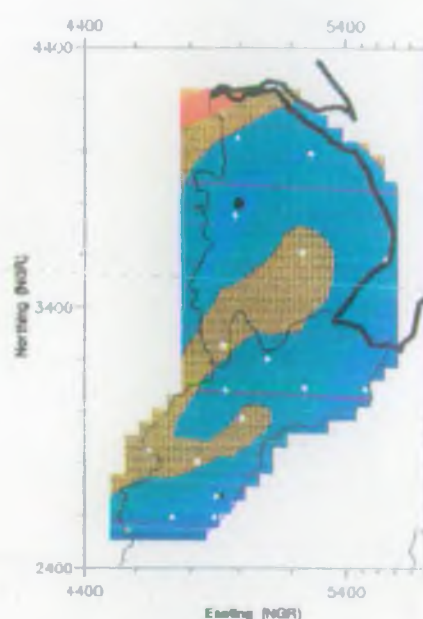
iv). interpolated raingauge
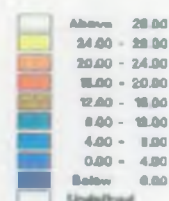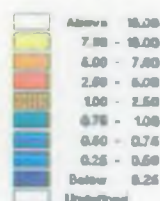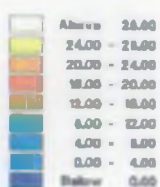
Figure 5.9b: Radar adjustment fields, 50%, 30th July 1989 (Ingham radar)
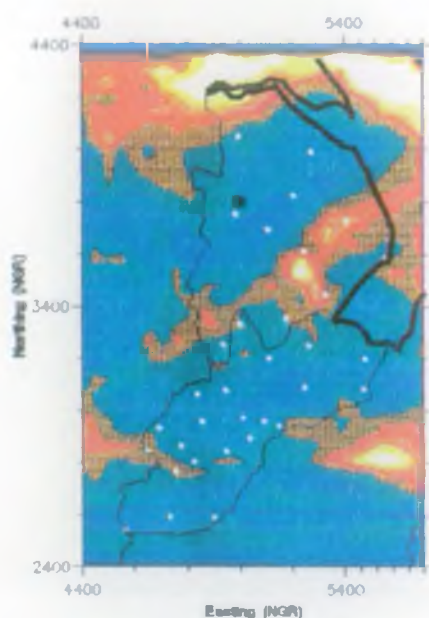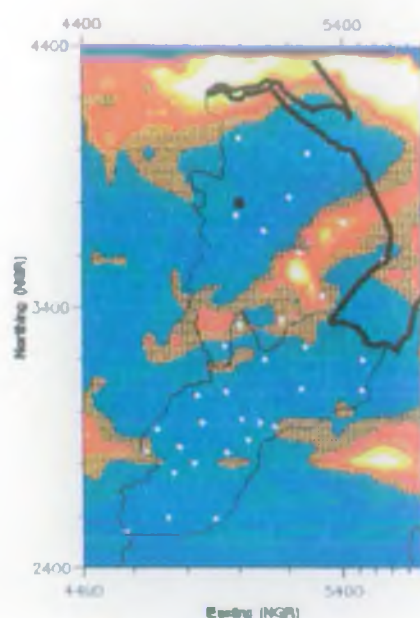
i). unadjusted radar

ii). adjusted radar
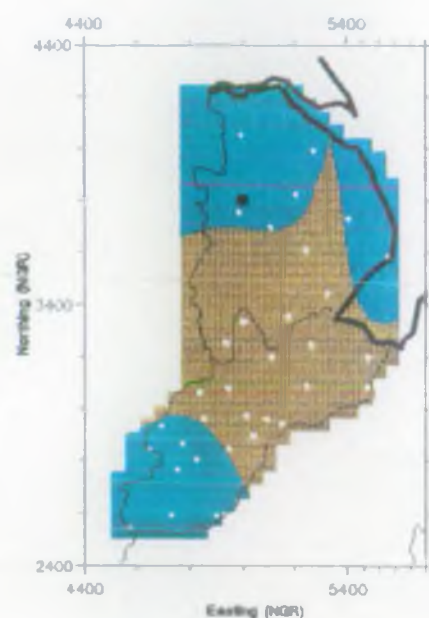
iii). assessment factors
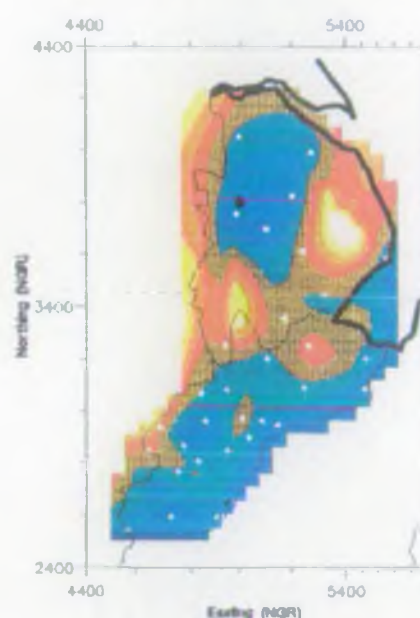
iv). interpolated raingauge
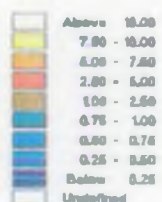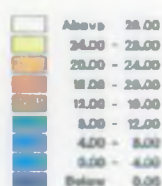
Figure 5.9c: Radar adjustment fields, 25%, 30th July 1989 (Ingham radar)

Table 5.3: <u>Areal rainfall estimation using different raingauge network densities:</u>
<u>30th July 1989</u>

Catchment	Raingauge network density				Mean	Maximum % difference
	25%	50%	75%	100%		
Fotheringhay	10.387	10.665	10.508	12.881	11.110	19.4
Islip	9.764	9.125	9.060	12.185	10.034	25.6
Harrowden	6.506	9.131	9.171	9.499	8.578	31.5
St Andrews	4.756	4.560	5.309	6.999	5.406	34.8
Upton	2.665	2.578	4.800	5.088	3.783	49.3

It is immediately apparent from this example that the representativeness of raingauges in rainfall systems with high spatial variation is limited and that quite different pictures of the rainfall can result from different raingauge topologies.

Cumulative hyetographs for each of the test catchments derived from all available raingauges (assumed truth), unadjusted radar data and radar data adjusted with the four different raingauge networks are shown in figures 5.10(a) - full network, (b) 75% network, (c) 50% network, and (d) 25% network. Visual inspection shows that the density of the raingauge network exerts a major influence on the areal totals derived from the adjusted radar data but unlike the stratiform case, there is no well defined relationship between the density of the raingauge network and the deviation of the areal rainfall estimates from the gauge-truth index. The lack of any consistent pattern is attributed to the high spatial variability of the rainfall event and the influence that even individual gauges can have on areal rainfall estimation when the spatial variation of the rainfall is high.

Figure 5.11 shows mean percentage 'error' (i.e. deviation from the 100% raingauge network derived amounts) in the adjusted radar rainfall amounts. Once again the lack of any consistent overall relationship between network density and error is observed. The results illustrated in figure 5.11 are statistically summarised in table 5.4. Here, a single statistic (RMSE) is computed for each error trace in the figure, and since there are five traces per catchment (unadjusted radar, 25%, 50%, 75%, and 100% error), each catchment has five RMSE statistics which provide an indication of mean percentage error over the entire 24 hour period. The results shown in table 5.4 are represented graphically in figure 5.12.
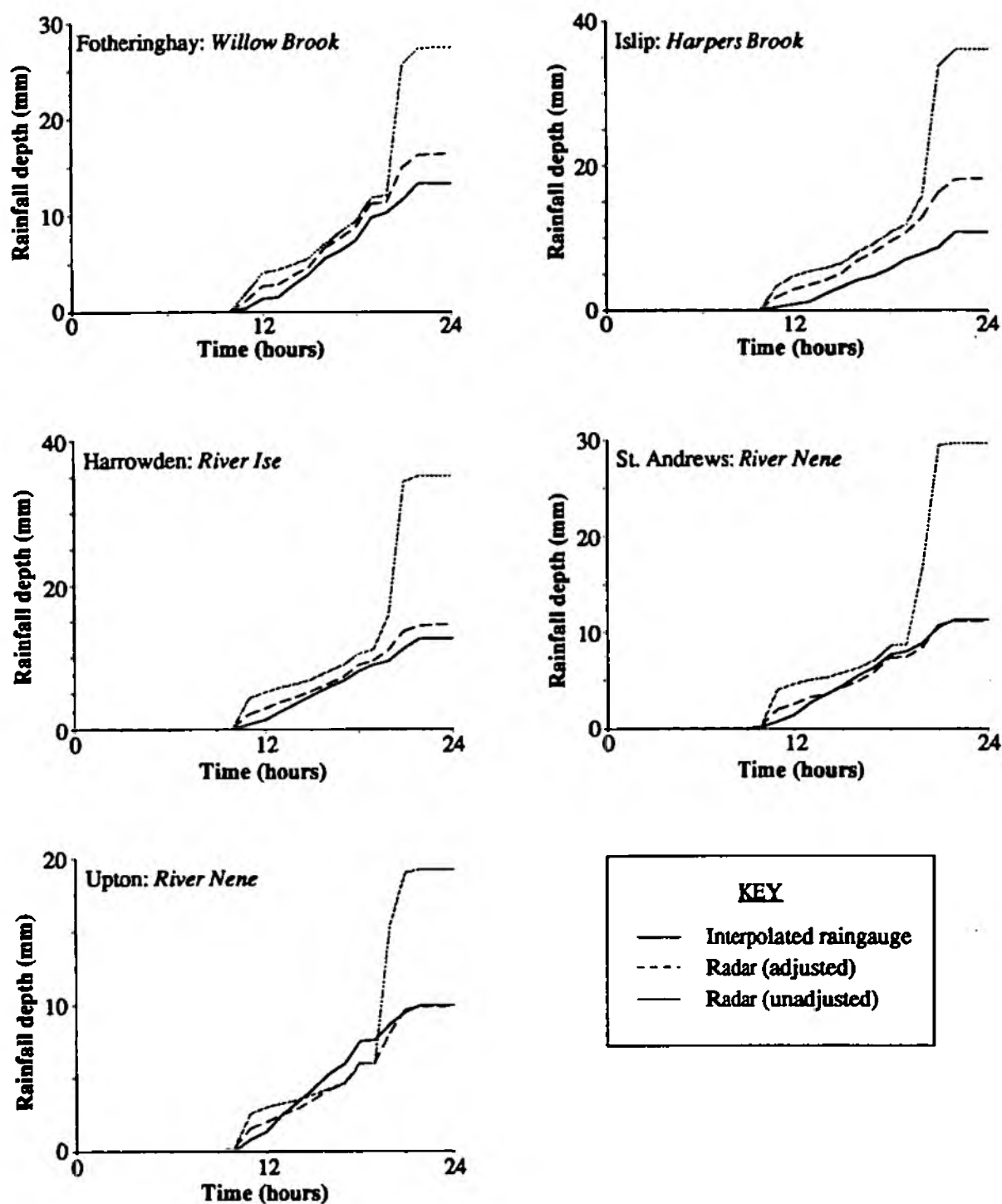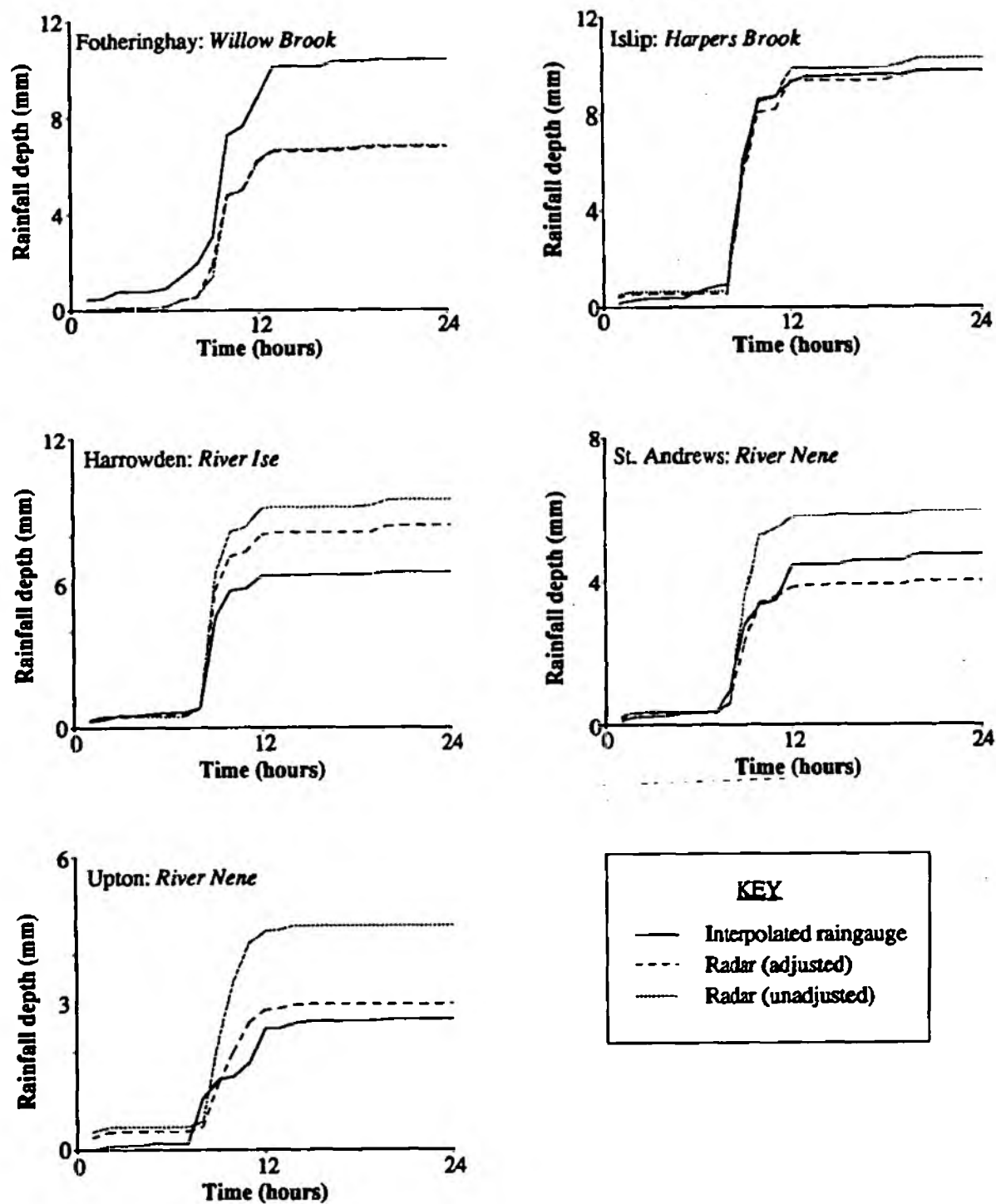
Figure 5.10(a): Catchment averaged rainfall amounts, 100% network: 30th July 1989
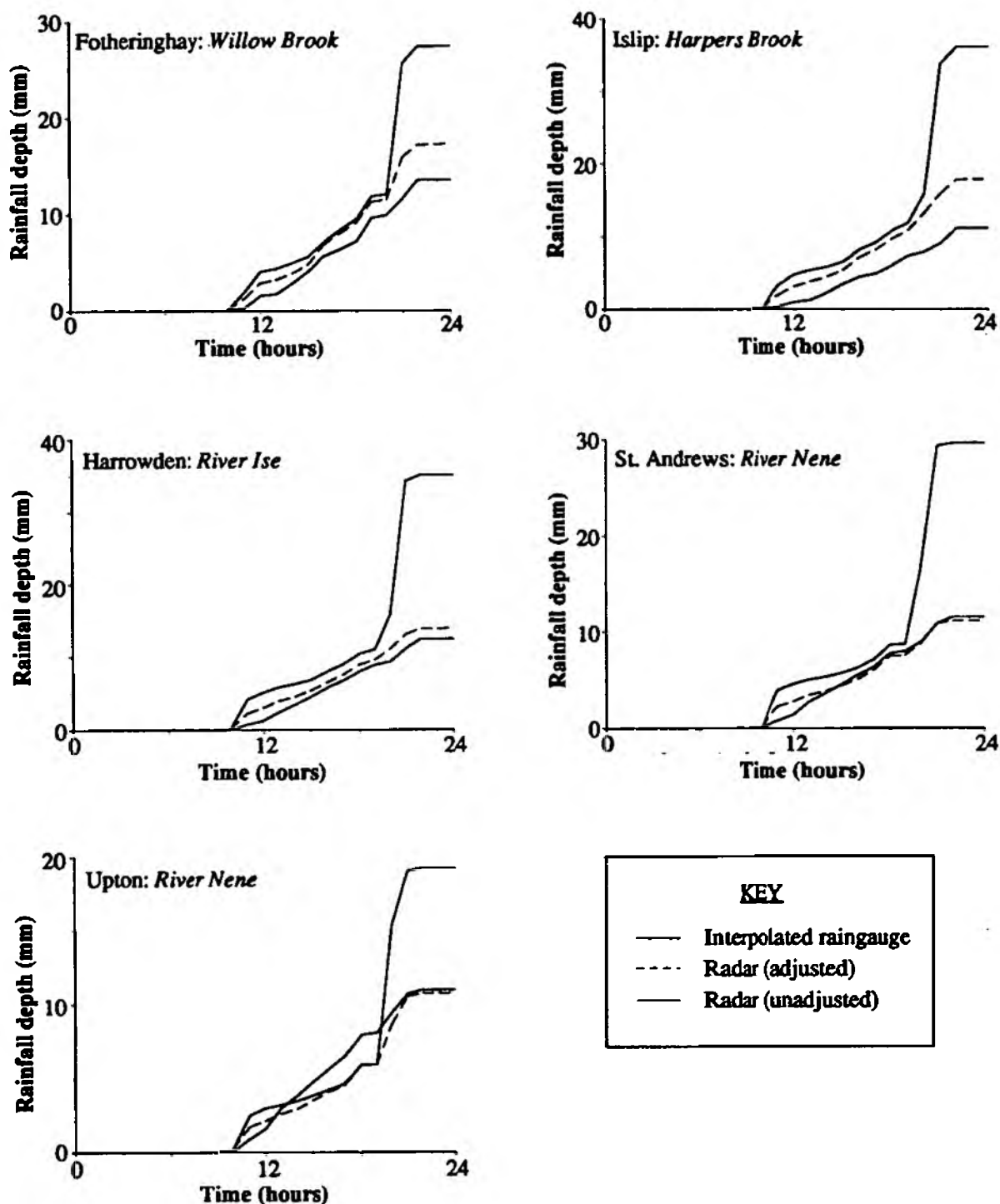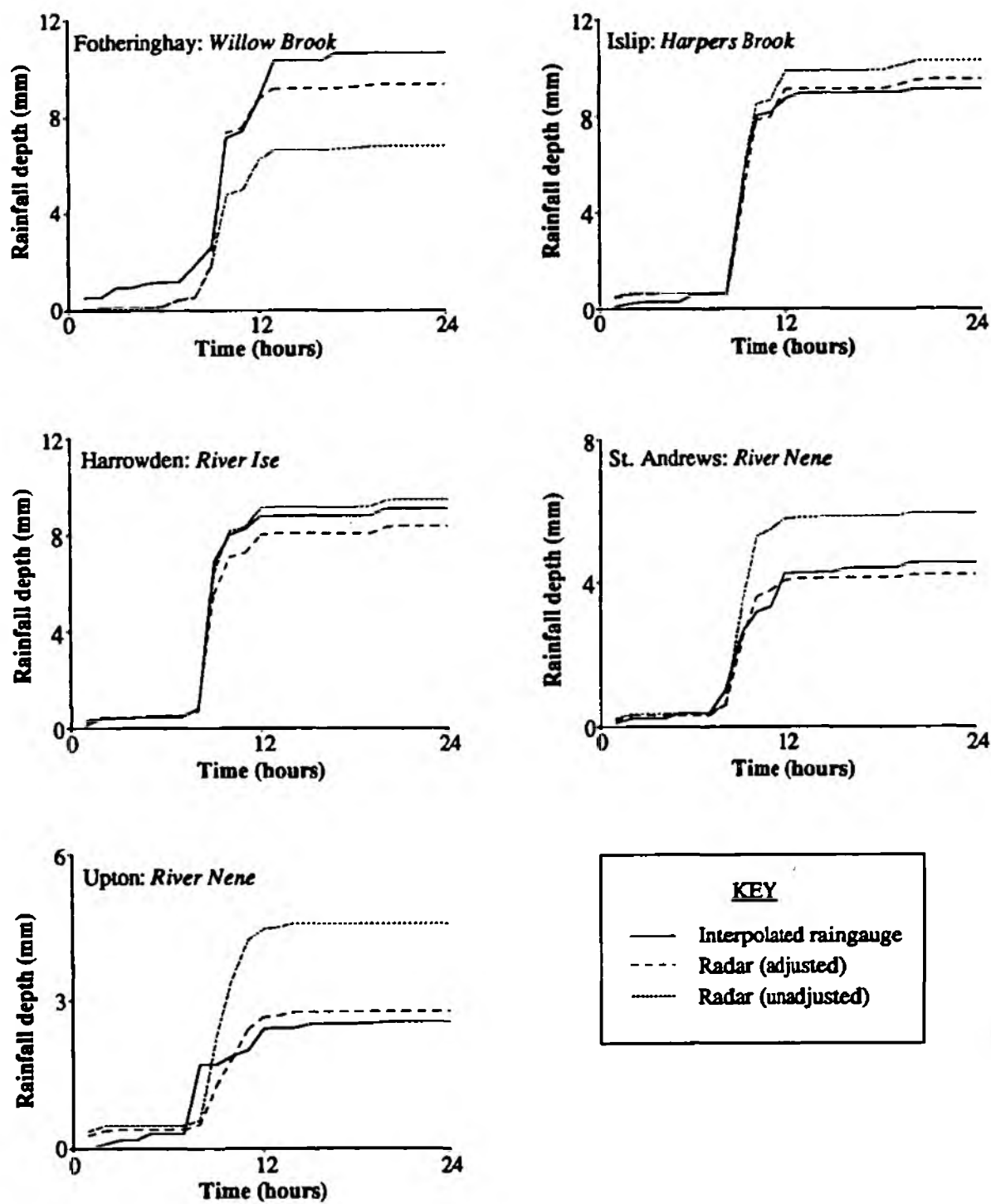
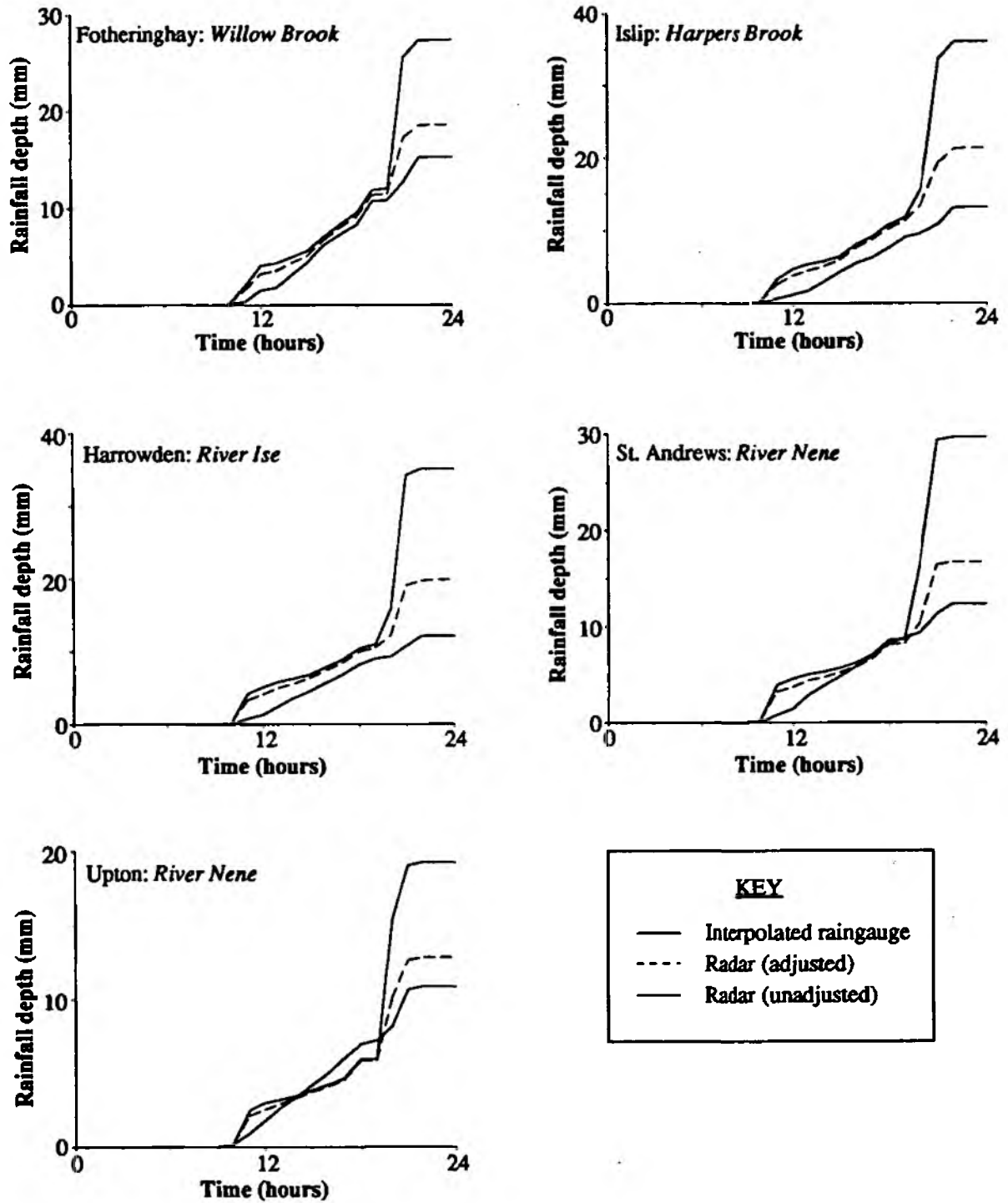Figure 5.10(b): Catchment averaged rainfall amounts, 75% network: 30th July 1989
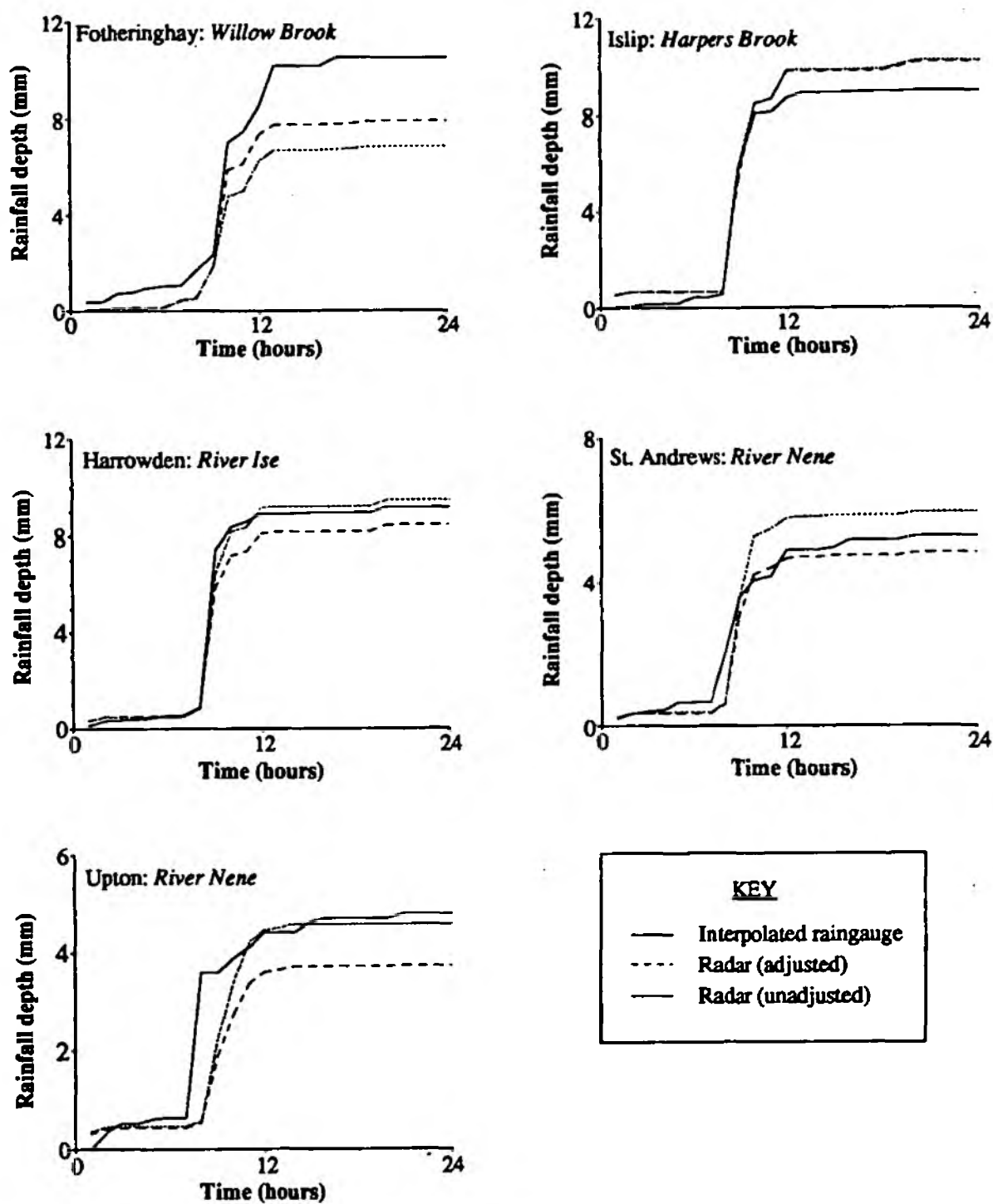
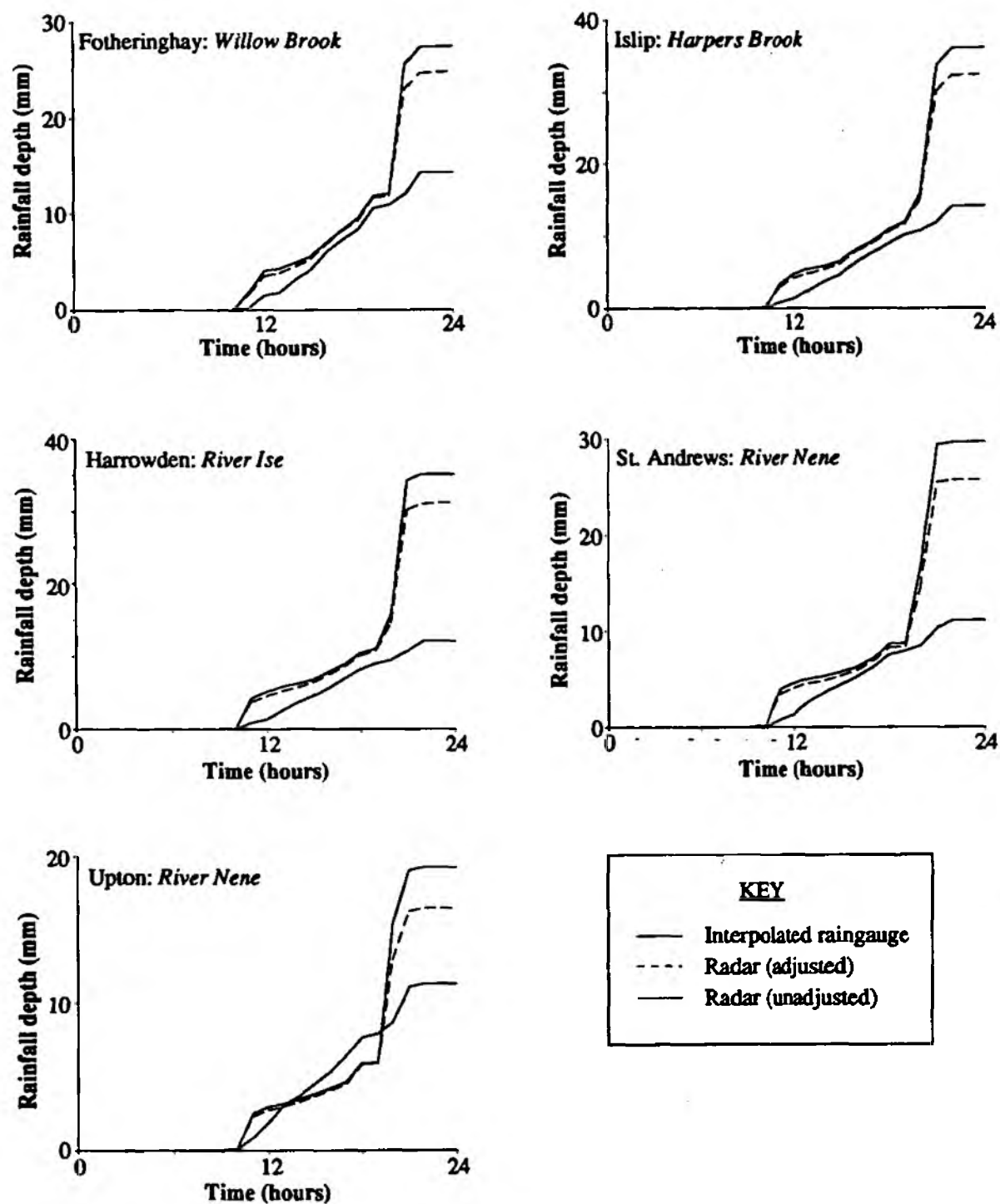Figure 5.10(c): Catchment averaged rainfall amounts. 50% network:
30th July 1989
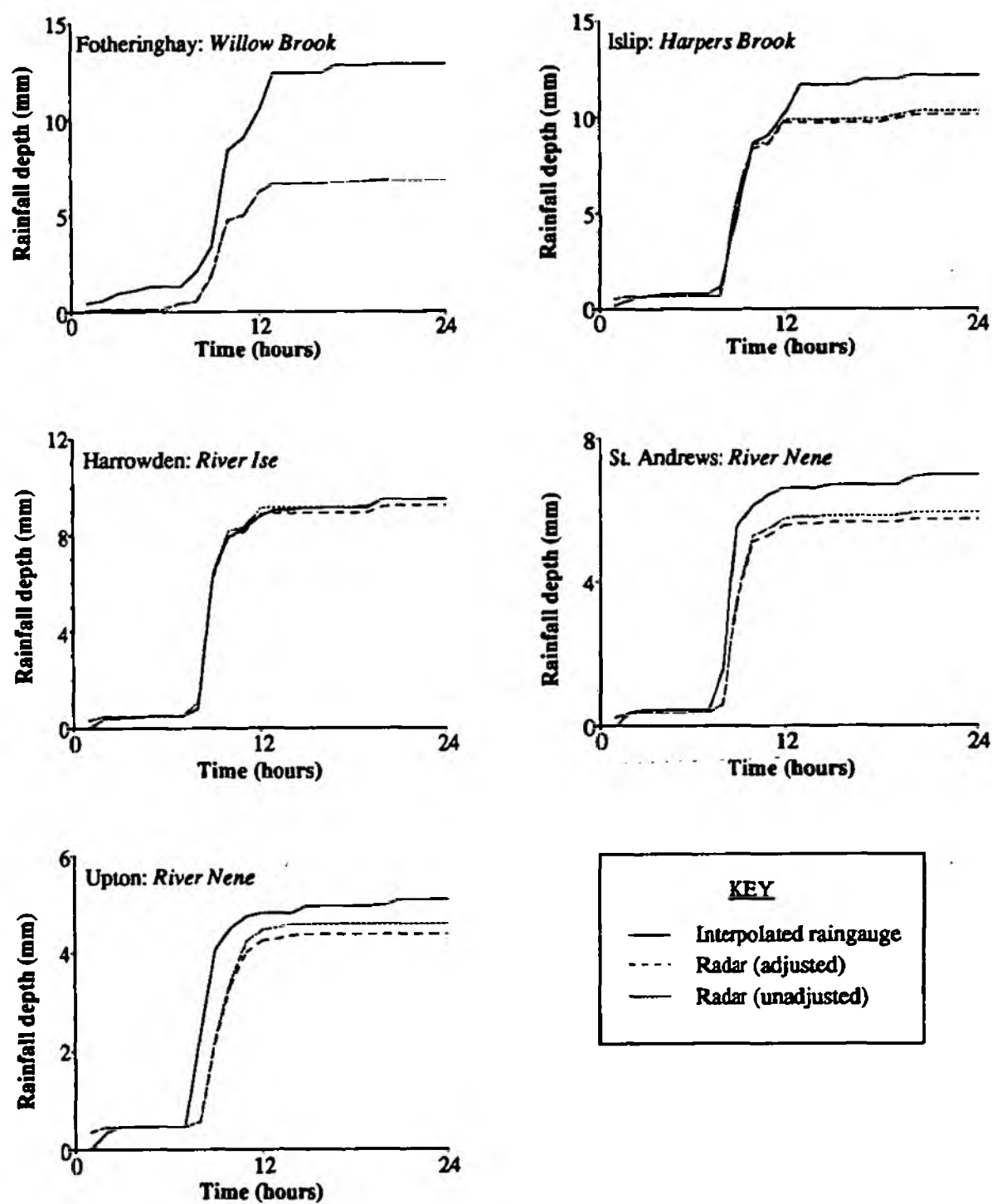
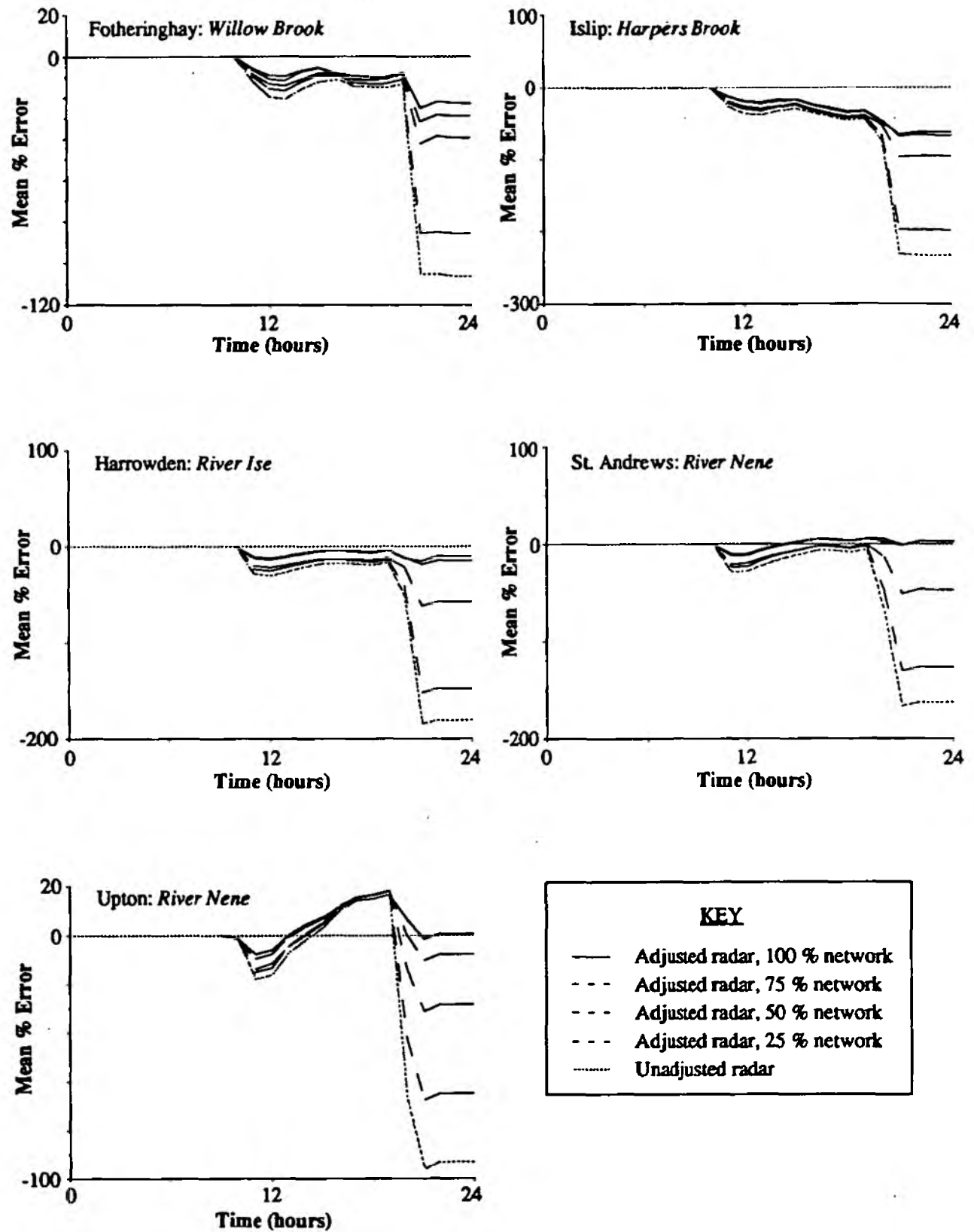Figure 5.10(d): Catchment averaged rainfall amounts, 25% network: 30th July 1989
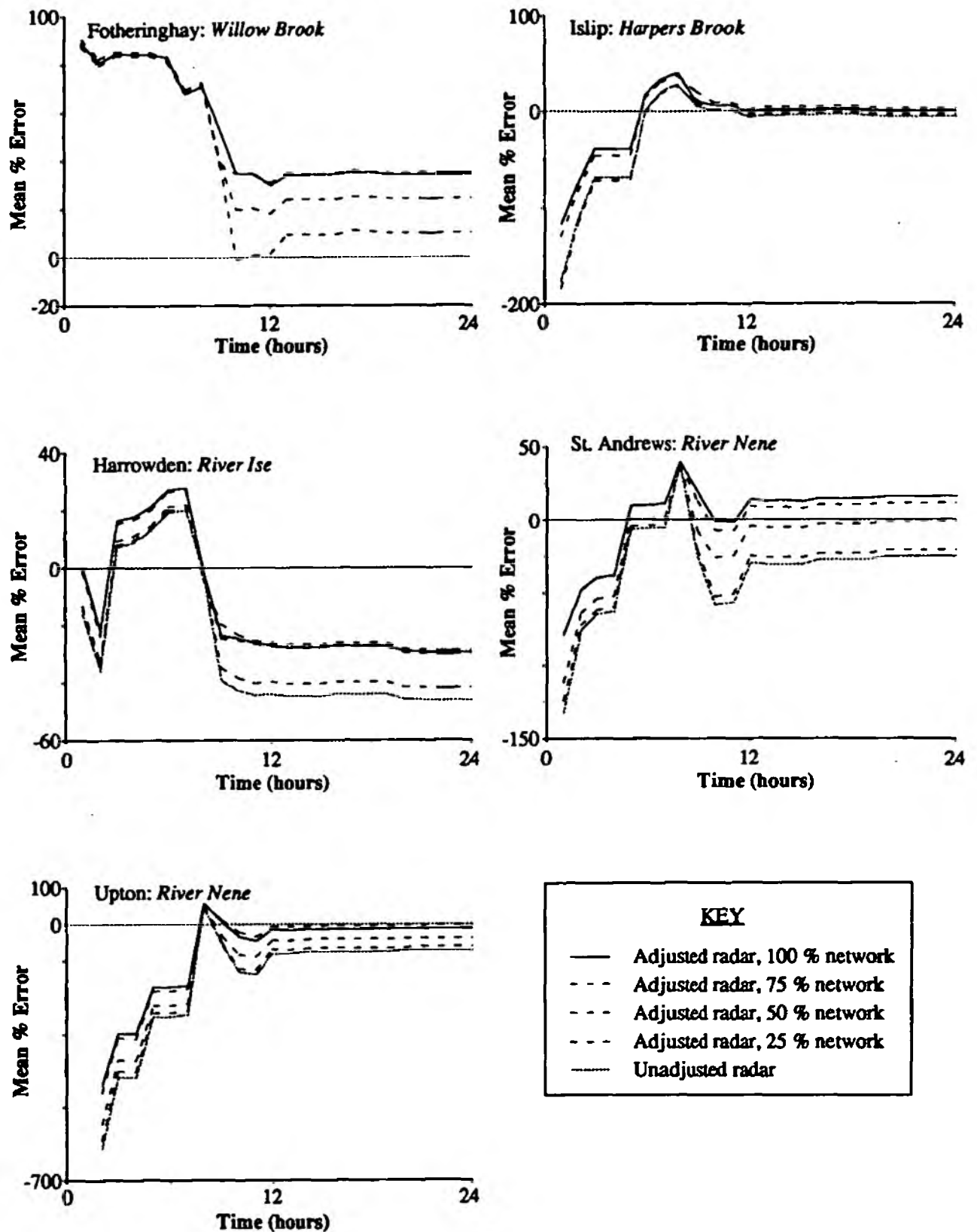
Figure 5.11: Error in cumulative catchment averaged rainfall: 30th July 1989 data

Table 5.4: Root mean square (%) error of areal rainfall estimates: 30th July 1989

| Catchment | Unadjusted | Network density | | | |
		100%	75%	50%	25%
Fotheringhay	49.8	50.9	33.2	42.9	49.9
Islip	25.3	18.2	21.6	26.1	24.6
Harrowden	34.7	23.9	23.3	24.0	31.9
St Andrews	37.0	20.4	18.1	17.8	33.2
Upton	147.9	77.3	76.1	115.0	139.0
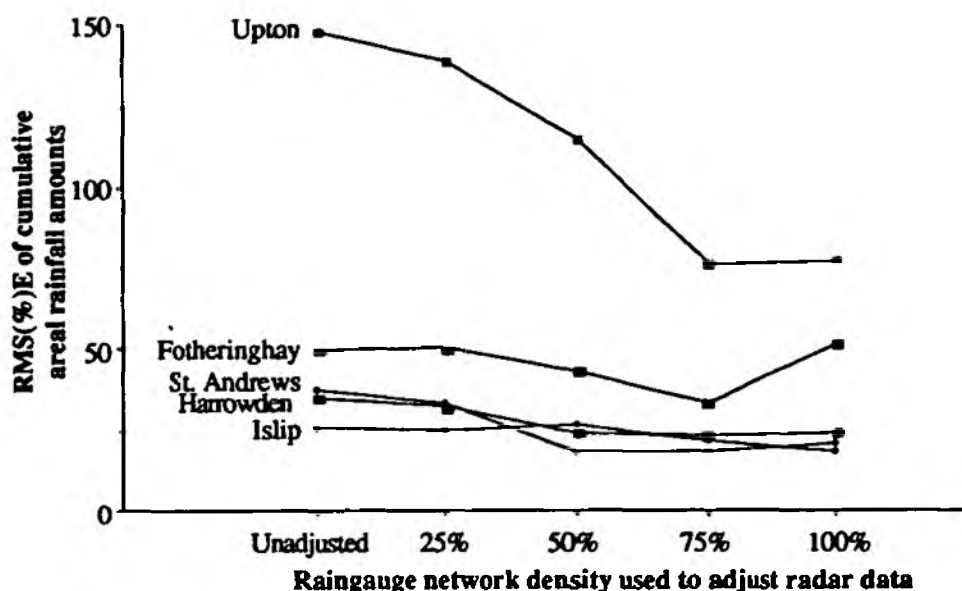
Figure 5.12: Mean RMS(%)E of areal rainfall estimates: 30th July 1989

Unlike the stratiform rainfall case there is no well defined relationship between the density of the raingauge network used for radar adjustment and the areal estimation error and the use of a high density network does not guarantee an overall reduction in areal rainfall estimates and in certain cases error actually increases as a result. It is probable that raingauge network density far exceeding that available for this study would be required to adequately represent high spatial variability rainfall.

5.2. Influence of Raingauge Network Density on Point Rainfall Estimates

This section presents the results of an analysis into the influence that the density of the raingauge network used for adjusting the radar data has on quantitative estimation of point rainfall.

The analysis has been restricted to one case study, a stratiform rainfall event on the 14th December 1989. Approximately 21 mm of evenly distributed rainfall occurred over the area through the 24 hour period, at an average intensity of just under 1 mm/hr. As with most stratiform rainfalls, the spatial variation was quite low with an inter-gauge standard deviation of 5 mm. A total of 66 raingauges were available for the day.

As with the areal rainfall study in described in section 5.1, radar data were adjusted using four different raingauge network densities corresponding to a full network, (i.e. all available raingauges), and 75%, 50% and 25% (sub)networks of 66, 47, 31 and 14 gauges respectively. To form the reduced density networks, raingauges were removed subjectively. An attempt was made to maintain even coverage across the entire adjustment area. The raingauges used for each network are tabulated in table 5.5. For the analysis, gauges not used in the formation of the assessment factor surface were used as verification gauges, providing an unbiased assessment of adjustment performance. Clearly, no independent verification gauges were available for the full (100%) network, with progressively more being available as the adjustment network became less dense.

Figure 5.13 shows the unadjusted (i) and adjusted (ii) radar rainfall fields and the raingauge rainfall fields (iii) together with the mean assessment factor field (iv) for the day for each of the raingauge network densities ([a] full network, [b] 75%, [c] 50%, [d] 25%). The figures provide a visual illustration of the impact of network density on the adjustment procedure. It is immediately apparent that as the density decreases, the impact of the adjustment lessens. Cumulative hyetographs of the raingauge data, unadjusted radar data and radar data adjusted with each of the four raingauge networks are shown in figure 5.14. The traces indicate that in general the deviation between the raingauge and radar hyetographs reduces as the density of the raingauge network used for adjustment increases.

The mean cumulative hyetographs of all the raingauges and overlying radar cells are shown in figure 5.15. This figure emphasises the influence of network density and shows that there is some benefit to be gained with even a relatively small network (i.e. 25%) in this type of rainfall system. The information is presented in a different form in figure 5.16.

Table 5.5: Raingauge Networks used for Rationalisation Analysis

i: Verification gauges

100 %	75 %	50 %	25 %	0 % (i.e. unadjusted)
None	S	S 5	S 3, 5, 7, 14	S 2, 3, 4, 5, 6, 7, 11, 13, 14, 16, 17, 18
	T	T 1, 2, 7	T 1, 2, 7	T 1, 2, 3, 5, 7, 10
	U 12, 14, 15, 23	U 4, 7, 12, 14, 15, 23, 25	U 1, 4, 6, 7, 12, 14, 15, 17, 18, 19, 21, 23, 25	U 1, 4, 5, 6, 7, 10, 11, 12, 14, 15, 17, 18, 19, 21, 23, 24, 25
	V 1, 6, 7, 13, 14, 20, 24, 25, 32, 34	V 1, 3, 5, 6, 7, 9, 11, 13, 14, 19, 20, 22, 24, 25, 27, 28, 29, 31, 32, 34	V 1, 3, 4, 5, 6, 7, 9, 10, 11, 13, 14, 15, 16, 17, 18, 19, 20, 22, 23, 24, 25, 27, 28, 29, 31, 32, 34	V 1, 3, 4, 5, 6, 7, 8, 9, 10, 11, 13, 14, 15, 16, 17, 18, 19, 20, 21, 22, 23, 24, 25, 26, 27, 28, 29, 30, 31, 32, 34
0 gauges	14 gauges	31 gauges	47 gauges	66 gauges

ii: Gauges sites used in construction of assessment factor field surface

100 %	75 %	50 %	25 %	0 % (i.e. unadjusted)
S 2, 3, 4, 5, 6, 7, 11, 13, 14, 16, 17, 18	S 2, 3, 4, 5, 6, 7, 11, 13, 14, 16, 17, 18	S 2, 3, 4, 6, 7, 11, 13, 14, 16, 17, 18	S 2, 4, 6, 11, 13, 16, 17, 18	None
T 1, 2, 3, 5, 7, 10	T 1, 2, 3, 5, 7, 10	T 3, 5, 10	T 3, 5, 10	
U 1, 4, 5, 6, 7, 10, 11, 12, 14, 15, 17, 18, 19, 21, 23, 24, 25	U 1, 4, 5, 6, 7, 10, 11, 17, 18, 19, 21, 24, 25	U 1, 5, 6, 10, 11, 17, 18, 19, 21, 24	U 5, 10, 11, 24	
V 1, 3, 4, 5, 6, 7, 8, 9, 10, 11, 13, 14, 15, 16, 17, 18, 19, 20, 21, 22, 23, 24, 25, 26, 27, 28, 29, 30, 31, 32, 34	V 3, 4, 5, 8, 9, 10, 11, 15, 16, 17, 18, 19, 21, 22, 23, 26, 27, 28, 29, 30, 31	V 4, 8, 10, 15, 16, 17, 18, 21, 23, 26, 30	V 8, 21, 26, 30	
66 gauges	52 gauges	35 gauges	19 gauges	0 gauges
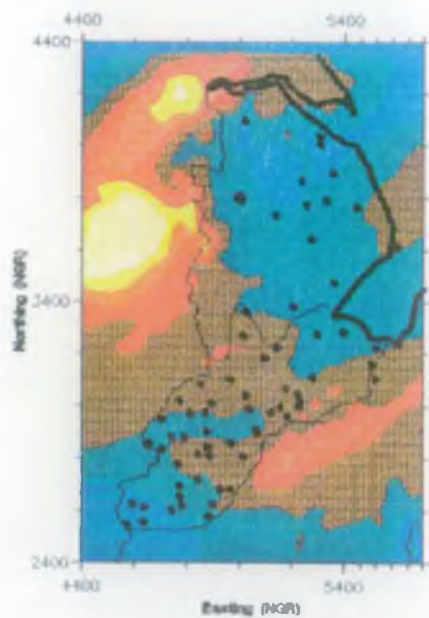
i). unadjusted radar
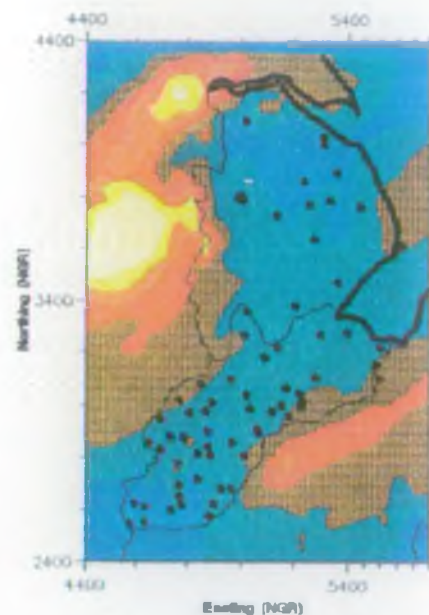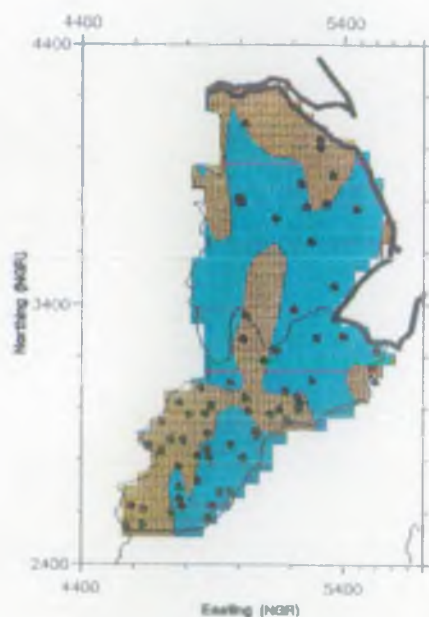
ii). adjusted radar

iii). assessment factors
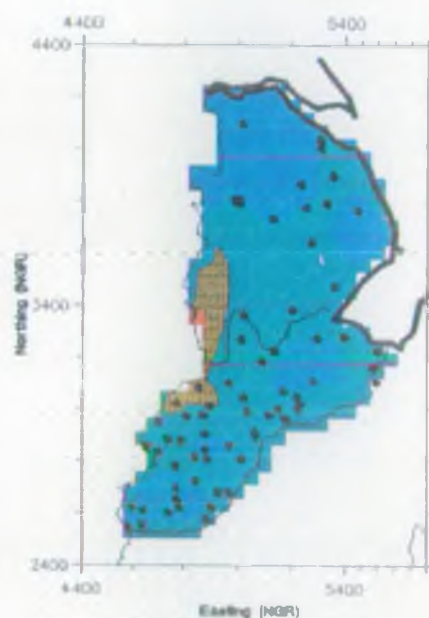
iv). interpolated raingauge

Figure 5.13a: Radar adjustment fields, 100%, 14th December 1989 (Ingham radar)
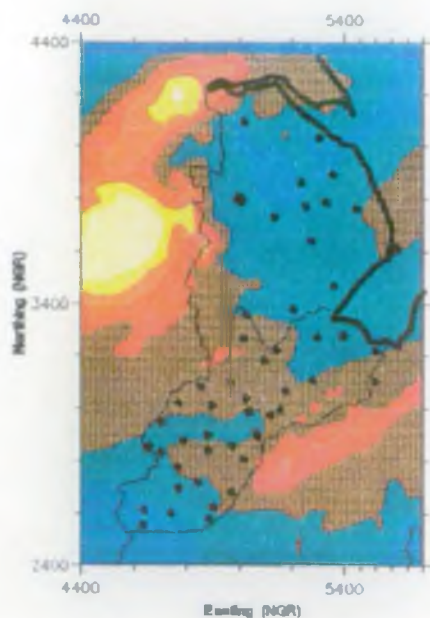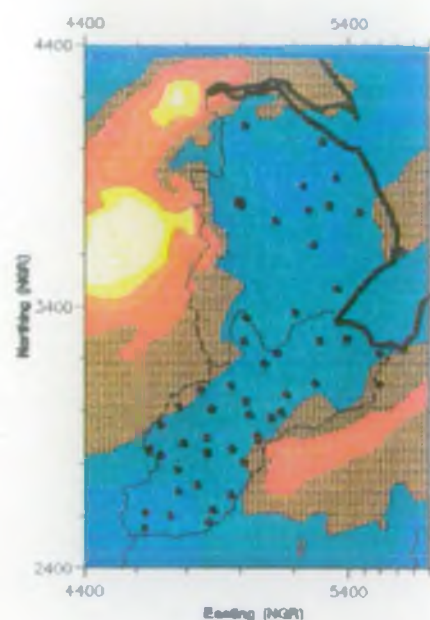
i). unadjusted radar
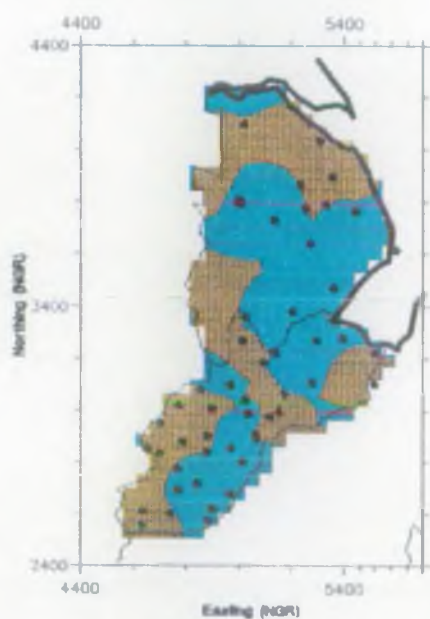
ii). adjusted radar

iii). assessment factors
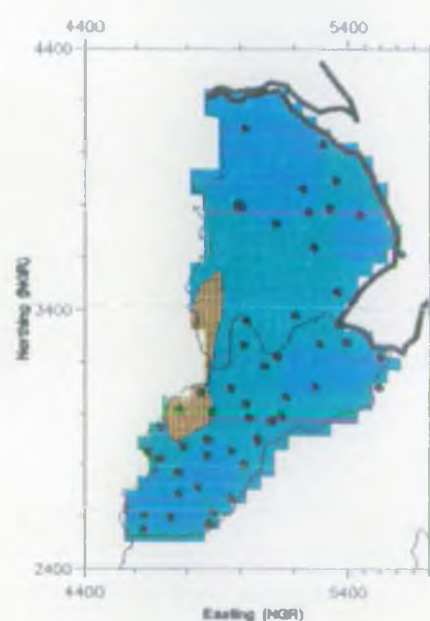
iv). interpolated raingauge
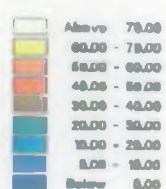
Figure 5.13b: Radar adjustment fields, 75%, 14th December 1989 (Ingham radar)
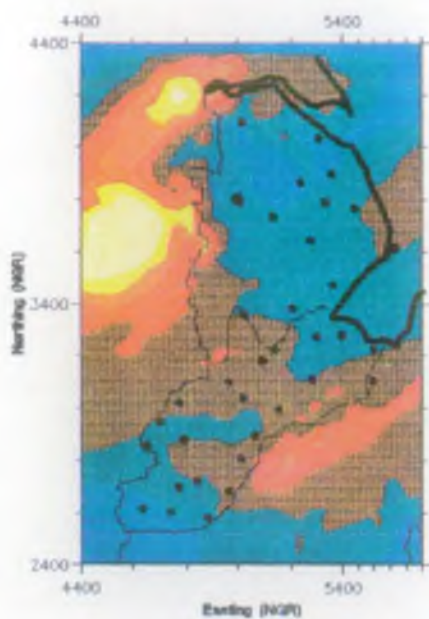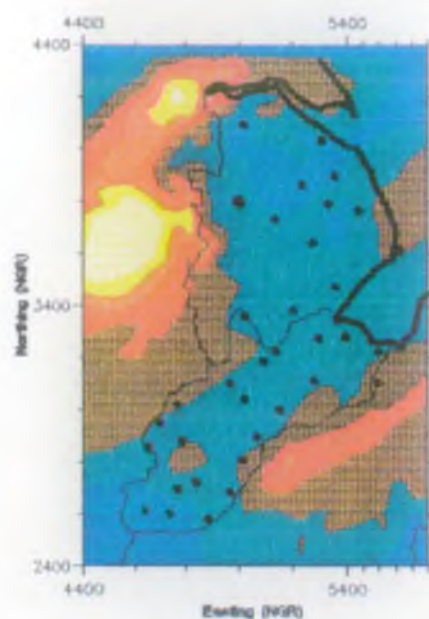
i). unadjusted radar
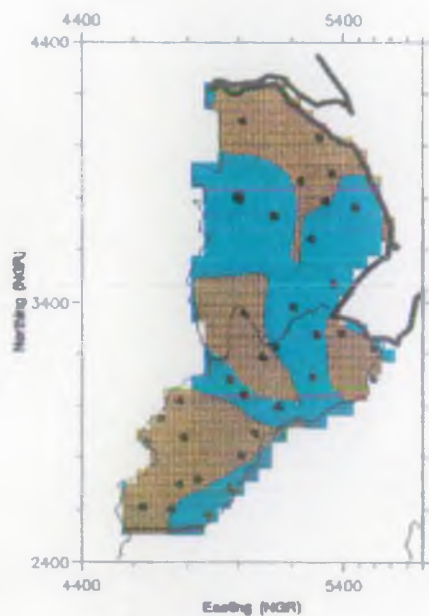
ii). adjusted radar

iii). assessment factors
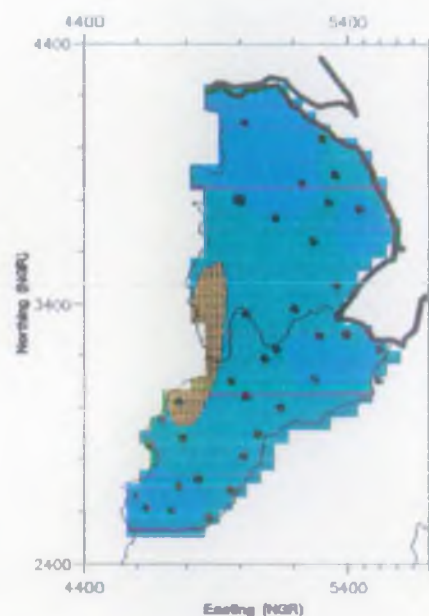
iv). interpolated raingauge
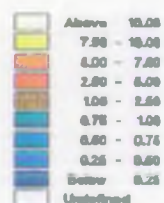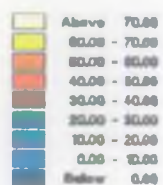
Figure 5.13c: Radar adjustment fields, 50%, 14th December 1989 (Ingham radar)
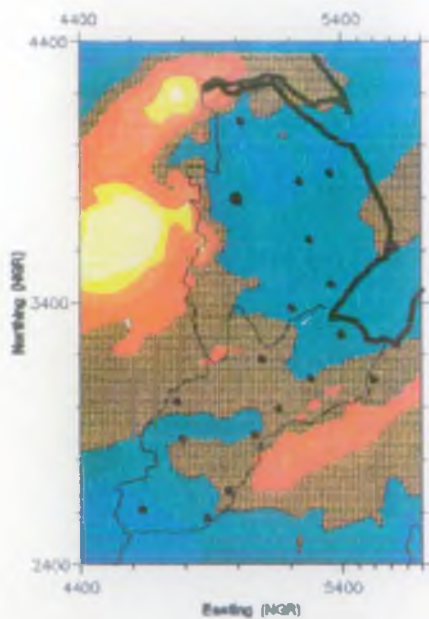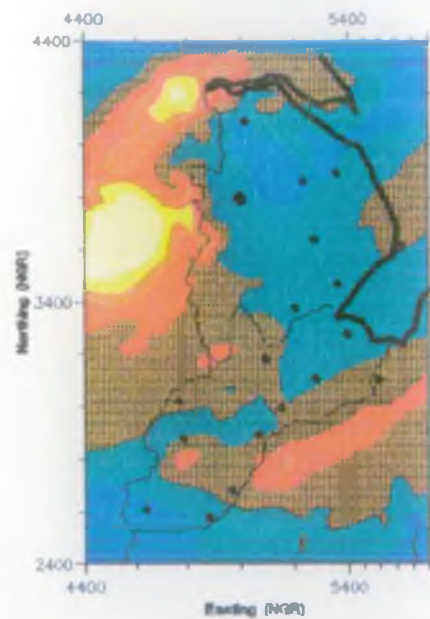
i). unadjusted radar
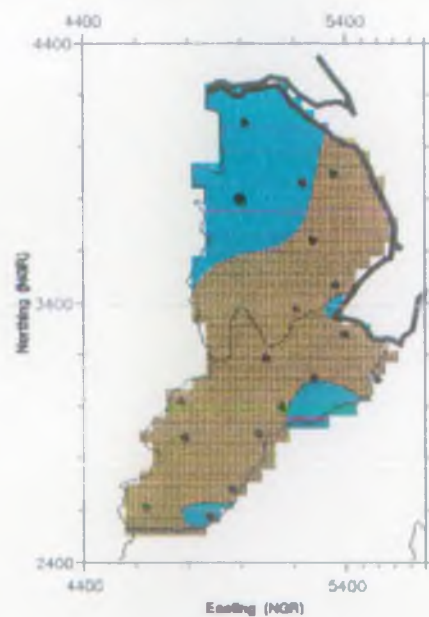
ii). adjusted radar

iii). assessment factors
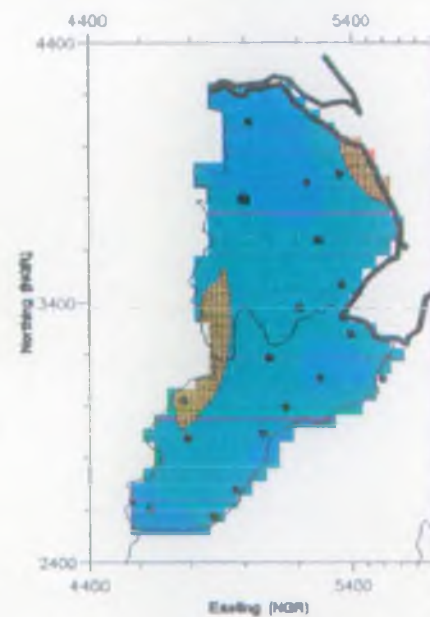
iv). interpolated raingauge
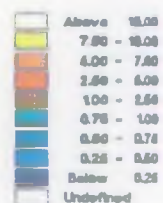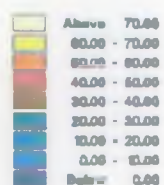
Figure 5.13d: Radar adjustment fields, 25%, 14th December 1989 (Ingham radar)
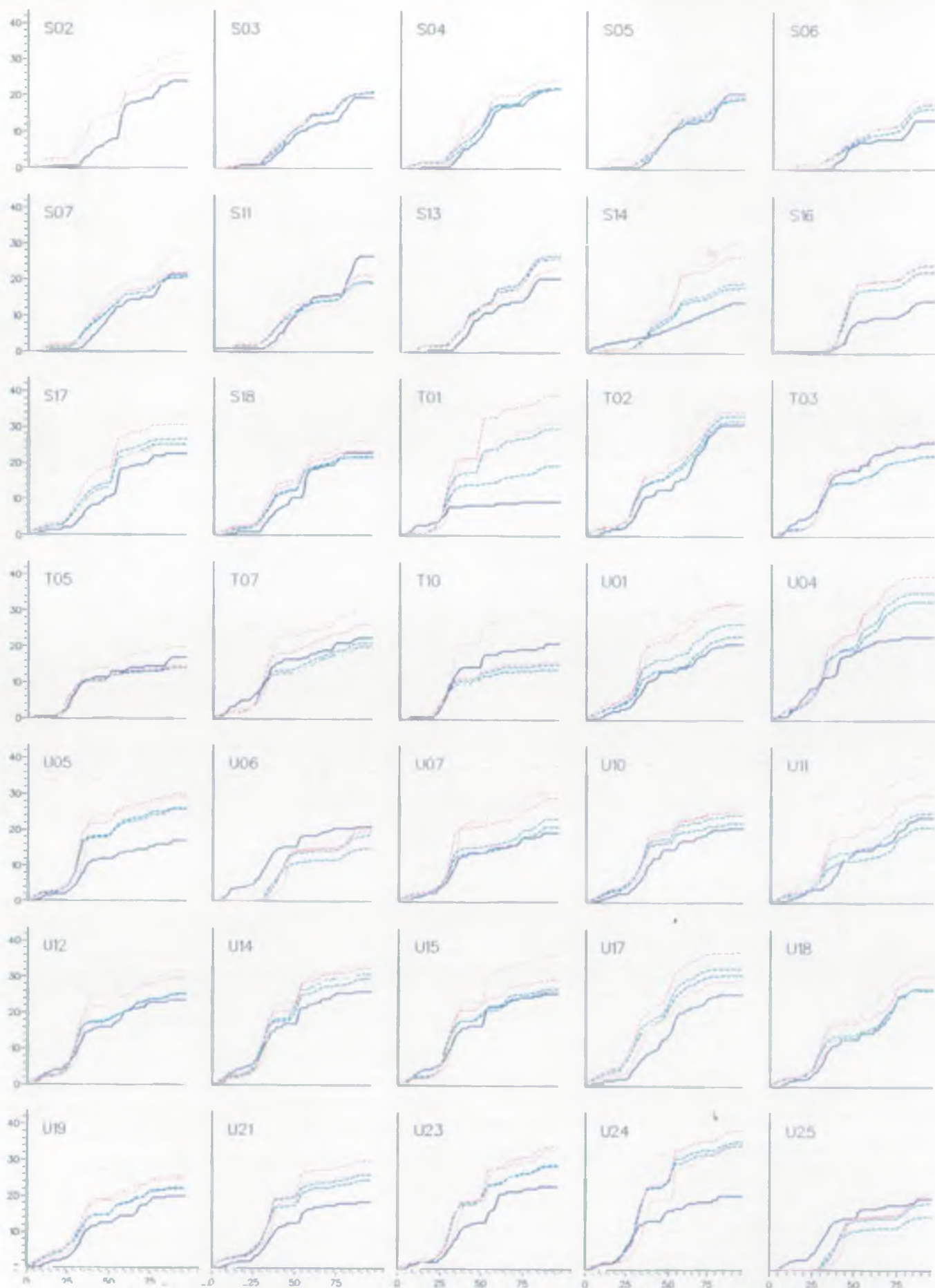
Figure 5.14a: Cumulative hyetographs from raingauge data and radar data adjusted and unadjusted by different density raingauge networks: 14th December 1989 (Ingham radar)
(dark blue-raingauge; red-unadjusted; pink-25%; lt. blue-50%; yellow-75%; green-100%)
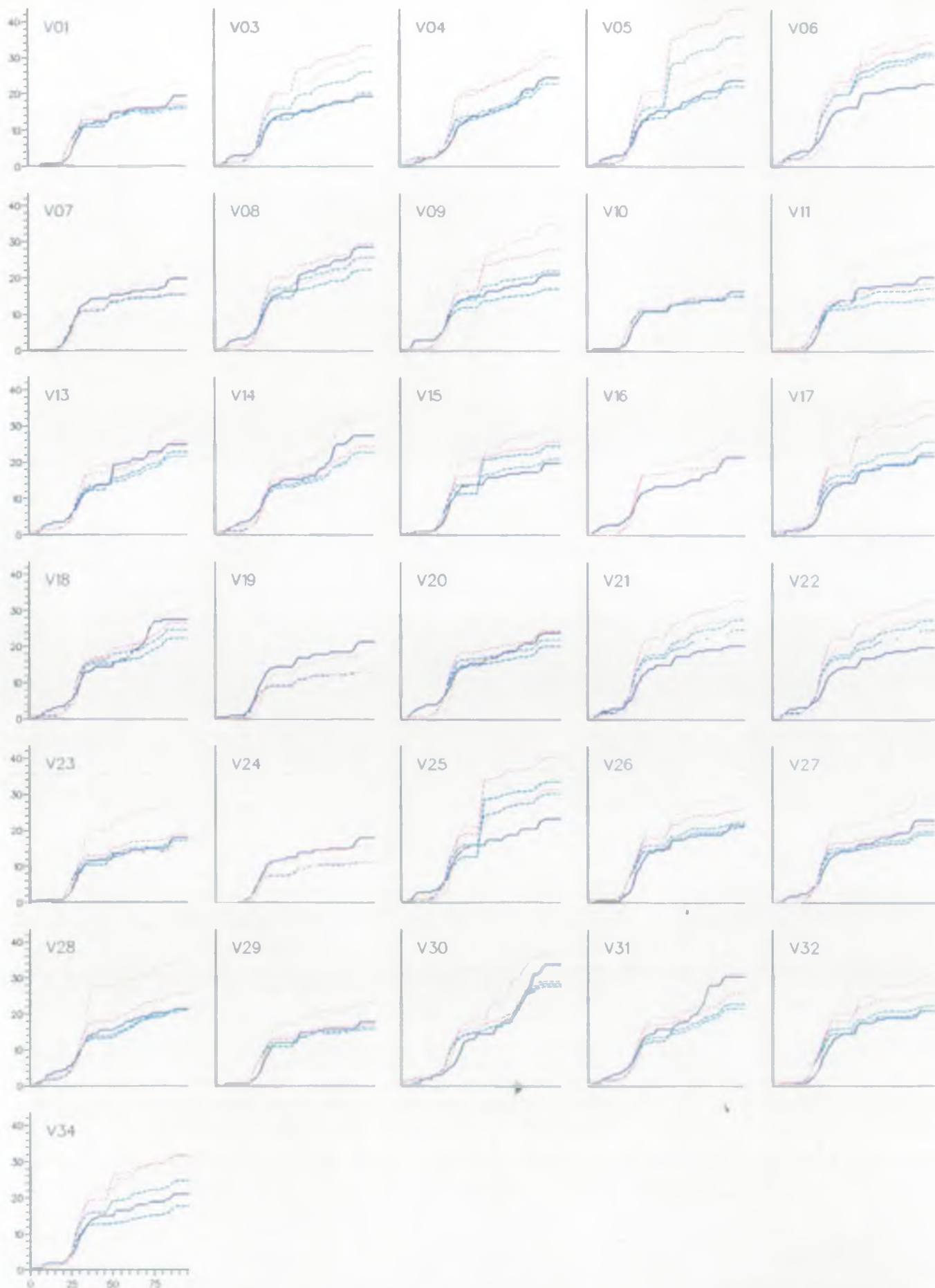
Figure 5.14b: Cumulative hyetographs from raingauge data and radar data adjusted and unadjusted by different density raingauge networks; 14th December 1989 (Ingham radar)

(dark blue-raingauge; red-unadjusted; pink-25%; lt. blue-50%; yellow-75%; green-100%)
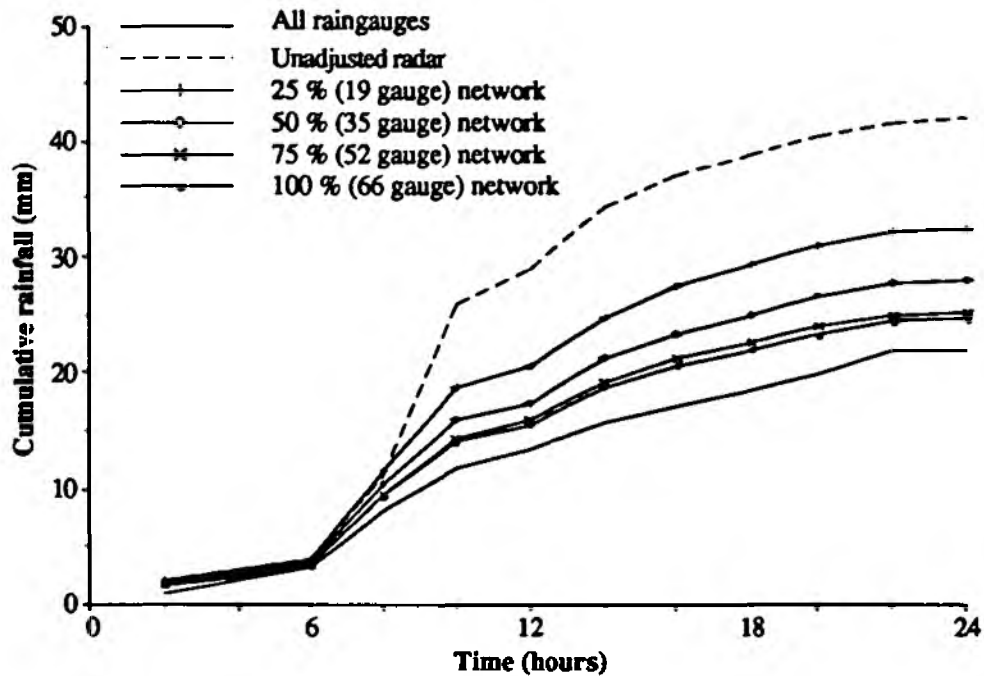
Figure 5.15: Mean cumulative hvetographs for raingauges and overlying radar cells:
14th December 1989

Figure 5.16 shows the mean percentage error at all raingauge sites (assuming gauge-truth), for cumulation periods ranging from 10-24 hours (10 hours corresponds to the period for which the mean raingauge rainfall catch exceeds 5 mm), for unadjusted and adjusted radar data. The figure indicates that error reduction is directly related to the density of the raingauge network used for adjustment. In addition, a law of diminishing returns seems to apply whereby error reduction does not increase much beyond a threshold network density. In part this is bound to be the case, because the gauge-truth is in this case not totally unbiased (i.e. gauges used for adjustment are also used to compute the gauge-truth index), but it is reasonable to expect a threshold of this type, particularly for stratiform rainfall. On the basis of this threshold it becomes apparent that only a marginal benefit will be realised by further expansion of the raingauge network. The figure suggests that a reduction of about 25% (i.e. a 75% network) does not have a major impact on point rainfall estimation and that a network of this density would constitute a reasonable compromise between error reduction and network size.
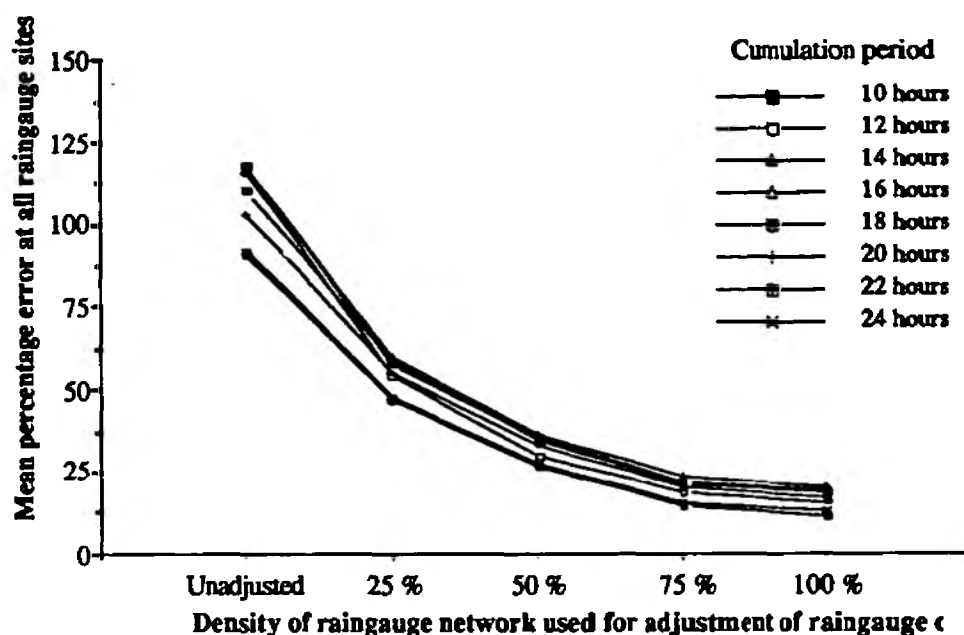
Figure 5.16: Mean % error in hyetographs for raingauges and overlying radar cells: 14th December 1989

Figure 5.17 presents cumulative rainfall hyetograph for raingauge and radar rainfall data adjusted by each of the raingauge networks at verification raingauge sites. The error statistics in table 5.6, and shown in the figure, do not replicate the biased assessment where error reduction was directly related to network density. This is probably because the density of the adjustment networks and therefore the verification gauge-truth varies. Thus figures 5.17(i), (ii), and (ii) are not strictly comparable.

5.3. Conclusions

This chapter has presented the results of an investigation into the influence of network density on areal and point rainfall estimation. The impact on areal estimation was investigated with two case study data sets, a winter stratiform rainfall event severely effected by bright-band, and a summer convective event. Significant rainfall occurred for both but whilst for the stratiform system the rainfall was widespread and uniformly distributed across the area, the rainfall associated with the convective system was more localised and confined to a smaller area. The influence on point estimates was investigated using a single case study, for stratiform rainfall (bright-band affected but not severely).

The low spatial variability of stratiform rainfall means that areal rainfall estimates derived from raingauge data from networks of different densities do not exhibit much variation. Despite this, network density has been found to have an important influence on the reduction of deviation between adjusted radar and raingauge rainfall amounts, error reduction being related to network

Raingauge network	Cumulation period (hours)	All raingauge locations		Verification locations			
		Absolute error (mm)	Percentage error (%)	Absolute error (mm)		Percentage error (%)	
				Adjusted	Unadjusted	Adjusted	Unadjusted
Unadjusted radar	6	0.73	22.5	-	-	-	-
	12	15.45	116.2	-	-	-	-
	18	20.27	109.9	-	-	-	-
	24	20.11	92.0	-	-	-	-
25 % network	6	0.65	20.3	0.80	0.82	26.3	26.8
	12	7.17	53.9	8.05	15.65	62.7	121.9
	18	10.72	58.1	11.03	19.94	60.7	109.8
	24	10.42	47.7	11.69	20.61	54.1	95.4
50 % network	6	0.50	15.5	1.15	1.28	41.6	46.2
	12	4.02	30.2	5.93	18.35	49.1	151.9
	18	6.54	35.5	8.42	22.32	47.7	126.5
	24	6.03	27.6	9.61	23.79	44.9	111.2
75 % network	6	0.18	5.4	2.59	3.23	201.0	251.2
	12	2.52	18.9	9.23	22.07	104.8	250.2
	18	4.02	21.8	12.35	24.96	82.1	166.0
	24	3.35	15.3	14.33	28.05	70.9	138.8
100 % network	6	0.14	4.2	-	-	-	-
	12	2.10	15.8	-	-	-	-
	18	3.44	18.7	-	-	-	-
	24	2.73	12.5	-	-	-	-

Table 5.6: Error Analysis of Radar Adjustment: 14th December 1989
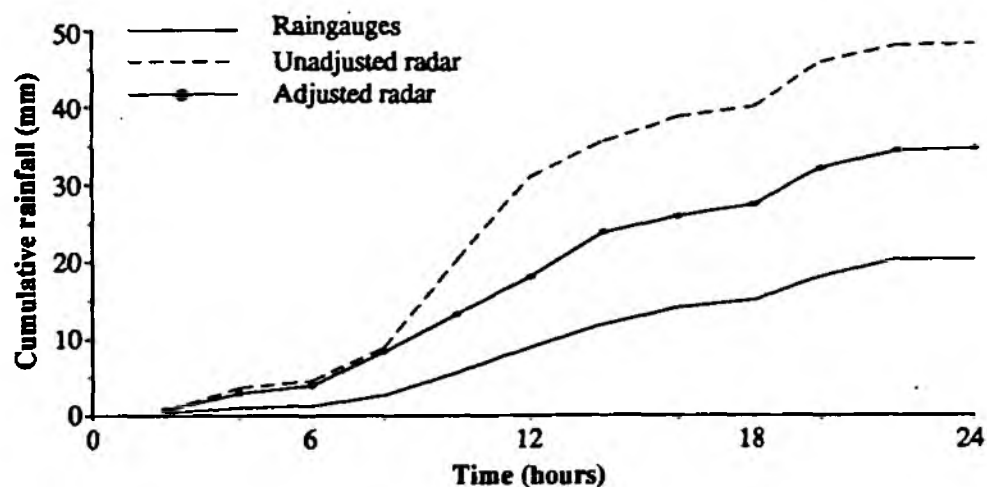
i). Verification of 75 % network (using 14 raingauges)
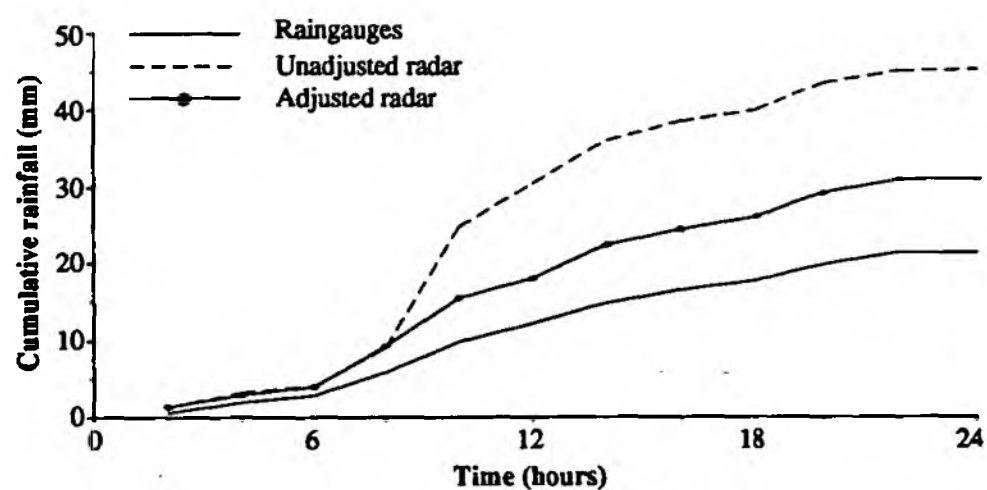
ii). Verification of 50 % network (using 31 raingauges)
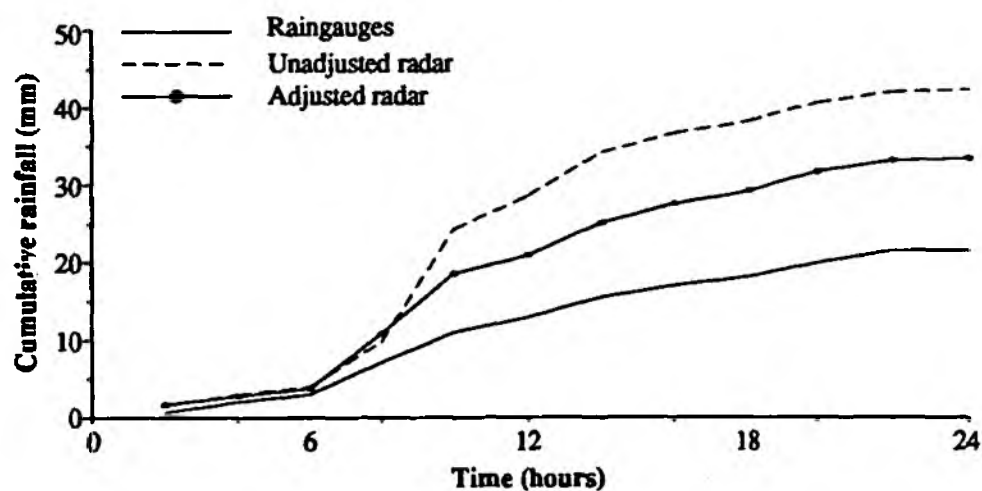
iii). Verification of 25 % network (using 47 raingauges)

Figure 5.17: Mean cumulative hyetographs for verification raingauges, and overlying 5 km radar cell: 14th December 1989

density by an S-curve relationship. Thus, increasing the adjustment network beyond an upper threshold does not result in significant improvement whilst error reduction resulting from adjustment using a small network has a limited impact on error reduction. Between these upper and lower bounds, a small increase in network density is seen to result in significant increases in error reduction.

In contrast, the high spatial variability of convective rainfall is reflected in substantially different areal rainfall estimates derived from directly from raingauge data of different densities. The analysis showed that individual raingauges can have a major impact on areal rainfall estimation, and also (consequently) on adjusted radar estimates. Spatial variability is attributed as the reason for the lack of any clear relationship between network density and error reduction.

The study has again shown that the spatial variability of rainfall is a most important factor for raingauge-based radar adjustment. Thus, in rainfall with high spatial variability, despite high point accuracy, raingauges can be unrepresentative of rainfall away from the point and over a larger area. For stratiform rainfall, representativeness is much higher. Clearly in the former case, adjustment of radar data (which has high spatial resolution, and generally high accuracy in convective rainfall) is fraught with problems. For all but the smallest areas (e.g < 50 km^2) a prohibitively costly number of raingauges would be required to overcome the representativeness problem.

For point rainfall estimation, adjustment with even a low density network has some benefit. The study also indicated that beyond an upper threshold, little additional benefit in terms of error reduction would result. An attempt at independent verification with unbiased raingauge data was largely inconclusive due to insufficient numbers of verification raingauges.

The estimation case studies for areal and point rainfall estimation in stratiform rainfall suggest that a network of approximately 185 km^2/gauge constitutes a good overall compromise between network size and error reduction in areal rainfall estimation. If this value is extrapolated over the entire Anglian Region (approximately 26803 km^2), a total of 145 raingauges would be required, broken down according to area: northern area 50 gauges; central area 46; eastern area 48. In the case of localised rainfall with high spatial variability, far greater numbers of raingauges are required to overcome the fundamental representivity problems, considerably in excess of numbers which are logistically reasonable or economic. The problem could be overcome partially by the employment of a dual density network strategy whereby 'sensitive areas' such as those prone to flooding, or urban centres, would be covered by a higher density of raingauges than are used in other less critical areas.

Chapter 6: Concluding Comments

This report has addressed a number of issues pertaining to the use of weather radar data adjusted by a locally operated raingauge network for hydrological applications. In addition, the influence of a number of factors that influence the accuracy and reliability of weather radar data have been investigated. The results of detailed analyses are presented including investigations into the influence of range from the radar on rainfall estimates, the influence of altitude on the rainfall process in the Region, the influence of storm type on radar adjustment, the utility of adjusted radar data for point and areal rainfall estimation, the influence of intensity resolution of the radar data, and the impact of the raingauge network density on direct areal rainfall estimation and on radar adjustment.

Range from the radar is a critical factor in rainfall estimation, principally because it determines beam-height. Because the effect is a function of time and space variant beam propagation characteristics and cloud/precipitation structure, it only becomes significant as data are cumulated. Consequently, a simple range correction algorithm to correct for systematic error in the radar data for long-term data accumulations (i.e. weeks) has been developed. The procedure is optimised for non bright-band conditions and for ranges up to 150 km. Beyond 150 km partial (conservative) correction consistent with the reduced rainfall information content of the radar signal is provided. A correlation between raingauge altitude and rainfall intensity in the Region has been observed. The relationship is duration dependent and is weak for periods of the order days to weeks, and even for a period of almost one month has only a small influence. Uncertainty and errors in the radar data tend to swamp any altitude effect which may be present.

A procedure for adjusting radar data in real-time using a locally operated network of ground-based raingauges has been developed. For reasons given in the preceding paragraph, neither range or altitude correction components are included in the procedure. The procedure includes computation of hourly assessment factors, fitting of a two-dimensional surface (using a bicubic spline algorithm) to the scattered assessment factors, and finally cell-by-cell adjustment of the radar data. The procedure implicitly assumes raingauge-truth at each raingauge site, although because the surface is not constrained to pass exactly through the assessment factors, the routine is robust to random error in the assessment factors (whether due to raingauge or radar). The assessment factor field derived from the fitted surface is constrained to be conservative in its adjustment towards the adjustment domain boundary - a technique which helps prevent instabilities towards the edge of the domain. Upper and lower bounds imposed on the assessment factors help prevent temporal instabilities in the surface. Surface smoothness is controlled by a single parameter which can be set by the user, although a single value has been found to adequate.

Over a 23 day evaluation period embracing rainfall data for a wide range of synoptic conditions,

the adjustment procedure achieves an error reduction in areal rainfall amounts of 29% (using raingauge derived amounts as a truth-index). The impact of the current real-time Meteorological Office 'calibration' procedure is shown to be slight and even the cause of additional errors in the data. This is primarily due to the relatively small number of raingauges used in the procedure (between four and seven).

The spatial variability of rainfall is an important factor in quantitative rainfall estimation and raingauge-based radar adjustment. In low spatial variability rainfall, the assumption that point raingauge measurements are generally representative of rainfall over a larger area is generally valid. Consequently radar adjustment can be very successful. In dynamic convective systems the spatial and temporal variability of the rainfall field can be extremely high and the representivity assumption may be seriously violated. Thus, whilst the adjustment procedure reduces the deviation between the unadjusted radar and raingauge rainfall amounts, an accurate rainfall field[1] is in fact being 'corrected' with a less accurate one. In such circumstances the potential for raingauge adjustment of weather radar data is judged to be limited. End-point application (EPA) analyses using a rainfall-runoff model for two test catchments confirm this, the best quality flow-forecasts being obtained from an unadjusted radar rainfall input.

The adjustment procedure possesses a significant bright-band error reduction capability. The potential to reduce often large errors due to bright-band is regarded as the most significant benefit of the adjustment procedure. Thus, even when a pronounced bright-band effect is present, the radar data can be used with higher confidence than if no local adjustment had been applied. However, the severest bright-band errors can be unacceptable for the more stringent data requirements of off-line applications, the so-called 'front-end' rainfall products. For example, in the severest bright-band situations, off-line storm return period estimation may be better conducted using interpolated raingauge data.

The number (density) of raingauges required for rainfall estimation and radar adjustment is a function of the spatial variability of the rainfall. In convective showers substantially different areal rainfall estimates are derived from raingauge networks of different densities. For low spatial variability rainfall, areal rainfall estimates derived from a range of different raingauge network densities do not exhibit much variation. Network analysis suggests a raingauge network of approximately 185 km^2/gauge (145 gauges Regionwide) constitutes a good compromise between gauge numbers and error reduction capability. In the case of localised rainfall with high spatial variability, far greater numbers of raingauges are required to overcome the fundamental representivity problems. For all but the smallest areas (e.g < 100 km^2) this would necessitate a prohibitively costly number of raingauges (in terms of real-time operation). The problem may be best addressed by the development of a dual density network strategy whereby 'sensitive areas' i.e. those prone to flooding, urban centres etc. area covered by a higher density of raingauges than elsewhere. Such a philosophy would fit in well with the Regional

---

[1] Weather radar data tend to be high quality in such rainfall systems because of the high spatial resolution and the absence of a bright-band to degrade quantitative accuracy

policy of raingauge clustering for polling.

The influence of the intensity resolution of radar data on front-end rainfall products has been investigated. For stratiform rainfall, adjustment reduces the difference between cumulative hyetographs derived from eight and three-bit radar data to the extent that storm frequency estimates for five test catchments did not differ significantly. For a convective event, the difference between the three and eight-bit cumulative hyetographs increases after adjustment. The difference between unadjusted three and eight-bit hyetographs is judged to be insignificant for hydrological applications (either front-end products or end-point applications), and that three-bit radar data are sufficient for a wide range of hydrological applications.

In summary, the adjustment procedure provides a significant bright-band correction capability resulting in radar data can be used operationally with higher confidence. In rainfall conditions where the adjustment raingauges are representative of rainfall, the procedure successfully combines the point accuracy of the raingauges whilst retaining the spatial information content of the radar data. This has been illustrated in the EPA assessment where areal rainfall estimates derived from adjusted radar data provide better forecast accuracy than either raingauge or unadjusted derived amounts.

References

Cline, A.K., and Renka, R.L. (1984) 'A storage efficient method for construction of a Theissen triangulation', *Rocky Mountain J. Math.*, **14**, 119-139.

Creutin J.D., and Obled, C. (1982) 'Objective analyses and mapping techniques for rainfall fields: an objective comparison, *Water Res. Research*, **18(2)**, 413-431.

Franke, R. and Neilson, G. (1980) Smooth interpolation of large sets of scattered data', *Internat. J. Numer. Methods Engng.*, **15**, 1691-1704.

Hall, A.J., and Barclay, P.A. (1975) 'Methods of determing areal rainfall from observed data', in Prediction in Catchment Hydrology, ed. Chapman X., and Dunin, X., Australia.

Krumbein, W.C. (1959) 'Trend surface analysis of contour-type maps with irregular control point spacing', *J. Geoph. Res.*, **64**, 823-834.

Lawson, C.L. (1977) 'Software for C^1 surface interpolation', In: 'Mathematical Software III', Rice, J.R. (ed.). Academic Press, New York, 161-194.

Moore, R.J., Watson, B.C., Jones. D.A., and Black, B.B. (1990) 'Local recalibration of weather radar data', *Proc, Int. Symp. on Hydrological Applications of Weather Radar*, Salford, U.K., August. (In Hydrological Applications of Weather Radar, Ed. Cluckie, I.D. and Collier, C.G., Ellis Horwood, U.K, 1990).

NERC (1975). Flood Studies Report, Five volumes.

Renka, R.L. (1984) 'Algorithm 624: Traingulation and interpolation of arbitrarily distributred data points in the plane', *ACM Trans. Math. Software*, **10**, 440-442.

Renka, R.L., and Cline, A.K. (1984) 'A triangle-based C1 interpolation method', *Rocky Mountain J. Math.*, **14**, 223-227.

Stol, P. Th. (1986) 'Conceptual rainfall interstation correlation functions for time-integrated rainfall depths', In: Integrated Design of Hydrological Networks, (Ed. Moss, M.E.), IAHS Pub. No. 158.

Shephard, D. (1968) 'A two-dimensional interpolation function for irregularly spaced data', *Proc. 23rd Nat. Conf. ACM, Brandon/Systems Press Inc.*, Princeton, 517-523.

ARIP Reports

ARIP Report 1: Preliminary Design Study (88 pages including Appendices)

ARIP Report 2: An Evaluation of the Influence of Radar Rainfall Intensity Resolution for Real-Time Operational Flood Forecasting (119 pages including Appendices)

ARIP Report 3: Transfer Function Models for Flood Forecasting in National River Authority: Anglian Region (65 pages including Appendix)

ARIP Report 4: Aspects of Precipitation Observation and Quantitative Estimation with Weather Radar (40 pages including Appendices)

Software Profiles

TFUH: Transfer Function Unit Hydrograph Software (February 1990, revised July 1990)

QUANTARE: Quantitative Areal Rainfall Estimation Software (June 1991)

RADGAP: Radar Gauge Adjustment Program Software (June 1991)

Appendices

Appendix 1: The U.K. Weather Radars

The U.K weather radar network has evolved over a number of years and was declared operational in 1985 with the commissioning of the Chenies radar in Buckinghamshire. Since then the network has expanded to its present state, incorporating a total of eleven radars in the U.K and Eire (see figure for the network in England and Wales) the most recent addition being a radar located at Jersey. Plans for further expansion are well advanced and includes a number of radars in Scotland. In addition to the national network the radar output also contributes to a pan-European 'COST' image (COST is an acronym for Co-operation in Science and Technology). Usually individual radars are funded jointly by the Meteorological Office and the Water Industry, consortiums overseeing the general management of the projects with day to day management decisions being made by the Meteorological Office (the Project Management Authority).
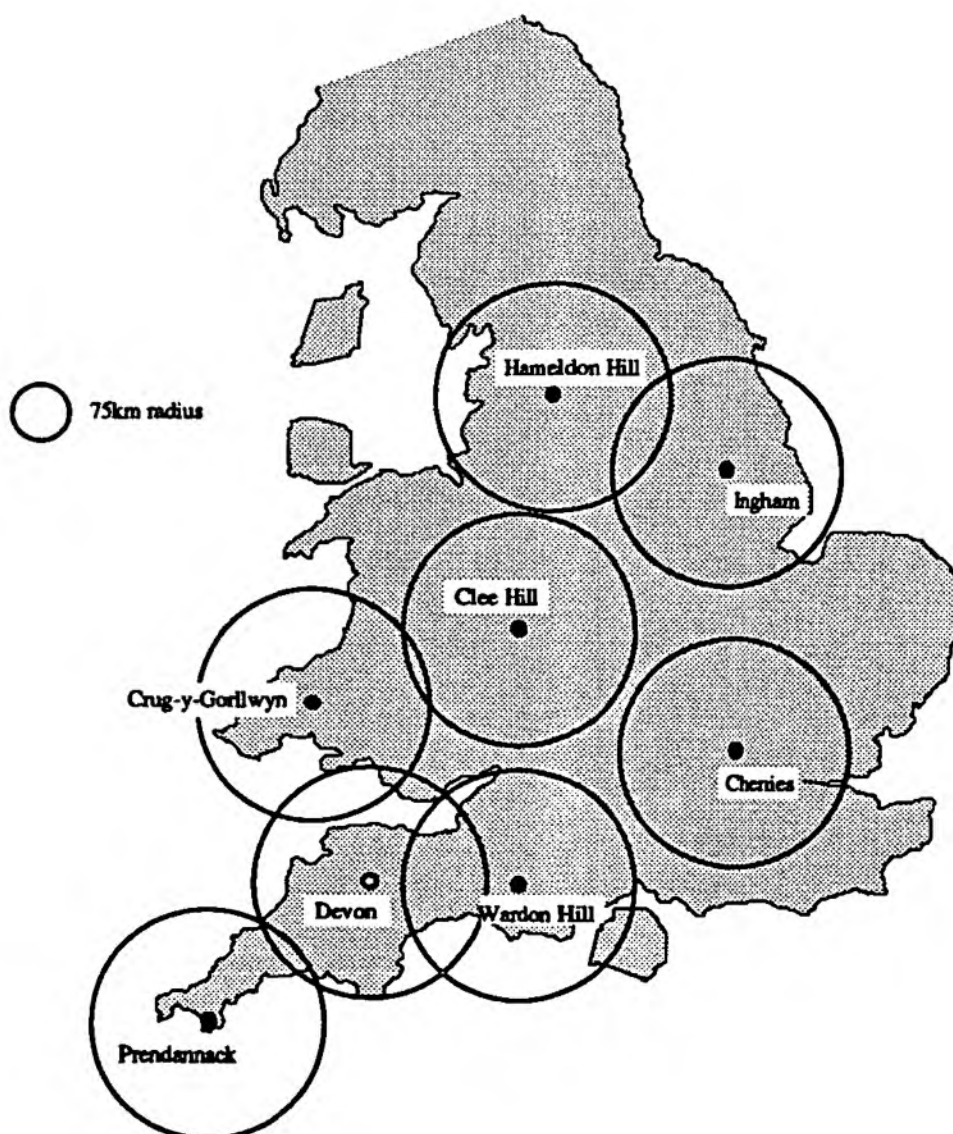
Appendix 2: Radar Specification

The radars are operationally unmanned and of the same specification (table A2.1). The radars operate in a PPI mode (see ARIP 4 section 2.3) and a cyclical five minute, contiguous scan strategy based upon a method discussed by Vasiloff *et al.* (1984) is utilised. In this mode successive 360° scans are made at (usually) four different beam elevations in the range 0.5°-4.0°. Each rotation takes about one minute, the fifth minute being reserved for at-site data processing (including conversion from polar to cartesian coordinates; ground clutter, attenuation and beam occultation corrections). An estimation of surface rainfall is made primarily from the lowest (surface) beam, but data from higher elevation beams are also used in areas where ground based obstructions or topography obstruct the lowest beam (see sections 3.2 and ARIP 4 section 3.3).

Table A2.1: Radar characteristics for Plessey type 45 C

Antenna: parabolic dish	
Diameter	*3.7 m*
Gain	*43 dB*
Polarization	*Vertical*
Beam width	*1°*
Side lobes	*Better than -25 dB relative to main beam*
Elevation	*-2° to +90°*
Elevation rate	*9° s-1*
Rotation rate	*0.1-6 rpm*
Transmitter	
Peak power	*250 kW*
Pulse width	*2 m*
Frequency	*5450 and 5825 MHz (i.e. 5.6 cm wavelength)*
Receiver	
Noise factor	*8.5 dB or better*
Characteristic	*Logarithmic*
Swept gain	*1/R^2 to 200 km*
Frequency control	*Automatic*
Environment	
Operating,	*external - 40°C to +55°C*
	internal +10°C to +35°C
Radome survival	*240kmh-1*

A variety of hardware is located at the radar site (in addition to the radome and radar reflector and antenna) which perform a variety of functions. The at-site hardware includes:

- Array Processor
- Radar / computer interface
- Computer / tape recorder and peripheral devices
- Monitoring equipment
- Power stabilising and distribution equipment
- Communication channel interface units
- Heating, lighting and air-conditioning equipment
- Display system for monitoring purposes.

Appendix 3: Radar Data Types

A variety of different data products are routinely produced by the weather radar network in real-time. These vary in terms of the fundamental properties of temporal, spatial and intensity resolution. The surface rainfall image is available at five minute intervals, but depending on the radar data product, may be averaged over a longer period such as fifteen or thirty minutes. All data products available commercially are based upon a cartesian grid representation. Spatial resolution for single site data is 2 km to a range of 76 km and 5 km to 210 km. The former are known as quantitative data (after the somewhat arbitrary condition of the centre of the 0.5° beam being below 1500 m in normal atmospheric conditions), and the later as qualitative data. Beyond 150 km range from the radar site, the return echo is weak, the centre of the 0.5° beam is 3000 m above the radar altitude and beyond this range the quality of the data start to deteriorate rapidly. The consequences of range from the radar on the accuracy of the radar data form a major part of investigations conducted as part of this report and are covered in detail in chapter 3. The intensity resolution of the data is controlled by the number of classes the analogue reflectivity data are quantised across. Two intensity resolutions are used, high intensity resolution eight-bit data (208 levels) and low intensity resolution three-bit data (8 levels, 'picture quality data'). The ranges used to derive three-bit data from eight-bit data are shown in table A3.1. Three bit data originally evolved due to a combination of factors existing at the time of production including digital communication logistics and graphic display capability.

Table A3.1: Intensity levels for eight-bit and three-bit data

Intensity Level	Eight-bit Range (mm/hr)	3-Bit values (mm/hr)
0	I < 0.125	0.0
1	0.125 ≤ I < 1	0.56
2	1 ≤ I < 4	2.5
3	4 ≤ I < 8	6.0
4	8 ≤ I < 16	12.0
5	16 ≤ I < 32	24.0
6	32 ≤ I < 126	79.0
7	≥ 126	319.0

It is convenient to classify data types into three fundamental categories:

- *Single-site:* data for one particular radar site. A variety of data types are available within this category.

- *Composited:* data formed by compositing data from a number of radar sites to provide an image covering a wide area. Current network images are available on a sub-national, national and pan-European scale.
- *Frontiers[1]:* data formed by compositing data from a number of radars, and from the METEOSAT weather satellite. The data consists of two distinct data streams, 'Actuals' and 'Forecasts'. These data are considered as an additional data group since they differs significantly in terms of production method from the other data types. For further information the reader is referred to any of the papers produced by the Meteorological Office(usually with K. Browning as the lead author).

The data streams produced and/or disseminated by the Meteorological Office are shown in table A3.2. Of these, the single site Type 1 and Type 2 data streams and the U.K network image are the most heavily utilised for hydrological applications. Real-time FRONTIERS forecast data is currently being assessed by two Regions of the NRA (North-west and Thames) and routine dissemination of the forecasts is imminent. In addition, off-line FRONTIERS forecast data has been appraised for hydrological applications for the past three years at Salford - Viner and Cluckie (1990); Viner, Cluckie, and Collier (1991). The potential of quantitative precipitation forecast data for a wide range of hydrological applications is at present largely unrealised, and the future utilisation of such data, and the realisation of the benefits afforded by the data remains a major challenge to the Water Industry.

It is worth noting that the real-time raingauge adjustment factors[2] can only be 'removed' from single-site, type II data. The national network data cannot be de-adjusted, since the network data header block does not contain information regarding the adjustment raingauge rainfall depths. The Frontiers network data has at-site adjustment removed in real-time in certain instances but incorporates additional adjustments subjectively applied by the Meteorological Office Frontiers operator. These factors have important consequences for any real-time adjustment procedure, when the choice of data stream is undecided.

---

[1]   FRONTIERS is an acronym for 'forecasting rain optimised using new techniques of interactively enhanced radar and satellite data.'.

[2] Adjustment factors are defined as the ratio of raingauge/radar rainfall value at raingauge locations. These are determined in real-time by the Meteorological Office from a small number of telemetering raingauges (usually 4 to 7) and applied as a correction to the radar rainfall estimates.

Table A3.2: Radar Data Types

Type 1 Data:	
Spatial resolution	*5 km grid to 210 km range*
Intensity resolution	*8 intensity levels (including zero rainfall)*
Temporal resolution	*data collected at 5 minute intervals but updated for transmission every 15 minutes*
Other Information:	*date, time, radar station number, calibration information, synoptic type*
Other data	*Subcatchment averaged rainfall totals every 15 minutes, hourly and daily totals*
Transmission rate	*1200 baud (asynchronous)*
Transmission time	*35 seconds.*
Type 2 Data:	
Spatial resolution	*2 km to 75 km range, 5 km to 210 km*
Intensity resolution	*208 intensity levels (eight bit data)*
Temporal resolution	*transmitted every 5 minutes*
Transmission rate	*1200 baud (asynchronous)*
Transmission time	*2 minutes*
Other Information	*date, time calibration information, synoptic type, height of bright band (if present)*
Other data	*subcatchment totals (updated every 15 minutes)*
Comments	*data can be processed by used*
Type 3 Data:	
Spatial resolution	*5 km to 210 km*
Intensity resolution	*208 intensity levels (eight bit data)*
Other Information	*date, time calibration information, synoptic type, height of bright band (if present)*
Transmission rate	*2400 baud (asynchronous)*
Transmission time	*27 seconds*
Comments	*used by the Met. Office for production of national network image*
Network Data	
Spatial resolution	*5 km (680 km*680 km coverage)*
Intensity resolution	*8 intensity levels (three-bit data)*
Temporal resolution	*transmitted every 5 minutes with updates at 15 minute intervals*
Transmission rate	*1200 baud (asynchronous)*
Transmission time	*25 minutes*
Other Information	*date, time, colour key for rainfall intensity, height of bright-band above radar site*
Comments	*suitable for display on graphics monitor*
COST-73 Data	
Spatial resolution	*20 km*
Intensity resolution	*8/1 intensity levels*
Temporal resolution	*60 minute*
Comments	*combines data from radars in 13 European countries*
Frontiers 'Actuals' Data	
Spatial resolution	*5 km (1280 km*1280 km coverage)*
Intensity resolution	*208/1 intensity levels*
Temporal resolution	*15 minute*
Transmission rate	*1200 baud (asynchronous)*
Comments	*at-site calibration removed, quality controlled in real-time, supplemented by satellite data*
Frontiers 'Forecast' Data	
Spatial resolution	*5km (1280 km*1280 km coverage)*
Intensity resolution	*208/1 intensity levels*
Temporal resolution	*30 minutes*
Transmission rate	*1200 baud (asynchronous)*
Other Information	*quantitative precipitation forecasts for 1,2,...,6 hours ahead*
Comments	*still under evaluation not routinely disseminated*

Appendix 4: Radar Coverage of Anglian Region

The Anglian Region is covered by two weather radars, one located north-west of London at Chenies (within the Thames Region of the NRA), and the other just north of Lincoln at Ingham. Further details of these radars is provided in table A4.1 and the Regional radar coverage is shown in figure A4.1. About one-third of Anglian Region falls inside the 'quantitative range' of the radar (75 km), with the furthermost range from either radar being about 175 km. Thus, although the entire Region has complete qualitative coverage, a significant area lies beyond the quantitative range of the radar. In these areas (for reasons discussed in ARIP 4 section 3.3.2 (earth curvature effects) the accuracy of the quantitative precipitation estimates becomes increasingly unreliable with increasing range. In particular, a corridor aligned east-west, running between the radars and beyond the quantitative coverage of either is noticeable. This area is hydrologically important containing a number of ungauged upland catchments and sources to some of the major rivers of the Region.

Table A4.1: _Details of weather radars serving the Anglian Region_

Name	_London (Chenies)_
Letter code	_E_
Site NGR	_5016 1999_
Grid centre NGR	_5000 2000_
Commissioned	_1985_
Beamwidth	_1°_
Antenna height	_150 m_
NW extent of grid	_84 * 84 - 2900 4100_
	_76 * 76 - 4240 2760_
Beam elevations	_0.5°, 1.5°, (2.5°, 4.0°)_
Calibration gauges	_Cranleigh (5041 1393), Chievely (4468 1739), Stansted (5504 2243), Bretch Hill (4439 2400), Chigwell (5423 1926)_
Name	_Lincoln (Ingham)_
Letter code	_I_
Site NGR	_4961 3830_
Grid centre NGR	_5000 3800_
Commissioned	_1988_
Beamwidth	_1°_
Antenna height	_80 m_
NW extent of grid	_84 * 84 - 2900 5900_
	_76 * 76 - 4240 4560_
Beam elevations	_0.5°, 1.1°, 1.5°, (2.5°)_
Calibration gauges	_Braunston (4838 3065), Ludford (5208 3893), High Mowthorpe (4888 4685), Hollingsclough (4066 3665), Worksop (4609 3791), Yaddlethorpe (4875 4058)_

The Chenies radar was funded by the London Weather Radar consortium, comprised of the following member bodies: Meteorological Office, Greater London Council, Southern Water Authority and Thames Water Authority. The Ingham radar consortium comprising the following bodies (financial contribution in 1987 prices):

Meteorological Office	£ 365 000
Anglian Water	£ 265 000
Severn-Trent Water	£ 70 000
Yorkshire Water	£ 30 000

The benefits to an industrial organisation of being a Consortium member and contributing to the design and installation costs of a radar are two-fold:

- Consortium members are able to exert a direct influence on the siting of the radar and the raingauges used for real-time adjustment, thereby ensuring their interests are best served by the radar.
- Data from the radar are subsequently available at a minimal charge[1]. Consequently, Anglian Region receive data from the Ingham radar at a nominal fee whilst Chenies data are charged at the full commercial tariff.

---

[1] radar data charges to the Water Industry are currently being reviewed within the context of reorganisation and formation of a National Rivers Authority.
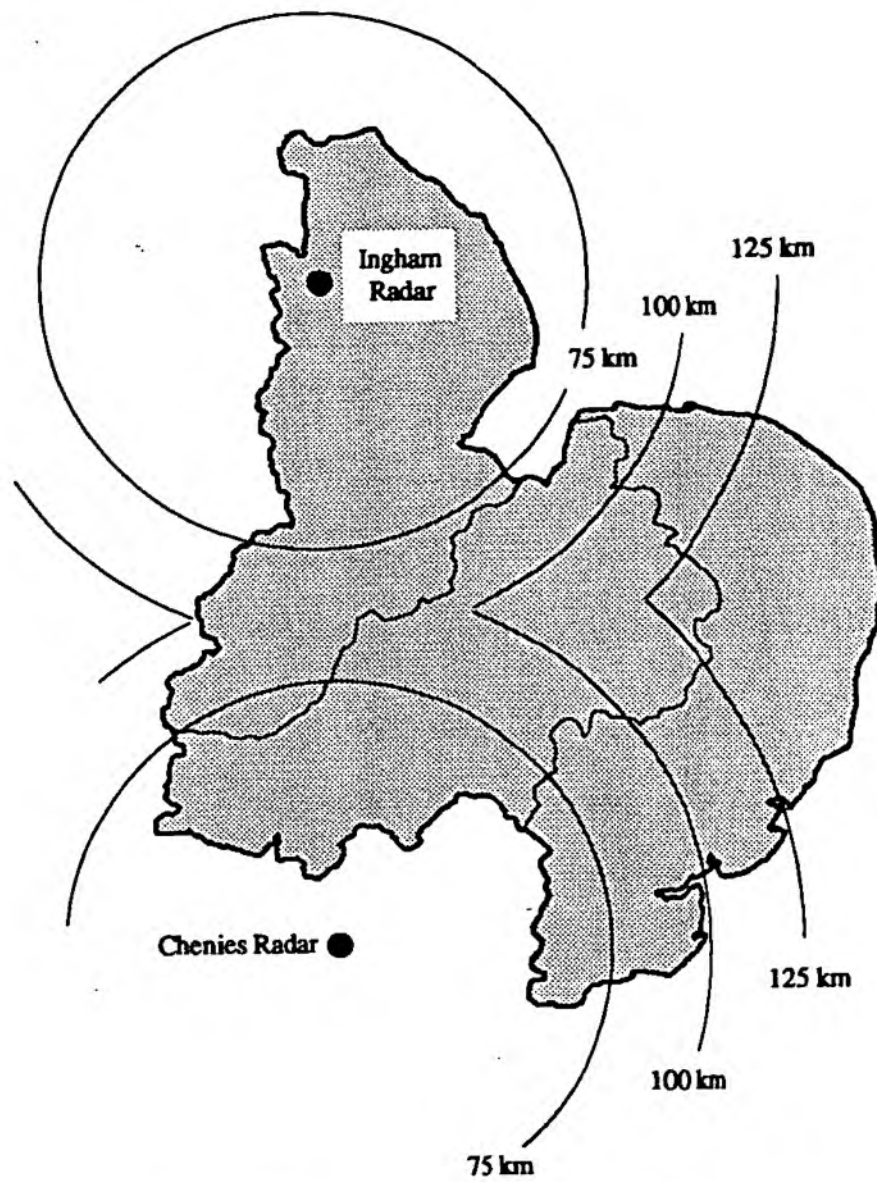
Figure A4.1: Weather Radar Coverage of NRA Anglian Region

Appendix 5: Radar Data used in ARIP

Radar rainfall data were obtained directly from the Meteorological Office in Bracknell. The data obtained were direct copies of the single-site data stream (i.e. data transmitted from the radar sites) after processing by the at-site computer (regrettably it is not possible to obtain the fundamental reflectivity data which would be the ideal data to work with). Consequently the data have already been processed to include:

- occultation correction (ARIP 4, section 3.2.2)
- clutter removal and interpolation (ARIP 4, sections 3.2.1)
- reflectivity to rainfall intensity (Z-R) conversion (ARIP 4, section 2.1)
- attenuation correction (ARIP 4, section 3.1.2)
- conversion from polar to cartesian coordinates
- adjustment using telemetering raingauges (ARIP 4, section 3.4.1)

Adjustment information (i.e. rainfall depths for the real-time telemetering adjustment raingauges, and the adjustment factors derived for each of the adjustment domains) is included. From this it is possible to remove the final stage of processing and de-adjustment procedures have been developed at Salford to perform this. All other corrections remain. The fundamental data type on the single-site data tapes are rainfall intensities on 2 km and 5 km cartesian grids with an eight-bit intensity resolution. Since full header information is also provided, these data can be de-adjusted to produce data free from the real-time, at-site raingauge adjustments applied by the Meteorological Office. It is a simple process to synthesise low intensity resolution three-bit data from these (eight-bit data) data (i.e. by applying table A3.1).

The Chenies data were received at an earlier stage of the ARIP project to facilitate hydrological modelling studies (refer to ARIP 3 Report), and were selected according to flow records for catchments primarily in the Central Area. The Ingham data were also received during the project and took the form of daily data identified on the basis of high rainfall to the north of the Region. The radar rainfall data for the Ingham radar are listed in table A5.1.

Event number	Start Time				End Time				Comments
1	00:00	19	October	1988	00:00	20	October	1988	
2	00:00	9	November	1988	00:00	10	November	1988	
3	00:00	19	November	1988	00:00	20	November	1988	Minimal rainfall in Region
4	00:00	29	November	1988	00:00	30	November	1988	
5	00:00	30	November	1988	00:00	31	November	1988	No raingauge data
6	00:00	24	February	1989	00:00	25	February	1989	
7	00:00	25	February	1989	00:00	26	February	1989	
8	00:00	2	March	1989	00:00	3	March	1989	
9	00:00	14	March	1989	00:00	15	March	1989	
10	00:00	20	March	1989	00:00	21	March	1989	
11	00:00	23	March	1989	00:00	24	March	1989	Minimal rainfall in Region
12	00:00	4	April	1989	23:59	4	April	1989	
13	00:00	9	April	1989	23:59	9	April	1989	
14	00:00	24	April	1989	23:59	24	April	1989	Minimal rainfall in Region
15	00:00	10	May	1989	23:59	11	May	1989	
16	00:00	11	May	1989	23:59	12	May	1989	
17	00:00	26	June	1989	23:59	26	June	1989	
18	00:00	27	June	1989	23:59	27	June	1989	
19	00:00	30	June	1989	23:59	30	June	1989	
20	00:00	7	July	1989	23:59	7	July	1989	No radar data 14:25 - 18:23
21	00:00	29	July	1989	23:59	29	July	1989	
22	00:00	30	July	1989	23:59	30	July	1989	
23	00:00	26	August	1989	23:59	26	August	1989	
24	00:00	13	December	1989	23:59	13	December	1989	No raingauge data
25	00:00	14	December	1989	23:59	14	December	1989	
26	00:00	16	December	1989	17:10	16	December	1989	
27	00:00	18	December	1989	23:59	18	December	1989	

Table A5.1: Ingham radar data used in ARIP

Appendix 6: Regional Radar Mapping

In order to facilitate the analysis, the 5 km Ingham radar grid has been mapped onto the Northern Area as shown in figure A6.1. This is a relatively simple process because all the cartesian radar grids of the U.K weather radars are routinely transformed by at-site processing so that the radar grid coincides directly with the National Grid (thus the radar site will not usually coincide with the grid centre). The shaded portion of the figure is the northern area radar coverage with a (minimum) 10 km mask applied around the area boundary.
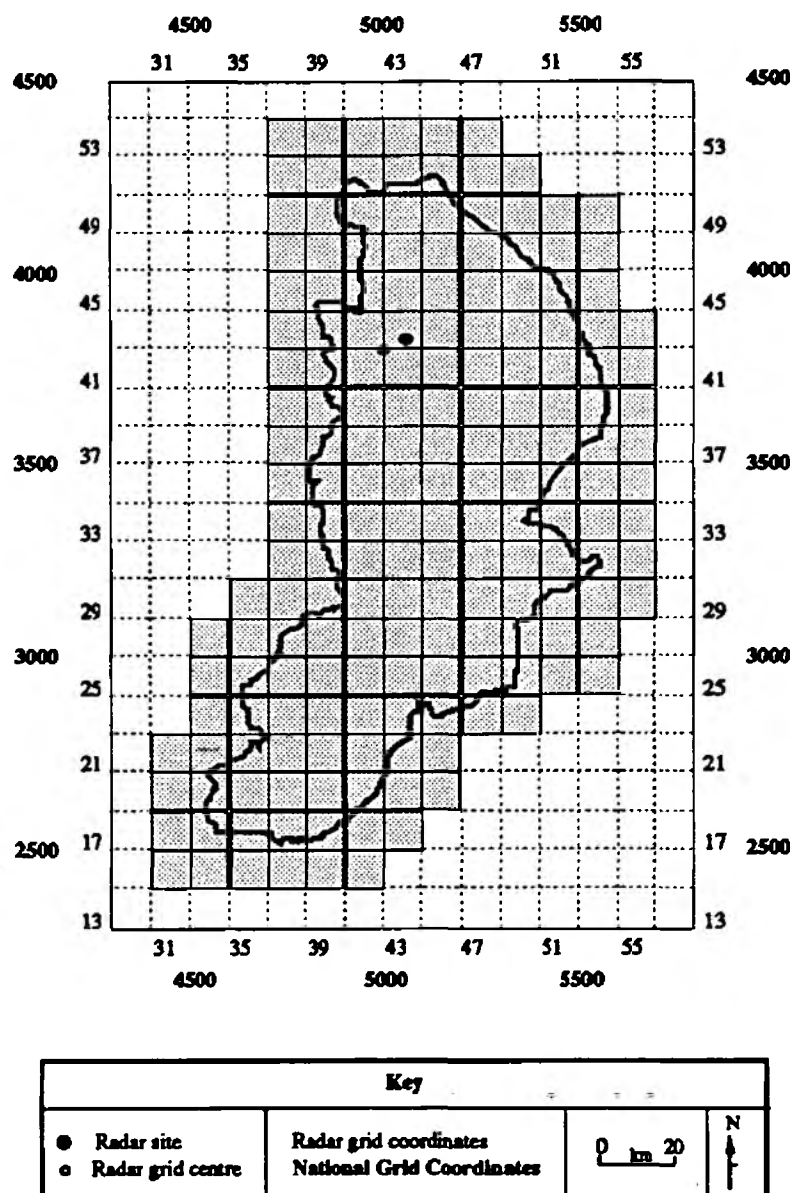

Figure A6.1: Coverage of Northern Area by Ingham radar (10 km grid)

Appendix 7: Regional Raingauge Network

The Regional raingauge network comprises of a number of tipping-bucket raingauges and rainfall loggers. Real-time rainfall data are only available from the former via interrogation over PSTN lines whilst the loggers are recording devices only, data becoming available some time later. Most of the instruments have an intensity resolution of 0.5 mm. The Regionwide network of raingauges and loggers (as of September 1989) is shown in figure A7.1. Of the order of 120 raingauges are envisaged for the Region (which would provide an average raingauge density of 248 sq km/gauge).

This study has concentrated largely on the Northern Area, primarily for two reasons:

- the area already had an established network of raingauges for which archived rainfall data were readily available.
- the Ingham radar is sited within the area and ranges up to 140 km from this radar could be analysed in conjunction with the raingauge data.
- radar data were freely available from the Meteorological Office by virtue of Anglian Region being a member of the Ingham radar Consortium.

The telemetering/ recording raingauge networks for the Northern Area are shown in figure A7.2 and A7.3, and a detailed listing of the raingauges covering the area is provided in table A7.1. The Regional raingauge coding scheme has been adopted throughout the study: raingauges each have a unique three character code - two digits preceded by a letter. Four letters are used, S, T, U and V. Generally S and T gauges are telemetering raingauges, whilst U and V gauges are rainfall loggers, though there are exceptions to this classification.

An attempt was made to collate Northern Area raingauge rainfall data for all periods for which Ingham radar data were available. This was largely achieved, and the exceptions are shown in the 'Comments' column of table A5.1. A full listing of daily raingauge totals for all the Northern Area raingauges may be found in Appendix 8.

Table A7.1: <u>Northern Area raingauge information and relations to Ingham radar</u>

Gauge Ref.	Location	NGR Coordinates	5 km radar grid cell coordinates	Altitude (m)	Azimuth relative to radar	Range (km)	Height of beam above gauge (km)†
S02	Burgh Sluice	5552 3586	54,38	3	112	63.9	0.80 ††
S03	Bardney	5106 3698	45,40	3	132	19.6	0.40 ††
S04	Fulsby	5241 3611	47,39	10	128	35.5	0.75 ††
S05	Baumber	5222 3740	47,41	60	109	27.6	0.52 ††
S06	Benniworth	5203 3826	47,43	95	90	24.2	0.40 ††
S07	Belchford	5296 3754	48,42	80	102	34.4	0.65 ††
S11	Raithby	5319 3859	49,44	45	85	35.9	0.34 †††
S13	Riseholme	4985 3756	42,42	40	162	7.8	0.17 †††
S14	Ulceby Cross	5405 3730	51,41	102	102	45.5	0.42
S16	Cadney	4996 4053	42,48	2	8	22.6	0.23
S17	Donnington Bridge	5174 3356	46,34	3	155	52.0	0.61
S18	Boston Grand Sluice	5324 3445	49,35	3	136	52.9	0.62
T01	Barford Bridge	4861 2831	40,23	77	185	100.4	1.39
T02	Braunston	4838 3065	39,28	110	189	77.5	0.92
T03	Castor	5124 2982	45,26	7	169	86.4	1.19
T05	Dodford	4627 2607	35,19	81	195	126.8	1.97
T07	Kingscliffe	5013 2975	43,26	43	176	85.7	1.14
T10	Yardley Hastings	4867 2574	40,18	74	184	126.0	1.96
U01	Bourne STW	5109 3202	45,31	4	166	64.5	0.80
U04	Corby Glen STW	4992 3247	42,31	76	176	58.4	0.63
U05	Crowland STW	5246 3091	47,28	2	158	79.2	1.06
U06	Dog-in-a-Doublet	5272 3993	48,46	2	62	35.1	0.38
U07	Etton PS	5143 3051	45,28	10	166	80.0	1.07
U08	Freemans	5177 3008	46,27	15	165	85.0	1.15
U09	Gunthorpe School	5183 3029	46,27	8	164	83.1	1.12
U10	Holbeach STW	5358 3258	50,32	3	145	69.6	0.89
U11	Manthorpe STW	5067 3164	44,30	15	170	67.4	0.84
U12	Paston School	5189 3029	46,27	8	164	83.3	1.13
U13	Peterborough STW	5201 2984	47,26	3	164	87.9	1.22
U14	Peterborough Tech	5201 3003	47,27	3	163	86.1	1.19
U15	Peterborough Town Hall	5193 2986	46,26	3	164	87.5	1.21
U16	Ridds Farm	4938 3255	41,32	118	182	57.5	0.58
U17	Ropsley STW	5001 3336	43,33	70	175	49.6	0.51
U18	Rutland Water	4946 3081	41,28	58	181	74.9	0.93
U19	Spalding STW	5262 3251	48,32	5	152	65.3	0.82
U20	Stamford STW	5071 3066	44,28	23	171	77.2	1.00
U21	Sutton Bridge	5476 3201	52,31	6	140	81.3	1.09
U22	Werrington School	5183 3029	46,27	8	164	83.1	1.12
U23	West Walton STW	5460 3140	52,29	5	144	85.2	1.17
U24	Wisbech Isle College	5472 3086	52,28	5	145	90.3	1.26
U25	Whittlesey STW	5274 3962	48,46	3	67	34.0	0.36
V01	Boughton Green	4760 2647	38,19	110	189	120.0	1.79
V02	Bozeat STW	4902 2593	41,18	70	182	123.8	1.91
V03	Brigstock STW	4948 2847	41,23	55	180	98.3	1.37
V04	Collyweston WT	5000 3024	43,27	93	177	80.7	0.99
V05	Corby Beaufield	4861 2888	40,24	125	186	94.7	1.23
V06	Chesterton	5148 2946	45,25	17	168	90.4	1.25
V07	Daventry R	4584 2619	34,19	183	197	126.8	1.87
V08	Dingley PS	4774 2867	38,24	148	190	98.1	1.27
V09	Draughton STW	4754 2768	38,22	105	191	108.2	1.53
V10	Duston Mill	4729 2596	37,18	60	190	125.6	1.96
V11	Gt. Billing STW	4882 2619	40,19	48	183	121.4	1.88
V12	Gt. Doddington STW	4879 2642	40,19	45	183	119.1	1.83

table continued over...

Table A7.1: Raingauge information (continued)

Gauge Ref.	Location	NGR Coordinates	Radar grid cell coordinates	Altitude (m)	Azimuth relative to radar	Range (km)	Height of beam above gauge (km)[†]
V13	Gt. Easton STW	4854 2926	40,26	55	187	91.0	1.23
V14	Hallaton STW	4795 2959	38,26	80	190	88.7	1.16
V15	Hannington Res	4826 2712	39,21	135	186	112.6	1.59
V16	Husbands Bosworth	4645 2847	35,23	137	197	103.3	1.39
V17	Islip STW	4991 2797	42,22	30	178	103.3	1.50
V18	Kibworth STW	4691 2936	36,25	92	196	93.4	1.24
V19	Litchborough	4624 2551	35,18	110	194	132.3	2.07
V20	Market Harborough	4727 2869	37,24	80	193	98.9	1.36
V21	Oundle PLC Office	5042 2883	43,24	35	175	95.0	1.33
V22	Oundle STW	5038 2897	43,24	32	173	93.6	1.30
V23	Pitsford Res	4757 2688	38,20	91	190	116.0	1.71
V24	Preston Capes	4567 2545	34,17	185	197	134.4	2.05
V25	Rothwell STW	4826 2807	39,23	91	187	103.2	1.44
V26	Rushden PS	4946 2675	41,20	40	180	115.5	1.75
V27	Sibbertoft Res	4691 2823	36,23	184	195	104.3	1.37
V28	Sibson	5090 2962	44,26	32	171	87.8	1.19
V29	Stimpson Ave	4768 2616	38,19	91	189	122.9	1.87
V30	Tugby	4760 3005	38,27	152	193	84.9	1.01
V31	Uppingham STW	4877 2994	40,26	110	185	84.0	1.04
V32	Wellingborough PS	4908 2674	41,20	40	182	115.7	1.76
V34	Kettering Office	4870 2799	40,22	91	185	103.5	1.44
Raingauges for which no data are available							
S01	Toft Newton	5033 3873	43,44	10	59	8.4	0.21[†††]
S08	Stenigot	5259 3829	48,43	148	90	29.8	0.16
S09	Welton le Wold	5282 3878	48,44	70	81	32.5	0.28
S10	Horncastle	5261 3702	48,41	30	113	32.6	0.66[††]
S12	Saltersford Rain	4926 3335	41,33	57	184	49.6	0.52
S15	Brant Broughton	4927 3546	41,37	11	186	28.6	0.29
S19	Covenham	5351 3967	50,46	3	70	41.3	0.46
S20	Tathwell	5323 3830	49,43	70	90	36.2	0.32
T04	Corby STW	4906 2889	49,06	97	183	94.3	1.25
T08	Ravensthorpe	4681 2703	36,21	98	193	116.1	1.71
T09	Stamford	5069 3065	44,28	23	171	77.3	1.00

[†]Notes:
(1) unless otherwise stated (see note [2]), beam height refers to the 0.5 degree beam
(2) where a raingauge is within the radar beam infill zone (see figure 9), height given is for the appropriate beam, i.e. 1.1[††] or 1.5[†††] degree
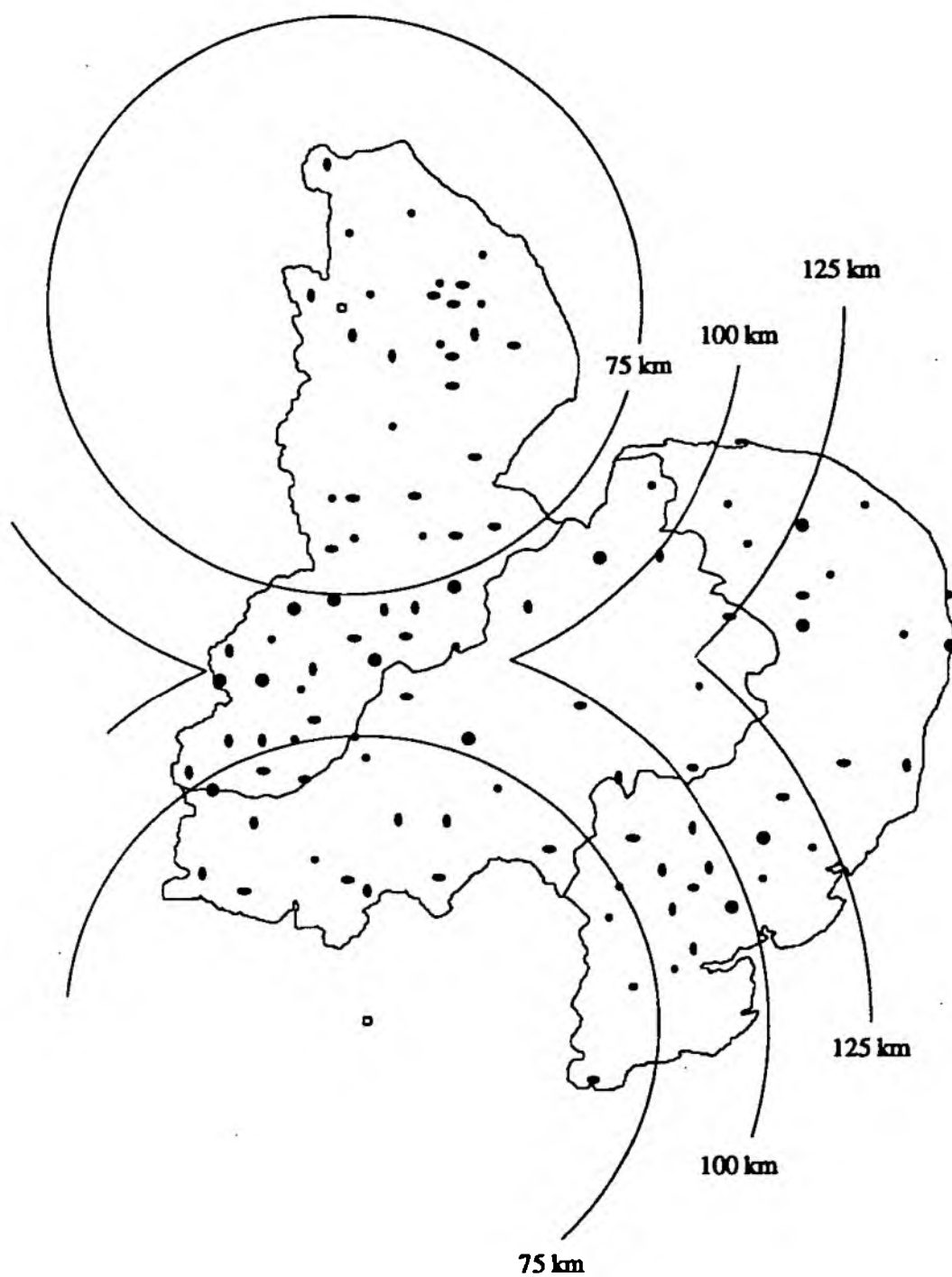(3) all raingauges have a depth resolution of 0.5mm.

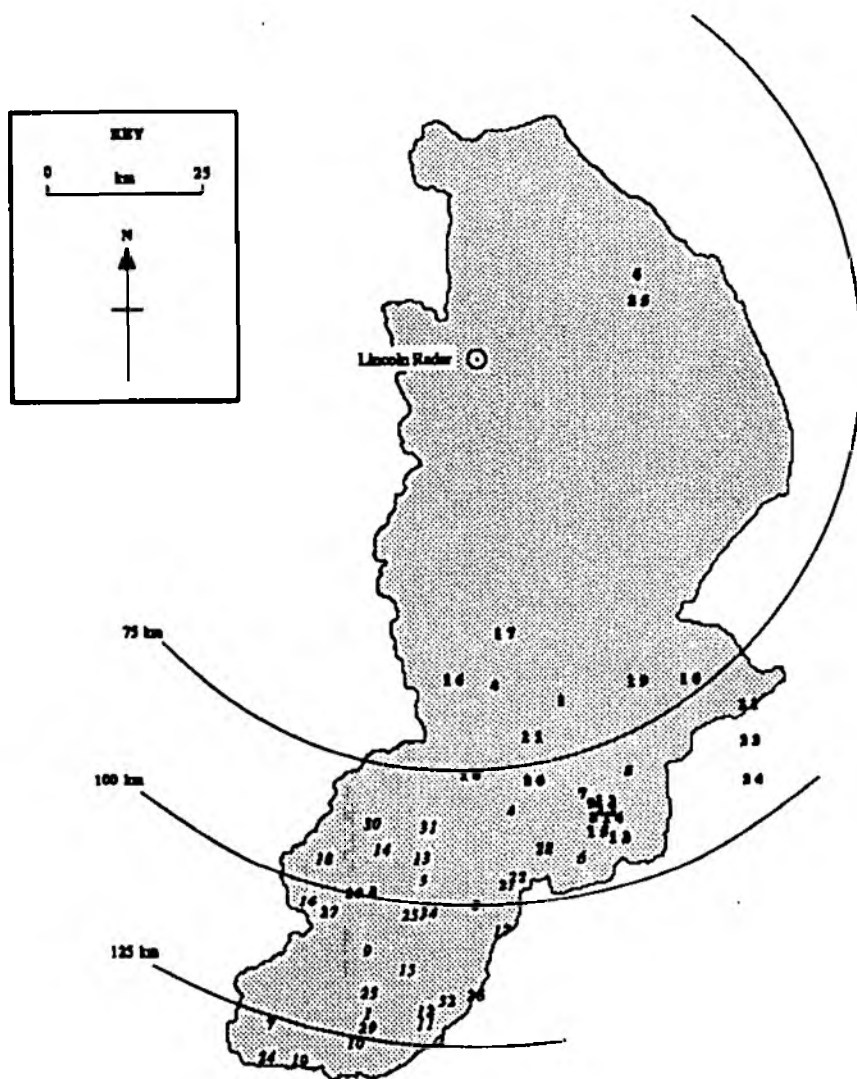Figure A7.1: Combined Radar and Telemetering Raingauge Coverage
(September 1989)

Figure A7.2: Recording rainfall loggers (Outline indicates
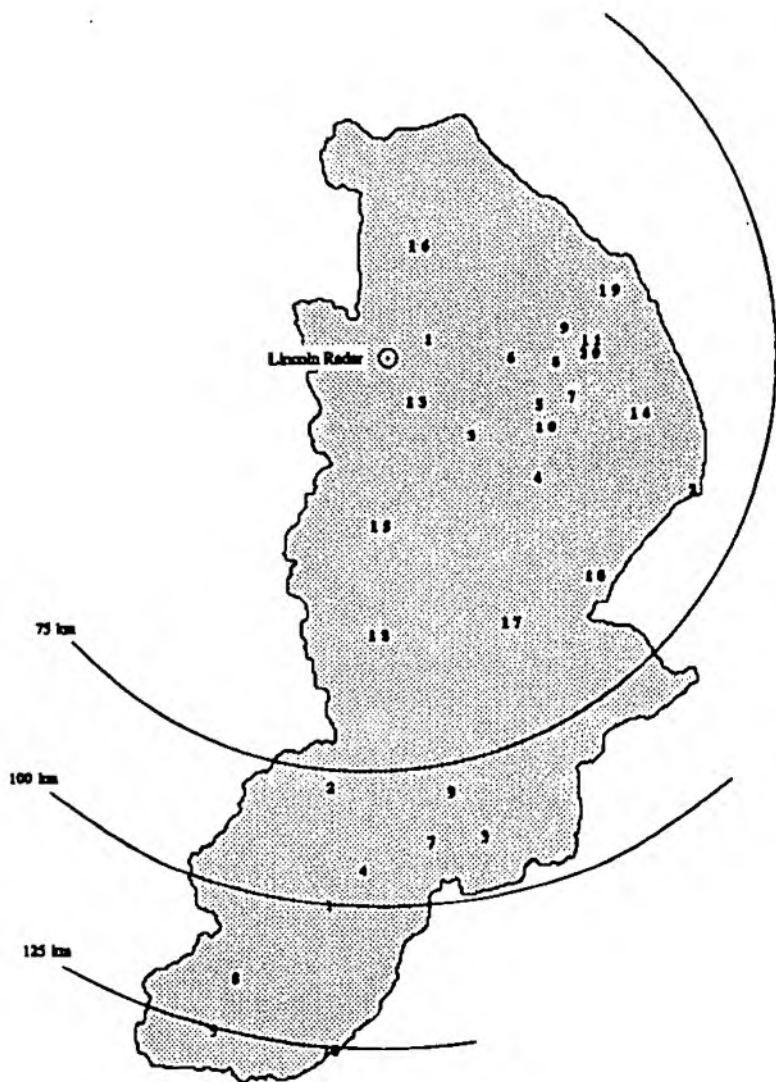group U gauges. *Italic* indicates group V gauges)

Figure A7.3: Telemetering raingauges (Bold indicates group S gauges. Plain indicates group T gauges)

	881019	881109	881119	881129	890224	890225	890302	890314	890320	890323	890404	890409	890424	890510	890511	890626	890627	890630	890707	890729	890730	890826	891214	891216	891218
S02	3.0	2.0	0.0	5.5	-	-	-	-	-	-	-	-	-	-	-	0.0	10.0	4.5	0.5	0.5	8.5	6.5	24.0	8.0	14.0
S03	-	-	-	-	-	-	-	-	-	-	-	-	-	-	-	-	24.0	12.5	-	-	3.0	-	19.5	11.5	14.0
S04	-	-	-	-	-	-	-	-	-	-	-	-	-	-	-	-	18.0	13.0	-	-	13.0	-	22.0	11.5	13.5
S05	-	-	-	-	-	-	-	-	-	-	-	-	-	-	-	-	15.0	17.0	-	-	4.5	-	21.0	12.0	15.0
S06	-	-	-	-	-	-	-	-	-	-	-	-	-	-	-	-	25.0	12.0	-	-	2.0	-	13.5	14.5	16.5
S07	9.0	5.0	0.0	6.0	-	-	-	-	-	-	-	-	-	-	-	0.0	6.5	7.5	2.5	0.0	3.0	12.0	21.5	10.5	16.0
S11	8.5	4.5	0.0	7.5	-	-	-	-	-	-	-	-	-	-	-	0.0	13.0	10.0	3.0	0.0	3.0	25.5	26.5	17.0	18.5
S13	7.0	7.5	0.0	10.5	-	-	-	-	-	-	-	-	-	-	-	3.0	22.0	12.0	2.0	0.0	5.0	8.0	20.5	13.5	15.5
S14	9.5	3.0	0.0	7.0	-	-	-	-	-	-	-	-	-	-	-	0.0	14.0	11.0	0.5	0.0	35.0	17.0	14.0	13.0	8.5
S16	5.5	4.0	0.5	6.5	-	-	-	-	-	-	-	-	-	-	-	14.5	2.0	13.0	2.5	0.0	11.0	17.0	14.5	19.0	14.5
S17	1.0	1.5	0.0	8.5	-	-	-	-	-	-	-	-	-	-	-	0.0	12.0	9.0	3.5	3.5	14.0	3.5	22.5	10.5	19.0
S18	4.0	1.0	0.0	9.0	-	-	-	-	-	-	-	-	-	-	-	0.0	7.5	5.0	4.5	0.5	11.0	7.5	23.0	10.5	19.0
T01	2.0	1.5	0.0	7.0	-	-	-	-	-	-	-	-	-	-	-	2.5	8.5	0.5	34.0	0.5	5.0	4.0	9.5	8.0	15.0
T02	0.0	3.0	0.0	11.5	-	-	-	-	-	-	-	-	-	-	-	5.0	4.5	5.5	30.0	15.0	11.5	6.5	31.0	13.0	20.0
T03	0.5	1.5	0.0	16.0	-	-	-	-	-	-	-	-	-	-	-	0.0	7.0	1.5	22.0	7.0	9.5	5.0	26.0	13.0	12.0
T05	1.0	1.0	0.0	11.5	-	-	-	-	-	-	-	-	-	-	-	6.0	2.0	1.0	30.0	0.0	0.0	8.0	17.0	12.5	16.0
T07	0.0	1.5	0.0	12.0	-	-	-	-	-	-	-	-	-	-	-	0.5	6.5	1.0	35.0	6.0	13.0	6.0	22.5	12.5	14.0
T10	0.0	3.5	0.0	13.0	-	-	-	-	-	-	-	-	-	-	-	0.0	1.5	0.0	39.5	-	-	4.0	21.0	16.5	18.5
U01	1.0	1.5	0.0	12.5	4.0	0.5	5.0	8.0	4.0	0.0	-	1.5	7.5	0.0	4.0	0.0	11.0	8.0	14.0	7.5	9.0	6.5	21.0	11.0	17.5
U04	0.0	1.5	0.0	11.5	8.5	2.0	6.5	12.0	4.0	0.5	5.5	1.5	11.0	0.0	4.0	2.5	8.5	9.0	8.5	29.0	20.5	3.0	23.0	7.5	20.0
U05	1.0	2.0	0.0	10.0	2.0	1.0	4.5	7.0	4.0	0.0	-	0.5	5.5	0.0	3.5	0.0	11.0	7.0	9.0	7.5	8.5	2.5	17.0	11.5	11.5
U06	2.5	2.5	0.0	9.5	1.0	0.5	4.5	8.5	4.0	0.0	3.0	0.5	6.0	0.0	5.5	0.0	6.0	2.0	20.5	3.0	7.5	5.5	21.0	13.0	15.5
U07	1.0	1.5	0.0	13.0	4.5	1.0	6.0	10.0	5.0	0.0	3.5	1.0	7.5	0.0	4.5	0.0	6.0	3.5	18.5	7.0	5.0	4.5	19.5	12.5	13.5
U08	1.0	-	-	-	-	-	-	9.0	4.0	0.5	3.0	1.0	8.0	0.0	4.0	0.0	10.0	2.0	-	5.0	11.0	-	-	-	-
U09	-	-	-	11.0	2.5	1.0	4.5	-	-	-	-	-	-	0.0											
U10	3.0	1.5	0.0	11.0	-	-	-	-	5.5	0.0	3.0	0.5	7.5	0.0	3.5	0.0	9.0	8.0	-	13.5	15.0	6.0	21.0	12.0	16.5
U11	0.5	1.5	0.0	9.0	5.0	1.0	5.5	8.0	4.0	0.0	6.0	1.0	8.5	0.0	4.5	0.0	7.0	8.0	22.5	6.0	12.5	10.5	24.0	11.5	14.5
U12	-	2.5	0.0	-	-	-	-	-	-	-	-	-	-	-	-	-	-	-	15.5	-	-	4.0	23.5	12.5	13.5
U13	1.0	2.0	0.0	12.5	1.5	1.5	4.5	9.0	4.5	0.5	3.0	1.0	7.5	0.0	4.5	0.0	3.0	1.5	20.5	5.5	14.0	4.5	-	-	-
U14	1.0	2.5	0.0	11.0	2.0	1.0	5.0	10.5	5.0	0.5	3.0	1.0	8.0	0.0	-	0.0	10.5	2.0	-	5.0	8.5	5.0	26.0	13.0	14.0
U15	1.0	2.5	0.0	12.0	1.5	1.5	4.5	9.0	4.5	0.5	3.5	1.0	8.0	0.0	-	0.0	5.5	1.5	-	4.5	11.5	5.0	25.5	13.0	14.5
U16	0.0	-	-	11.0	12.5	3.0	8.5	8.0	4.5	0.0	9.0	1.5	4.0	-	6.0	-	-	-	-	11.0	13.5	3.5	2.0	-	0.0
U17	1.0	-	-	10.0	9.0	1.5	8.0	7.0	5.0	0.0	7.0	2.0	9.5	-	5.5	3.0	13.5	10.0	3.0	0.5	24.0	5.5	25.5	10.5	19.0
U18	0.0	2.0	0.0	12.0	10.0	2.0	6.0	10.5	4.5	0.0	8.0	2.0	6.5	-	4.0	4.5	11.0	10.0	10.0	4.5	8.0	5.5	27.0	13.0	19.0
U19	7.5	1.5	0.0	13.5	3.0	1.5	6.0	7.0	5.5	0.5	3.5	0.5	7.5	0.0	4.0	0.0	10.0	10.0	-	19.0	16.5	6.5	20.0	12.0	17.5
U20	0.5	1.5	0.0	10.5	2.5	1.5	5.0	-	-	-	-	-	-	-	-	-	-	-	-	-	-	-	-	-	-
U21	7.5	7.0	0.5	10.5	1.0	2.5	-	7.0	5.5	0.5	1.5	0.5	10.5	0.0	4.0	0.0	7.5	7.5	-	15.5	10.5	-	18.5	6.5	11.0

Table A8.1: Raingauge Daily Rainfall Totals

	881019	881109	881119	881129	890224	890225	890302	890314	890320	890323	890404	890409	890424	890510	890511	890626	890627	890630	890707	890729	890730	890826	891214	891216	891218
U22	0.0	2.5	0.0	-	-	-	-	11.0	5.0	0.5	2.5	1.0	8.5	0.0	4.5	0.0	9.0	3.0	19.0	8.0	8.0	3.5	-	-	-
U23	4.5	7.0	0.5	5.5	2.0	3.5	-	8.5	5.0	0.0	-	-	-	-	-	0.0	10.0	6.5	5.0	12.5	7.5	4.5	23.0	12.5	12.0
U24	4.0	8.5	0.0	11.5	1.5	7.5	-	7.5	4.5	0.5	2.5	0.5	8.5	0.0	5.5	-	-	-	-	8.0	3.5	7.0	20.5	11.0	12.5
U25	1.5	2.0	0.0	11.5	0.5	0.5	-	8.0	4.5	0.5	2.0	1.0	6.5	0.0	6.5	0.0	5.0	1.5	13.5	5.5	14.5	4.0	20.0	13.0	13.5
V01	1.0	0.5	0.0	-	6.0	2.5	4.0	10.5	4.5	0.5	0.0	0.0	1.5	0.5	7.5	2.0	8.5	-	30.5	-	-	5.0	19.5	12.5	18.5
V02	1.0	2.5	0.0	11.5	3.5	10.5	6.0	9.5	7.5	0.5	5.5	1.5	-	-	6.0	0.0	6.0	0.0	42.5	0.5	2.5	10.5	-	-	-
V03	2.0	1.0	0.0	12.5	5.5	2.0	3.5	10.5	4.5	0.5	6.0	2.0	7.5	0.0	4.5	1.5	13.5	0.0	30.0	0.5	10.5	4.5	19.5	15.0	13.0
V04	0.0	1.5	0.0	12.0	6.5	1.5	-	10.0	4.0	0.5	5.0	1.0	5.0	0.0	5.0	1.0	8.0	2.0	37.5	7.0	3.5	5.0	24.5	10.5	17.0
V05	1.5	-	-	13.0	8.5	1.0	6.0	12.5	4.5	1.0	6.5	2.0	9.0	0.0	5.0	1.5	5.0	0.5	39.0	17.0	7.0	1.0	24.0	11.0	3.0
V06	1.0	2.5	0.0	13.5	5.0	1.5	5.0	11.0	5.0	1.0	3.5	1.5	8.5	0.0	5.0	0.0	5.5	1.0	23.0	0.0	0.0	2.5	23.0	13.5	8.5
V07	1.0	-	-	10.5	8.0	2.0	4.5	9.5	4.5	0.0	2.5	1.5	6.0	0.0	5.0	4.5	7.0	-	37.5	2.0	3.5	3.5	20.0	14.5	19.0
V08	7.5	-	-	14.0	9.5	1.5	6.0	12.5	4.0	1.0	5.0	2.5	8.5	0.0	3.5	2.5	13.5	0.5	31.0	4.5	14.0	1.0	28.5	12.0	19.0
V09	0.5	2.0	0.0	12.5	9.5	1.5	-	-	-	-	-	-	10.5	0.0	3.0	2.0	5.5	0.0	44.5	1.0	6.5	8.0	21.0	14.5	16.0
V10	-	-	-	-	-	-	-	-	-	-	5.0	1.0	12.5	0.0	7.0	1.0	3.0	-	28.5	1.5	2.0	11.5	16.5	12.0	18.5
V11	0.0	0.5	0.0	12.5	4.0	4.0	4.5	9.0	4.5	0.5	-	-	-	-	8.5	0.5	4.0	0.0	39.5	0.5	3.0	11.5	20.5	13.5	17.5
V12	5.0	1.0	0.0	12.5	3.0	5.0	5.0	9.0	5.5	0.0	6.0	1.5	14.5	0.0	8.5	0.0	4.0	0.0	38.5	0.5	3.0	10.5	1.5	-	0.5
V13	4.0	-	-	13.5	11.0	1.0	7.0	10.5	4.0	0.5	5.0	2.5	10.0	0.0	7.0	0.5	2.0	0.0	0.0	0.0	0.0	3.5	25.0	8.5	14.5
V14	7.5	-	-	11.5	10.5	1.5	5.5	8.5	4.5	0.5	9.0	2.0	9.5	0.0	5.5	4.0	4.0	0.0	53.5	-	-	7.5	27.5	12.0	17.0
V15	2.5	0.5	0.0	15.5	5.5	2.0	4.5	10.5	4.5	0.5	3.5	2.0	8.5	0.0	7.0	-	-	-	-	0.5	4.0	6.5	20.0	16.0	18.0
V16	0.5	2.0	0.0	14.0	12.0	1.0	5.0	12.0	4.0	1.0	4.5	2.0	7.5	-	-	6.0	9.5	0.5	36.5	7.0	13.5	0.0	21.5	11.0	16.5
V17	0.5	2.0	0.0	13.0	6.0	2.0	3.5	9.5	4.5	0.5	0.0	1.0	11.0	0.0	8.0	-	-	-	37.5	1.0	5.0	8.0	22.0	14.0	14.0
V18	3.0	2.0	0.0	12.5	11.5	0.0	5.5	11.5	5.0	-	7.0	2.5	7.5	0.0	4.0	6.5	7.0	-	41.5	4.0	20.0	9.5	27.5	6.0	8.0
V19	1.0	1.0	0.0	16.0	11.5	5.5	7.0	11.5	4.5	0.5	4.0	2.0	11.0	-	-	3.0	13.0	0.5	34.0	2.5	2.5	3.0	21.5	15.0	20.5
V20	3.0	2.0	0.0	13.5	9.5	0.5	6.5	13.5	4.0	1.0	6.0	2.0	7.0	0.0	4.5	3.5	11.5	-	33.0	8.5	11.0	1.0	24.0	10.5	19.5
V21	1.0	2.0	0.0	13.0	5.5	1.5	3.5	9.5	4.5	0.5	5.5	1.0	9.5	0.0	4.5	0.5	5.0	0.5	21.0	3.5	13.5	2.5	20.5	13.0	13.0
V22	0.5	2.0	0.0	11.5	1.0	0.0	-	10.0	4.0	0.5	5.0	1.0	8.5	0.0	4.0	0.5	5.0	0.5	25.5	8.0	9.5	2.0	20.0	12.5	13.5
V23	0.5	0.0	0.0	10.0	8.5	2.0	5.5	10.0	4.5	0.0	3.0	1.5	9.0	0.0	5.5	2.5	6.5	0.5	34.5	0.5	1.5	3.5	18.0	13.0	16.0
V24	2.0	0.5	0.5	13.0	11.5	4.5	5.5	9.0	4.5	0.5	3.5	2.0	9.5	0.0	5.0	2.5	8.5	0.5	33.5	3.5	4.0	4.5	18.0	14.0	18.5
V25	2.5	1.0	0.0	13.0	7.5	1.0	6.5	12.5	7.0	2.0	-	-	-	0.0	4.0	2.0	6.0	0.0	36.5	1.0	12.0	6.5	23.5	13.5	18.0
V26	0.0	2.5	0.0	13.0	5.5	5.0	0.0	11.0	5.0	0.5	0.0	0.0	0.0	0.0	7.5	0.0	4.5	0.0	34.5	0.5	2.5	9.5	21.5	13.5	18.0
V27	0.0	1.5	0.0	15.0	12.0	0.5	6.5	13.5	4.0	1.0	6.5	3.0	7.0	0.0	4.5	5.0	10.5	0.5	41.0	7.5	12.5	1.0	23.0	13.0	18.0
V28	0.0	1.5	0.0	13.5	0.5	0.0	3.0	9.5	3.5	0.5	3.5	1.0	8.0	0.0	4.0	0.0	8.5	1.5	4.5	9.0	9.0	4.0	21.5	11.5	11.5
V29	0.0	0.0	0.0	10.5	5.5	4.5	4.5	9.0	5.5	0.5	4.0	1.0	9.0	0.0	8.5	0.5	3.0	0.0	30.5	1.0	2.0	9.0	18.0	13.5	17.5
V30	-	-	-	12.5	8.5	1.5	-	-	-	0.5	9.0	1.0	9.0	0.0	4.0	3.0	10.5	-	39.0	7.5	18.0	7.0	34.0	12.0	18.0
V31	1.5	-	-	15.0	9.0	1.0	6.0	9.5	5.0	-	9.0	2.0	5.5	0.0	6.0	2.5	6.0	0.5	38.5	3.5	8.0	7.0	30.5	11.5	18.0
V32	9.5	1.5	0.0	18.5	3.5	4.0	4.5	8.0	4.0	0.5	6.0	1.5	11.0	0.0	7.5	0.0	4.5	0.0	35.5	0.5	2.5	9.5	21.0	12.0	16.0
V34	-	-	-	-	-	-	-	-	-	-	-	-	-	-	-	-	-	-	-	-	-	-	21.0	13.5	17.5
No. of gauges	65	58	58	64	54	50	42	48	49	48	46	48	48	45	47	62	66	60	58	63	67	65	68	66	68

Table A8.1: Raingauge Daily Rainfall Totals (continued from previous page)

Appendix 9: Two-dimensional Interpolation

The routines described in this Appendix are part of the Numerical Algorithms Group Fortran Library (see references under NAG). Some of the following material is from the relevant routine documentation.

Renka and Cline Method

This routine constructs an interpolating surface $F(x,y)$ through a set of M scattered data points (x_r, y_r, f_r), for $r=1,2,...M$, using a method due to Renka and Cline. In the (x,y) plane, the data points must be distinct. The constructed surface is continuous and has continuous first order derivatives.

The method involves firstly creating a triangulation with all the (x,y) data points as nodes, the triangulation being as nearly equi-angular as possible (Cline and Renka, 1984). Then gradients in the x- and y-directions are estimated at node r, for $r=1,2,...,M$, as the partial derivatives of a quadratic function of x and y which interpolates the data value f_r, and which fits the data values at nearby nodes (those within a certain distance chosen by the algorithm) in a weighted least square sense. The weights are chosen such that closer nodes have more influence than more distant nodes on derivative estimates at node r. The computed partial derivatives, with the f_r values, at the three nodes of each triangle define a piecewise polynomial surface of certain form which is the interpolant on that triangle. More detailed information on the algorithm is provided in Renka and Cline (1984), Lawson (1977), and Renka (1984).

The interpolant $F(x,y)$ can be subsequently evaluated at any point (x,y) inside or outside the domain of the data in the second stage routine (see below). Points outside the domain of the data are determined by extrapolation.

The second stage routine computes the interpolant for a specified grid. The routine takes as input the parameters defining the interpolant $F(x,y)$ of a set of scattered data points (x_r, y_r, f_r), for $r=1,2,...,M$, and evaluates the interpolant at the point (px,py). If (px,py) is equal to (x_r, y_r) for some value of r, the returned value will be equal to fr. If (px,py) is not equal to (x_r, y_r) for any r, the derivatives passed to the routine are used to compute the interpolant. A triangle is sought which contains the point (px,py), and the vertices of the triangle along with the partial derivatives and f_r values at the vertices are used to compute the value $F(px,py)$. If the point (px,py) lies outside the triangulation defined by the input parameters, the returned value is obtained by extrapolation. In this case, the interpolating function F is extended linearly beyond the triangulation boundary.

Modified Shepherd Method

This routine constructs and interpolating surface $F(x,y)$ through a set of M scattered data points (x_r, y_r, f_r), for $r=1,2,...M$, using a modification of Shepherd's method. The surface is continuous and has continuous first derivatives.

The basic Shepherd method, described in Shepherd (1968), interpolates the input data with the weighted mean:

$$F(x,y) = \frac{\displaystyle\sum_{r=1}^{M} w_r \, (x,y) \, f_r}{\displaystyle\sum_{r=1}^{M} w_r \, (x,y)} \quad \text{where} \quad w_r \, (x,y) = \frac{1}{d_r^2} \quad \text{and} \quad d_r^r = (x-x_r)^2 + (y-y_r)^2$$

(eq. A9.1)

The basic method is global in that the interpolated value at any point depends on all the data, but the method uses a modification due to Franke and Neilson (1980), whereby the method becomes local by adjusting each $w_r(x,y)$ to be zero outside a circle with centre (x_r, y_r) and some radius R_w. Also, to improve the performance of the basic method, each f_r above is replaced by a function $f_r(x,y)$ which is a quadratic fitted by weighted least-squares to data local to (x_r, y_r) and forced to interpolate (x_r, y_r, f_r). In this context, a point (x,y) is defined to be local to another point if it lies within some distance R_q of it. Computation of these quadratics constitutes the main work done by this routine. If there are less than five other points within distance R_q from (x_r, y_r) the quadratic is replaced by a linear function. In cases of rank deficiency, the minimum norm solution is computed.

The values for R_w and R_q can be specified explicitly but it is usually easier to choose instead two integers N_w and N_q, from which the routine computes R_w and R_q These integers can be thought of as the average number of data points lying within distances R_w and R_q respectively from each node. Default values are utilised by the procedure.

The timing of the routine is approximately proportional to the number of data points M, provided that N_q is of the same order as its default vale (18). If N_q is increased so that the method becomes more global, the time taken becomes approximately proportional to M^2.

The radii R_w and R_q are computed as:

$$\frac{D}{2}\sqrt{\frac{N_w}{M}} \quad \text{and} \quad \frac{D}{2}\sqrt{\frac{N_q}{M}}$$

(eq. A9.2)

where D is the maximum distance between any pairs of data points.

Default values $N_w=9$ and $N_q=18$ work quite well when the data points are fairly uniformly distributed. However, for data having some regions with relatively few points or for small data sets ($M<25$), a larger value of N_w may be needed. This is to ensure a reasonable number of data points within a distance R_w of each node, and to avoid some regions in the data area being left outside all the discs of radius R_w on which the weights $w_r(x,y)$ are non-zero. Maintaining N_q approximately equal to $2.N_w$ is usually an advantage. Increasing N_w and N_q does not improve the quality of the interpolant in all cases: it does increase the computational time and makes the method less local.

The interpolant $F(x,y)$ can be subsequently evaluated at any point (x,y) inside or outside the domain of the data in the second stage routine (see below).

The second stage routine computes the interpolant for a specified grid. The routine takes as input the parameters defining the interpolant $F(x,y)$ of a set of scattered data points (x_r, y_r, f_r) for $r=1,2,...,M$, and evaluates the interpolant at the point (px,py). If (px,py) is equal to (x_r, y_r) for some value of r, the returned value will be equal to f_r. If (px,py) is not equal to (x_r, y_r) for any r, all points that are within a prescribed distance of (px,py), along with the corresponding nodal functions will be used to compute a value of the interpolant.

Appendix 10: Two-dimensional Surface Fitting

The routines described in this Appendix are part of the Numerical Algorithms Group Fortran Library (see references under NAG). Some of the following material is from the relevant routine documentation.

Bicubic Spline Surface Fitting

The knots of the spline are located automatically, but a single parameter must be specified to control the trade-off between closeness of fit and smoothness of fit.

The routines determine a smooth bicubic spline approximation $s(x,y)$ to the set of data points (x_r, y_r, f_r) with weights w_r for $r=1,2,...,m$ (scattered data only). The approximation domain is considered to be the rectangle $[x_{min}, x_{max}]*[y_{min}, y_{max}]$, where $x_{min}(y_{min})$ and $x_{max}(y_{max})$ denote the lowest and highest data values of $x(y)$, though the domain can be extended by augmenting the data with two artificial data points $(a,c,0)$ and $(b,d,0)$ with zero weight, where $[a,b]*[c,d]$ denotes the enlarged approximation rectangle.

The spline is given by the B-spline representation:

$$s(x,y) = \sum_{i=1}^{n_x-4} \sum_{j=1}^{n_y-4} c_{ij} \, M_i(x) \, N_j(y)$$

(eq. A10.1)

where $M_i(x)$ and $N_j(y)$ denote normalised B-splines, the former defined on the knots l_i to l_{i+4} and the latter on the knots m_j to m_{j+4}. The total numbers n_x and n_y of these knots and there values $l_1,...,l_{n(x)}$ and $m_1,...,m_{n(y)}$, are chosen automatically by the routine. The knots $l_5,...,l_{n(x)-4}$ are the interior knots; they divide the approximation domain $[x_{min}, x_{max}]*[y_{min}, y_{max}]$, into $(n_{x-7})*(n_{y-7})$ subpanels $[l_i, l_{i+1}]*[m_j, m_{j+1}]$, for $i=4,5,...,n_{x-4}$; $j=4,5,...,n_{y-4}$. Then, the coefficients c_{ij} are determined as the solution of the following minimisation problem:

minimise

η, subject to the constraint:

$$\theta = \sum_{r=1}^{m} \epsilon_r^2 \le S$$

(eq. A10.2)

where:

η is a measure of the (lack of) smoothness of $s(x,y)$. Its value depends on the discontinuity jumps in $s(x,y)$ across the boundaries of the subpanels. It is zero only where there are no discontinuities and is positive otherwise, increasing with the size of the jumps.

ε_r denotes the weighted residual $w_r(f_r - s(x_r, y_r))$,

S is a non-negative number specified by the user.

By means of the parameter S, the 'smoothing factor', the balance between smoothness and closeness and of fit, as measured by the sum of the squares of the residual in eq. A10.2. can be controlled. If S is too large, the spline will be too smooth (underfit) and if S is too small the spline will pick up too much noise (overfit) In the extreme cases the method returns an interpolating spine $(\theta=0)$ i.e. if S is set very small, and returns the least squares bicubic polynomial $(\eta=0)$ if S is set very large. Determination of the best value of S involves an adaptive search for locating the knots of the bicubic spline (depending on the function underlying the data and on the value S), and an iterative method for solving the constrained minimisation problem once the knots have been determined.

First suitable knot sets are built up in stages (starting with no interior knots). At each stage a bicubic spline is fitted to the data by least-squares and θ, the sum of the squares of the residuals is computed. If $\theta>S$, a new knot is added to one knot set or the other so as to reduce θ at the next stage. The new knot is located in an interval where the fit is particularly poor. When $\theta\leq S$ the knot sets are accepted. The routine goes on to compute a spline which has these knot sets and which satisfies the full fitting criterion specified by the minimisation requirement. The theoretical solution has $\theta=S$. The routine computes the spline by an iterative scheme which is ended when $\theta=S$ within a relative tolerance (of 0.001). The main part of each iteration consists of a linear least-squares computation of the special form. If the routine finds that even with no interior knots $(N=8)$, the least squares spline already has its sum of squares of residuals $\leq S$. In this case, since this spline (simply a bicubic polynomial) also has an optimal value for the smoothness measure η, namely zero, it is returned at once as the trivial solution (usually meaning S has been chosen too large). The timing of the routine depends on the complexity of the shape of the data, the value of the smoothing factor S, and the number of data points. Choosing S to be very small significantly increases the computation time.

Values of the computed spline are subsequently computed using a second phase evaluation routine (as with the routines described in Appendix 9).
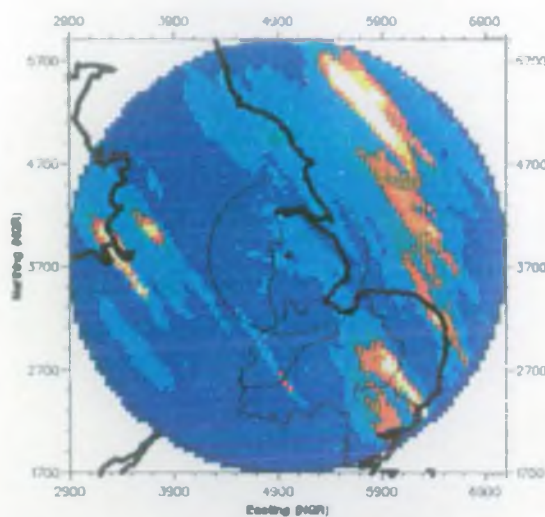
A11.1: 19th October 1988
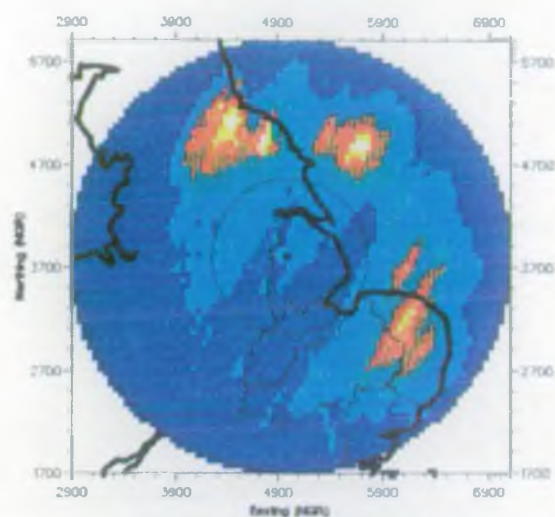
A11.2: 9th November 1988
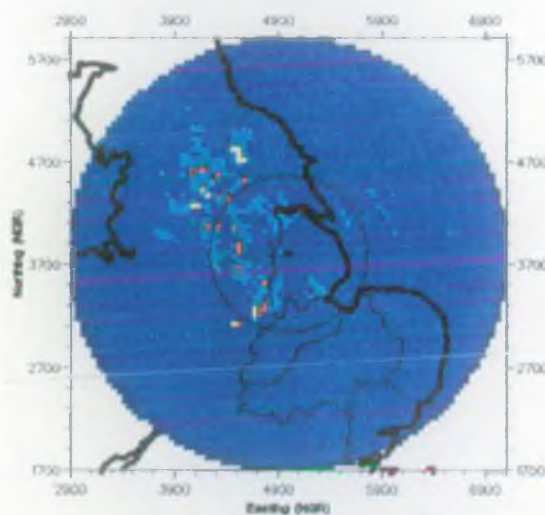
A11.3: 19th November 1988
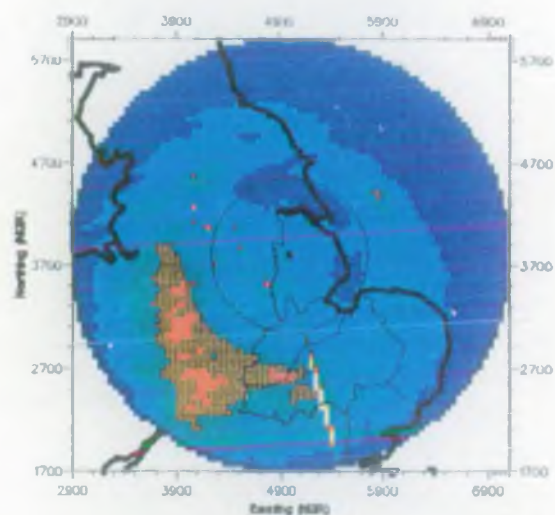
A11.4: 29th November 1988
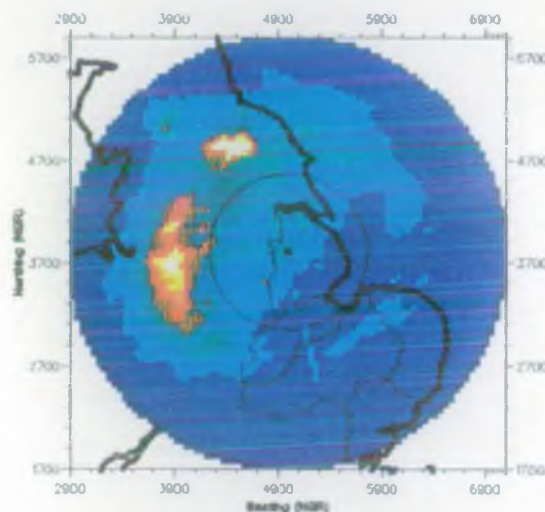
A11.5: 30th November 1988

Rainfall depth (mm)

Above	24.00
21.00 -	24.00
18.00 -	21.00
15.00 -	18.00
12.00 -	15.00
9.00 -	12.00
6.00 -	9.00
3.00 -	6.00
Below	3.00

Appendix 11a: Cumulated daily radar rainfall images
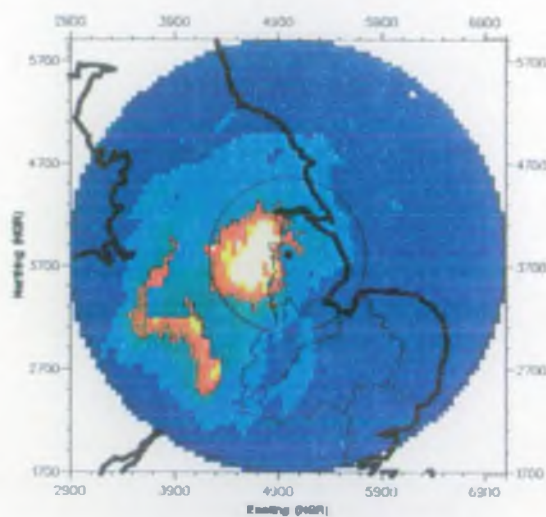
A11.6: 24th February 1989
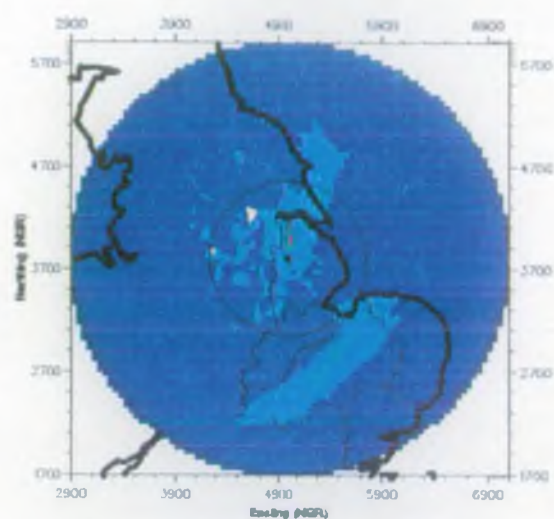
A11.7: 25th February 1989
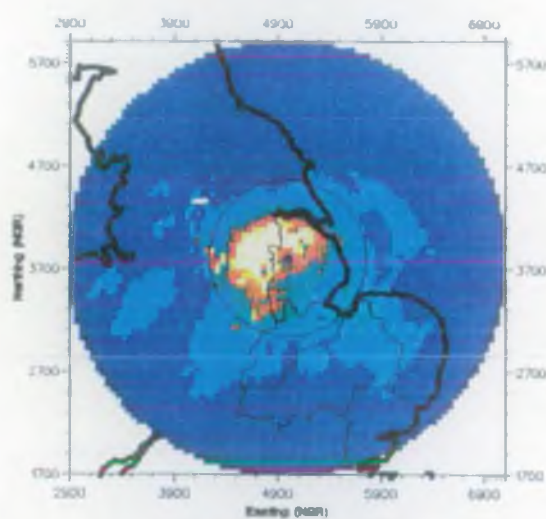
A11.8: 2nd March 1989
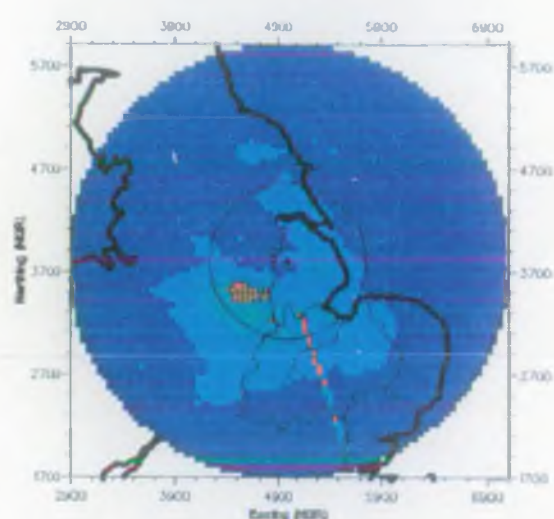
A11.9: 14th March 1989
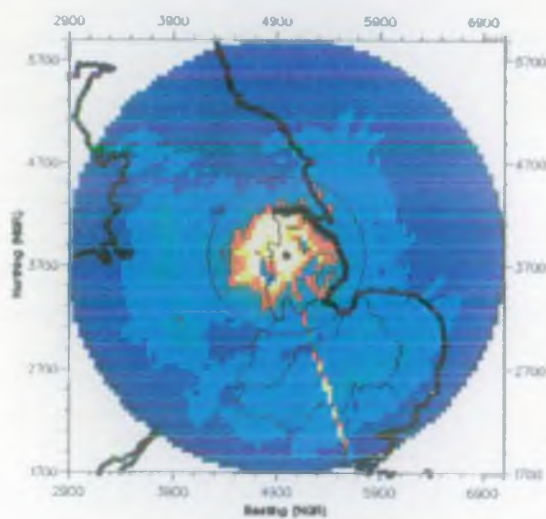
A11.10: 20th March 1989

Rainfall depth (mm)

Above	24.00
21.00	- 24.00
18.00	- 21.00
15.00	- 18.00
12.00	- 15.00
9.00	- 12.00
6.00	- 9.00
3.00	- 6.00
Below	3.00

Appendix 11b: Cumulated daily radar rainfall images
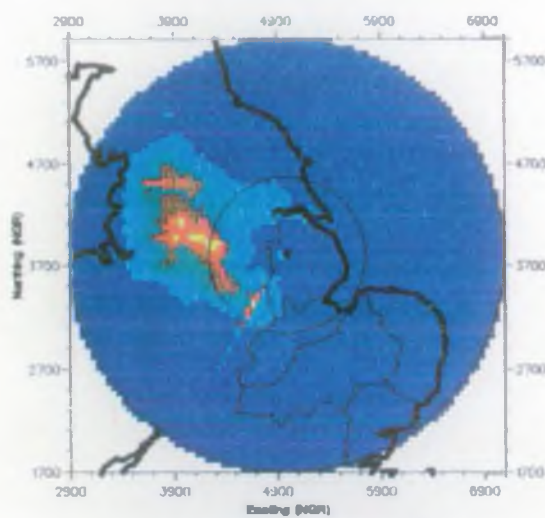
A11.11: 23rd March 1989
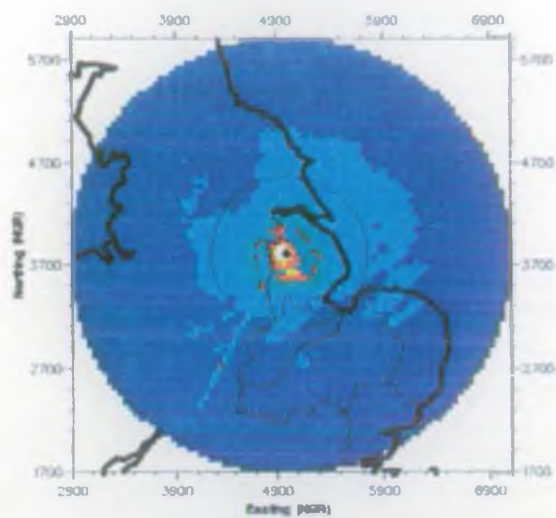
A11.12: 4th April 1989
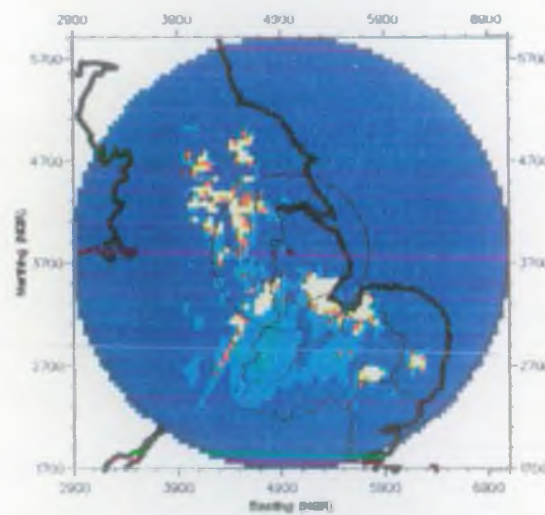
A11.13: 9th April 1989
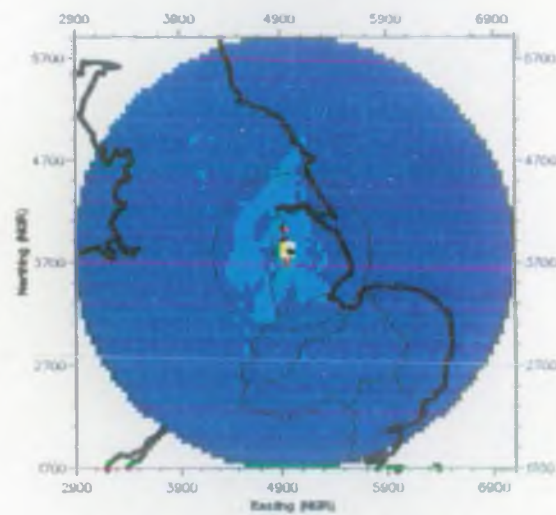
A11.14: 24th April 1989
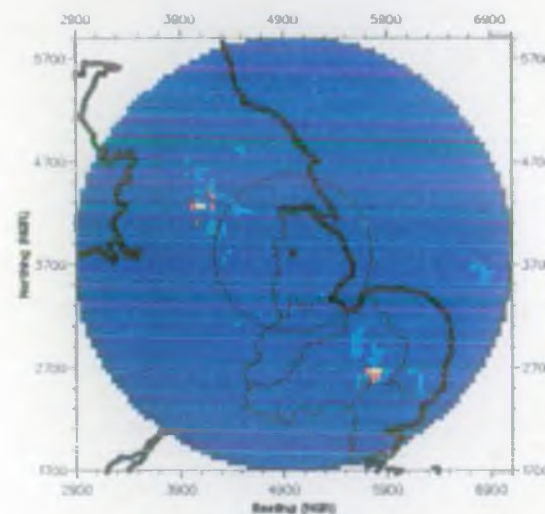
A11.15: 10th May 1989

Rainfall depth (mm)

	Above 24.00
	21.00 - 24.00
	18.00 - 21.00
	15.00 - 18.00
	12.00 - 15.00
	9.00 - 12.00
	6.00 - 9.00
	3.00 - 6.00
	Below 3.00

Appendix 11c: Cumulated daily radar rainfall images
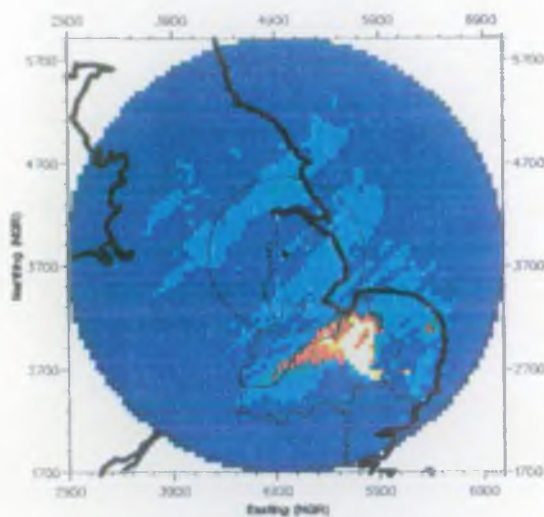
A11.16: 11th May 1989
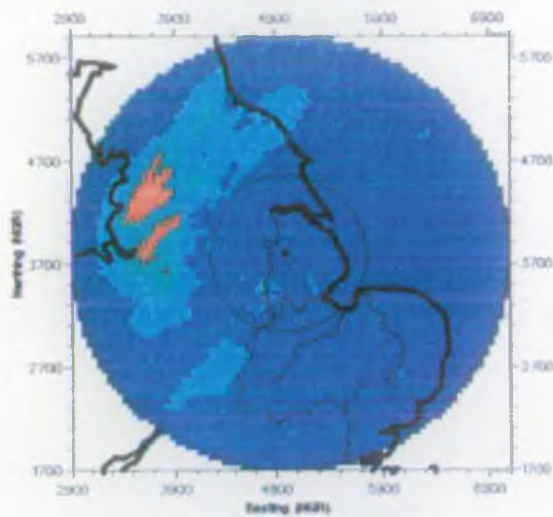
A11.17: 26th June 1989
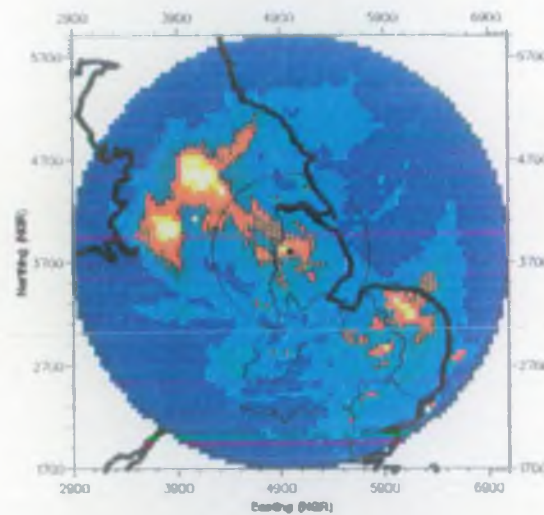
A11.18: 27th June 1989
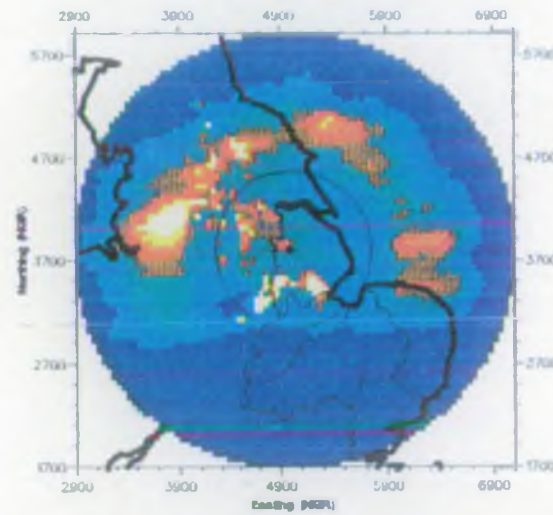
A11.19: 30th June 1989
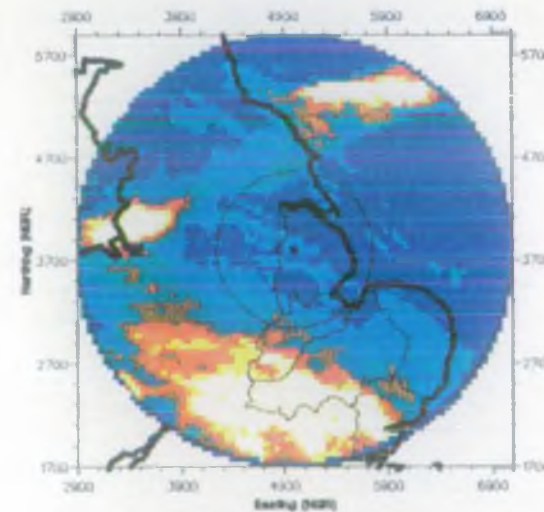
A11.20: 7th July 1989

Rainfall depth (mm)

	Above 24.00
	21.00 - 24.00
	18.00 - 21.00
	15.00 - 18.00
	12.00 - 15.00
	9.00 - 12.00
	6.00 - 9.00
	3.00 - 6.00
	Below 3.00

Appendix 11d: Cumulated daily radar rainfall images
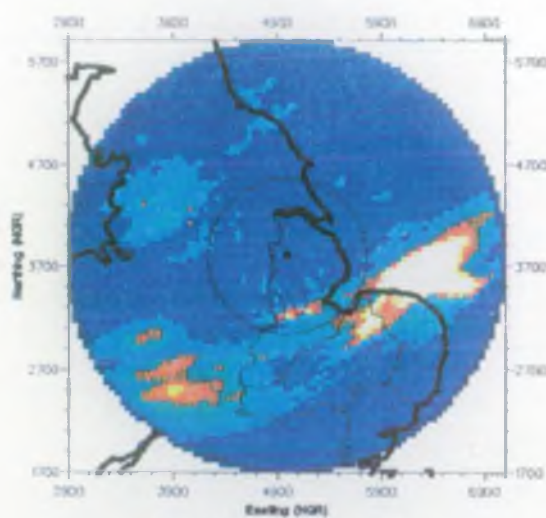
A11.21: 29th July 1989
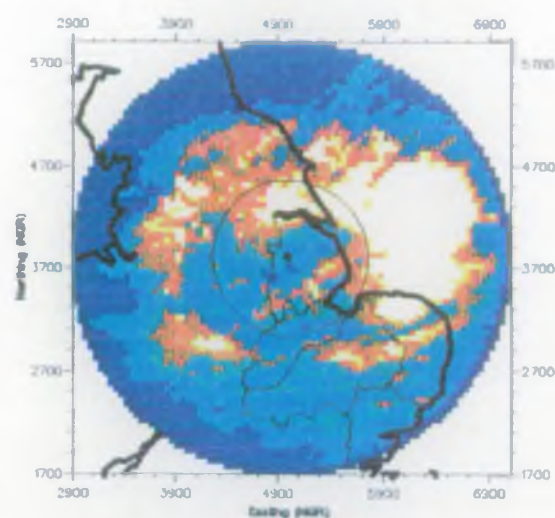
A11.22: 30th July 1989
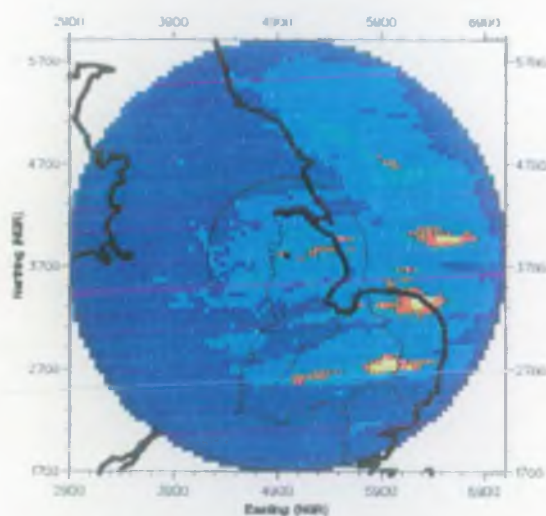
A11.23: 26th August 1989
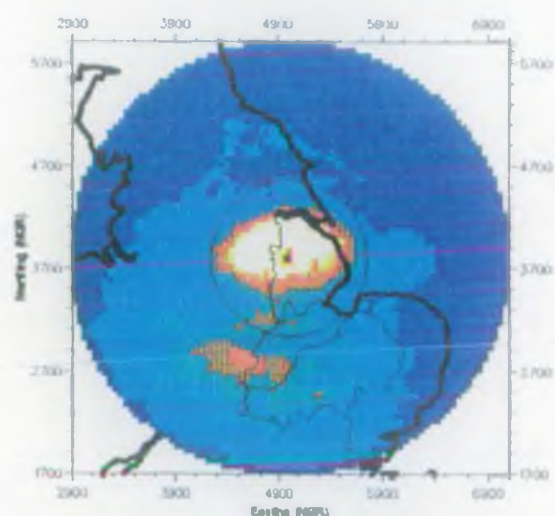
A11.24: 13th December 1989

A11.25: 14th December 1989

Rainfall depth (mm)

Above	24.00
21.00 -	24.00
18.00 -	21.00
15.00 -	18.00
12.00 -	15.00
9.00 -	12.00
6.00 -	9.00
3.00 -	6.00
Below	3.00

Appendix 11e: Cumulated daily radar rainfall images
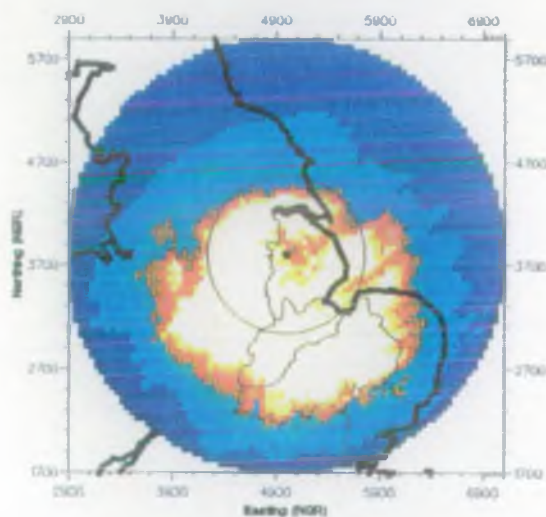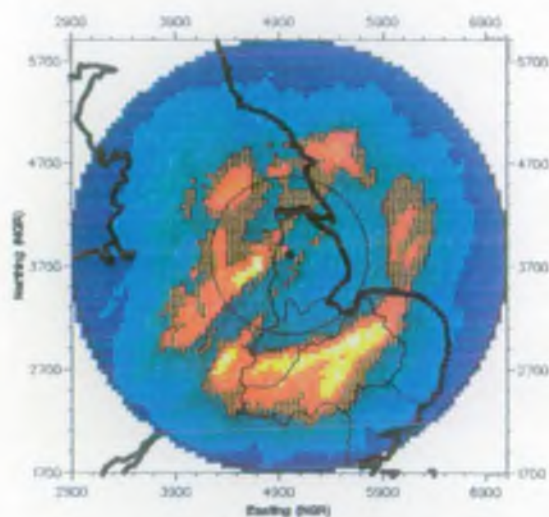
A11.26: 16th December 1989

A11.27: 18th December 1989

Rainfall depth (mm)

|	
	Above 24.00
	21.00 - 24.00
	18.00 - 21.00
	15.00 - 18.00
	12.00 - 15.00
	9.00 - 12.00
	6.00 - 9.00
	3.00 - 6.00
	Below 3.00
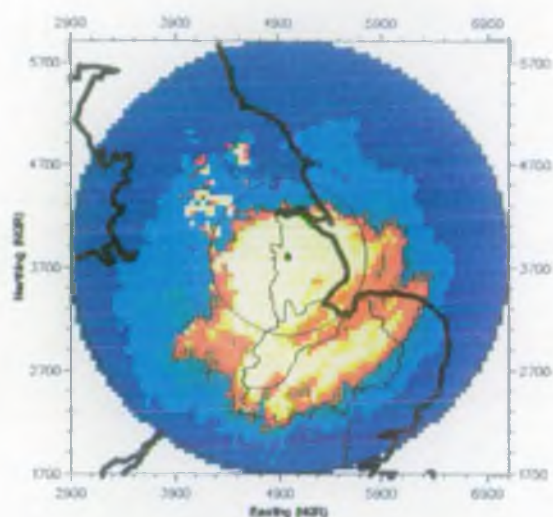
Appendix 11f: Cumulated daily radar rainfall images
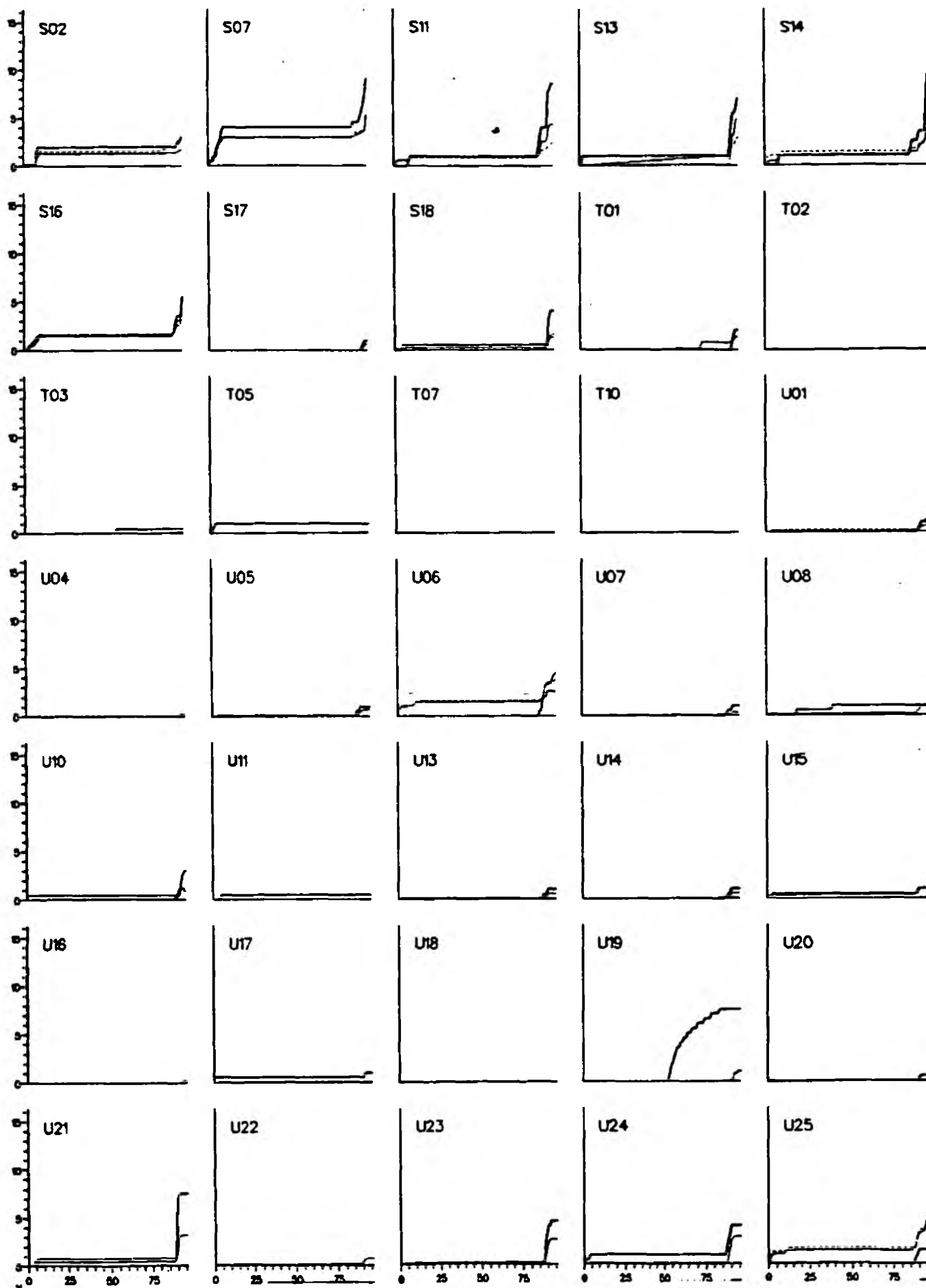
Appendix 12.1a: Comparative radar raingauge cumulative hyetographs: 19th October 1988

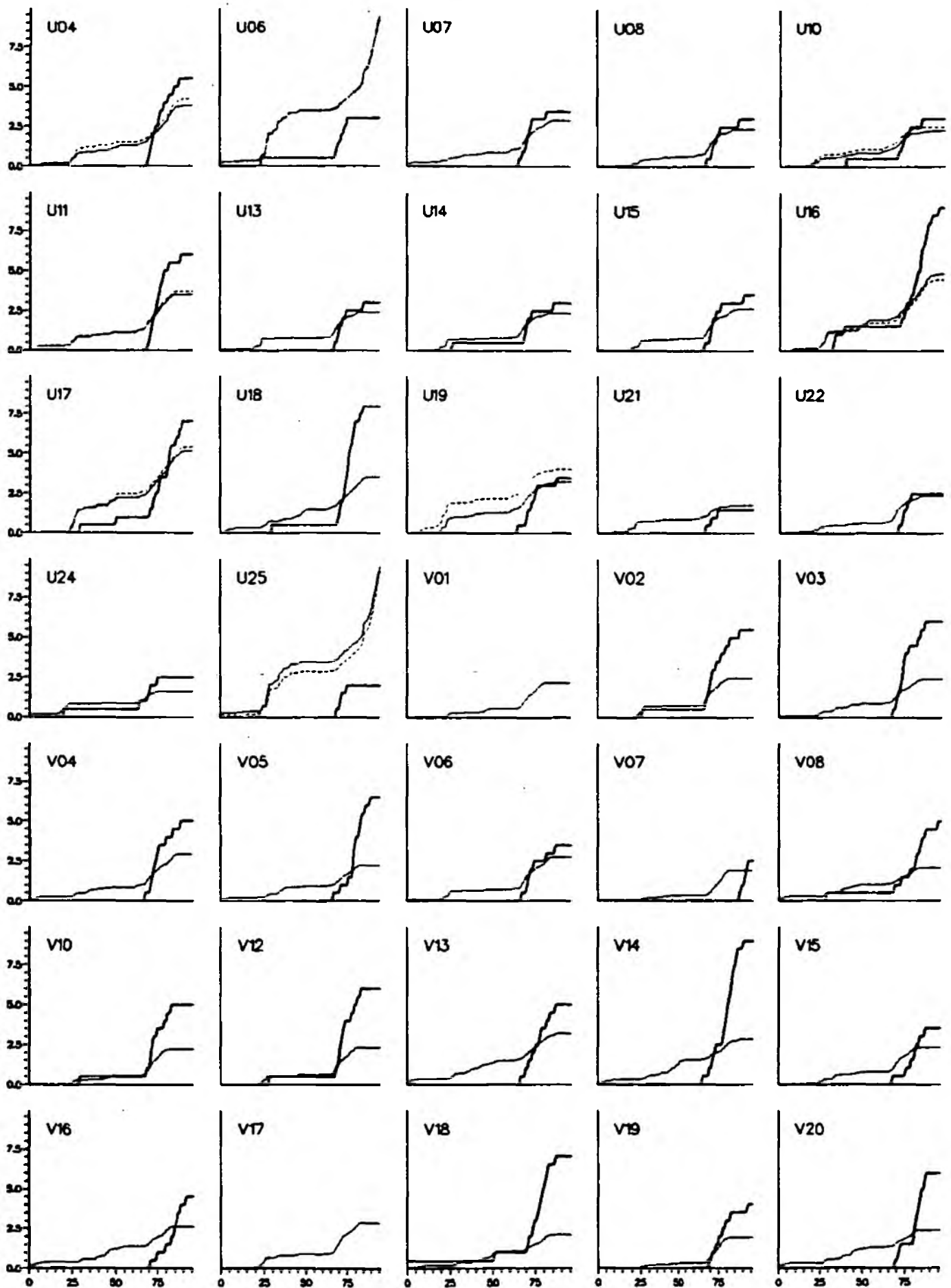(heavy solid - raingauge: medium dashed - 2 km (where available): light dotted - 5 km)
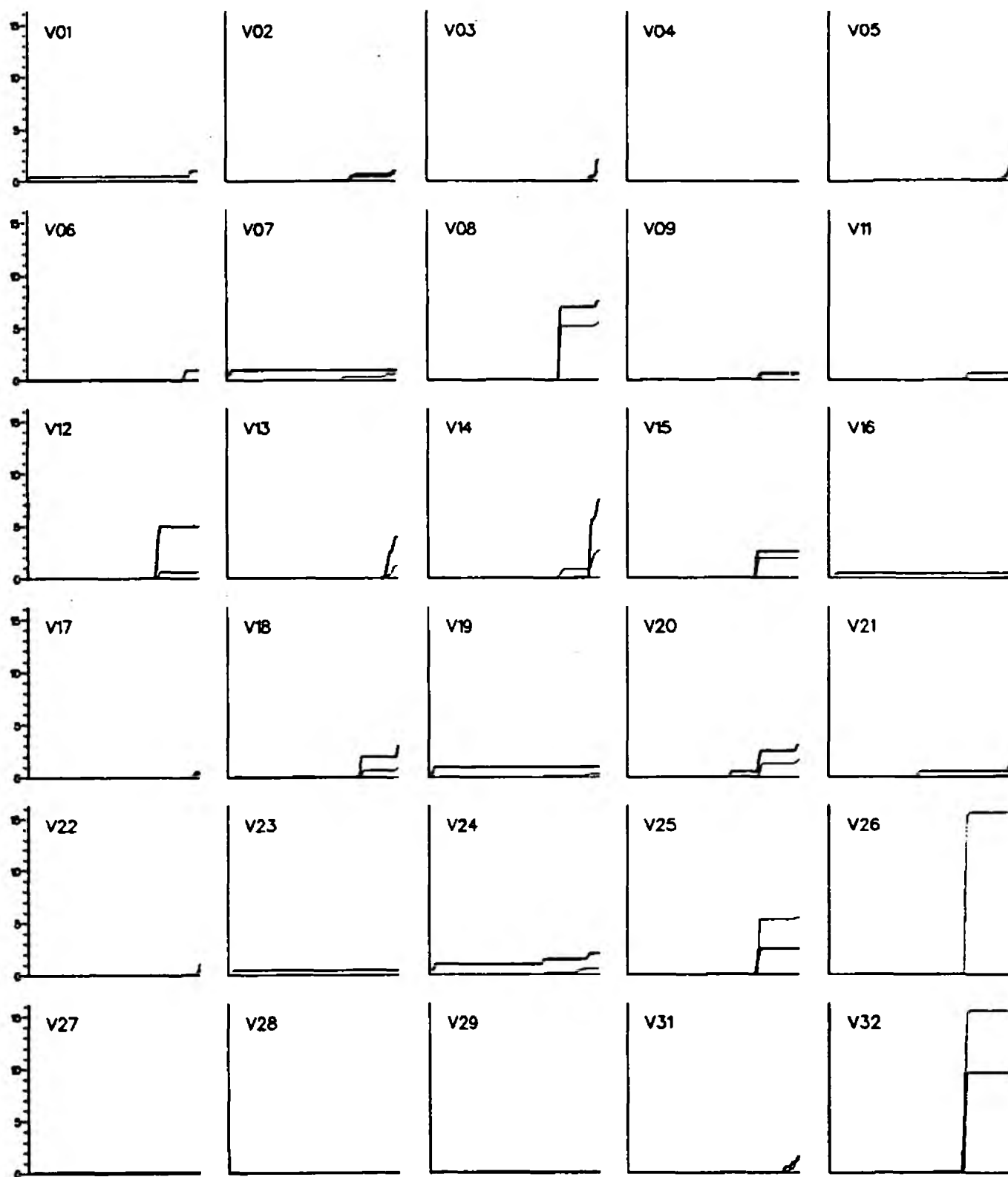
Appendix 12.1b: <u>Comparative radar raingauge cumulative hyetographs: 19th October 1988</u>

<u>(heavy solid - raingauge: medium dashed - 2 km (where available): light dotted - 5 km)</u>
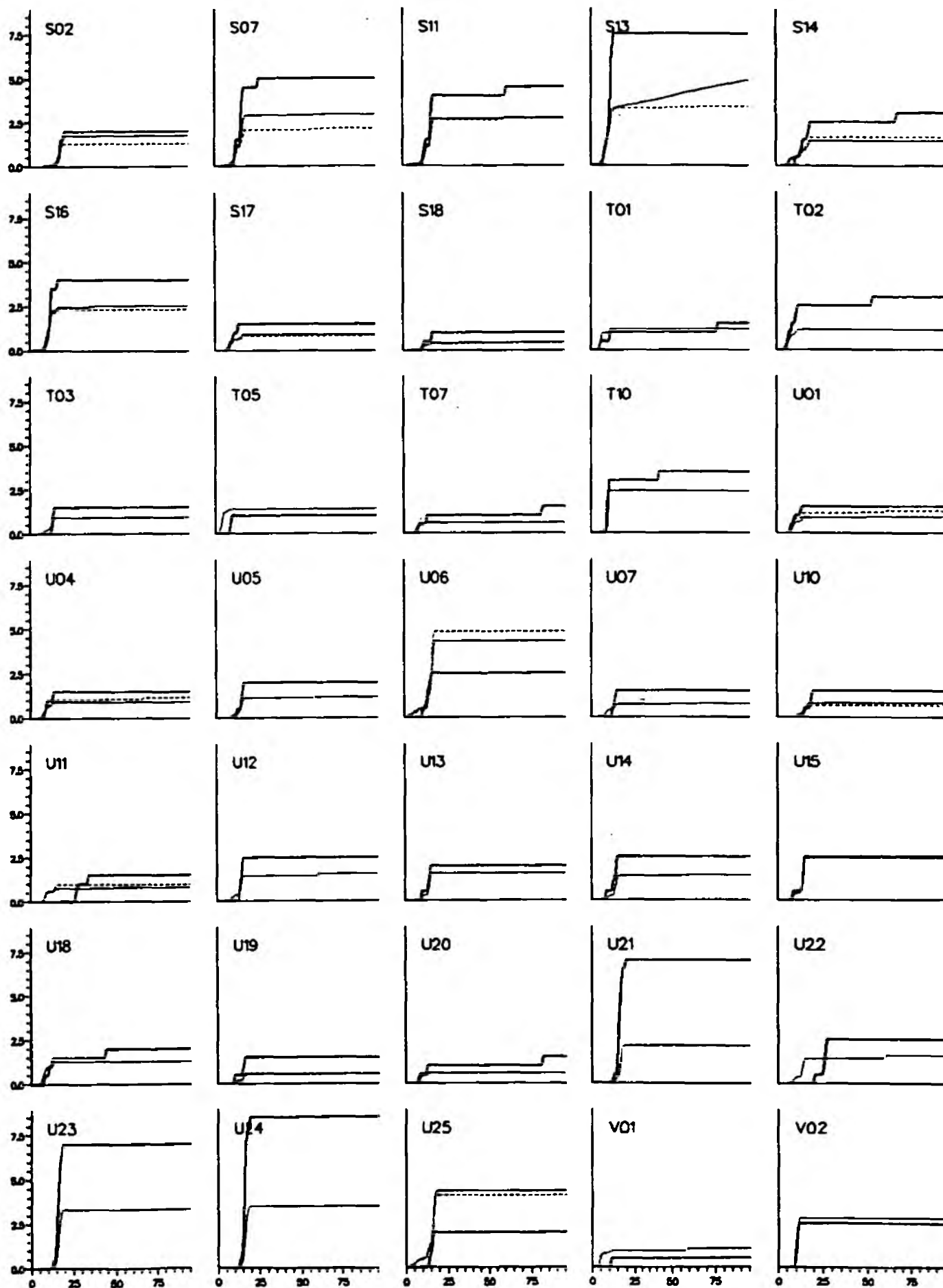
Appendix 12.2a: Comparative radar raingauge cumulative hyetographs: 9th November 1988

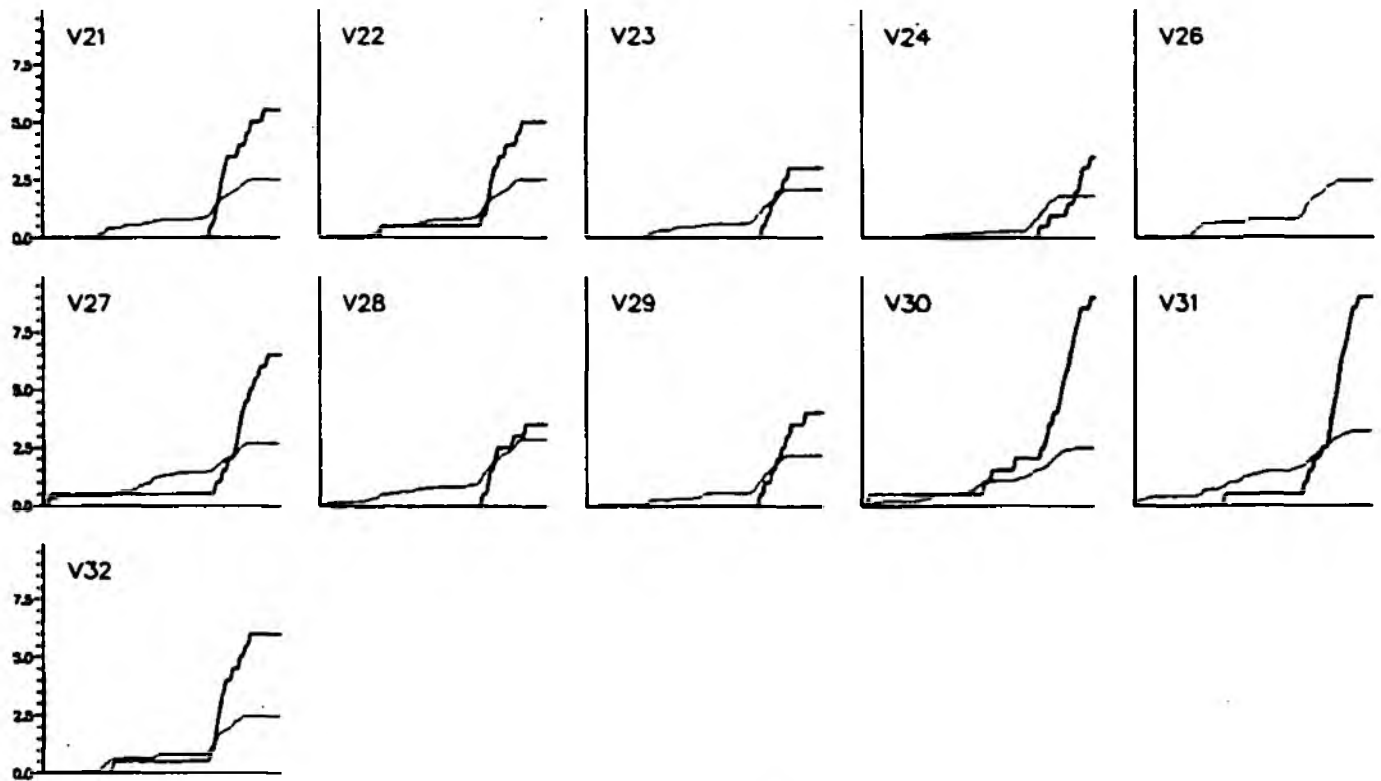(heavy solid - raingauge; medium dashed - 2 km (where available); light dotted - 5 km)
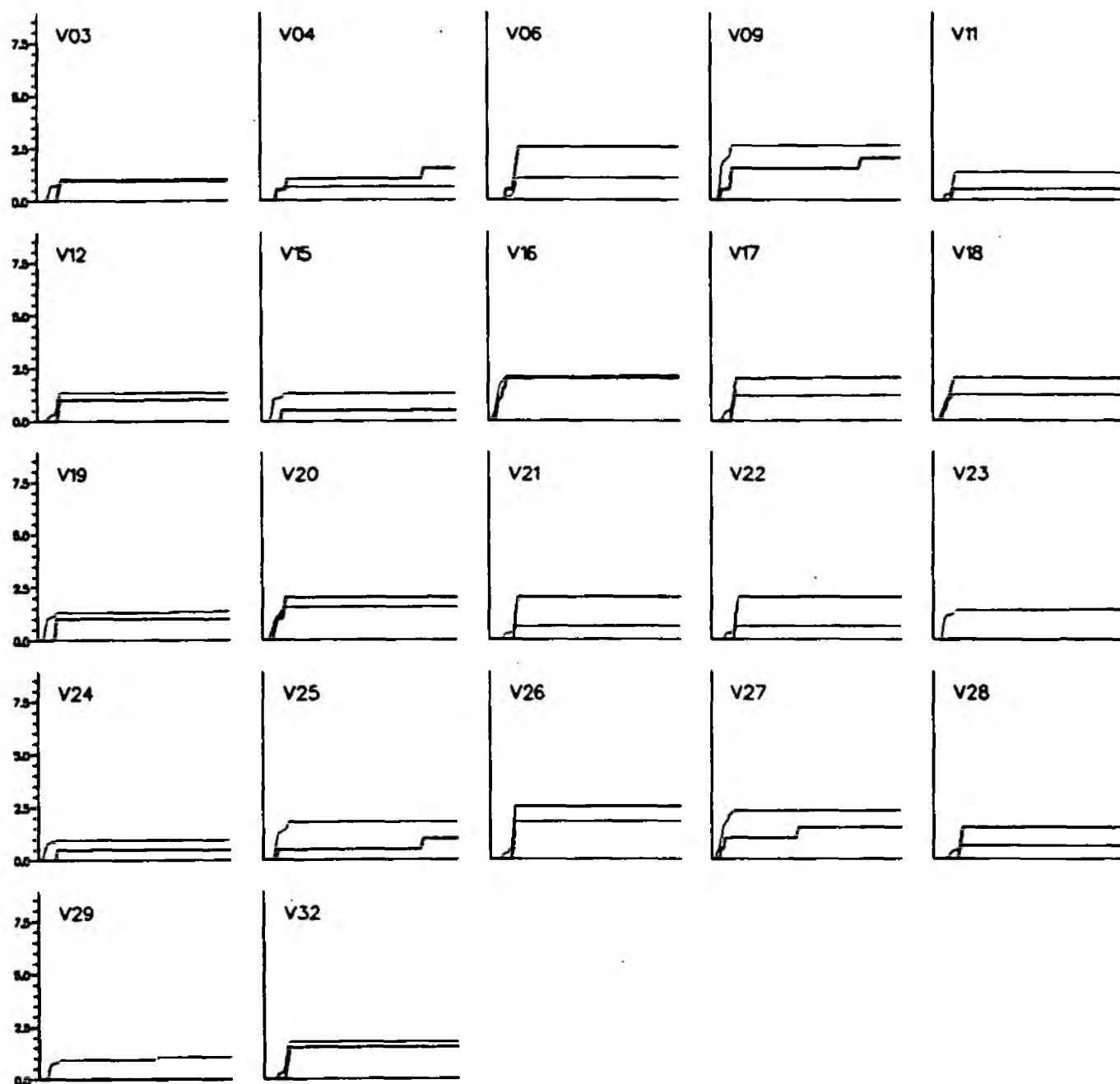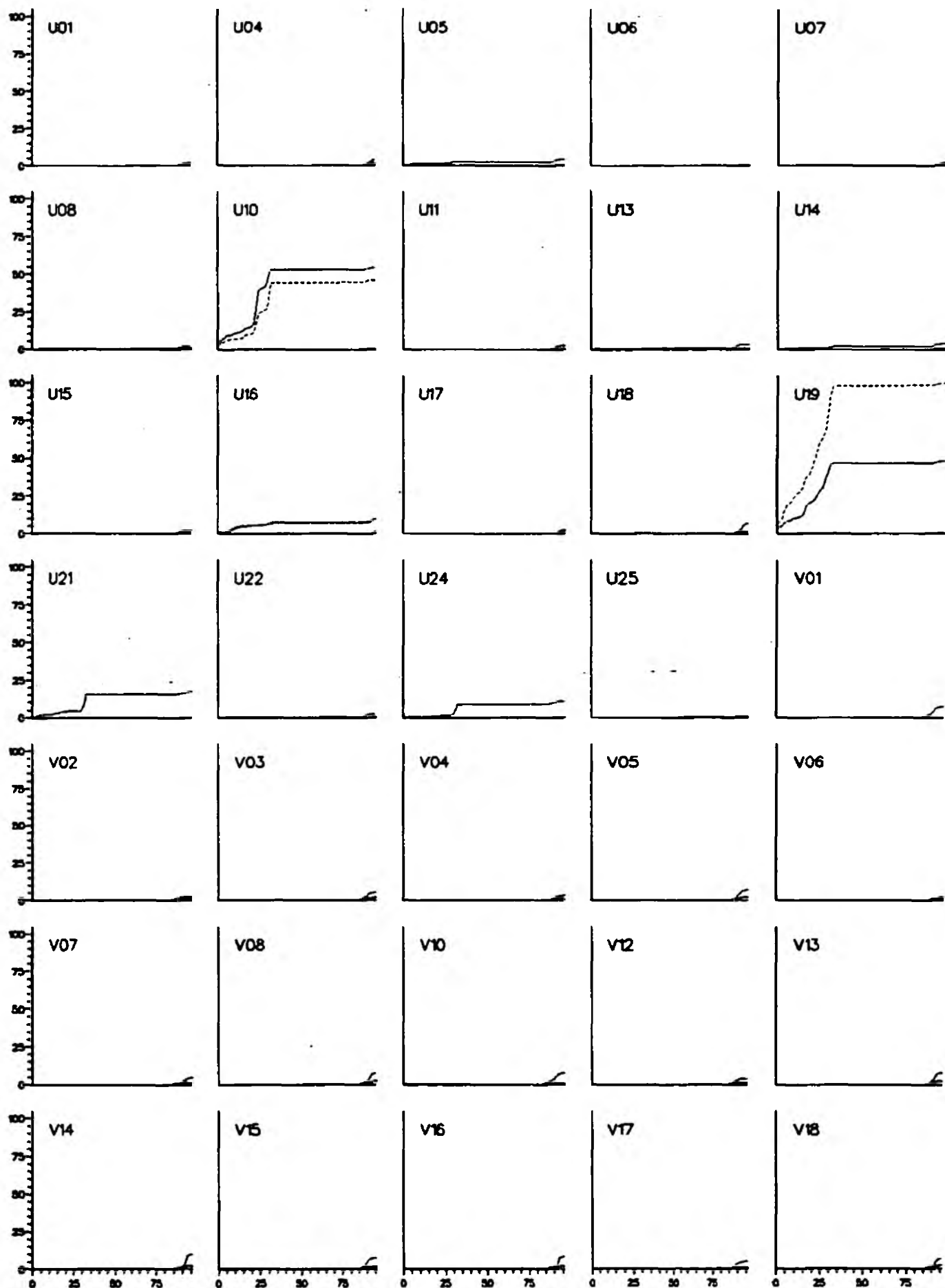
Appendix 12.2b: Comparative radar raingauge cumulative hyetographs: 9th November 1988

(heavy solid - raingauge: medium dashed - 2 km (where available): light dotted - 5 km)
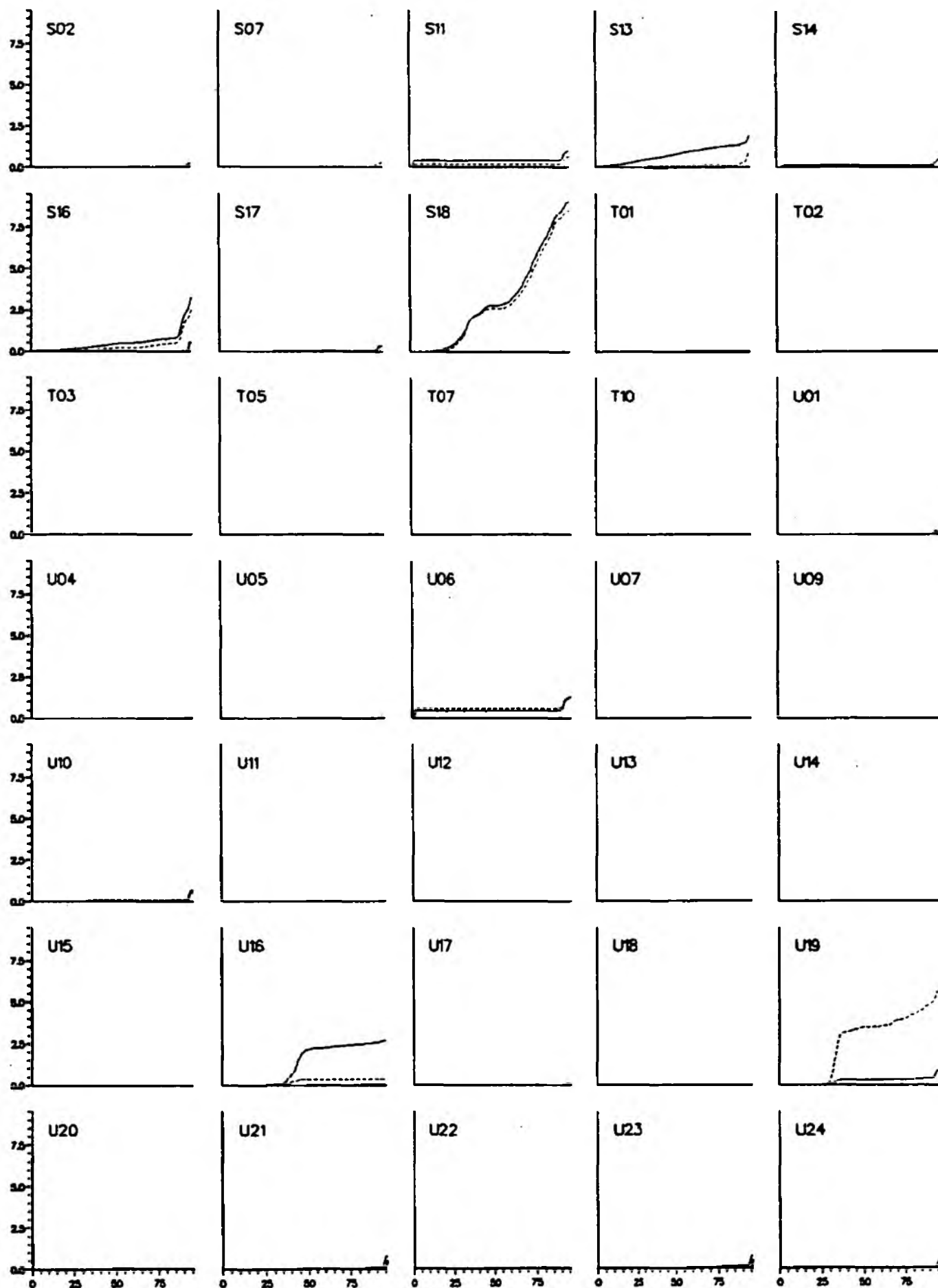
Appendix 12.3a: Comparative radar raingauge cumulative hyetographs: 19th November 1988
(heavy solid - raingauge: medium dashed - 2 km (where available): light dotted - 5 km)
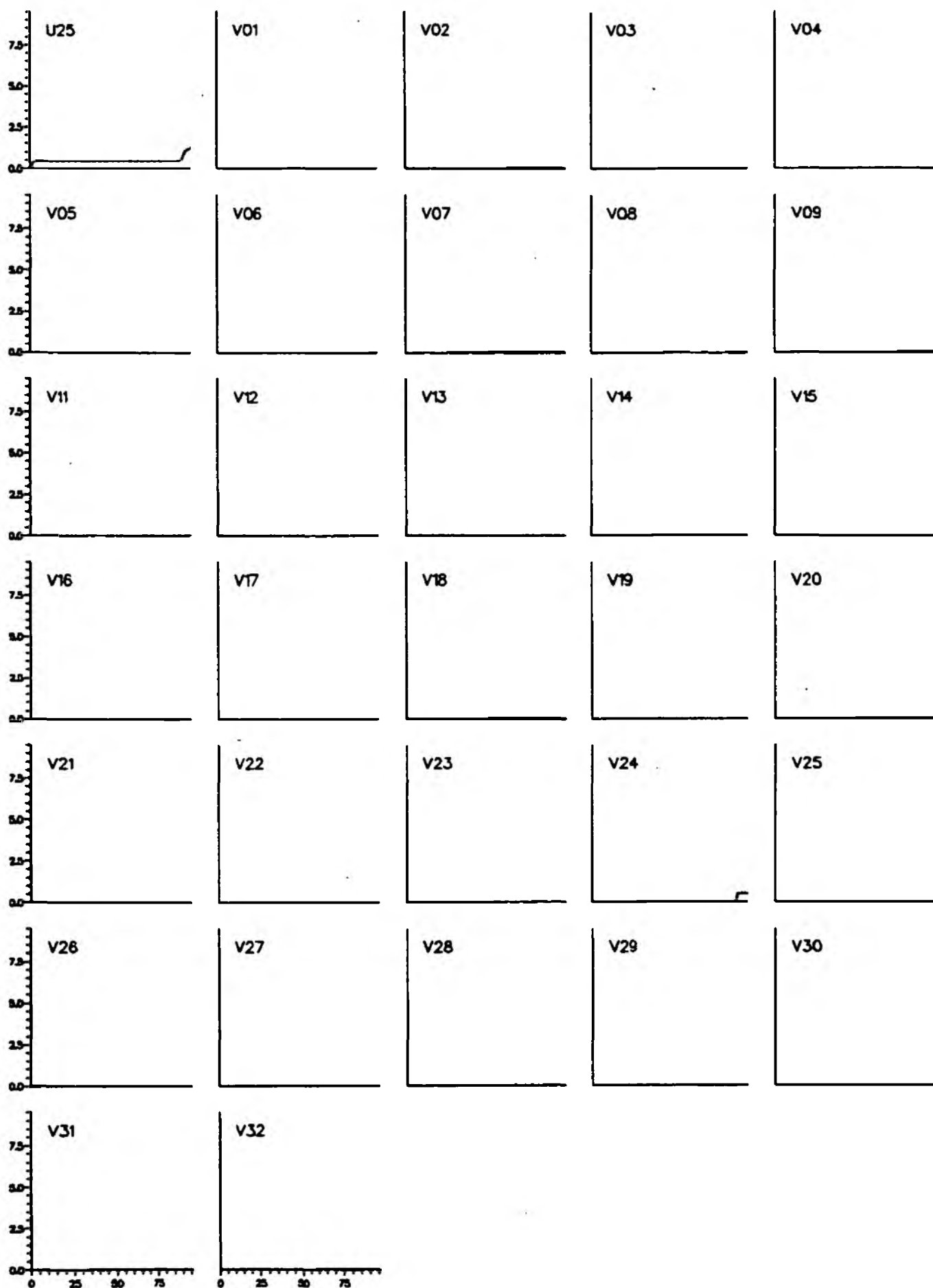
Appendix 12.3b: Comparative radar raingauge cumulative hyetographs: 19th November 1988

(heavy solid - raingauge: medium dashed - 2 km (where available): light dotted - 5 km)
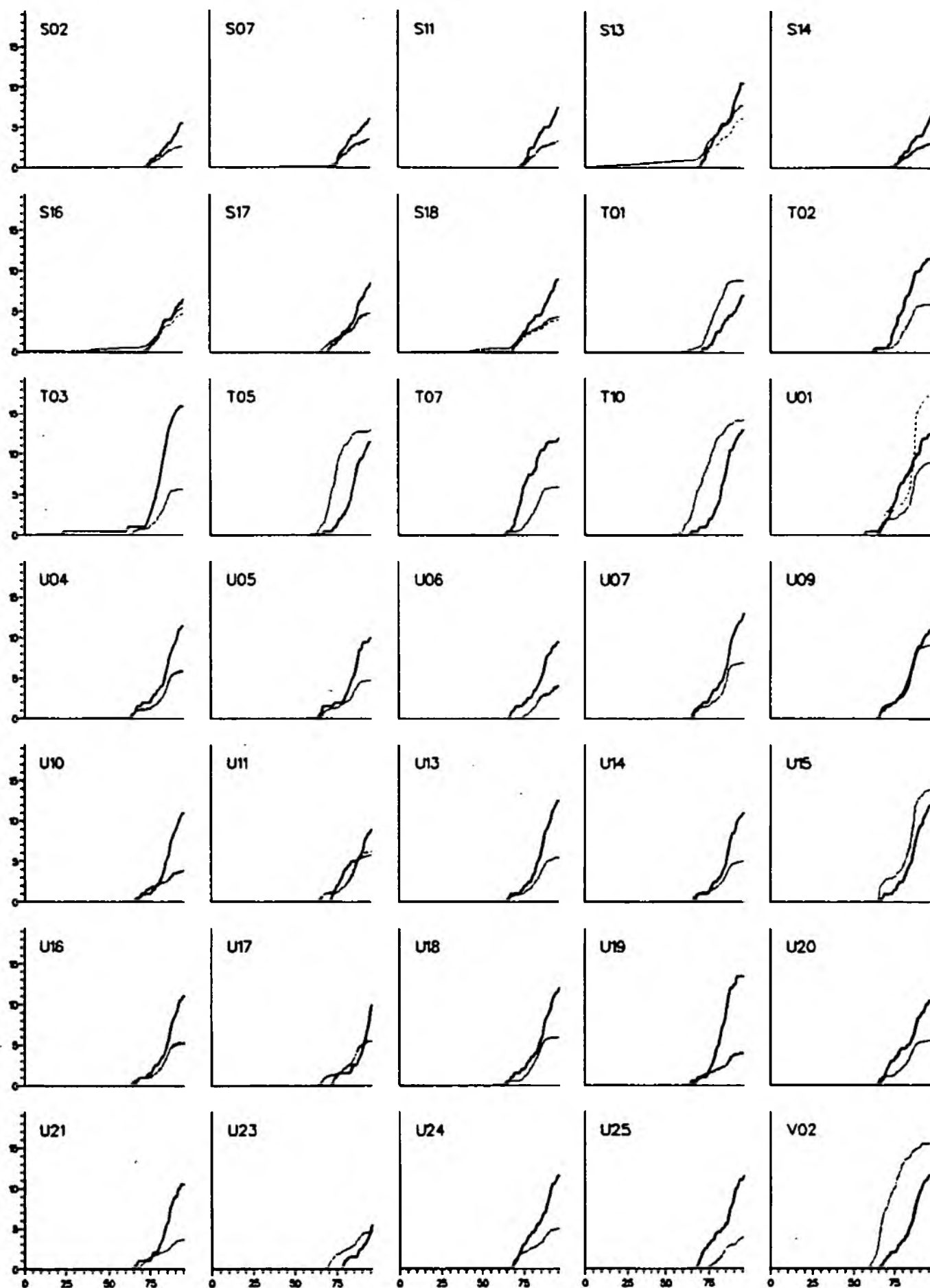
Appendix 12.4a: Comparative radar raingauge cumulative hyetographs: 29th November 1988

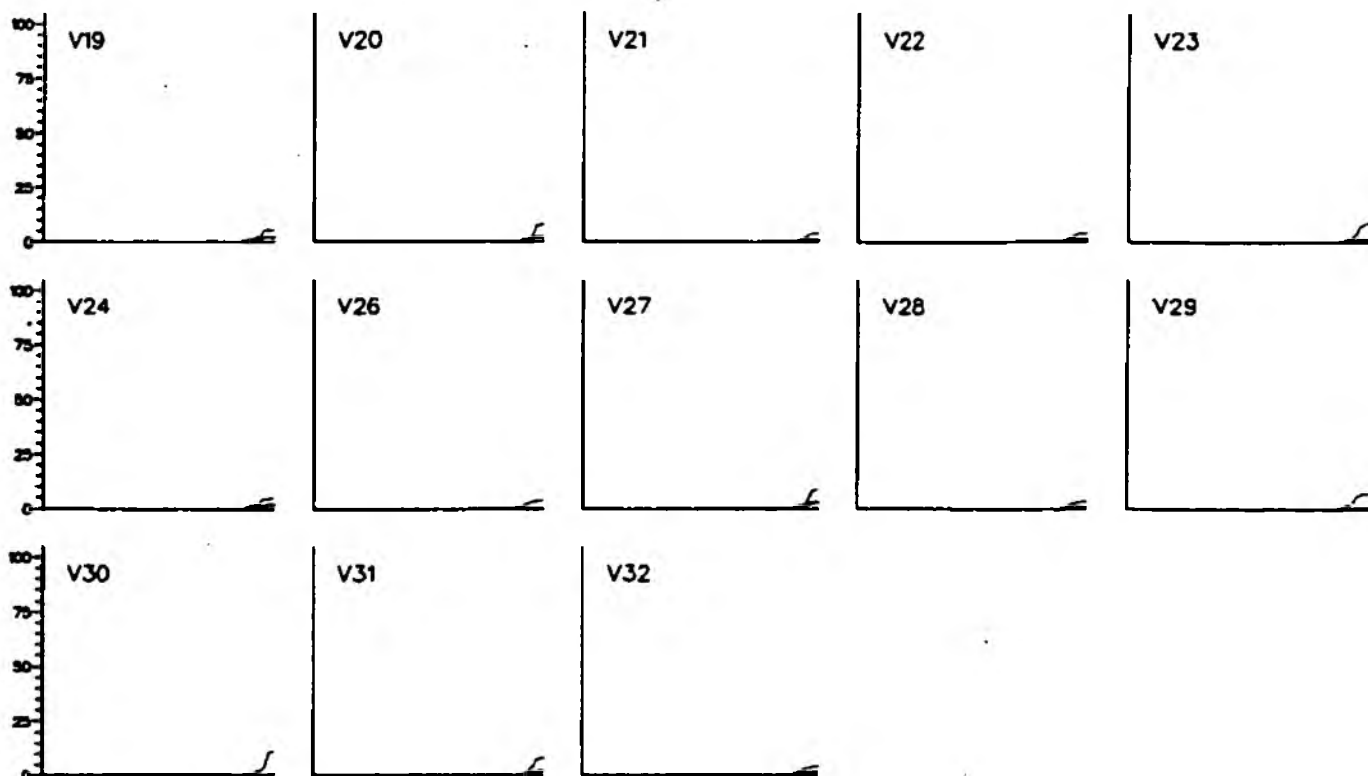(heavy solid - raingauge; medium dashed - 2 km (where available); light dotted - 5 km)
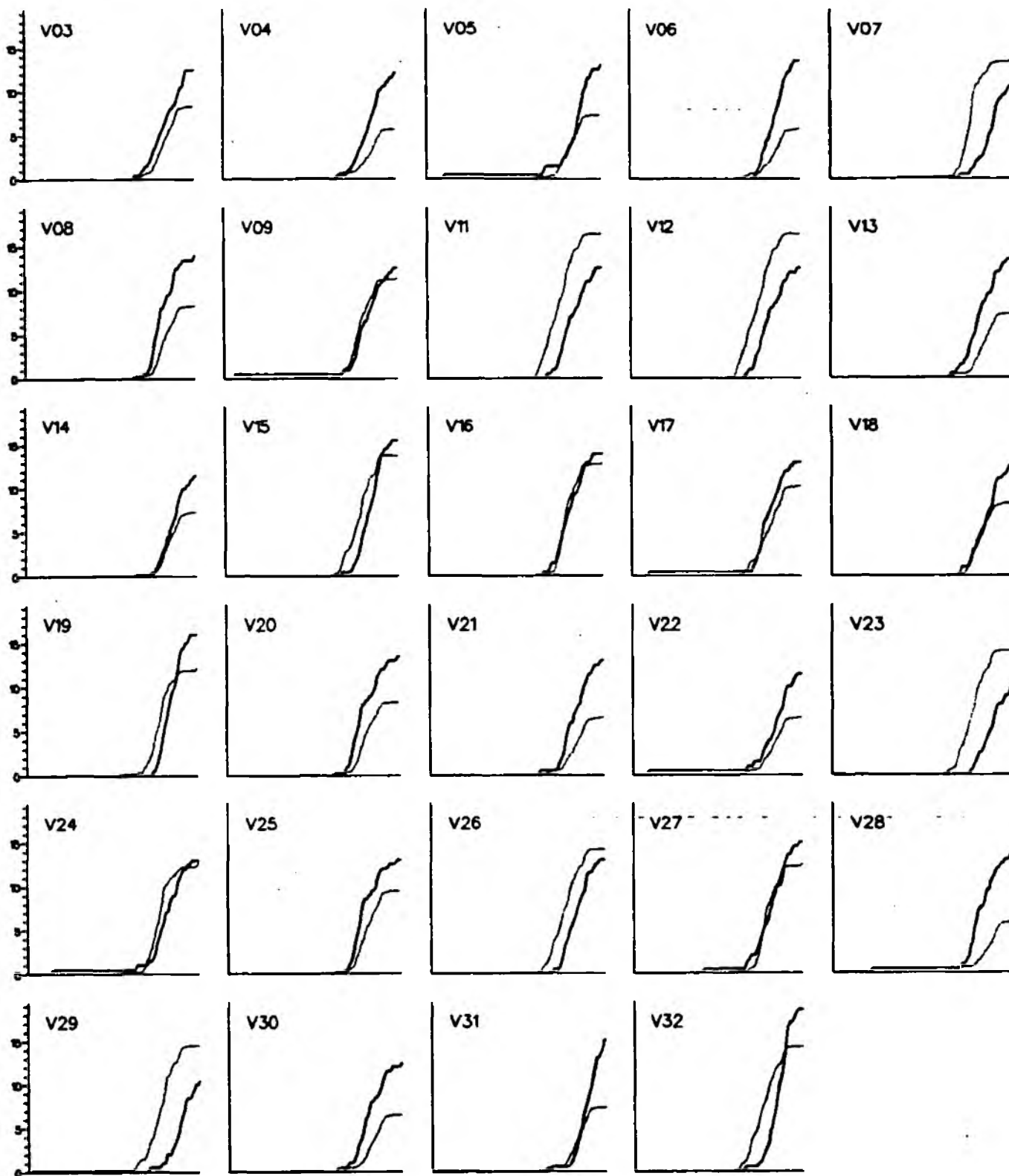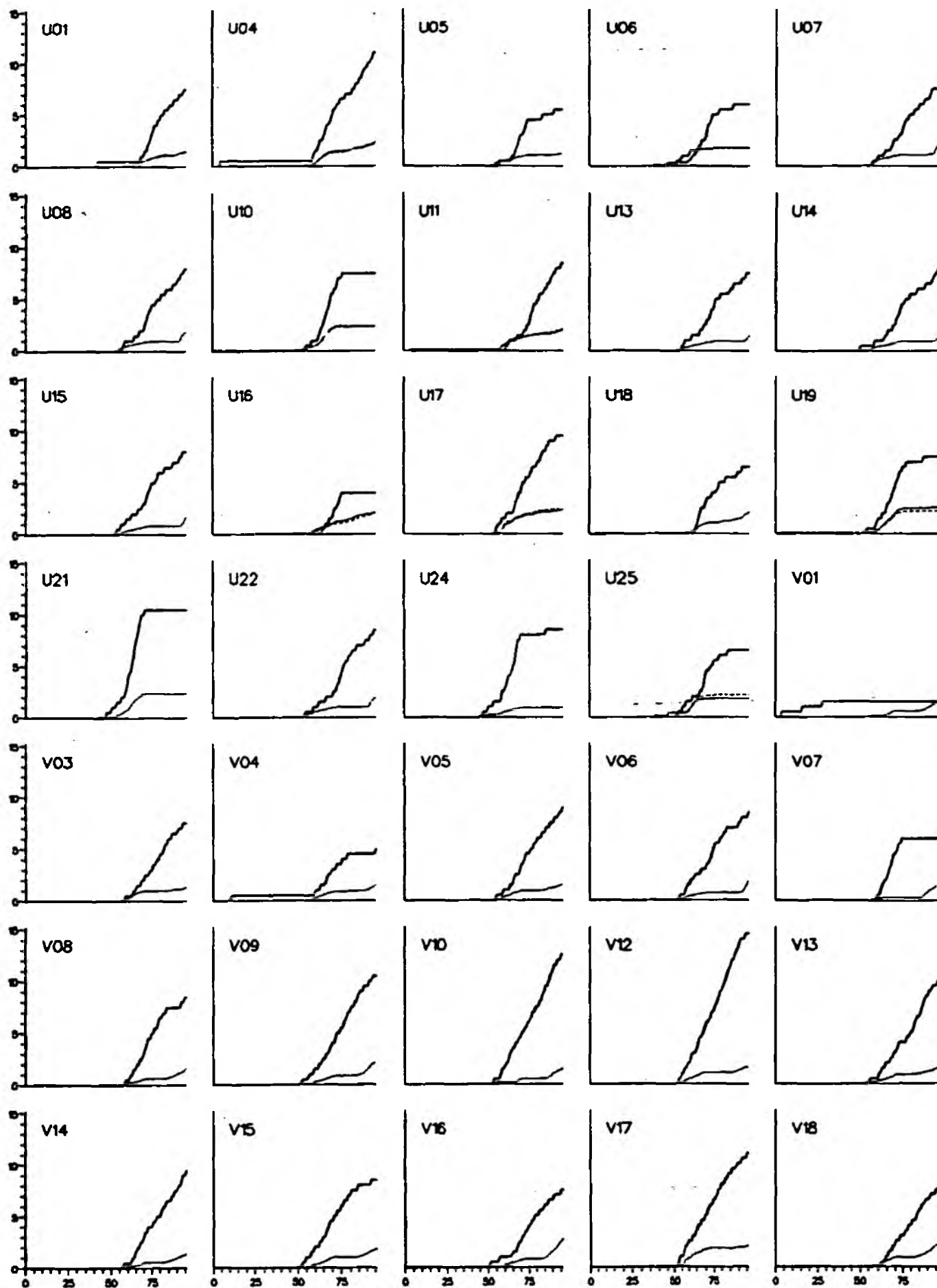
Appendix 12.4b: <u>Comparative radar raingauge cumulative hyetographs: 29th November 1988</u>
<u>(heavy solid - raingauge; medium dashed - 2 km (where available); light dotted - 5 km)</u>
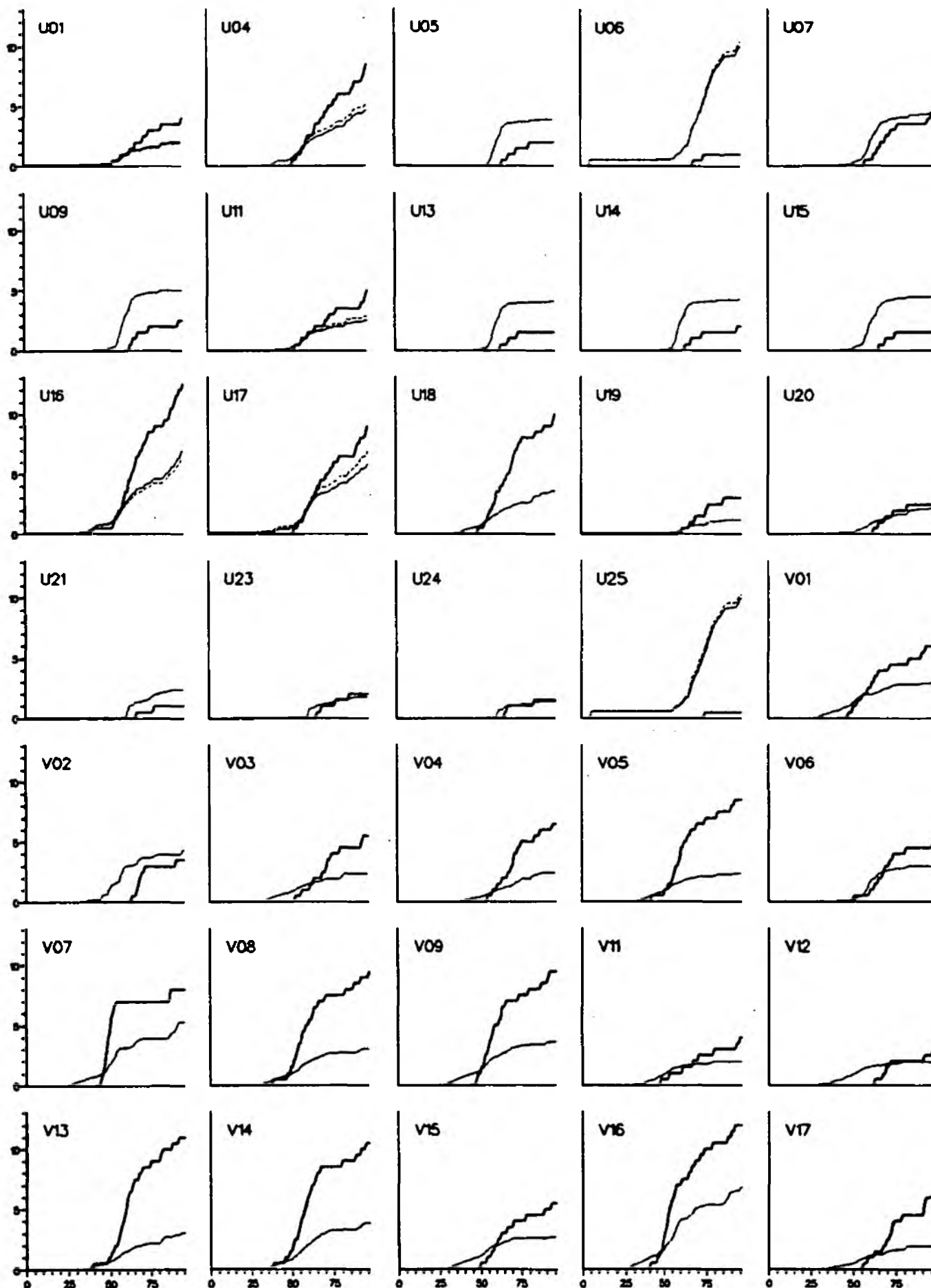
Appendix 12.5a: Comparative radar raingauge cumulative hyetographs: 24th February 1989

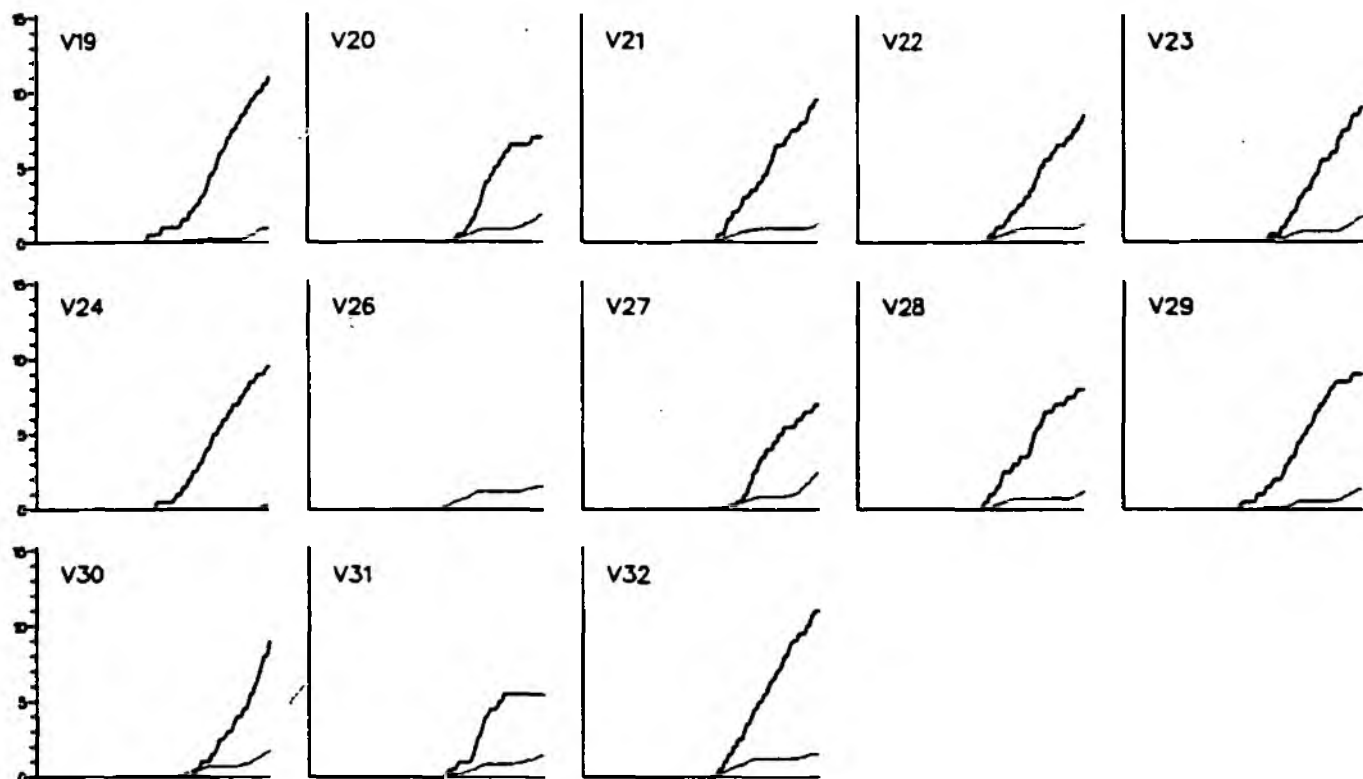(heavy solid - raingauge; medium dashed - 2 km (where available); light dotted - 5 km)
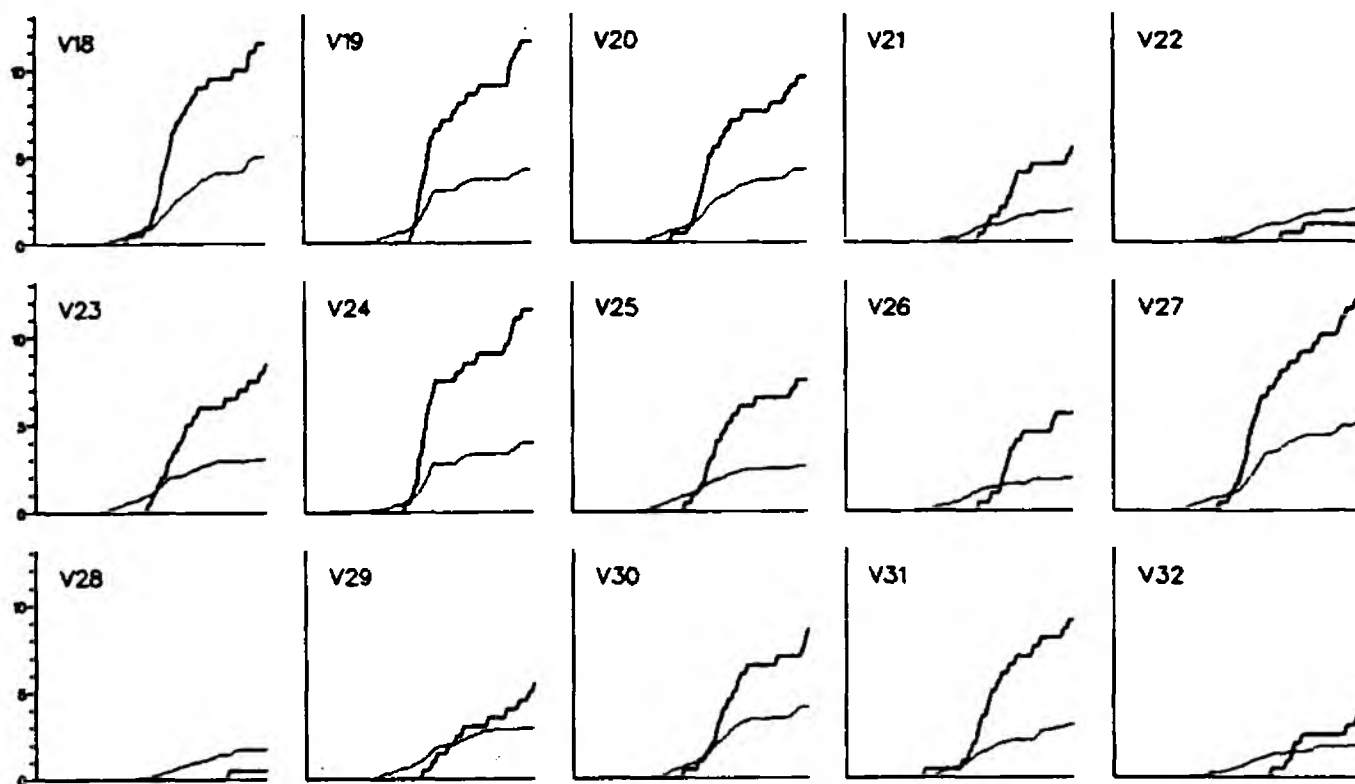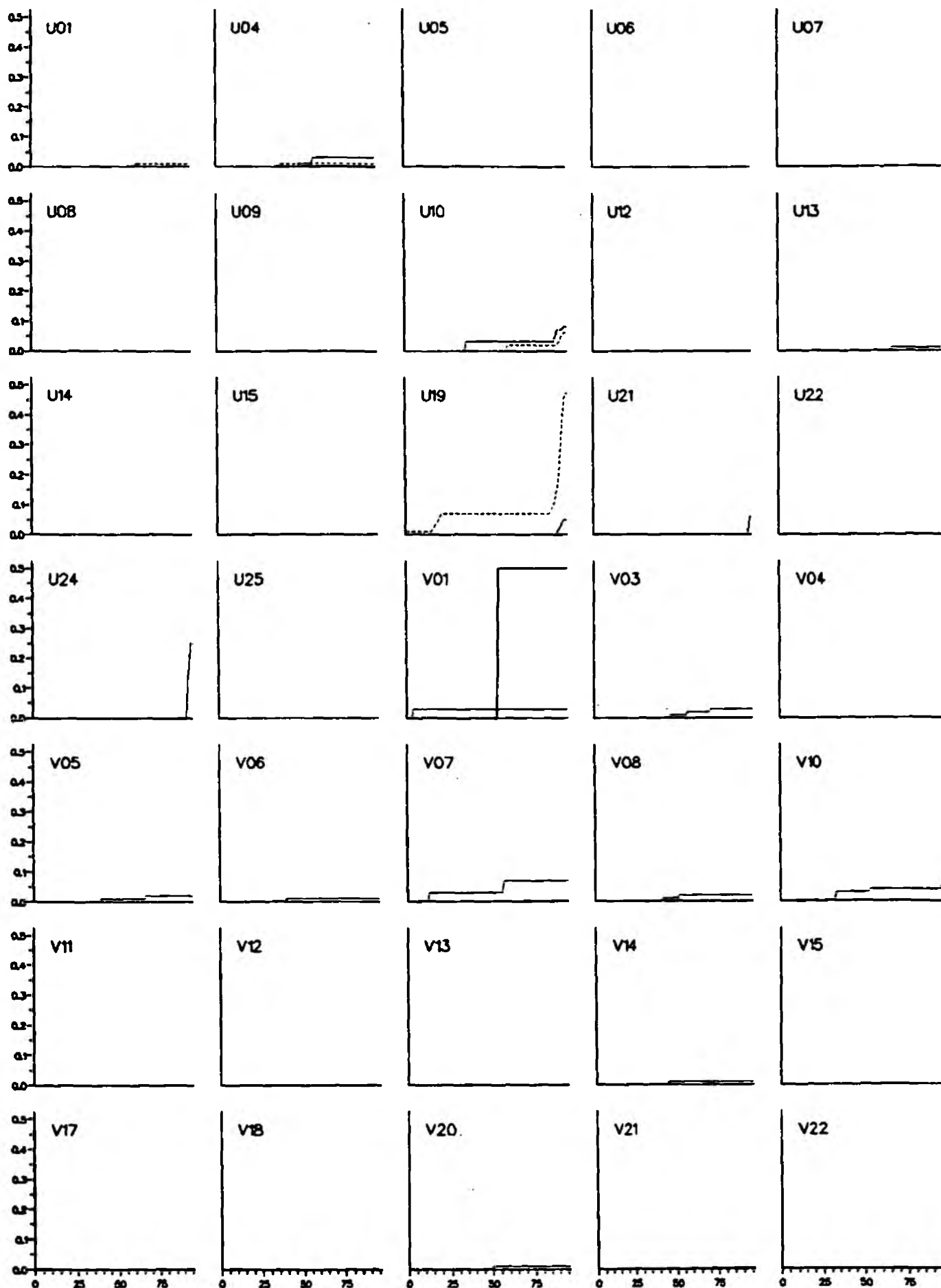
Appendix 12.5b: Comparative radar raingauge cumulative hyetographs: 24th February 1989

(heavy solid - raingauge; medium dashed - 2 km (where available); light dotted - 5 km)
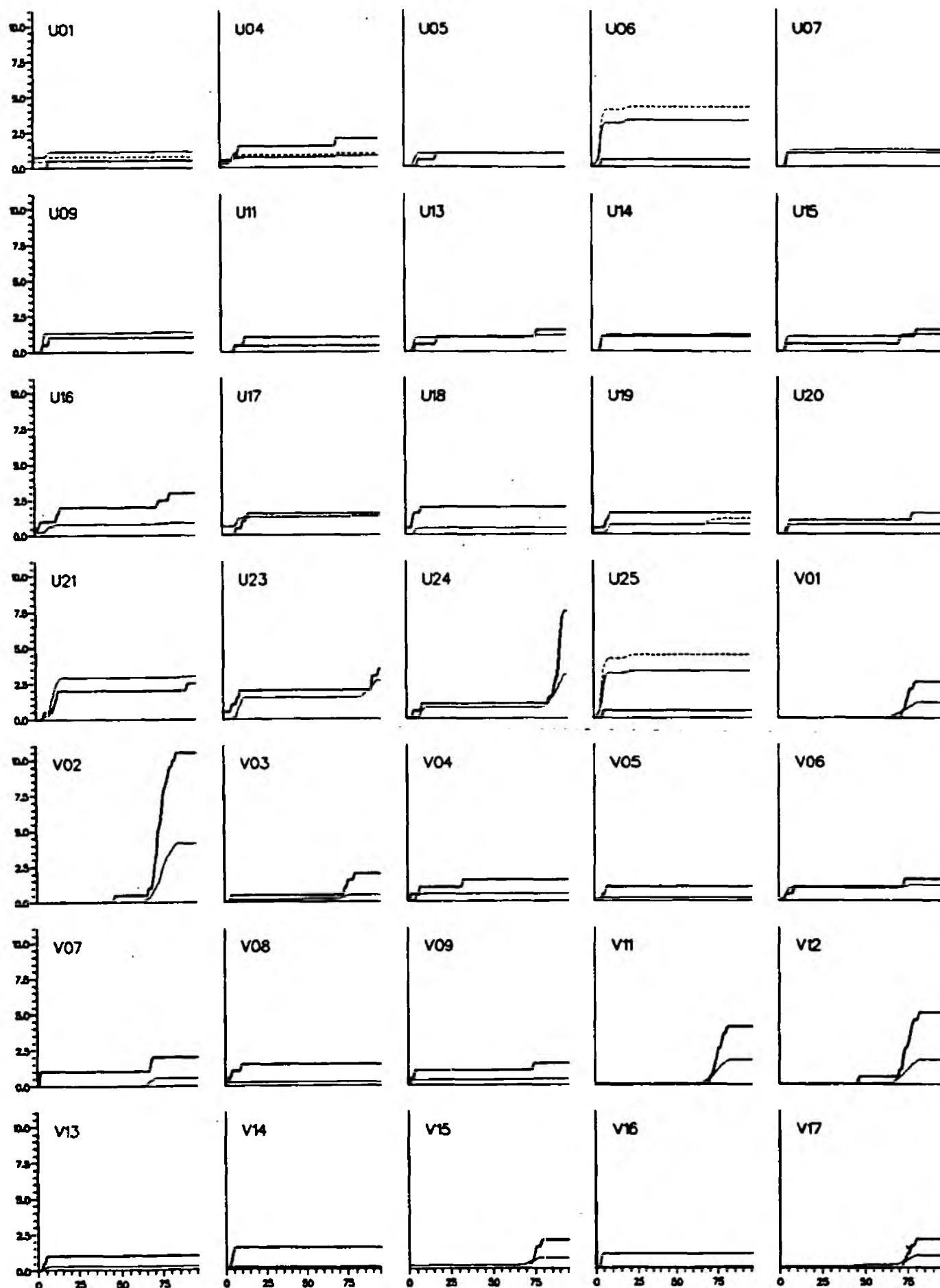
Appendix 12.6a: Comparative radar raingauge cumulative hyetographs: 25th February 1989

(heavy solid - raingauge; medium dashed - 2 km (where available); light dotted - 5 km)
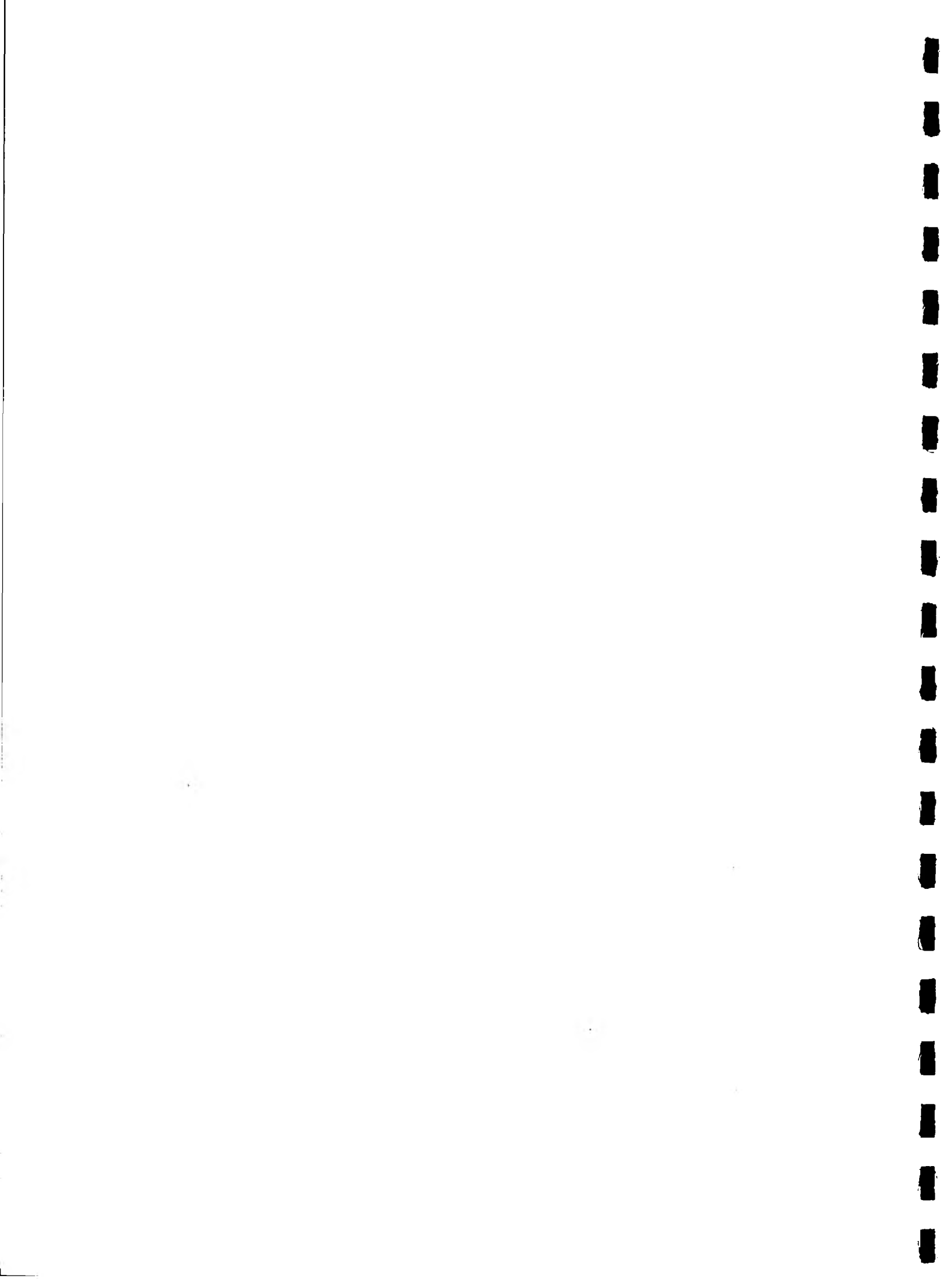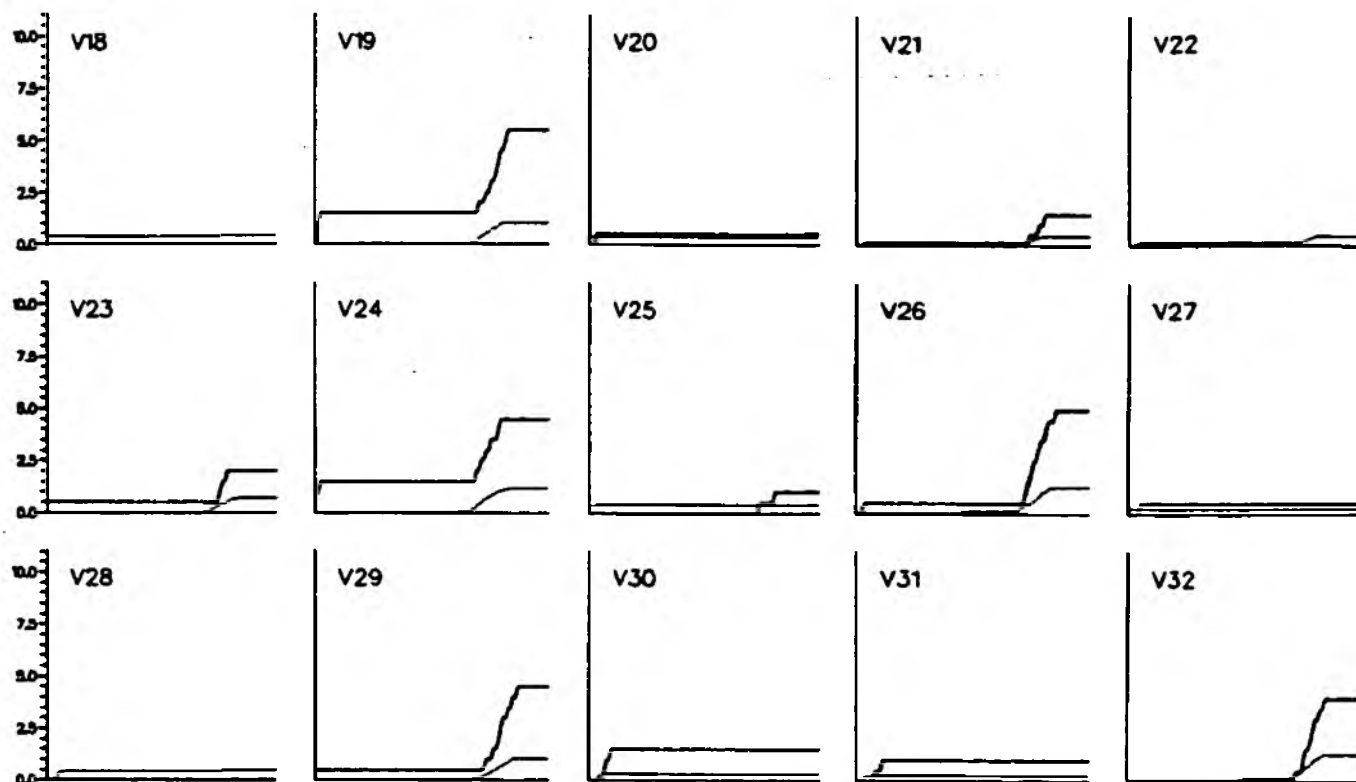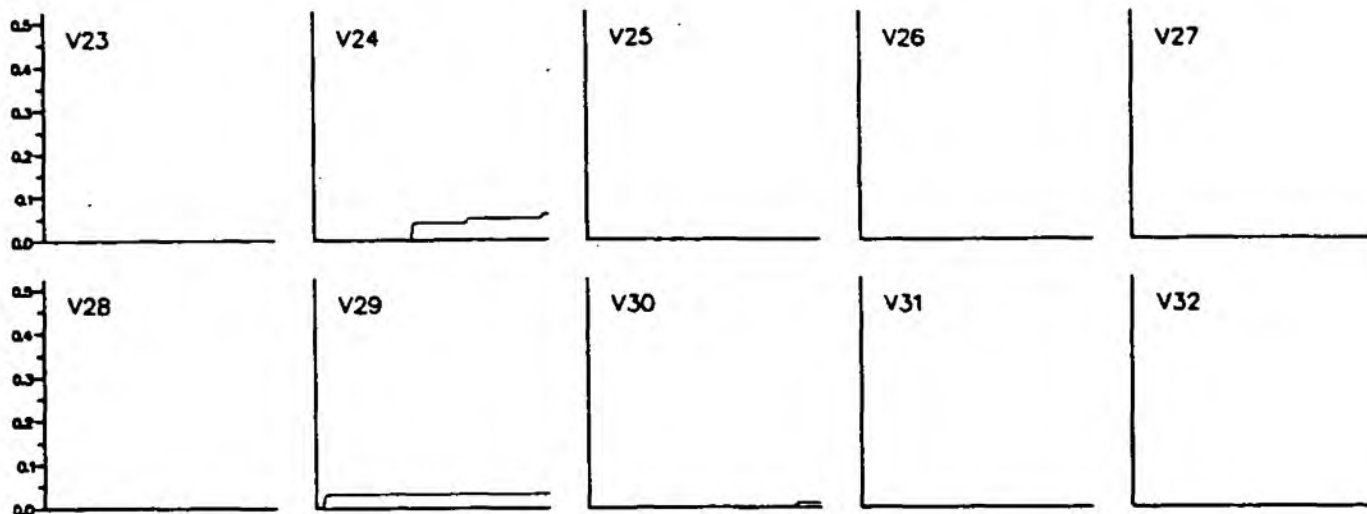
Appendix 12.6b: Comparative radar raingauge cumulative hyetographs: 25th February 1989

(heavy solid - raingauge: medium dashed - 2 km (where available): light dotted - 5 km)
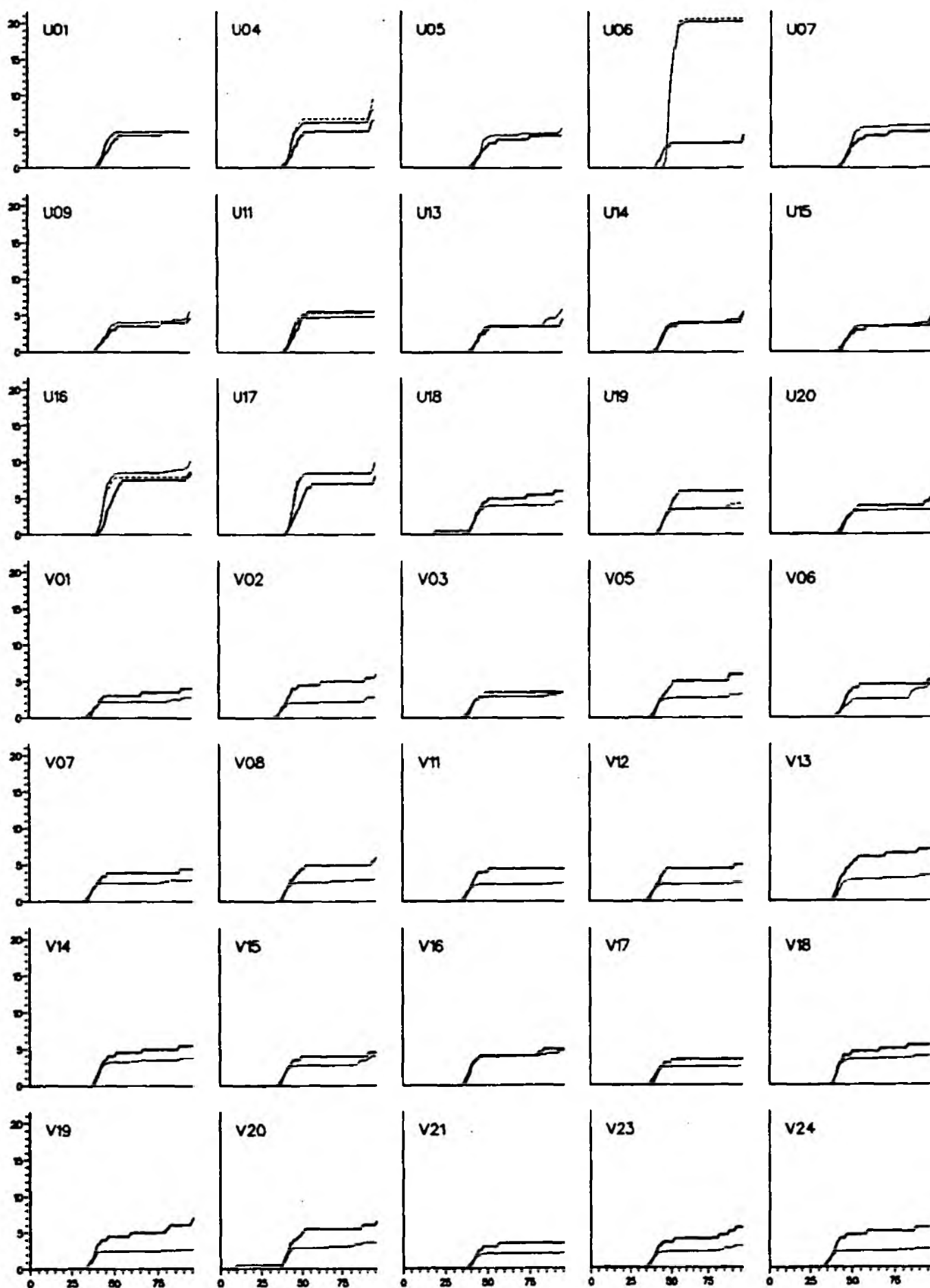
Appendix 12.7a: Comparative radar raingauge cumulative hyetographs: 2nd March 1989
(heavy solid - raingauge: medium dashed - 2 km (where available): light dotted - 5 km)
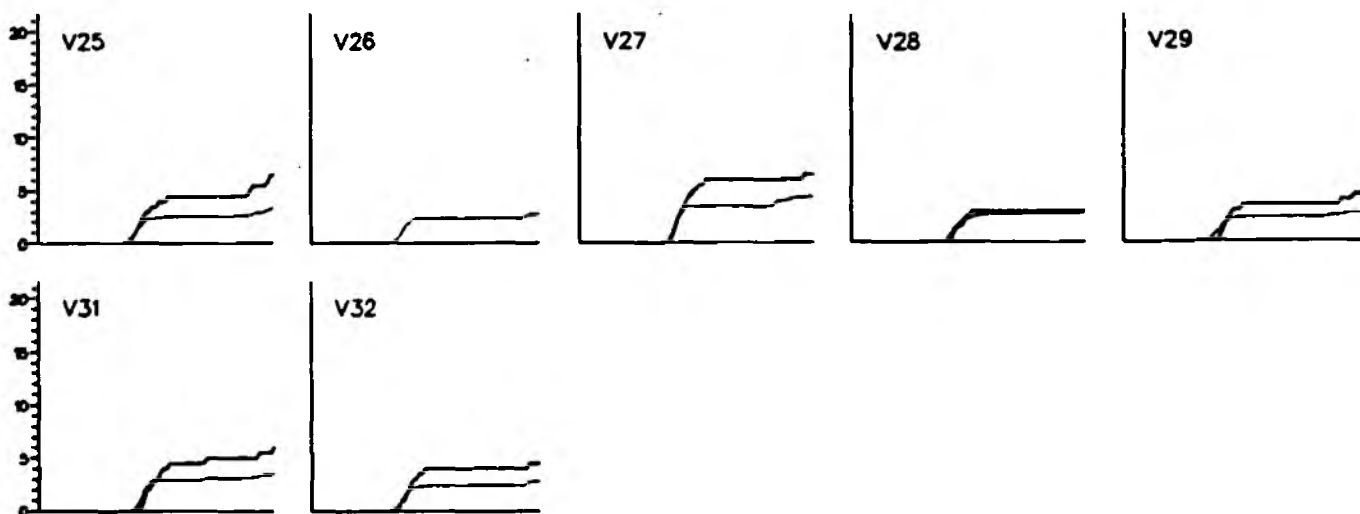
Appendix 12.7b: Comparative radar raingauge cumulative hyetographs: 2nd March 1989
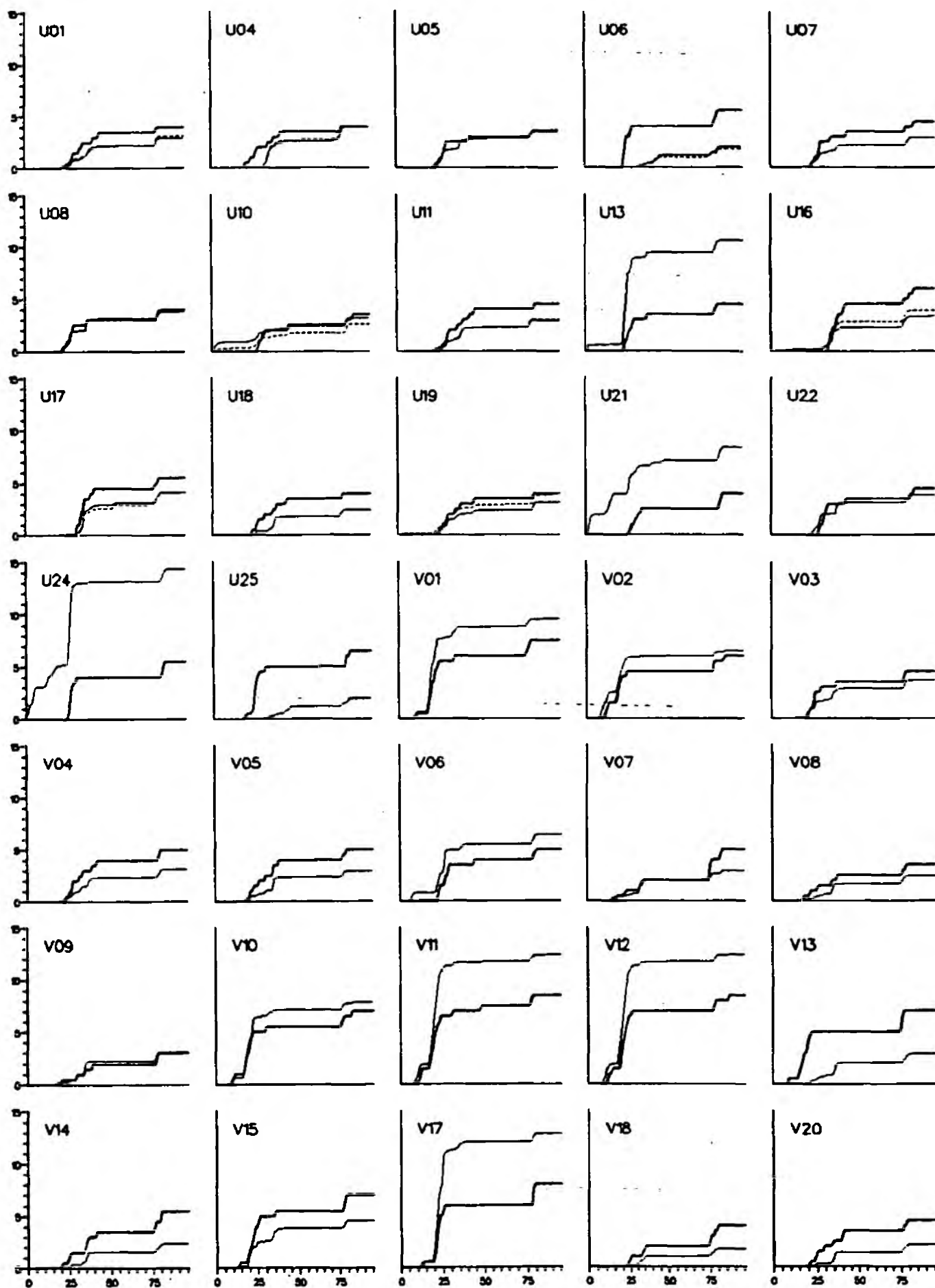(heavy solid - raingauge; medium dashed - 2 km (where available); light dotted - 5 km)
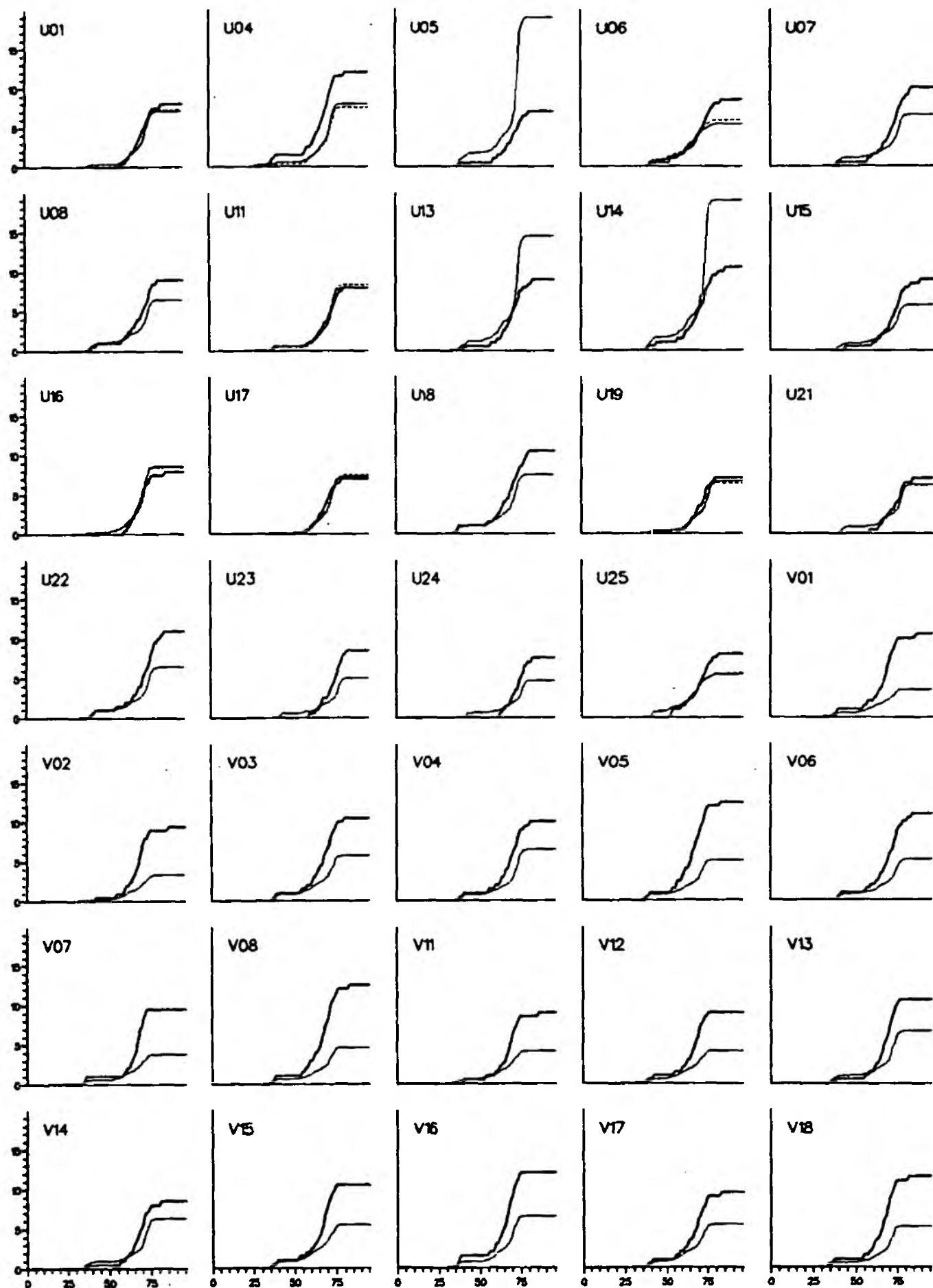
Appendix 12.8a: Comparative radar raingauge cumulative hyetographs: 14th March 1989

(heavy solid - raingauge: medium dashed - 2 km (where available): light dotted - 5 km)
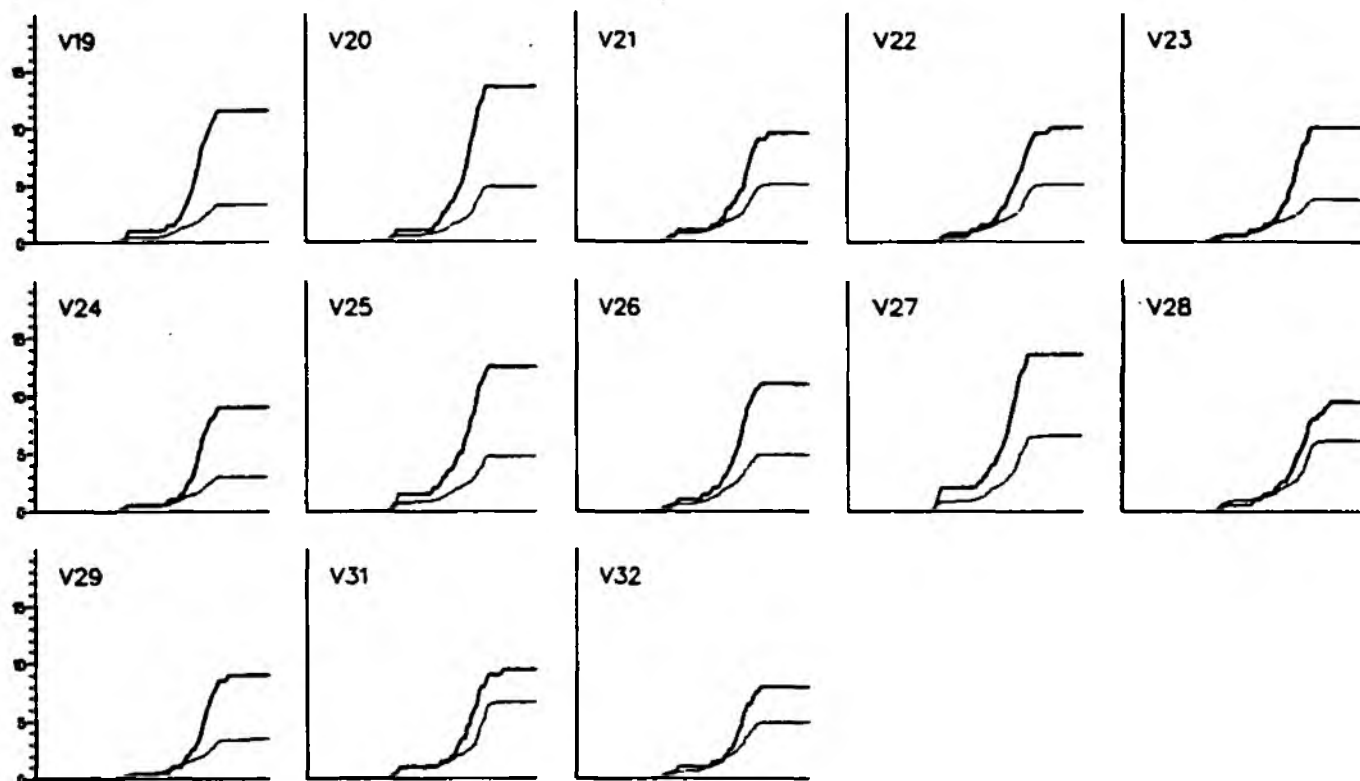
Appendix 12.8b: Comparative radar raingauge cumulative hyetographs: 14th March 1989
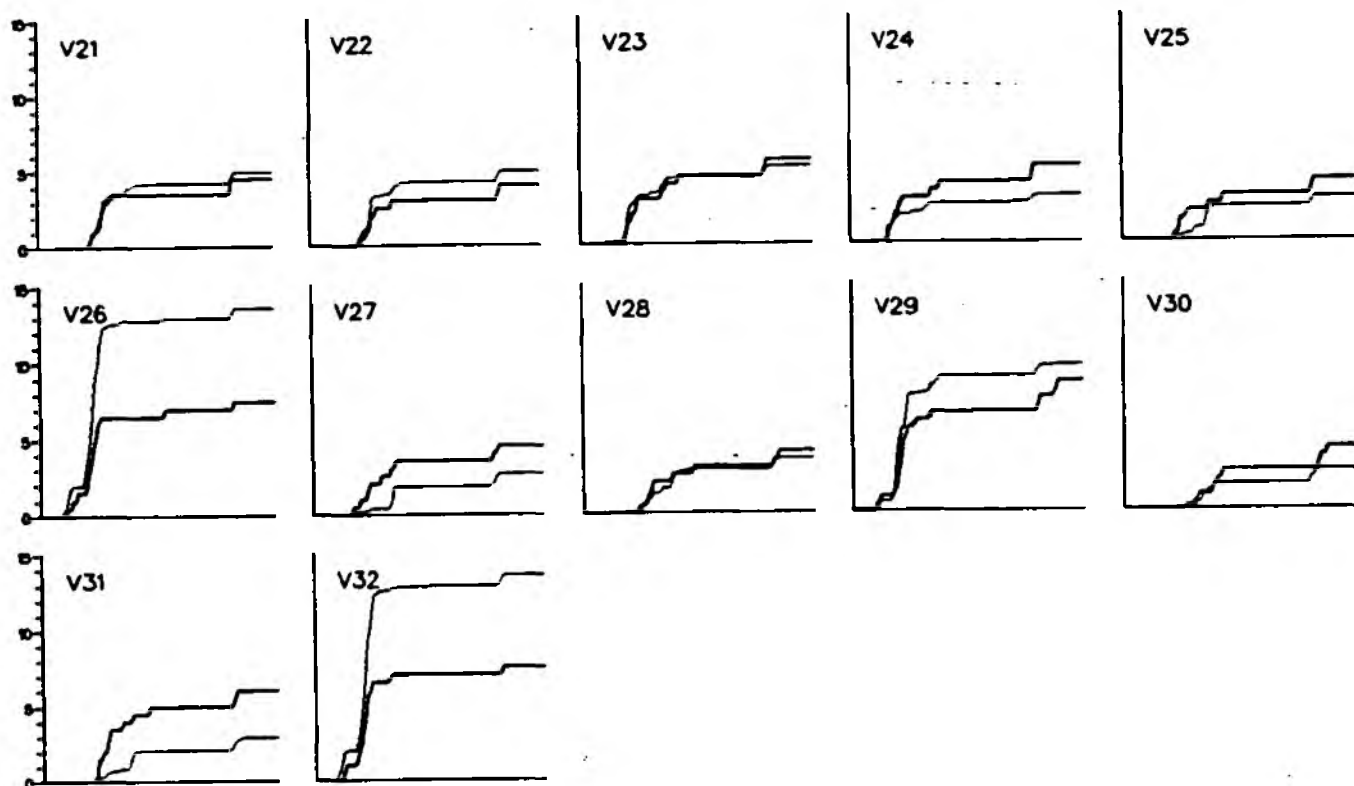(heavy solid - raingauge; medium dashed - 2 km (where available); light dotted - 5 km)
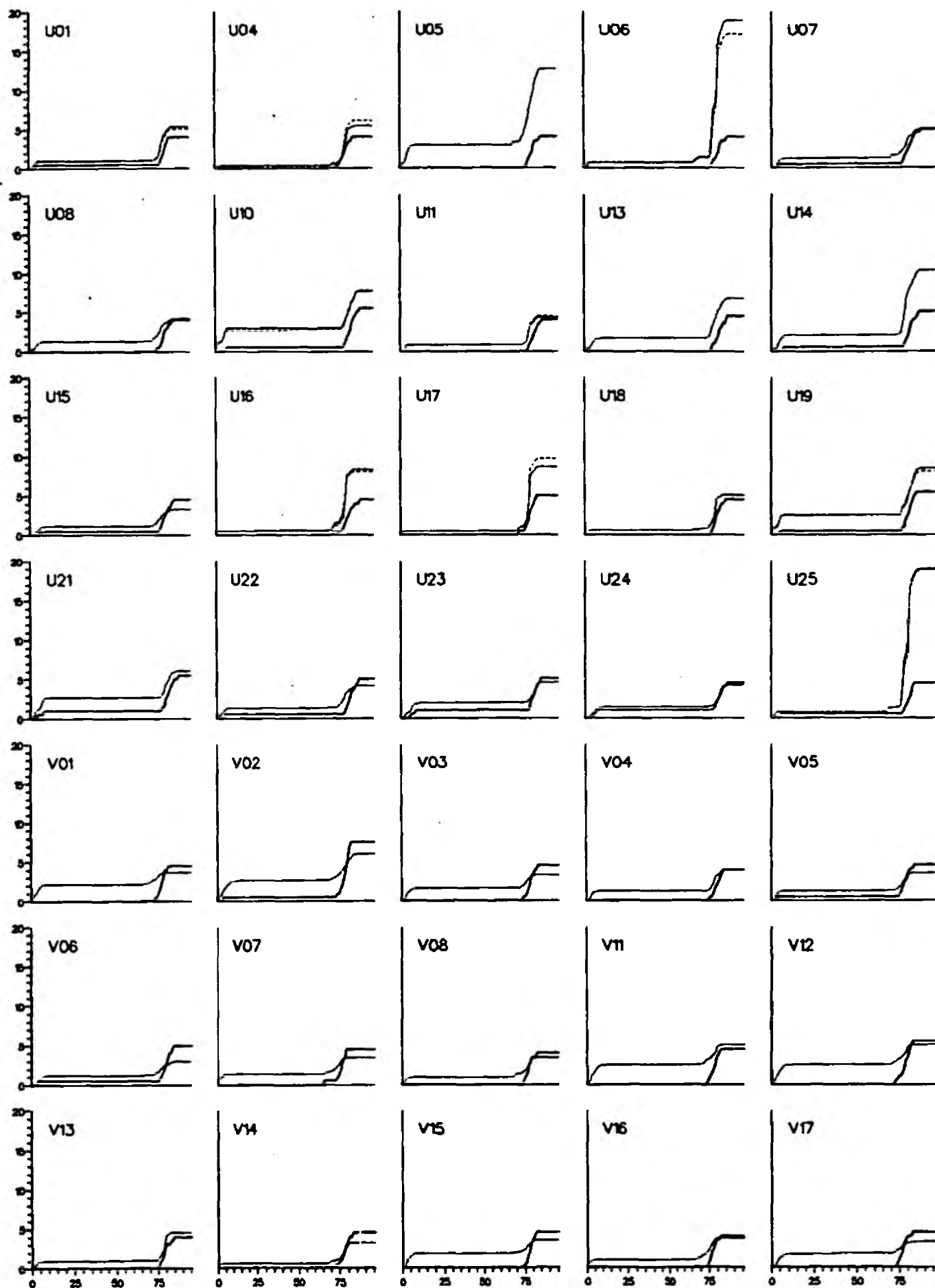
Appendix 12.9a: Comparative radar raingauge cumulative hyetographs: 20th March 1989

(heavy solid - raingauge; medium dashed - 2 km (where available); light dotted - 5 km)
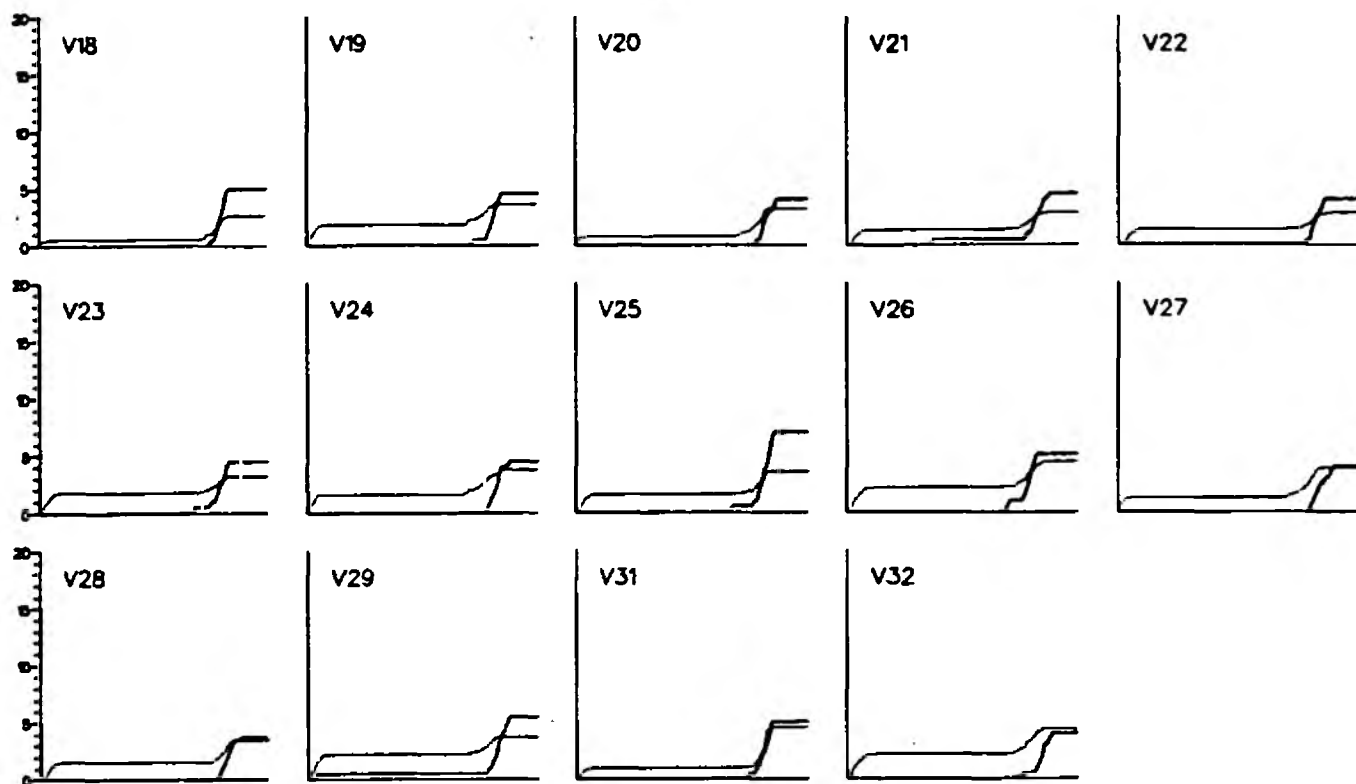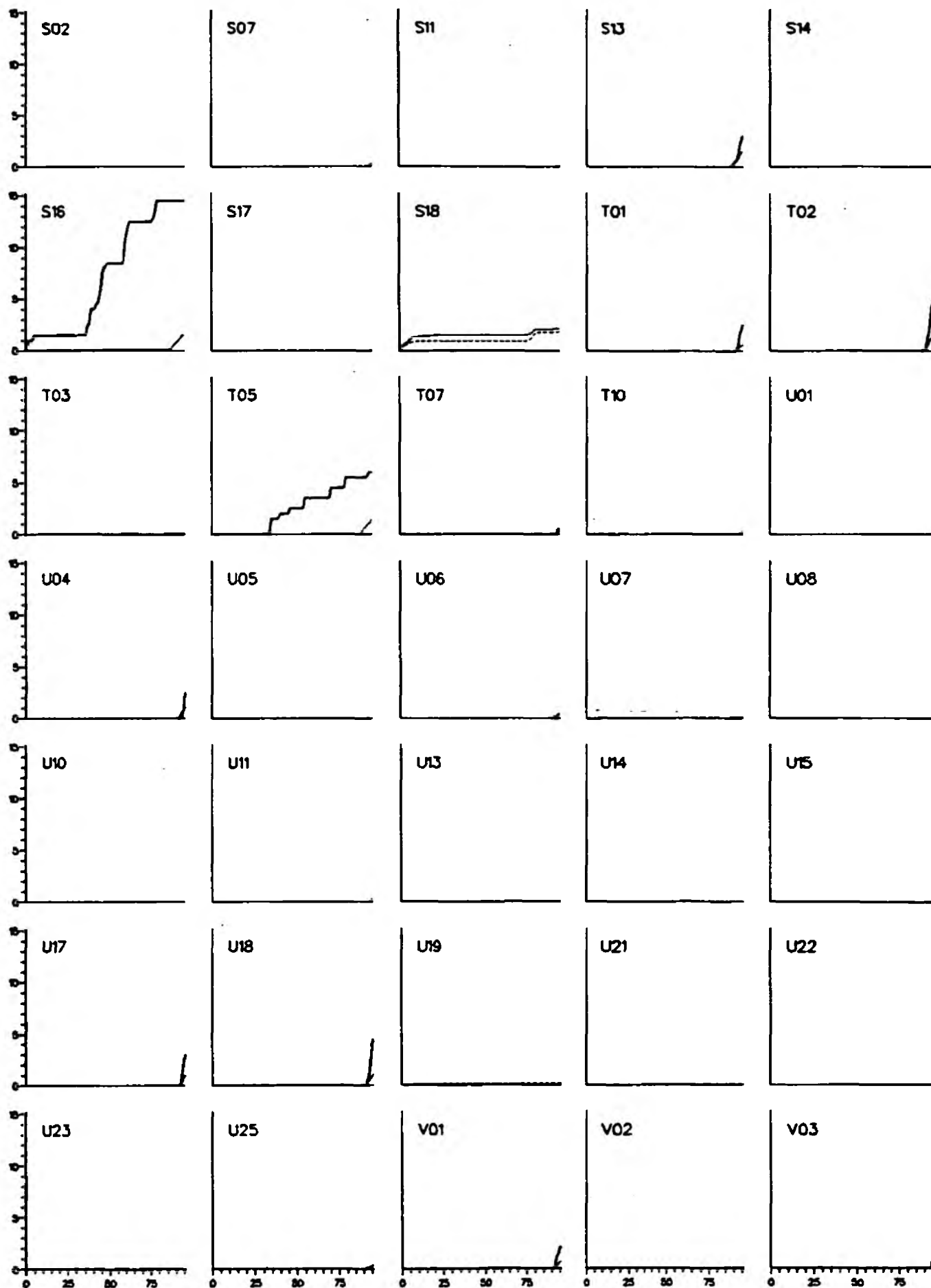
Appendix 12.9b: Comparative radar raingauge cumulative hyetographs: 20th March 1989

(heavy solid - raingauge: medium dashed - 2 km (where available): light dotted - 5 km)
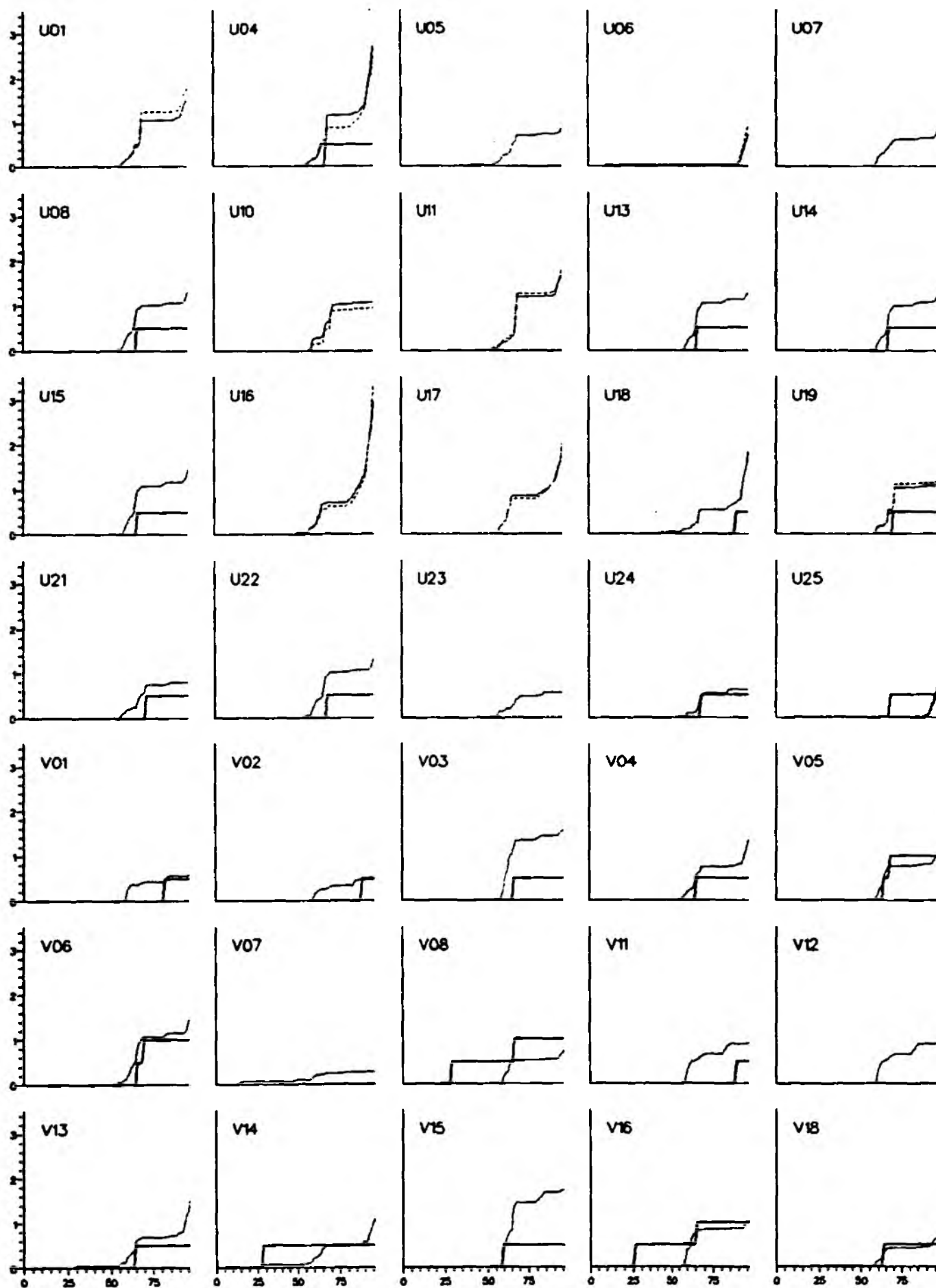
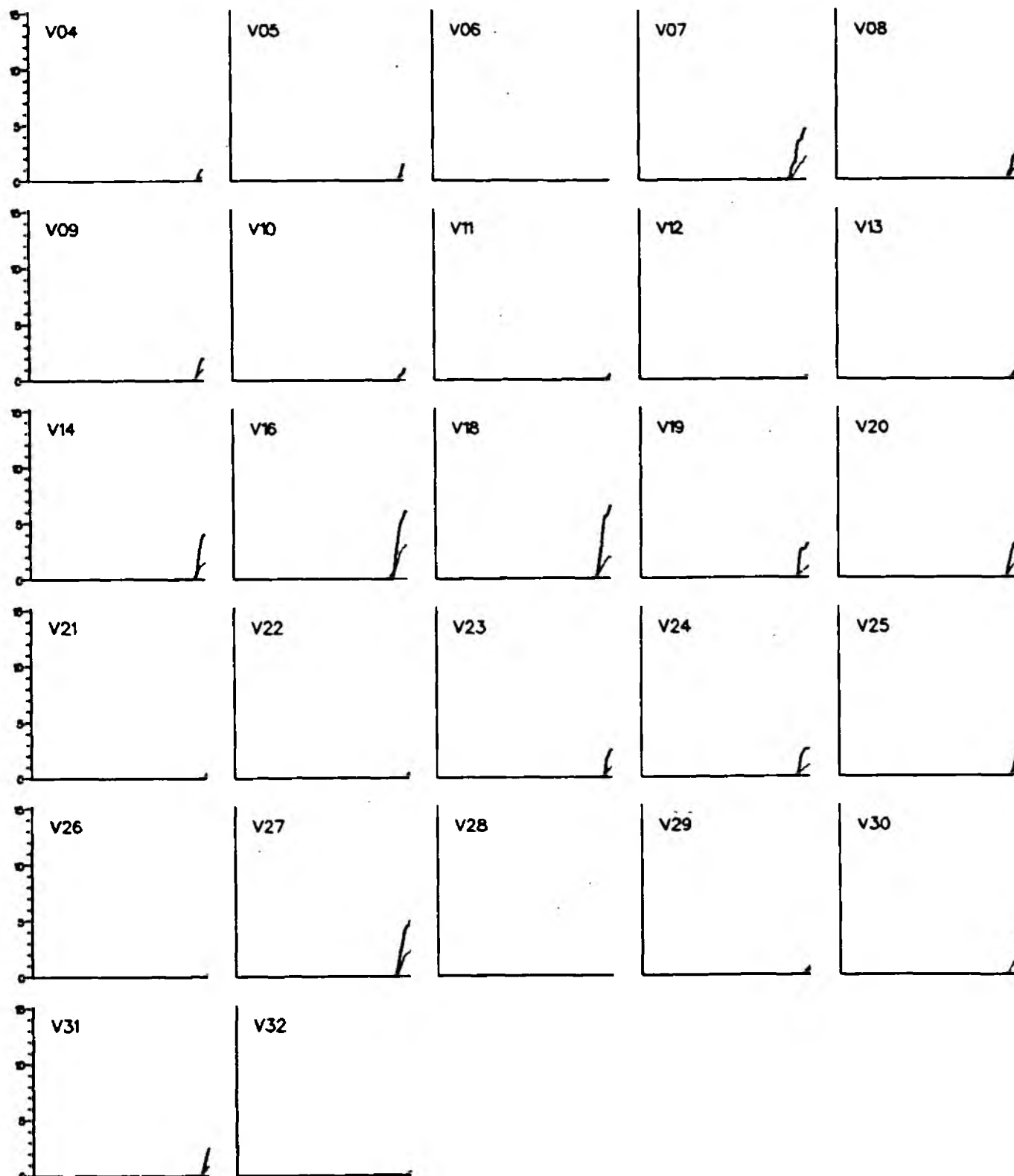**Appendix 12.10a:** Comparative radar raingauge cumulative hyetographs: 23rd March 1989
(heavy solid - raingauge: medium dashed - 2 km (where available): light dotted - 5 km)
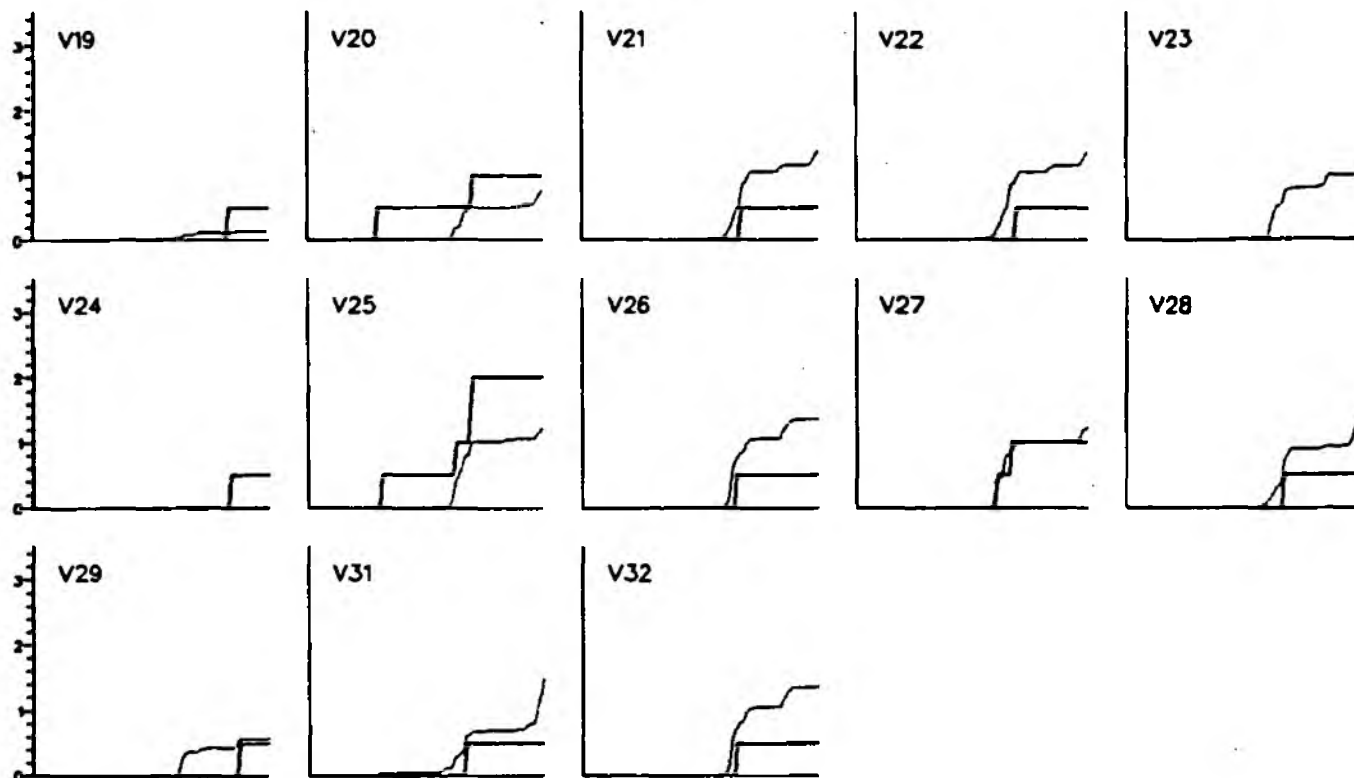
Appendix 12.10b: Comparative radar raingauge cumulative hyetographs: 23rd March 1989
(heavy solid - raingauge: medium dashed - 2 km (where available): light dotted - 5 km)

Appendix 12.11a: Comparative radar raingauge cumulative hyetographs: 4th April 1989

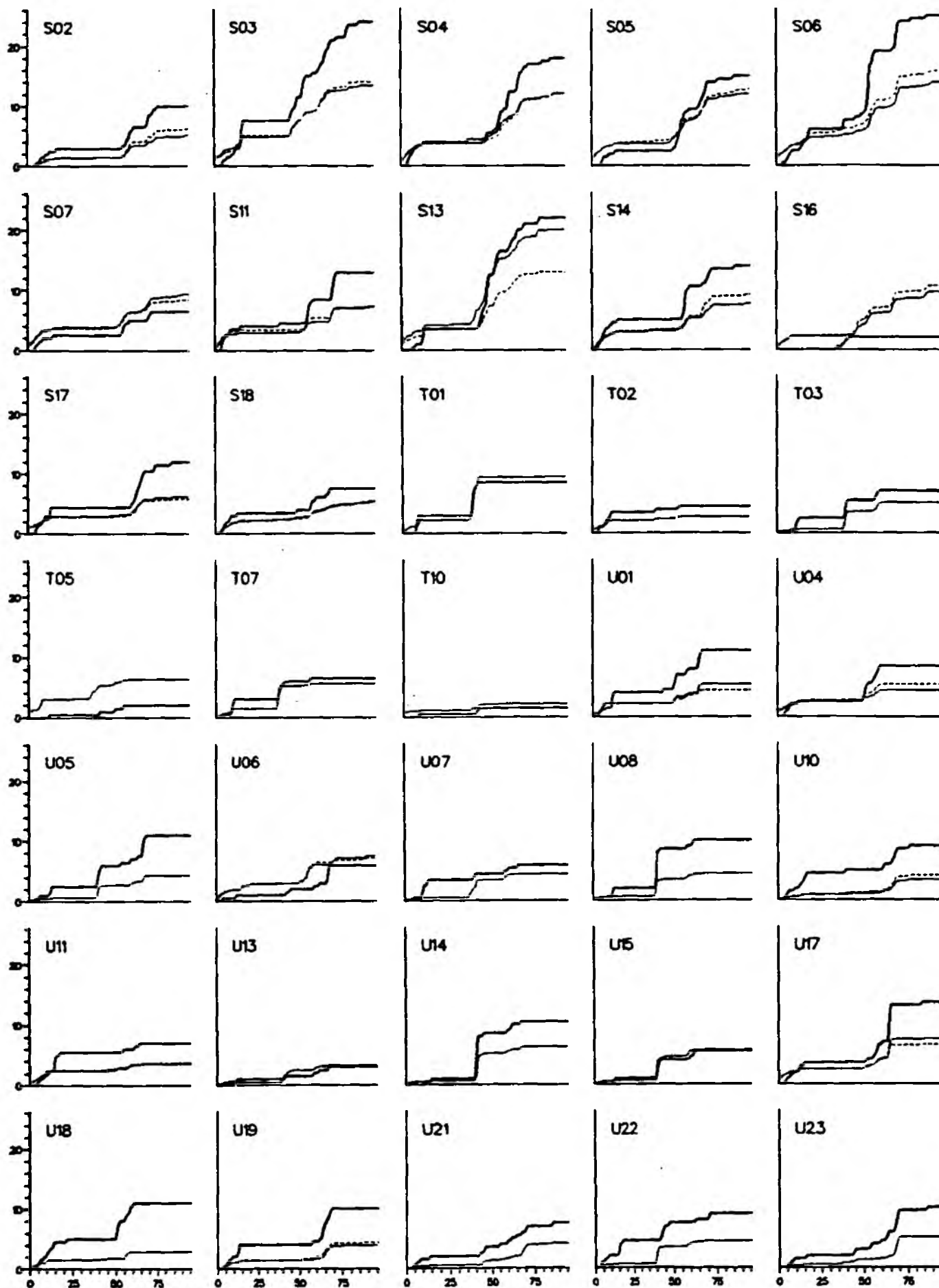(heavy solid - raingauge; medium dashed - 2 km (where available); light dotted - 5 km)

Appendix 12.11b: Comparative radar raingauge cumulative hyetographs: 4th April 1989
(heavy solid - raingauge; medium dashed - 2 km (where available); light dotted - 5 km)
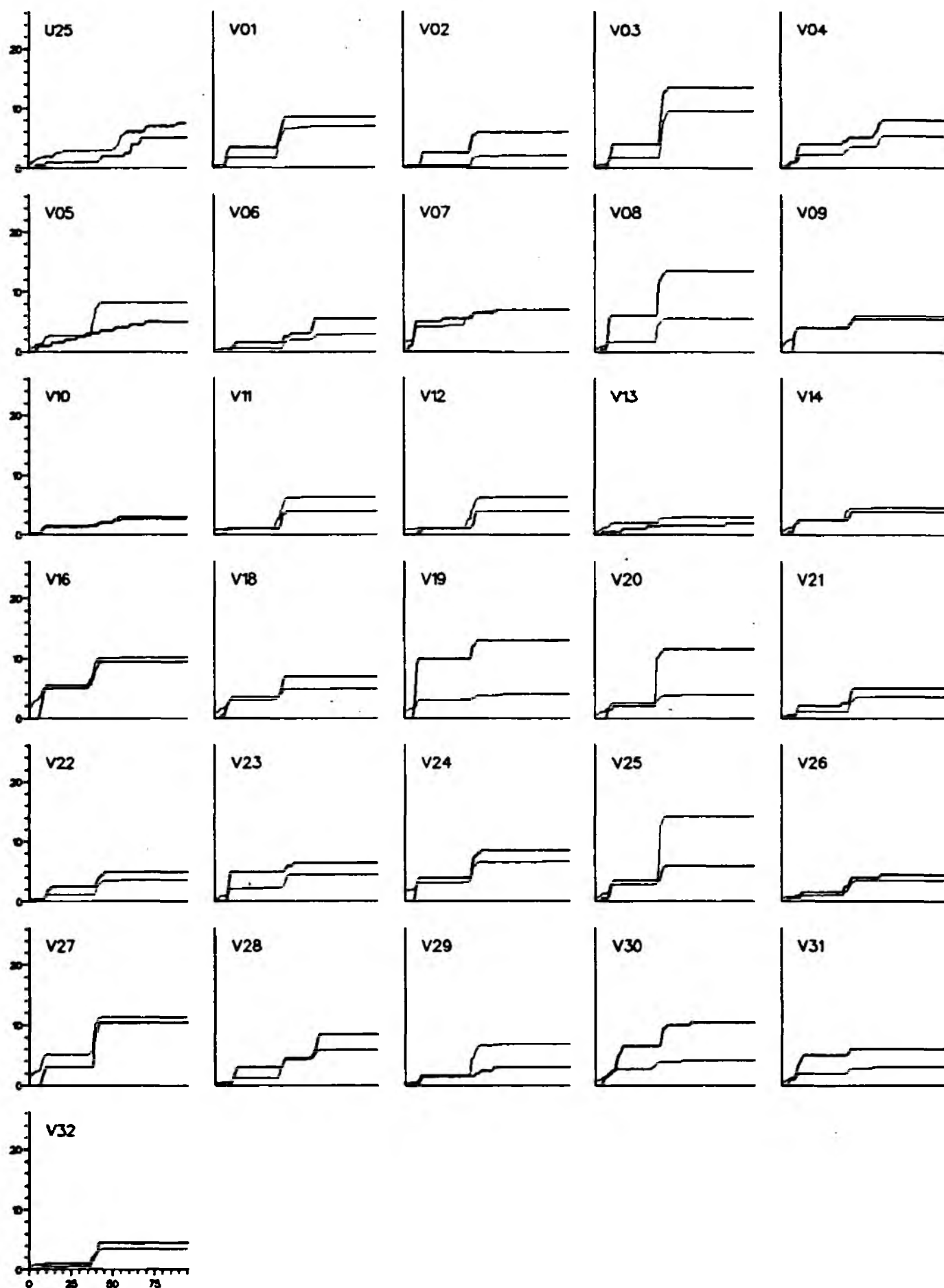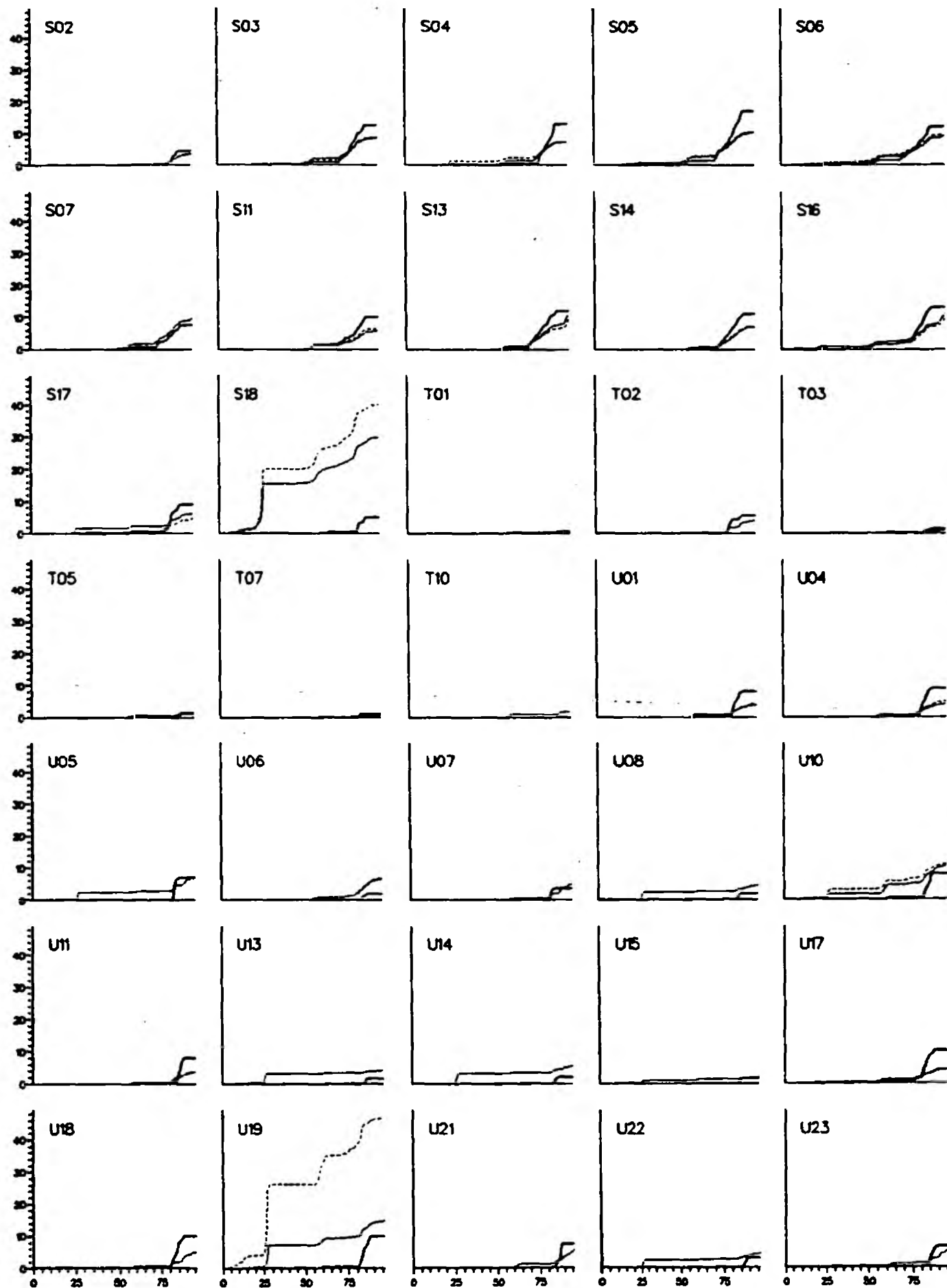
Appendix 12.12a: Comparative radar raingauge cumulative hyetographs: 9th April 1989

(heavy solid - raingauge: medium dashed - 2 km (where available): light dotted - 5 km)

V19   V20   V21   V22   V23

V24   V26   V27   V28   V29

V30   V31   V32

Appendix 12.12b: Comparative radar raingauge cumulative hyetographs: 9th April 1989

(heavy solid - raingauge: medium dashed - 2 km (where available): light dotted - 5 km)

Appendix 12.13a: Comparative radar raingauge cumulative hyetographs: 24th April 1989

(heavy solid - raingauge; medium dashed - 2 km (where available); light dotted - 5 km)
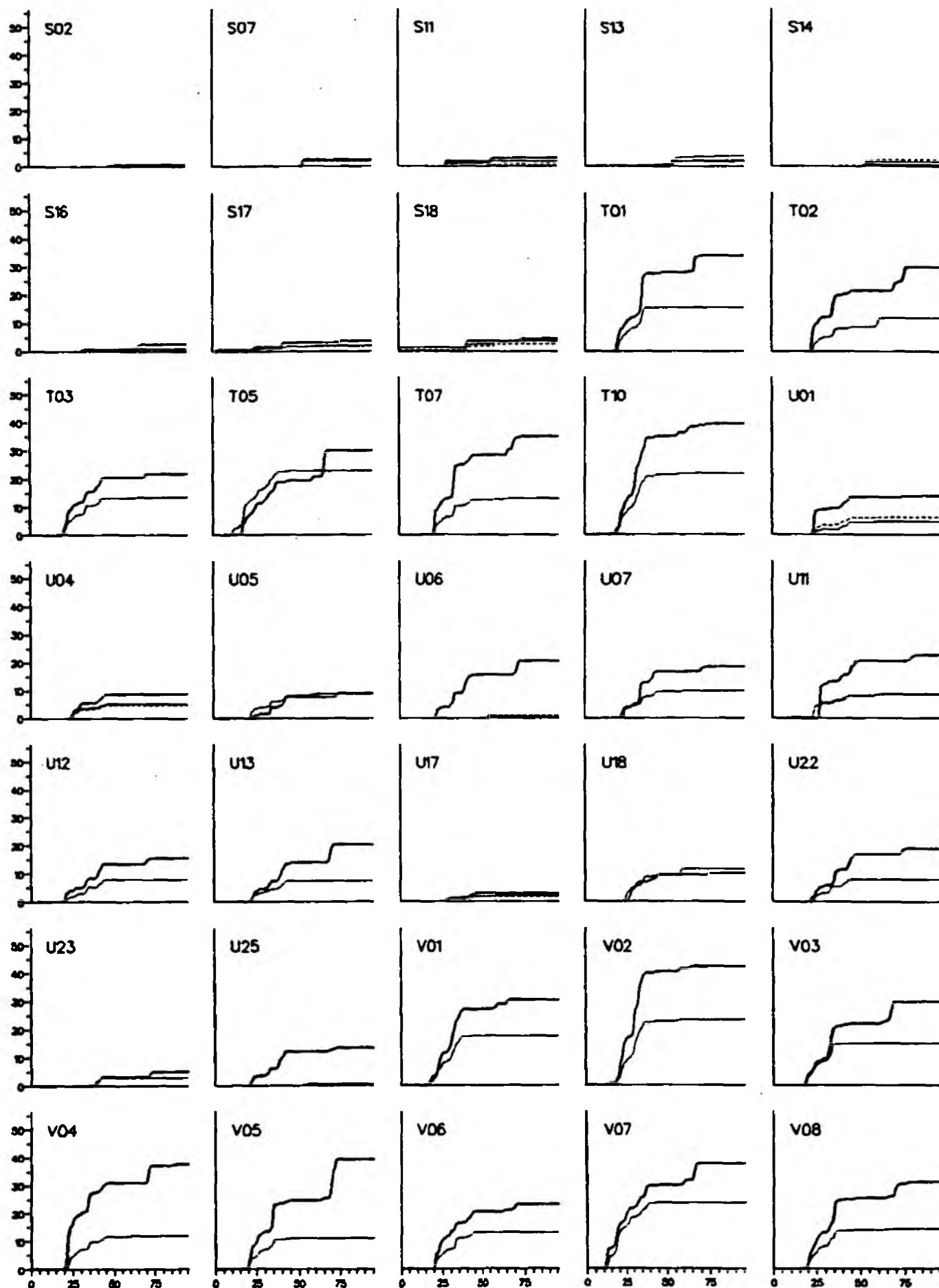
Appendix 12.13b: Comparative radar raingauge cumulative hyetographs: 24th April 1989
(heavy solid - raingauge; medium dashed - 2 km (where available); light dotted - 5 km)

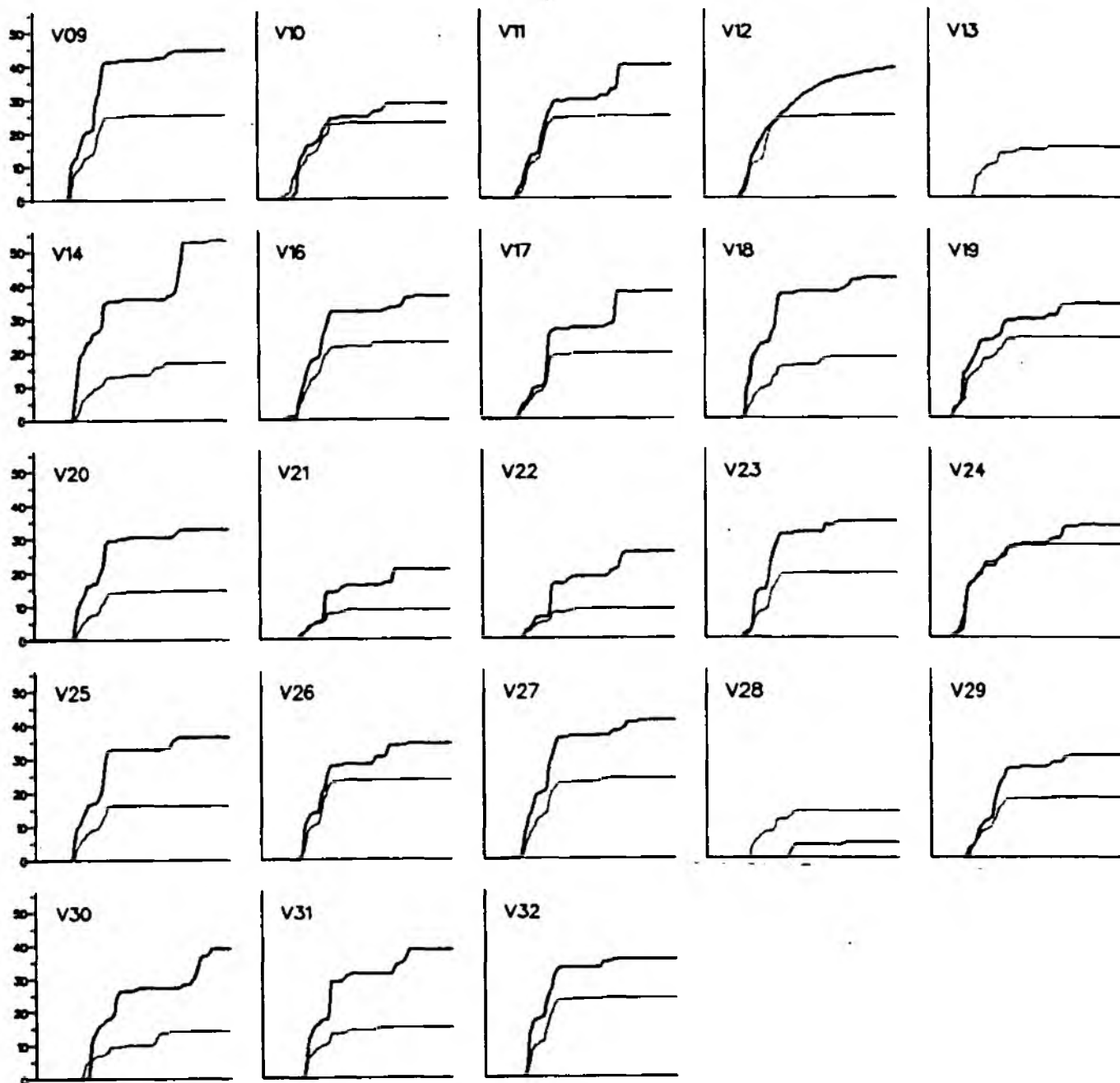Appendix 12.14a: Comparative radar raingauge cumulative hyetographs: 10th May 1989

(heavy solid - raingauge: medium dashed - 2 km (where available): light dotted - 5 km)

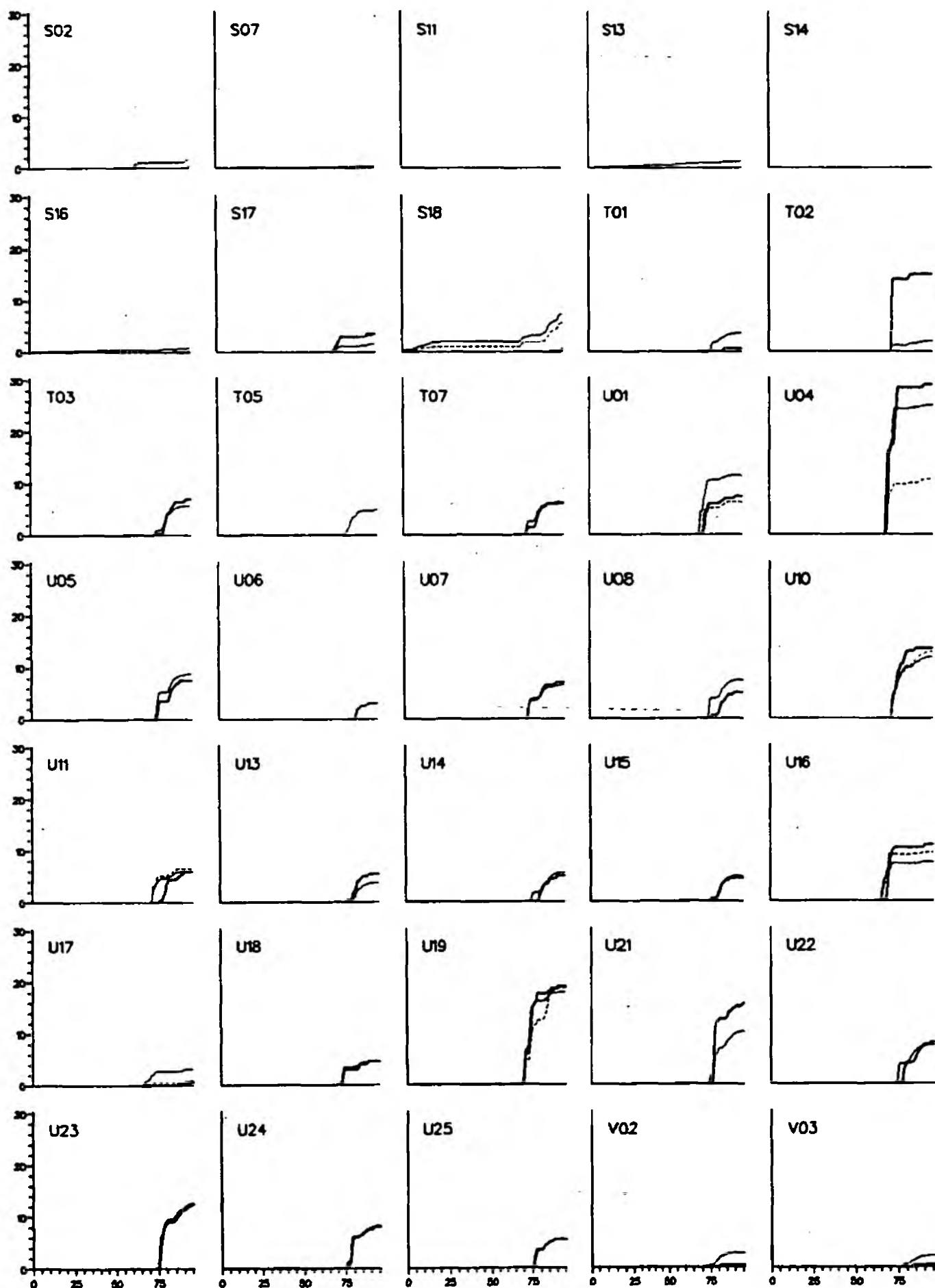Appendix 12.14b: Comparative radar raingauge cumulative hyetographs: 10th May 1989
(heavy solid - raingauge: medium dashed - 2 km (where available): light dotted - 5 km)
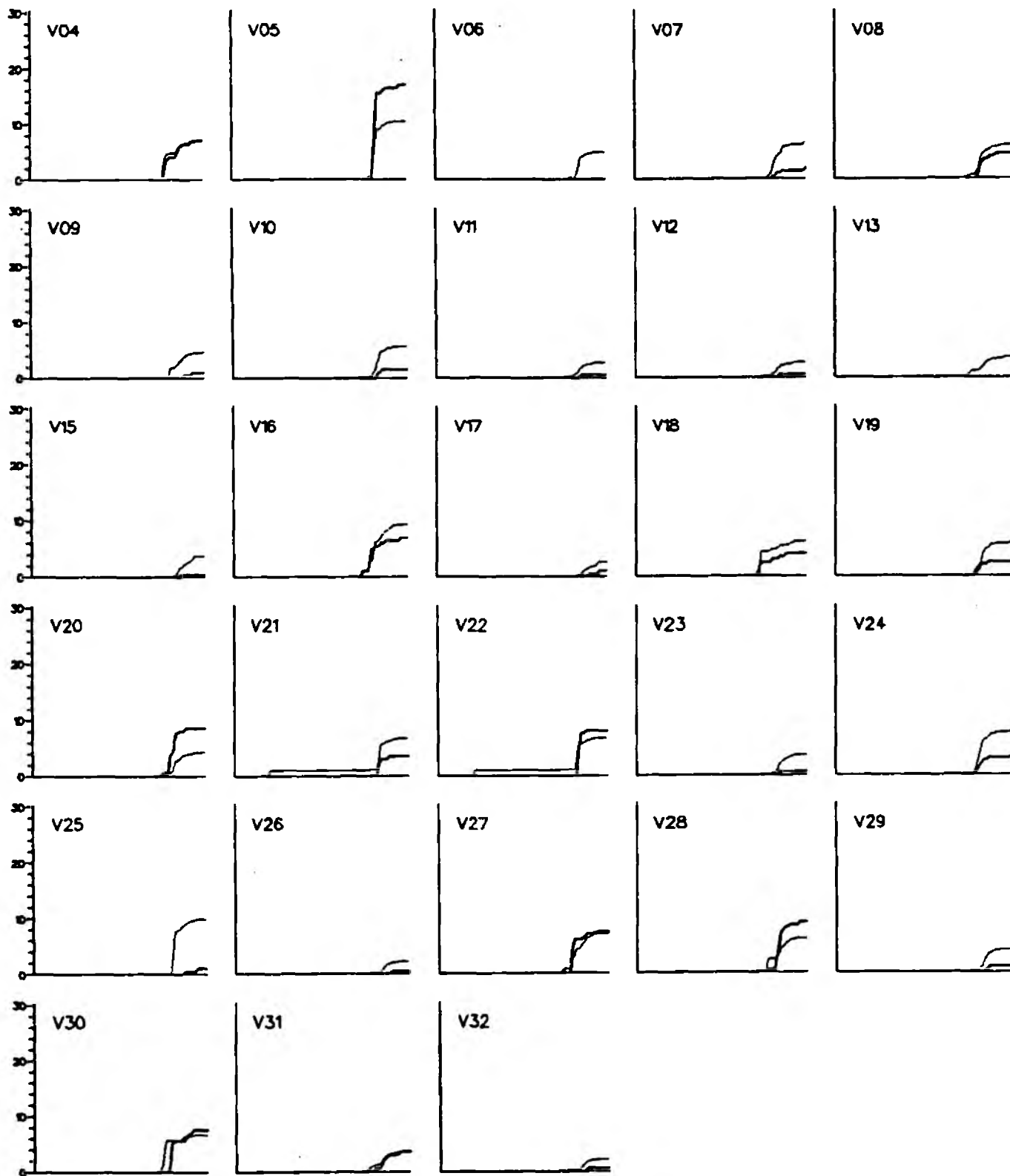
Appendix 12.15a: Comparative radar raingauge cumulative hyetographs: 11th May 1989

(heavy solid - raingauge; medium dashed - 2 km (where available); light dotted - 5 km)

Appendix 12.15b: Comparative radar raingauge cumulative hyetographs: 11th May 1989

(heavy solid - raingauge; medium dashed - 2 km (where available); light dotted - 5 km)
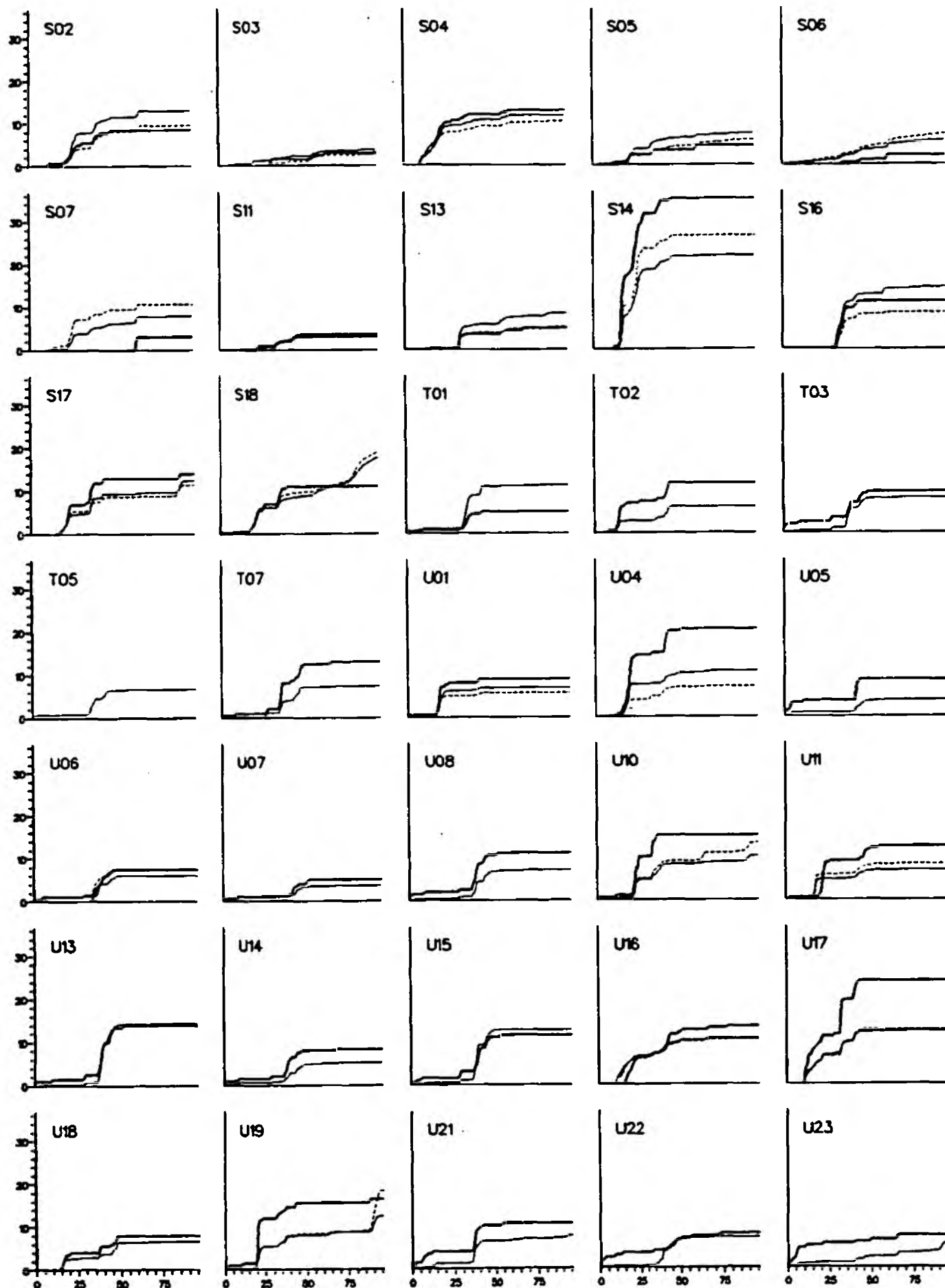
Appendix 12.16a: Comparative radar raingauge cumulative hyetographs: 26th June 1989

(heavy solid - raingauge: medium dashed - 2 km (where available): light dotted - 5 km)

Appendix 12.16b: Comparative radar raingauge cumulative hyetographs: 26th June 1989

(heavy solid - raingauge; medium dashed - 2 km (where available); light dotted - 5 km)

Appendix 12.17a: Comparative radar raingauge cumulative hyetographs: 27th June 1989

(heavy solid - raingauge; medium dashed - 2 km (where available); light dotted - 5 km)
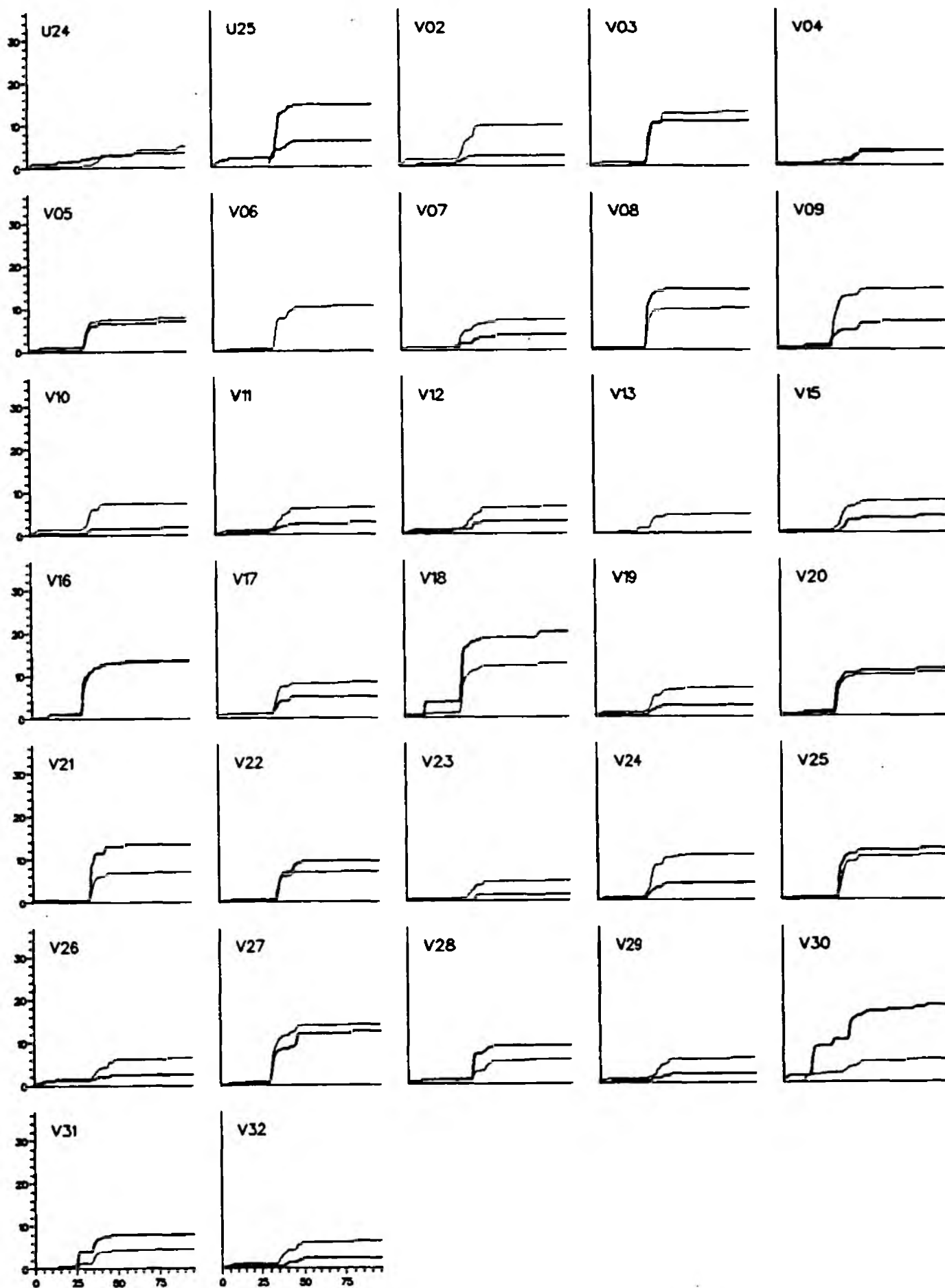
Appendix 12.17b: Comparative radar raingauge cumulative hyetographs: 27th June 1989

(heavy solid - raingauge; medium dashed - 2 km (where available); light dotted - 5 km)

Appendix 12.18a: Comparative radar raingauge cumulative hyetographs: 30th June 1989

(heavy solid - raingauge; medium dashed - 2 km (where available); light dotted - 5 km)

Appendix 12.19a: Comparative radar raingauge cumulative hyetographs: 7th July 1989

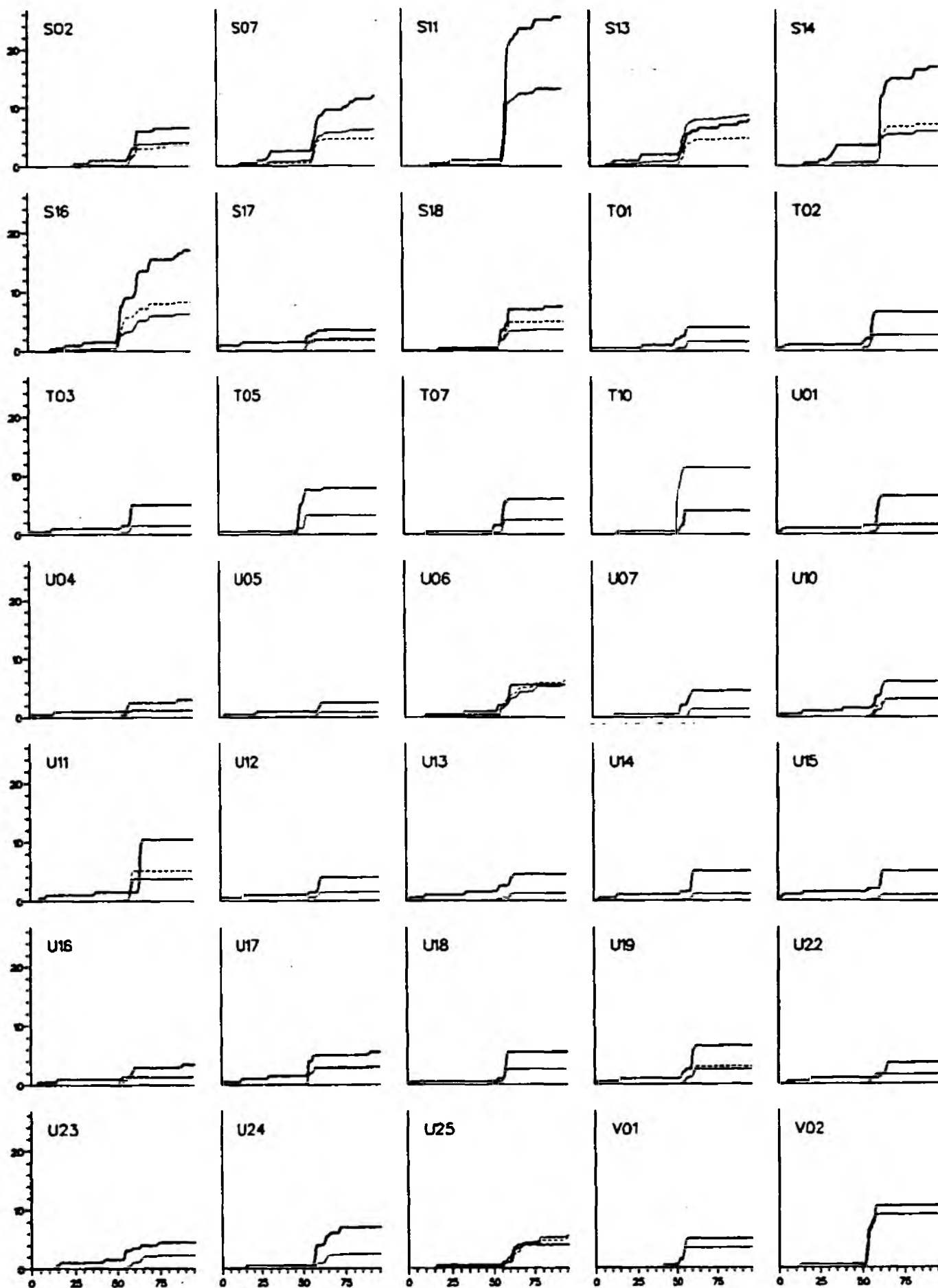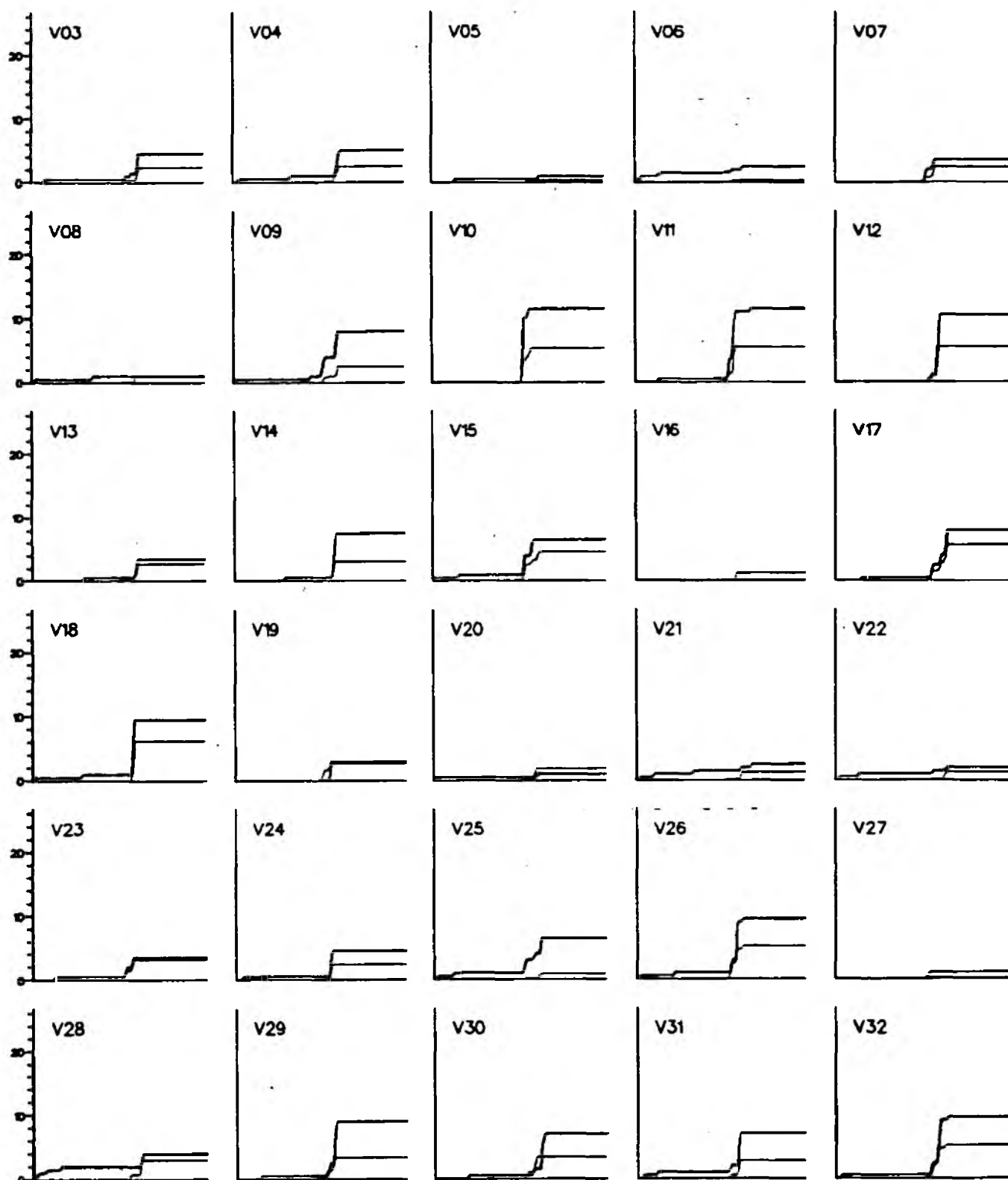(heavy solid - raingauge; medium dashed - 2 km (where available); light dotted - 5 km)

Appendix 12.19b: Comparative radar raingauge cumulative hyetographs: 7th July 1989

(heavy solid - raingauge: medium dashed - 2 km (where available); light dotted - 5 km)

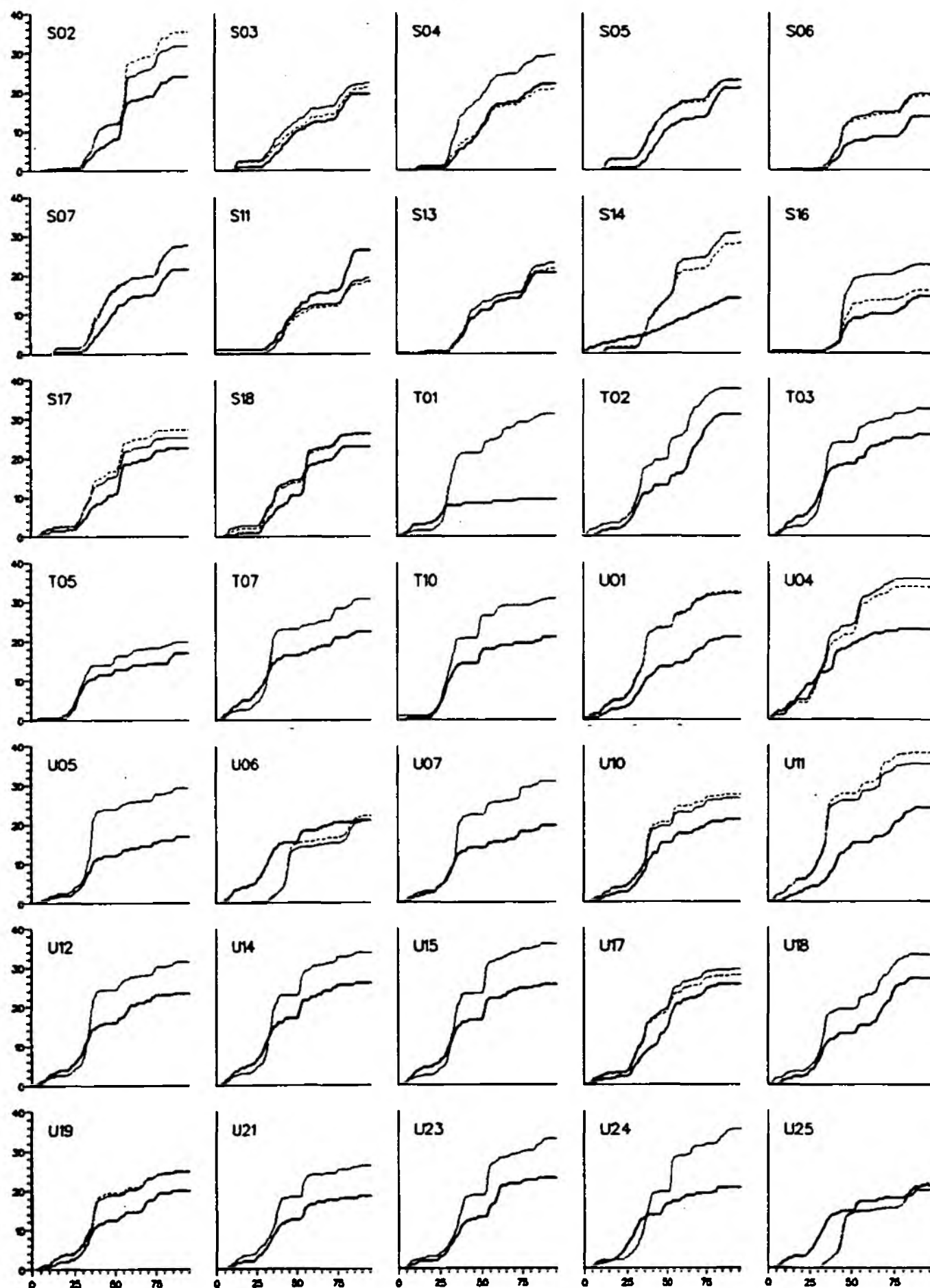Appendix 12.20a: Comparative radar raingauge cumulative hyetographs: 29th July 1989
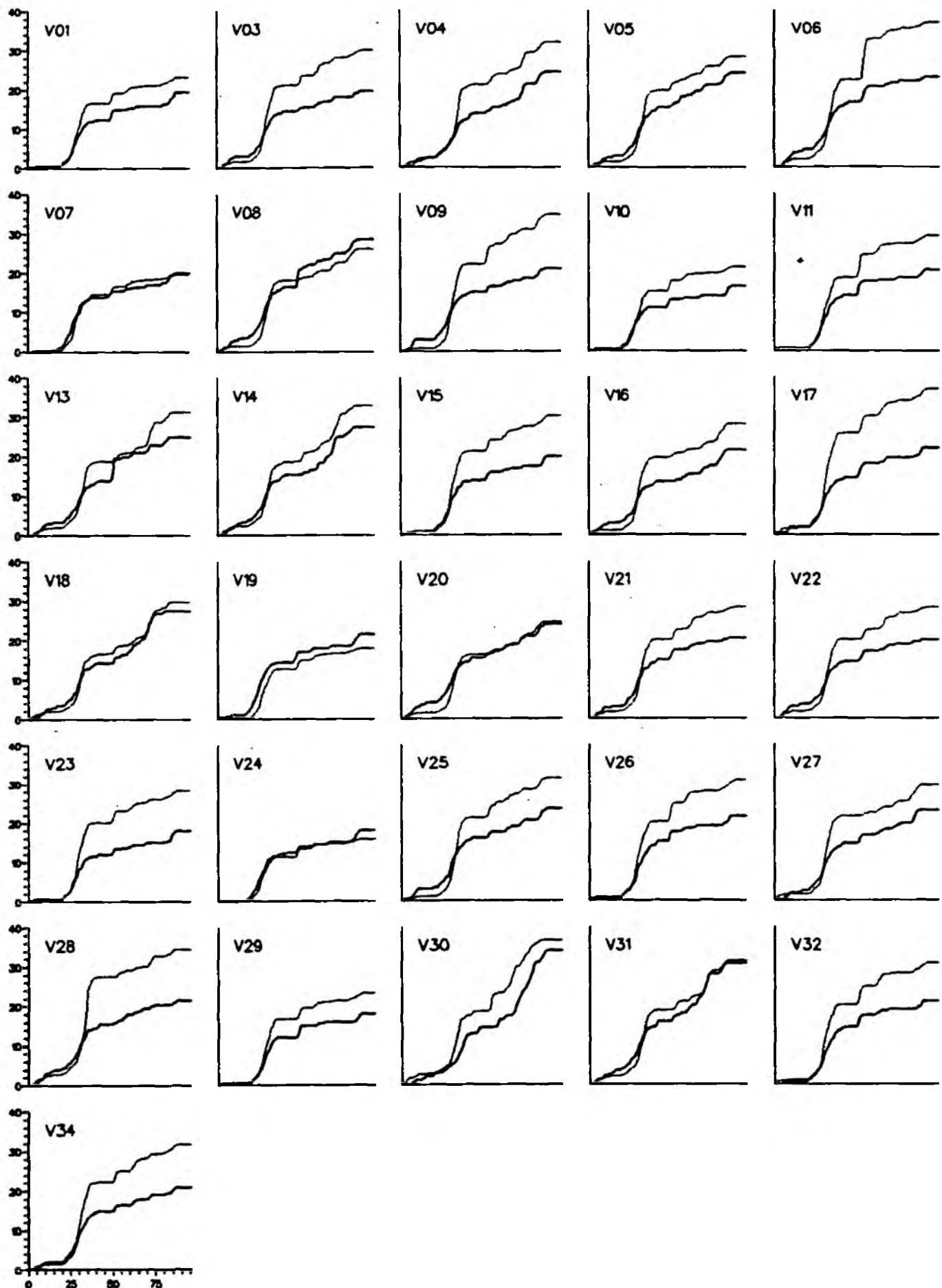
(heavy solid - raingauge: medium dashed - 2 km (where available): light dotted - 5 km)

Appendix 12.20b: Comparative radar raingauge cumulative hyetographs: 29th July 1989

(heavy solid - raingauge: medium dashed - 2 km (where available): light dotted - 5 km)

Appendix 12.21a: Comparative radar raingauge cumulative hyetographs: 30th July 1989
(heavy solid - raingauge: medium dashed - 2 km (where available): light dotted - 5 km)

Appendix 12.21b: Comparative radar raingauge cumulative hyetographs: 30th July 1989

(heavy solid - raingauge: medium dashed - 2 km (where available): light dotted - 5 km)

Appendix 12.22a: Comparative radar raingauge cumulative hyetographs: 26th August 1989

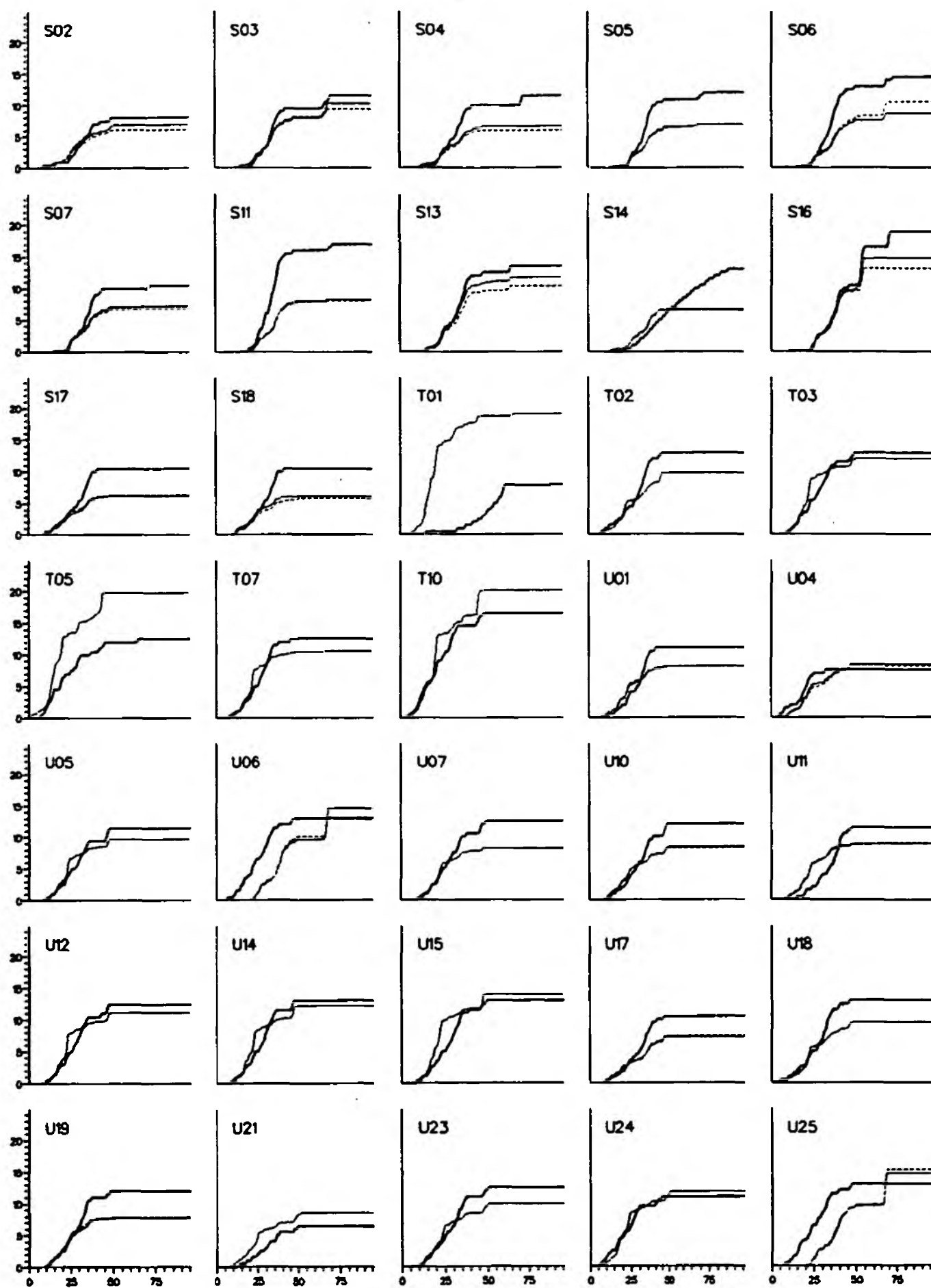(heavy solid - raingauge; medium dashed - 2 km (where available); light dotted - 5 km)

Appendix 12.22b: Comparative radar raingauge cumulative hyetographs: 26th August 1989

(heavy solid - raingauge; medium dashed - 2 km (where available); light dotted - 5 km)

Appendix 12.23a: Comparative radar raingauge cumulative hyetographs: 14th December 1989

(heavy solid - raingauge: medium dashed - 2 km (where available): light dotted - 5 km)
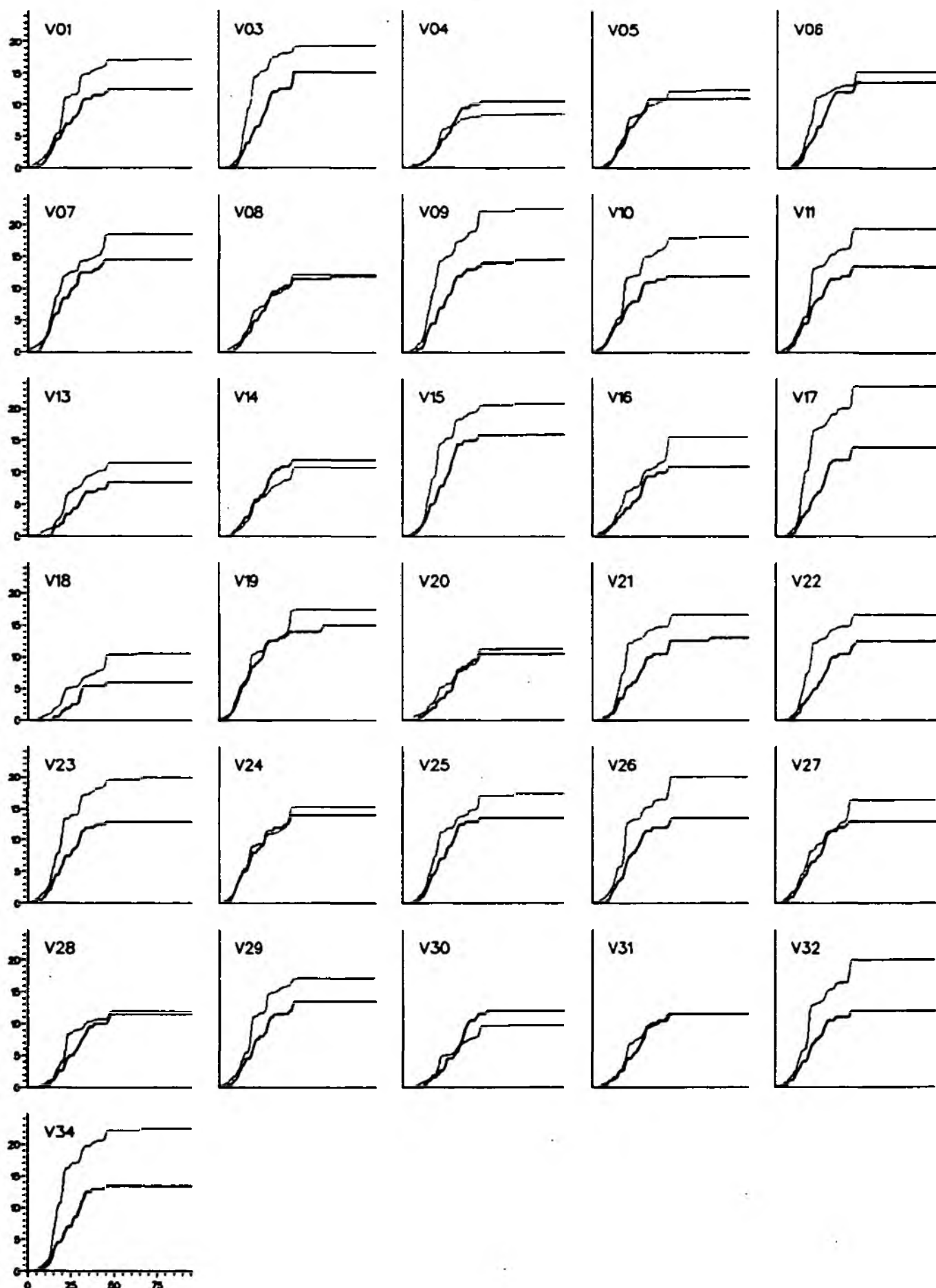
Appendix 12.23b: Comparative radar raingauge cumulative hyetographs: 14th December 1989

(heavy solid - raingauge; medium dashed - 2 km (where available); light dotted - 5 km)
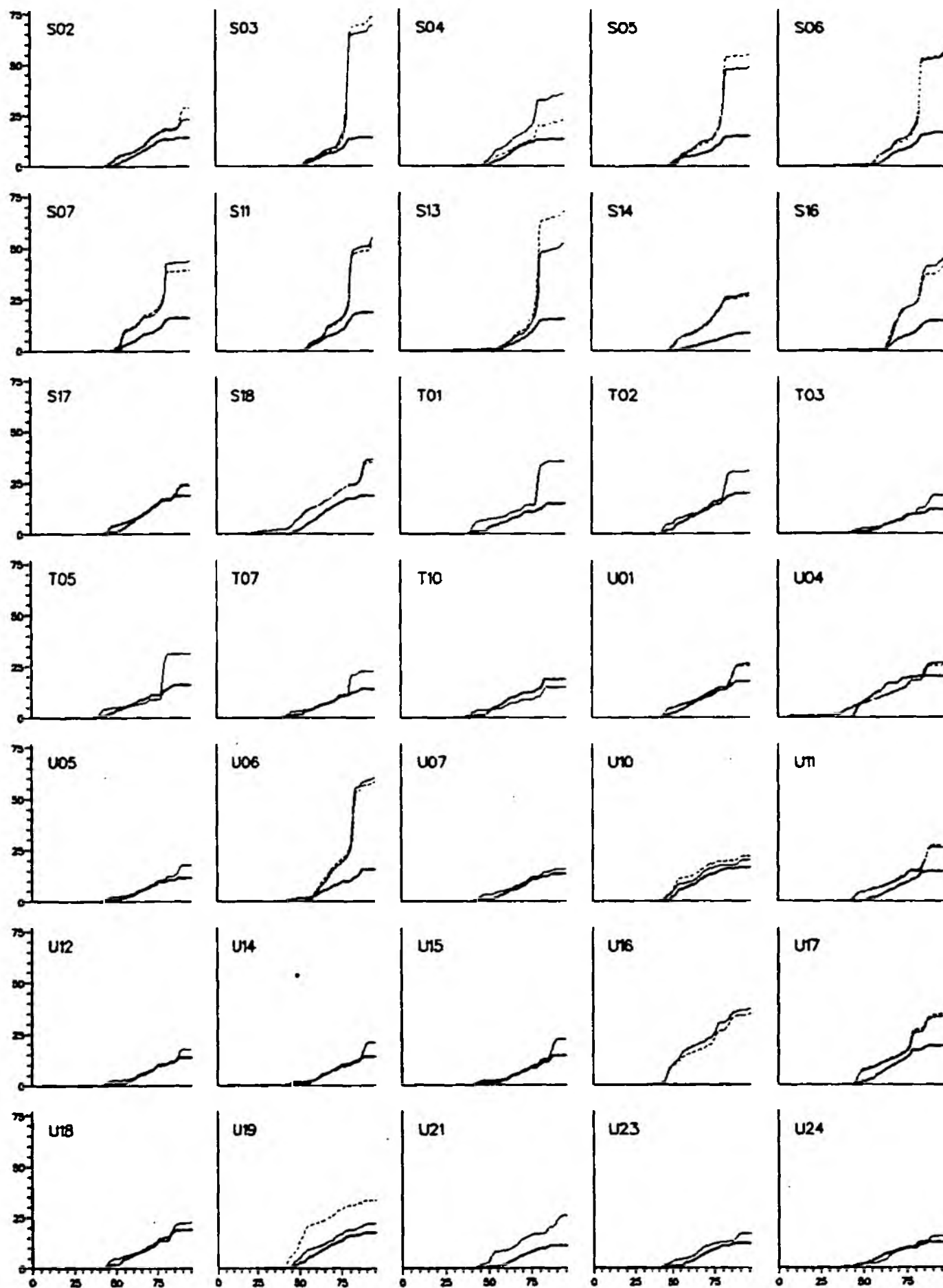
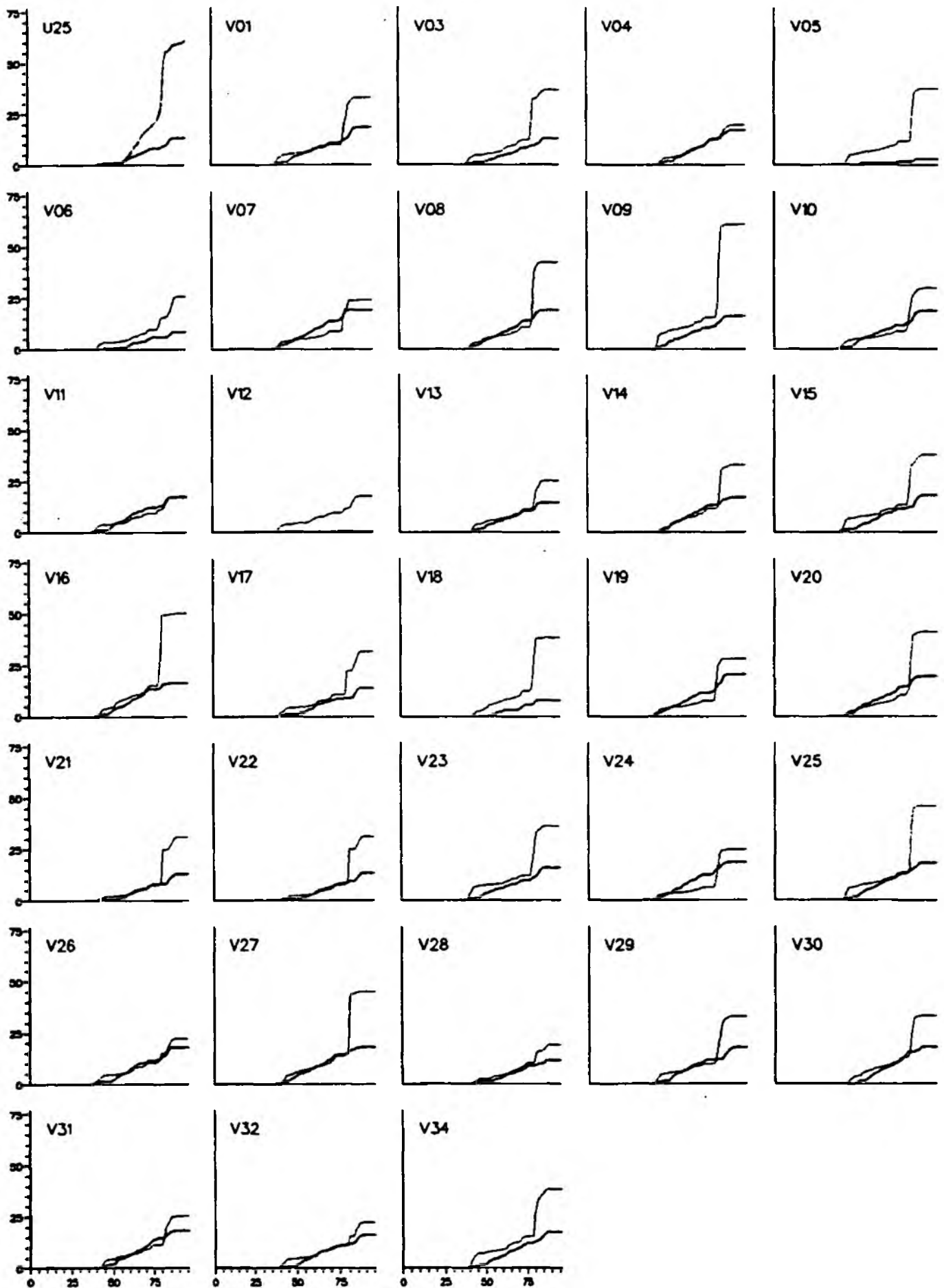Appendix 12.24a: Comparative radar raingauge cumulative hyetographs: 16th December 1989

(heavy solid - raingauge; medium dashed - 2 km (where available); light dotted - 5 km)

Appendix 12.24b: Comparative radar raingauge cumulative hyetographs: 16th December 1989

(heavy solid - raingauge: medium dashed - 2 km (where available): light dotted - 5 km)

Appendix 12.25a: Comparative radar raingauge cumulative hyetographs: 18th December 1989

(heavy solid - raingauge; medium dashed - 2 km (where available); light dotted - 5 km)

Appendix 12.25b: Comparative radar raingauge cumulative hyetographs: 18th December 1989

(heavy solid - raingauge: medium dashed - 2 km (where available): light dotted - 5 km)

River Witham
at Colsterworth

Willow Brook
at Fotheringay

Harpers Brook
at Old Mill Bridge

Ise Brook
at Harrowden

River Nene
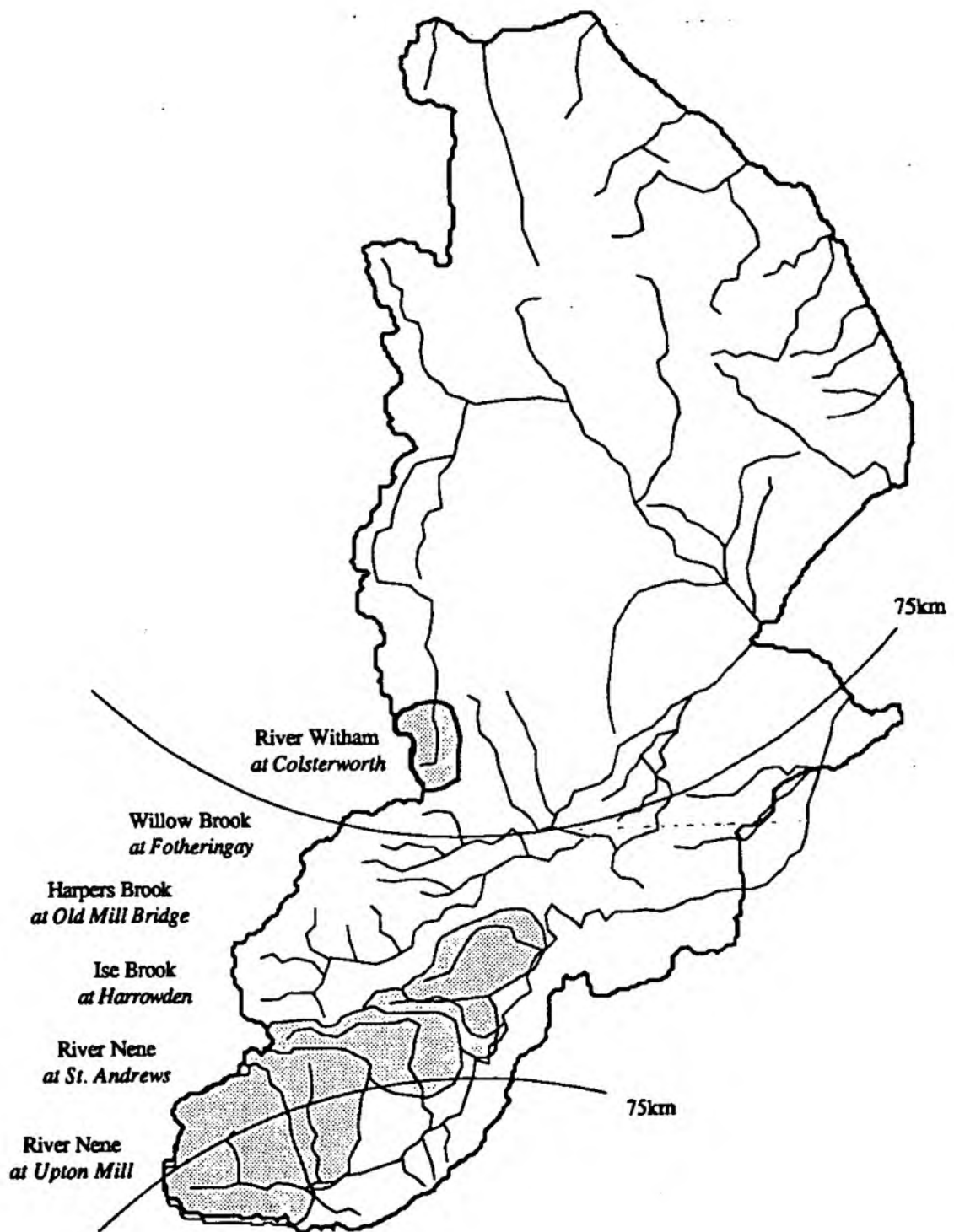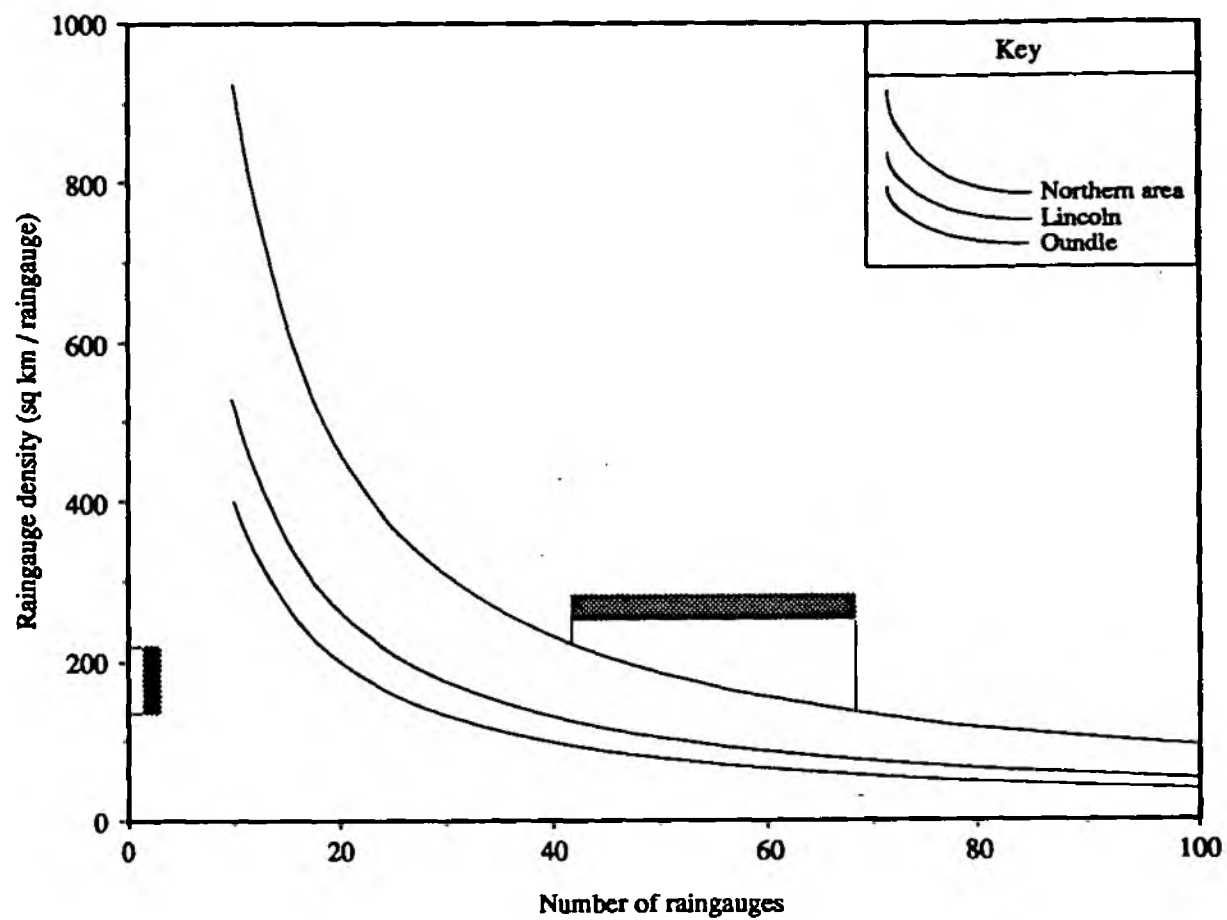*at St. Andrews*

River Nene
at Upton Mill

75km

75km

Figure A13.1: Test River Catchments

Figure A14.1: Raingauge Network Density